FACULTAD DE CIENCIAS QUÍMICAS E INGENIERÍA

DR. LUIS ENRIQUE PALAFOX MAESTRE
DIRECTOR DE LA FAC. DE CS. QCAS. E INGENIERÍA
P R E S E N T E :

Una vez revisado el trabajo que presenta la **M.C. SELENE LILETTE CÁRDENAS MACIEL** correspondiente al tema: CONTROL DE MOVIMIENTO DE ROBOT BÍPEDO UTILIZANDO MÉTODOS DE COMPUTACIÓN INTELIGENTE en la opción TESIS para optar por el grado académico de DOCTOR EN CIENCIAS consideramos que reúne los requisitos de calidad y otorgamos nuestro voto aprobatorio para proceder a la segunda etapa del examen profesional.

A T E N T A M E N T E
Tijuana, B. C., a 9 de diciembre de 2015

Oscar Castillo

DR. OSCAR CASTILLO LÓPEZ
Presidente

C.c.p. Mtra. Nayelli Salazar Piñón.- Jefa del Depto. de Servicios Estudiantiles y Gestión Escolar-Tijuana
C.c.p. expediente

FACULTAD DE CIENCIAS QUÍMICAS E INGENIERÍA

DR. LUIS ENRIQUE PALAFOX MAESTRE
DIRECTOR DE LA FAC. DE CS. QCAS. E INGENIERÍA
P R E S E N T E :

Una vez revisado el trabajo que presenta la **M.C. SELENE LILETTE CÁRDENAS MACIEL** correspondiente al tema: CONTROL DE MOVIMIENTO DE ROBOT BÍPEDO UTILIZANDO MÉTODOS DE COMPUTACIÓN INTELIGENTE en la opción TESIS para optar por el grado académico de DOCTOR EN CIENCIAS consideramos que reúne los requisitos de calidad y otorgamos nuestro voto aprobatorio para proceder a la segunda etapa del examen profesional.

A T E N T A M E N T E
Tijuana, B. C., a 9 de diciembre de 2015

DR. LUIS TUPAK AGUILAR BUSTOS
Secretario

C.c.p. Mtra. Nayelli Salazar Piñón.- Jefa del Depto. de Servicios Estudiantiles y Gestión Escolar-Tijuana
C.c.p. expediente

FACULTAD DE CIENCIAS QUÍMICAS E INGENIERÍA

DR. LUIS ENRIQUE PALAFOX MAESTRE
DIRECTOR DE LA FAC. DE CS. QCAS. E INGENIERÍA
P R E S E N T E :

Una vez revisado el trabajo que presenta la **M.C. SELENE LILETTE CÁRDENAS MACIEL** correspondiente al tema: CONTROL DE MOVIMIENTO DE ROBOT BÍPEDO UTILIZANDO MÉTODOS DE COMPUTACIÓN INTELIGENTE en la opción TESIS para optar por el grado académico de DOCTOR EN CIENCIAS consideramos que reúne los requisitos de calidad y otorgamos nuestro voto aprobatorio para proceder a la segunda etapa del examen profesional.

A T E N T A M E N T E
Tijuana, B. C., a 9 de diciembre de 2015

DR. ANTONIO RODRÍGUEZ DÍAZ
Sinodal

C.c.p. Mtra. Nayelli Salazar Piñón.- Jefa del Depto. de Servicios Estudiantiles y Gestión Escolar-Tijuana
C.c.p. expediente

FACULTAD DE CIENCIAS QUÍMICAS E INGENIERÍA

DR. LUIS ENRIQUE PALAFOX MAESTRE
DIRECTOR DE LA FAC. DE CS. QCAS. E INGENIERÍA
P R E S E N T E :

Una vez revisado el trabajo que presenta la **M.C. SELENE LILETTE CÁRDENAS MACIEL** correspondiente al tema: CONTROL DE MOVIMIENTO DE ROBOT BÍPEDO UTILIZANDO MÉTODOS DE COMPUTACIÓN INTELIGENTE en la opción TESIS para optar por el grado académico de DOCTOR EN CIENCIAS consideramos que reúne los requisitos de calidad y otorgamos nuestro voto aprobatorio para proceder a la segunda etapa del examen profesional.

A T E N T A M E N T E
Tijuana, B. C., a 9 de diciembre de 2015

DRA. ELBA PATRICIA MELIN OLMEDA
Sinodal

C.c.p. Mtra. Nayelli Salazar Piñón.- Jefa del Depto. de Servicios Estudiantiles y Gestión Escolar-Tijuana
C.c.p. expediente

FACULTAD DE CIENCIAS QUÍMICAS E INGENIERÍA

DR. LUIS ENRIQUE PALAFOX MAESTRE
DIRECTOR DE LA FAC. DE CS. QCAS. E INGENIERÍA
P R E S E N T E :

Una vez revisado el trabajo que presenta la **M.C. SELENE LILETTE CÁRDENAS MACIEL** correspondiente al tema: CONTROL DE MOVIMIENTO DE ROBOT BÍPEDO UTILIZANDO MÉTODOS DE COMPUTACIÓN INTELIGENTE en la opción TESIS para optar por el grado académico de DOCTOR EN CIENCIAS consideramos que reúne los requisitos de calidad y otorgamos nuestro voto aprobatorio para proceder a la segunda etapa del examen profesional.

A T E N T A M E N T E
Tijuana, B. C., a 9 de diciembre de 2015

DR. GUILLERMO LICEA SANDOVAL
Presidente

C.c.p. Mtra. Nayelli Salazar Piñón.- Jefa del Depto. de Servicios Estudiantiles y Gestión Escolar-Tijuana
C.c.p. expediente

FACULTAD DE CIENCIAS QUÍMICAS E INGENIERÍA

DR. LUIS ENRIQUE PALAFOX MAESTRE
DIRECTOR DE LA FAC. DE CS. QCAS. E INGENIERÍA
P R E S E N T E :

Una vez revisado el trabajo que presenta la **M.C. SELENE LILETTE CÁRDENAS MACIEL** correspondiente al tema: CONTROL DE MOVIMIENTO DE ROBOT BÍPEDO UTILIZANDO MÉTODOS DE COMPUTACIÓN INTELIGENTE en la opción TESIS para optar por el grado académico de DOCTOR EN CIENCIAS consideramos que reúne los requisitos de calidad y otorgamos nuestro voto aprobatorio para proceder a la segunda etapa del examen profesional.

A T E N T A M E N T E
Tijuana, B. C., a 9 de diciembre de 2015

DR. JUAN RAMÓN CASTRO RODRÍGUEZ
Suplente

C.c.p. Mtra. Nayelli Salazar Piñón.- Jefa del Depto. de Servicios Estudiantiles y Gestión Escolar-Tijuana
C.c.p. expediente

TESIS DEFENDIDA POR

Selene Lilette Cárdenas Maciel

Y APROBADA POR EL SIGUIENTE COMITÉ

Dr. Oscar Castillo López

Director del Comité

Dr. Luis Tupak Aguilar Bustos

Director del Comité

Dr. Antonio Rodríguez Díaz

Miembro del Comité

Dra. Elba Patricia Melín Olmeda

Miembro del Comité

Dr. Guillermo Licea Sandoval

Miembro del Comité

Enero de 2016

Universidad Autónoma de Baja California

MAESTRÍA Y DOCTORADO EN CIENCIAS E INGENIERÍA

CONTROL DE MOVIMIENTO DE ROBOT BÍPEDO UTILIZANDO MÉTODOS DE COMPUTACIÓN INTELIGENTE

TESIS

que para obtener el grado de

DOCTOR EN CIENCIAS

Presenta:

SELENE LILETTE CÁRDENAS MACIEL

Director:

Dr. Oscar Castillo López

Co-Directores:

Dr. Luis Tupak Aguilar Bustos **Dr. Guillermo Licea Sandoval**

Tijuana, Baja California, México, Enero de 2016

RESUMEN de la tesis de **SELENE LILETTE CÁRDENAS MACIEL**, presentada como requisito parcial para la obtención del grado de DOCTOR EN CIENCIAS. Tijuana, Baja California, Enero de 2016.

CONTROL DE MOVIMIENTO DE ROBOT BÍPEDO UTILIZANDO MÉTODOS DE COMPUTACIÓN INTELIGENTE

Resumen aprobado por:

Dr. Oscar Castillo López	Dr. Luis Tupak Aguilar Bustos
Director de Tesis	Director de Tesis

Esta tesis presenta contribuciones en control de movimientos de caminata en un robot bípedo con grado de subactuación uno. Métodos de computación inteligente son utilizados para determinar movimientos de caminata periódica y para diseñar un controlador retroalimentado. El caso de estudio considera movimientos de caminata periódica para un robot bípedo de tres enlaces que no presenta actuación en el torso. Los movimientos periódicos deseados son descritos como polinomios parametrizados por una coordenada de configuración del robot. El problema consiste en el diseño de un controlador que realice seguimiento de las trayectorias de salida que contiene en su definición los polinomios que representan el movimiento deseado. Los resultados de simulación del sistema en lazo cerrado verifican que la ley de control permite realizar estabilización a una órbita.

Palabras Clave: Robot bipédo, control de caminata, movimientos periódicos, sistemas difusos, ANFIS, algoritmos genéticos.

ABSTRACT of the thesis presented by **SELENE LILETTE CÁRDENAS MACIEL**, in partial fulfillment of the requirements of the degree of DOCTOR IN SCIENCES. Tijuana, Baja California, Enero de 2016.

MOTION CONTROL OF BIPED ROBOT USING COMPUTATIONAL INTELIGENCE METHODS

This thesis presents contributions to the walking control problem for a biped robot with one degree of underactuation. Computational intelligent methods are considered to obtain periodic walking motions and for designing a walking motion feedback controller. As a case of study is considered the problem of producing periodic walking motions in a three-link biped robot with underactuation at torso. The periodic motions reference are described by configuration coordinate parameterized-polynomials. The problem consists in the controller design for output trajectory tracking such that outputs definitions are the polynomials which represents desired motion. The closed-loop system simulation results shows that control law enables to perform orbit stabilization.

Keywords: Biped robot, walking control, periodic motions, fuzzy systems, ANFIS, genetic algorithm.

A Zohe y Nohé.

Agradecimientos

A mi familia.

A mis directores de tesis: Dr. Oscar Castillo López y Dr. Luis Tupak Aguilar Bustos.

A Universidad Autónoma de Baja California.

En especial al pueblo de México por financiar mis estudios a través de CONACyT.

Contenido

Contenido (continuación)

Lista de Figuras

Figura Página

Lista de Figuras (continuación)

Figura Página

Lista de Tablas

Capítulo 1

Introducción

Los robots caminantes han capturado el interés de los investigadores desde hace medio siglo debido a que tienen una estructura que permite mejor desplazamiento en ambientes pocos estructurados, si se compara con los robots móviles. En particular para robots caminantes con dos piernas también conocidos como robots bípedos, su estructura frecuentemente consiste en enlaces y articulaciones con o sin actuadores que implican que la dinámica de esta estructura cuando se mueve sea modelada a través de ecuaciones matemáticas altamente no lineales, que incluyen eventos discretos asi como grados de libertad subactuados que se forman debido a las interacciones de los extremos de las piernas con la superficie. Esto agrega dificultades al diseñar algoritmos de control que permitan asignar y dirigir de manera exitosa el movimiento de estos mecanismos, al imponer requisitos que el algoritmo de control debe satisfacer para preservar la configuración que mantiene la estructura estable mientras ejecuta el movimiento.

Para asegurar que los movimientos conservan la estructura estable se utilizan diferentes enfoques:

- Mantener la proyección del centro de masa del robot dentro del polígono de soporte que esta conformado por los pies, lo que produce movimientos de caminata a baja velocidad;

- Satisfacer que el punto en donde las fuerzas de reacción cuando el pie está en contacto con el suelo no produzcan momento (punto de momento cero - PMC)(Vukobratovic y Juricic (1969)), esta idea ha permitido a los robots realizar movimientos de manera versátil, pero el gasto de energía es considerable (Kuo (2007));

- Producir movimientos en el robot que muestran un patrón cíclico, nombrado como *limit cycle walking*. Un ejemplo representativo que obtiene esta clase de movimientos es el trabajo realizado por (McGeer (1990)) al colocar un robot (sin actuadores) en una pendiente y logra la caminata mientras baja la pendiente utilizando solamente la fuerza de gravedad.

Obtener movimientos periódicos no es una actividad trivial, pues su representación formal se establece como órbitas periódicas en las variables del modelo, y el algoritmo de control debe ser capaz de llevar al sistema, a producir el comportamiento descrito por la órbita. Este proceso regularmente inicia determinando aquellos movimientos que son factibles de llevarse a cabo por el sistema definidos como una función en el tiempo (planeación de movimiento o trayectorias), y posteriormente obtener la ley de control para que produzca el movimiento establecido (seguimiento de trayectorias).

Se han aplicado metodologías de control moderno en estos temas. Sin embargo, otras contribuciones que difieren en realizar seguimiento de esta forma de trayectorias fueron reportadas en (Canudas-de Wit *et al.* (2002)), (Shiriaev *et al.* (2005)) y (Aguilar *et al.* (2009)), donde establecen una metodología para el diseño de controladores para mecanismos con grado de subactuación uno que forzan a mostrar movimientos periódicos sin requerir de una trajectoria de referencia, que después es probada para robots bípedos en (Canudas-de Wit (2004)), (Mettin *et al.* (2007)) y (La Hera *et al.* (2013)). En (Grizzle *et al.* (2001)) se muestra la síntesis del controlador para un robot bípedo, demostrando estabilidad orbital a través de extensiones de la teoría de Poincaré para modelos que incluye el efecto de impulsos. El método linealización por retroalimentación parcial se utiliza en (Grizzle *et al.* (2005)) para sistemas subactuados que tienen una articulación subactuada cíclica, dentro de su análisis muestran la construcción de funciones de salida que al introducirla en la retroalimentación propician un seguimiento asintótico de la trayectoria de la salida. Mientras que en (Wang y Chevallereau (2011)) reportan un controlador variante en el tiempo que resuelve el problema de seguimiento de trayectorias, el controlador modifica los eigen valores del mapa de Poincaré linealizado tal que garantiza que la caminata en un robot bípedo sea estable.

Existe una vasta cantidad de publicaciones donde los métodos de computación inteligente tienen una intervención en la síntesis de caminata (planeación de movimiento) y en el diseño de controladores para robots humanoides como lo muestra (Katic y Vukobratovic (2003)) en su artículo de revisión y otras citas hechas en los capítulos 4 y 5 de este documento. Las contribuciones de estos últimos autores es que utilizan el enfoque de PMC como componente importante en su diseño, los sistemas robóticos son actuados en sus articulaciones y el algoritmo de control no refieren que esta diseñado para producir movimiento cíclico.

1.1 Descripción del problema

Esta tesis trata el uso de métodos de computación inteligente para producir movimiento coordinado de caminata periódica en un robot bípedo subactuado, sin pies, donde la caminata se representa por un modelo híbrido continuo-discreto. Este modelo fue empleado para determinar movimientos de caminata periódica estable.

1.2 Objetivos

- Diseñar de una ley de Control Inteligente, tal que un robot bípedo de cinco grados de libertad siga una trayectoria predefinida, para producir movimiento coordinado.
- Análizar y diseñar un controlador Inteligente en Sistemas Complementarios.

1.3 Meta

Proporcionar una ley de control inteligente que realice estabilización orbital de un robot bípedo de cinco grados de libertad.

1.4 Organización del documento

El resto del documento se organiza como sigue. En el Capítulo 2 presenta las definiciones y métodos de computación inteligente involucrados en el trabajo de tesis. En el Capítulo 3 se describe el robot bípedo de tres enlaces, las suposiciones de movimiento del robot y muestra el modelo matemático que rige su dinámica. La estrategia de solución para obtener movimientos de caminata periódica para el robot bípedo y resultados se muestran en el Capítulo 4. En el Capítulo 5 se describe la estrategia para la síntesis del controlador de caminata y presenta los resultados a nivel simulación obtenidos. Algunos comentarios a manera de conclusión e ideas relacionadas a problemas por resolver a futuro son establecidas en Capítulo 6.

Capítulo 2

Teoría sobre Computación Inteligente

En este capítulo se presentan las definiciones y descripción sucinta de los modelos de computación inteligente que serán empleados en capítulos posteriores. El contenido de este capítulo trata sobre

- Conjuntos difusos.
- Sistemas difusos.
- Algoritmos genéticos.
- Sistemas Neuro-difusos.

2.1 Modelos de Computación Inteligente

2.1.1 Conjuntos y sistemas difusos

Conjuntos y sistemas difusos tipo-1

Un ***conjunto difuso tipo-1***, denotado A es caracterizado por pares $(x, \mu_A(x))$ el cual se define

$$A = \{(x, \mu(x)) | \forall x \in X\} \tag{2.1}$$

donde $\mu_A(x)$ es una función $\mu : \Re \rightarrow [0, 1]$ que mapea cada número $x \in X$ a un valor entre 0 y 1, a esta función es llamada *función de membresia tipo-1*, la cual asocia a cada elemento x un grado de pertenencia al conjunto A.

De allí la diferencia con un conjunto tradicional donde solo existe un grado de pertenencia 0 o 1, y por ende, las generalizaciones a las operaciones clásicas de teoría de conjuntos y de la teoría de Lógica que permiten crear los sistemas de inferencia difusa , cuyo tratamiento detallado se encuentra en (Zadeh (1965)), (Zadeh (1973)), (Zadeh (1975a)), (Zadeh (1975b)) y (Zadeh (1996)).

Los ***sistemas difusos tipo-1*** conocidos tambien como sistemas de inferencia difusa o modelos difusos, contempla la aplicación de la teoría de conjuntos difusos y lógica difusa para realizar modelos de razonamiento aproximado, que involucra una función que mapea de un espacio n-dimensional U a otro espacio m-dimensional W. Los sistemas difusos que reportan frecuentemente son el sistema difuso de Mamdani (Mamdani y Assilian (1975), Mamdani (1976)); el sistema difuso de Takagi-Sugeno-Kang (TSK) conocido también como sistema difuso de Sugeno (Takagi y Sugeno (1985), Sugeno y Kang (1988)); el sistema difuso de Tsukamoto (Tsukamoto (1979)).

La estructura básica conceptual del sistema difuso tipo-1 (véase Figura 2.1) consta de: una *base de reglas difusas*; un método de *fusificación* que toma números reales y le asocia un valor de membresía considerando los conjuntos difusos definidos; un *mecanismo de razonamiento* que realiza el proceso de inferencia y un método de *defusificación* que transforma conjuntos difusos a números reales.

Cada regla de la base de reglas difusas se denota como sigue:

$$\begin{array}{lll} R^l\text{:} & \text{IF} & x_1 \text{ is } A_{1,i} \text{ AND } x_2 \text{ is } A_{2,i} \text{ AND ... } x_n \text{ is } A_{j,i} \\ & \text{THEN} & u_l = f(x_1, x_2, \ldots, x_n). \end{array} \tag{2.2}$$

La regla difusa tiene la forma IF *antecedente* THEN *consecuente.* En el antecedente se colocan las variables de entrada $(x_1, \ldots, x_n)$, los conjuntos difusos $(A_{1,i}, \ldots, A_{j,i})$

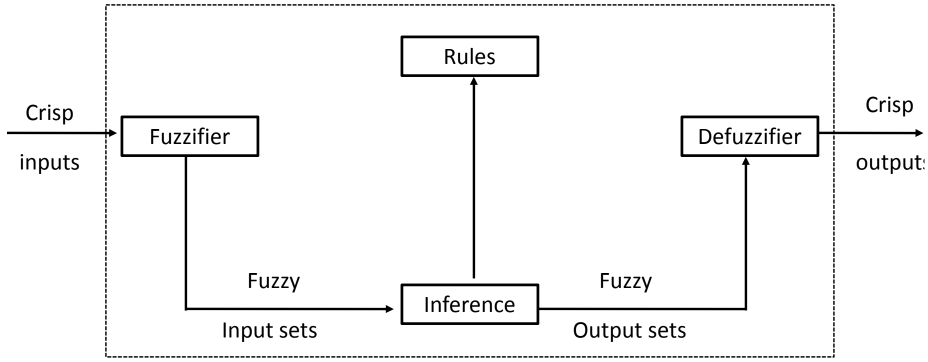

Figura 2.1. Sistema de inferencia difusa tipo-1 (Mendel (2001)).

conectados a través de operadores de conjuntos difusos (AND - unión), donde $A_{j,i} \subset U_j$, $j = 1, 2, \ldots, n$, las cuales forman al aplicarse las operaciones de conjuntos difusos una *relación difusa* $U = U_1 \times U_2 \times \cdots \times U_n$. En el consecuente se expresan las variables de salida ($u \subset W$) la cuales estan expresadas como una función matemática en términos de las variables de entrada, la regla difusa expresada en (2.2) se utiliza en el sistema difuso de TSK. Entonces el mecanismo de inferencia, aplica la teoría de razonamiento aproximado (Zadeh (1973)) para realizar el mapeo del espacio U al espacio W para toda la base de reglas.

Los métodos de defusificación varian de acuerdo al tipo de sistema difuso. Para el sistema difuso de Sugeno no se aplica un método de defusificación debido a que en el consecuente de cada regla difusa no se tiene conjuntos difusos. El operador de agregación que permite obtener la salida del sistema difuso se realiza como un promedio ponderado que se define como

$$u = \frac{\sum_{k=1}^{l} \omega_k u_k}{\sum_{k=1}^{l} \omega_k} \tag{2.3}$$

donde u_k se determina por la función f dada en (2.2), $k = 1, 2, \ldots, l$ representa el número de regla difusa y ω_k es la fuerza de disparo del antecedente de cada regla difusa.

2.1.2 Algoritmos genéticos

Los Algoritmos Genéticos (AGs) son algoritmos de búsqueda basado en los principios de selección y genética natural, estos algoritmos son inicialmente propuestos por Holland (1975), y han sido aplicados para resolver problemas de optimización pues difieren de métodos de optimización tradicional en que: (i) utilizan información basada en una función objetivo, no estan basados en derivadas, (ii) tienen una codificación de parámetros, utilizan reglas probabilísticas como una herramienta para guiar la búsqueda (Michalewicz (1994)).

La idea principal del AG es mantener un grupo de soluciones (*población de individuos*) dentro un proceso que imita los principios en los cual esta basado, lo cual produce competencia y una variación controlada de las soluciones que junto con ciertas heurísticas producen con el tiempo soluciones más adecuadas para resolver el problema.

La implementación del AG inicia con la elección de las variables de decisión para resolver el problema, las cuales son entonces llevada a una *representación codificada* que sirve como plantilla para formar los *individuos*, que son la versión codificada de las soluciones al problema; se construye una *función objetivo* que toma la codificación del individuo y la transforma en un valor numérico llamado *aptitud*, que indica que tan apta es la solución para resolver el problema; se crean los individuos de acuerdo a la plantilla mencionada y se lleva a cabo el proceso de evolución de los individuos.

El proceso evolutivo que imita el AG se puede describir por una secuencia de etapas que suceden de manera iterada: en la ***inicialización*** se crea de forma aleatoria un grupo de individuos (*población*) con la representación elegida; en la etapa de ***selección***, se evalua cada individuo mediante la *función objetivo* y se elige mediante un método que incluye reglas probabilísticas un subconjunto de individuos, por lo que los que tienen mayor *aptitud* tienen mayor posibilidad de ser elegidos que los que tienen menor *aptitud*; enseguida los individuos seleccionados se someten a la ***reproducción*** que se denota mediante las operaciones de *cruce* y *mutación* cuya aplicación se basa en probabilidades, la primera operación se da una combinación de porciones de la representación codificada de pares de individuos obteniendose dos nuevos individuos, la segunda operación introduce una alteración dentro de una porción de la representación de un individuo; después se construye una población considerando los individuos que resultan de la reproducción y los individuos que son los progenitores, esta etapa se le conoce como ***reemplazo***. La secuencia de etapas de selección - reproducción, se le conoce como *generación*, por lo que el resultado de realizar el proceso evolutivo es un conjunto de individuos que satisfacen de la mejor manera a los requisitos especificados en la función objetivo y al menos uno es la mejor solución. Esta explicación se expresa en forma resumida a través del siguiente algoritmo

Algoritmo

1. Inicio
2. $i \leftarrow 0$
3. Crea una población P_i de N individuos
4. Evalua la aptitud de los individuos de la población: $P_i^e \leftarrow Fitness(P_i)$
5. Repite los siguientes pasos hasta que las condiciones establecidas se satisfacen

(a) `Selecciona los individuos para reproducción:` $P_i^s \leftarrow Select(P_i, P_i^e)$

(b) `Aplica cruce y mutación:` $P_i^g \leftarrow Genetic\_Operation(P_i^s)$

(c) $i \leftarrow i+1$

(d) `Crea nueva población:` $P_i \leftarrow Replacement(P_i^g, P_{i-1})$

(e) `Evalua aptitud de los individuos de la población:` $P_i^e \leftarrow Fitness(P_i)$

6. `Muestra el mejor individuo`

7. `Fin`

2.2 Sistemas Neuro-Difusos

2.2.1 Redes Adaptativas

Es una estructura de red que contiene *nodos* conectados a través de *enlaces direccionales* que especifican las relaciones causales entre los nodos conectados. La característica de adaptación se debe a que cada nodo esta compuesto de *parámetros* que son modificables a través de una *regla de aprendizaje*, lo cual permiten modelar un sistema ajustando los parámetros de cada nodo en la red teniendo conocimiento de datos de las variables de entrada y salida (*datos de entrenamiento*).

La señal de salida de un nodo $x_{l,i}$ de una red con propagación hacia adelante que esta compuesta de L capas y cada capa l tiene $N(l)$ nodos, se define mediante una función nodo que depende de las señales de entrada y un conjunto de parámetros del nodo como

$$x_{l,i} = f_{l,i}(x_{l-1,1}, \ldots, xl-1, N(l-1), \alpha, \beta, \gamma, \ldots), \tag{2.4}$$

donde α, β, γ son los parámetros del nodo.

Proporcionando el conjunto de datos de entrenamiento como una matriz de P renglones, considerando cada renglón como un vector, se define la medida de error

$$E_p = \sum_{k=1}^{N(L)} (d_k - x_{L,k})^2, \tag{2.5}$$

donde E_p representa la suma de los errores al cuadrado, donde el error se determina como la diferencia entre cada componente del p-esimo vector de salida deseado y cada componente del vector de salida proporcionado por los nodos de la red en su última capa, al introducir los datos de entrenamiento del p-esimo vector. La medición del error total se define como sigue

$$E = \sum_{p=1}^{P} E_p \tag{2.6}$$

que lleva a un problema de minimización de E, que requiere la adaptación de los parámetros de cada nodo, mediante la *regla de aprendizaje de retropropagación* (Rumelhart *et al.* (1986), que determina un vector gradiente definido como la derivada de la medida del error con respecto a cada parámetro, es decir

$$\frac{\partial^+ E_p}{\partial \alpha} = \frac{\partial^+ E_p}{\partial x_{l,i}} \frac{\partial^+ f_{l,i}}{\partial \alpha} = \epsilon_{l,i} \frac{\partial^+ f_{l,i}}{\partial \alpha}, \tag{2.7}$$

donde $\epsilon_{l,i}$ es la señal de error del i-esimo nodo de la l-ésima capa (Werbos (1974)) y se define

$$\epsilon_{l,i} = \sum_{m=1}^{N(l+1} \frac{\partial^+ E_p}{\partial x_{l+1,m}} \frac{\partial^+ f_{l+1,m}}{\partial x_{l,i}} = \sum_{m=1}^{N(l+1} \epsilon_{l+1,m} \frac{\partial^+ f_{l+1,m}}{\partial x_{l,i}}, \tag{2.8}$$

con $0 \leq l \leq L-1$ y cuando se quiere obtener la señal de error en un nodo de la última capa $\epsilon_{L,i} = \frac{\partial^+ E_p}{\partial x_{L,i}} = \frac{\partial E_p}{\partial x_{L,i}}$.

La derivada de la medida del error total E con respecto a α es

$$\frac{\partial^+ E}{\partial \alpha} = \sum_{p=1}^{P} \frac{\partial^+ E_p}{\partial \alpha}. \tag{2.9}$$

A través del método de paso descendente, se determina la actualización de los parámetros α utilizando la siguiente expresión

$$\Delta\alpha = -\eta \frac{\partial^+ E}{\partial \alpha}, \tag{2.10}$$

donde η es la tasa de aprendizaje, que varia la velocidad de convergencia y se define

$$\eta = \frac{\kappa}{\sqrt{\sum_\alpha (\frac{\partial E}{\partial \alpha})^2}}, \tag{2.11}$$

y κ es el tamaño de paso.

2.2.2 Sistemas de inferencia Neuro-Difusa Adaptativa (ANFIS)

ANFIS es una clase de red neuronal adaptativa, la diferencia con respecto a una red neuronal tradicional estriba en como esta definida la estructura (*arquitectura*) de la red, la función que tienen los nodos en cada capa y la regla de aprendizaje. Este modelo de red neuronal fue propuesta por (Jang (1993)) con el propósito de incorporar las capacidades de las metodologías de Sistemas difusos y Redes Neuronales Artificiales, la cual permite obtener un modelo difuso a partir de datos de entrada y salida del sistema.

La arquitectura de ANFIS consiste en cinco capas y se tiene que un nodo puede tener una familia de funciones dependiendo de la capa en la que es ubicado.

Capa 1

Cada nodo de esta capa es adaptativo, su función de nodo es

$$O_i^1 = \mu_{A_i}(x), \tag{2.12}$$

donde el subindice i indentifica al nodo, x es la entrada al nodo y A_i es la etiqueta lingüística asociada con el nodo. O_i^1 representa la función de membresía del conjunto difuso A_i, la salida de este nodo especifica el grado que la entrada x satisface el cuantificador A.

La funcion de membresía $\mu_{A_i}(x)$ puede ser parametrizada por

$$\mu_{A_i}(x) = \exp\{-\frac{1}{2}(\frac{x - c_i}{a_i})^2\}, \tag{2.13}$$

donde a_i y c_i son los *parámetros premisa.*

Capa 2

Los nodos en esta capa son fijos y estan etiquetados con Π, su salida es el producto de todas las señales entrantes. Considerando el caso base de definir dos variables lingüísticas A y B y a cada una le asociamos dos conjuntos difusos. Entonces la salida del i-ésimo nodo de esta capa es obtenida por

$$O_i^2 = w_i = \mu_{A_i}(x)\mu_{B_i}(y) \quad , \quad i = 1, 2. \tag{2.14}$$

Cada nodo representa la fuerza de disparo de una regla, que considerando el caso base corresponde a la fuerza de disparo de una regla que tiene como antecedente

$$\texttt{Si } x \texttt{ es } A_i \texttt{ y } y \texttt{ es } B_i.$$

Capa 3

Cada nodo en esta capa es un nodo fijo que es etiquetado con N. En este clase de nodos se calcula la razón de la fuerza de disparo de la i-ésima regla difusa a la suma de todas las fuerzas de disparo de las reglas difusas. La salida de esta capa se le conoce como *fuerza de disparo normalizada* $\bar{w}_i$, que para el caso base de tener dos variables con dos conjuntos difusos cada una de ellas, la expresión se define como

$$O_i^3 = \bar{w}_i = \frac{w_i}{\sum i w_i} \quad , \quad i = 1, 2. \tag{2.15}$$

Capa 4

Cada nodo de esta capa es adaptativo, su función de nodo en torno al caso base es

$$O_i^4 = \bar{w}_i f_i = \bar{w}_i (p_i x + q_i y + r_i), \quad i = 1, 2. \tag{2.16}$$

donde p_i, q_i, r_i son los parámetros del nodo, estos representan los parámetros del consecuente de una regla difusa que pertenece al modelo difuso de TSK, la cantidad de parámetros en el consecuente obedece a la cantidad de variables lingüísticas de entrada que estan ponderadas por la fuerza de disparo que se produjo en el antecedente de la regla difusa.

Capa 5

Contiene solo un nodo fijo que es etiqueta con Σ, pues calcula la suma de todas las señales que provienen de la capa anterior, esto se expresa como

$$O_i^5 = \sum_i \bar{w}_i f_i = \frac{\sum_i w_i f_i}{\sum_i w_i}. \tag{2.17}$$

En resumen, esta arquitectura de red tiene implicita en su definición un sistema difuso tipo TSK.

La *regla de aprendizaje* combina el método de paso descendente (método basado en gradiente) y estimación de mínimos cuadrados que le permiten identificar los parámetros de la red (parámetros de los nodos de la capa uno y cuatro) que minimizan la métrica del error (2.6) que se describe en el mecanismo de adaptación que se describe en el inicio de esta sección. La generalización de la arquitectura solo implica el aumento del número de nodos que inicia desde la primer capa. El proceso iterativo de adaptación proporciona como resultado los parámetros de un modelo difuso Takagi-Sugeno. Si se asume que el modelo contiene variables de entrada x_1, x_2,..., x_j y variables de salida u_1, u_2,...,u_k sus reglas toman la forma

$$
\begin{array}{lll}
R^l\text{:} & \text{If} & x_1 \text{ is } A_{1,i} \text{ and } x_2 \text{ is } A_{2,i} \text{ and ... } x_j \text{ is } A_{j,i} \\
 & \text{Then} & u_1 = G(x_1, ..., x_j; p_{1,1}, p_{1,2}, ..., p_{1,j}, p_{1,j+1}) \\
 & & \text{and ... and} \\
 & & u_k = G(x_1, ..., x_j; p_{k,1}, p_{k,2}, ..., p_{k,j}, p_{k,j+1}),
\end{array}
\tag{2.18}
$$

donde $A_{j,i}$ con $i = 1, 2, ..., m_1$ y $j = 1, 2, ...m_2$, son el $i$ésimo conjunto difuso de la j-ésima variable de entrada; u_k con $k = 1, 2, ..., m_3$, es el consecuente representado como una función no difusa continua en términos de las entradas con $k(j + 1)$ parámetros p.

Capítulo 3

Robots Bípedos

En este capítulo se introduce el modelo dinámico que describe la **caminata** del robot bípedo el cual es utilizado para realizar las verificaciones numéricas de este trabajo. Se inicia estableciendo la nomenclatura necesaria, posteriormente se menciona brevemente suposiciones bajo las cuales se deduce el modelo del robot bípedo para concluir su expresión matemática.

3.1 Nomenclatura

Un robot bípedo es una cadena cinemática que esta formada principalmente de dos subcadenas que representan las piernas y una subcadena denominada torso, las cuales estan conectadas a través de la cadera. La locomoción del robot bípedo esta asociada principalmente a las fuerzas inducidas a través de los actuadores en el robot y las interacciones del robot con su entorno, donde la interacción con el entorno es considerada como el contacto de las piernas del robot con el suelo o superficie. Cuando una de las piernas esta en contacto con el suelo se le conoce como *pierna de soporte* y a la otra pierna se le llama *pierna en balanceo*.

La caminata en su forma básica se describe a través de la ***fase de soporte doble*** donde ambos pies tienen contacto con la superficie; y la ***fase de soporte simple*** o *fase libre* donde solo un pie presenta contacto con el suelo mientras la otra pierna presenta movimiento hacia el frente sin tocar la superficie. Entonces, la ***caminata*** se define como la alternancia de fases de soporte simple y doble.

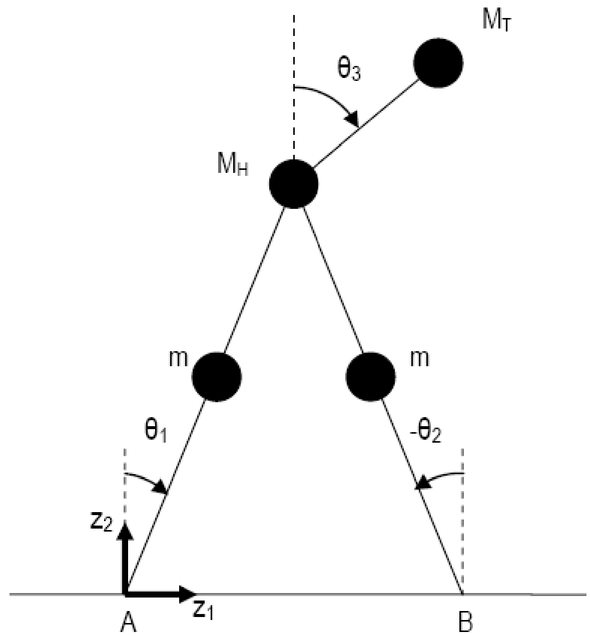

Figura 3.1. Robot bípedo de tres enlaces.

El *plano sagital* es el plano longitudinal que divide un objeto en sección derecha y sección izquierda. El *plano frontal* es el plano paralelo al eje longitudinal del objeto y perpendicular al plano sagital, el cual separa al objeto en porción delantera y trasera.

3.2 Robot Bípedo

En este trabajo, el robot bípedo es planar. El robot esta formado de un torso, cadera y dos piernas de longitud idéntica, sin pies, no tiene rodillas, ni tobillos. Las masas de los enlaces se consideran que estan concentradas, cada una en una parte de cada enlace. Un par es aplicado entre el torso y la pierna de soporte, el otro par es aplicado entre el torso y la pierna en balanceo. La definición de las coordenadas angulares y la disposición de la masa de los enlaces se muestran en la Figura 3.1. Los ángulos positivos se determinan en el sentido de las manecillas del reloj con respecto a la línea vertical.

3.2.1 Suposiciones del movimiento del robot bípedo

Las suposiciones relacionadas al movimiento del robot bípedo son: la caminata se restringe para llevarse a cabo en el plano sagital y a nivel del suelo; en la fase de soporte simple, la pierna de soporte se comporta como un pivote ideal y la pierna en balanceo inicia su movimiento por detrás de la pierna de soporte, continua el movimiento hacia delante hasta que sucede la fase de soporte doble la cual es instantánea.

Debido a que el robot bípedo tiene piernas de igual longitud y no tiene rodillas, en algún momento de la fase de soporte simple la pierna en balanceo puede arrastrarse y presentar contacto con el suelo. Para evitar este inconveniente, se supone que la pierna en balanceo se mueve hacia el plano frontal y retorna al plano de movimiento cuando el ángulo de la pierna de soporte alcanza un valor deseado (McGeer (1990)).

3.3 Modelo Dinámico

Tomándose en cuenta las suposiciones de movimiento del robot bípedo, el modelo dinámico que describe la caminata del robot bípedo comprende un modelo continuo que representa la fase de soporte simple y un modelo que corresponde al evento de contacto de la pierna en balanceo con el suelo.

3.3.1 Modelo de la fase de soporte simple

El modelo del robot durante la fase de soporte simple es un sistema de ecuaciones diferenciales de segundo orden obtenido de la aplicación del método de Euler-Lagrange (Kelly *et al.* (2005)), cuya representación matricial es

$$M(\theta)\ddot{\theta} + C(\theta,\dot{\theta})\dot{\theta} + G(\theta) = Bu, \tag{3.1}$$

donde $\theta = [\theta_1, \theta_2, \theta_3]^T$ representa a las coordenadas angulares, de las cuales θ_1 parametriza a la pierna de soporte, θ_2 a la pierna en balanceo y θ_3 al torso; $u = [u_1, u_2]^T$ es el vector de entrada.

Su representación en espacio de estados, queda como sigue

$$\begin{aligned} \dot{x} &:= \frac{d}{dt}\begin{bmatrix} \theta \\ \dot{\theta} \end{bmatrix} = \begin{bmatrix} \dot{\theta} \\ M^{-1}(\theta)[-C(\theta,\dot{\theta})\dot{\theta} - G(\theta)] \end{bmatrix} + \begin{bmatrix} 0 \\ M^{-1}(\theta)B \end{bmatrix} u, \\ &:= f(x) + g(x)u. \end{aligned} \tag{3.2}$$

donde $x = [\theta, \dot{\theta}]^T = [\theta_1, \theta_2, \theta_3, \dot{\theta}_1, \dot{\theta}_2, \dot{\theta}_3]^T$.

3.3.2 Modelo de Impacto

Un impacto ocurre cuando la pierna en balanceo tiene contacto con el suelo, lo cual lleva al inicio de la fase de soporte doble. El modelo que representa el impacto es debido a (Hurmuzlu y Marghitu (1994)), quien lo modela como un contacto entre dos cuerpos rígidos. Las suposiciones que considera son:

1. el impacto sucede en un instante de tiempo infinitesimalmente pequeño;
2. el impacto no provoca que la pierna en balanceo deslice ni rebote;
3. en el momento del impacto, la pierna de soporte se levanta del suelo sin que exista interacción;
4. las fuerzas externas durante el impacto pueden representarse como impulsos;

5. las fuerzas impulsivas podrian producir un cambio instantáneo en las velocidades generalizadas pero las posiciones permanecen continuas;

6. los pares que provienen de los actuadores no son impulsivos.

El modelo permite calcular las velocidades angulares después de que sucede el impacto utilizando las velocidades de los extremos inferiores de las piernas y las fuerzas de reacción que resultan del contacto con el suelo. Considerando la suposición 3, las fuerzas de reacción de la pierna de soporte es cero por lo que las fuerzas de reacción consideradas incluyen solo las que produce la pierna en balanceo. Se definen como coordenadas generalizadas $\theta_e = [\theta_1, \theta_2, \theta_3, z_1, z_2]$ donde z_1 y z_2 representan las coordenadas cartesianas del extremo final de la pierna de soporte. Al aplicar el método de Euler-Lagrange se obtiene

$$M_e(\theta_e)\ddot{\theta}_e + C_e(\theta_e, \dot{\theta}_e)\dot{\theta}_e + G_e(\theta_e) = B_e(\theta_e)u + \delta F_{ext}, \tag{3.3}$$

donde δF_{ext} son las fuerzas externas que actuan en el robot cuando la pierna en balanceo tiene contacto con el suelo.

Al integrarse (3.3) sobre la duración del impacto se obtiene (Hurmuzlu y Marghitu (1994))

$$M_e(\theta_e^+)\dot{\theta}_e^+ - M_e(\theta_e^-)\dot{\theta}_e^- = F_{ext}, \tag{3.4}$$

donde $F_{ext} = \int_{t^-}^{t^+} \delta F_{ext}(\tau)d\tau$, $\dot{\theta}_e^-$ son las velocidades antes del impacto y $\dot{\theta}_e^+$ son las velocidades después del impacto. F_{ext} se calcula mediante

$$F_{ext} = E_2(\theta_e)^T F_2, \tag{3.5}$$

$F_2 = [F_T, F_N]^T$ son las fuerzas tangenciales y normales aplicadas en el extremo de la pierna en balanceo, y

$$E_2 := \frac{\partial \Upsilon(\theta_e)}{\partial \theta_e} = \begin{bmatrix} r\cos(\theta_1) & -r\cos(\theta_2) & 0 & 1 & 0 \\ -r\sin(\theta_1) & r\sin(\theta_2) & 0 & 0 & 1 \end{bmatrix}, \tag{3.6}$$

donde

$$\Upsilon(\theta) := \begin{bmatrix} z_1 + r\sin(\theta_1) - r\sin(\theta_2) \\ z_2 + r\cos(\theta_1) - r\cos(\theta_2) \end{bmatrix} \tag{3.7}$$

denotan las coordenadas cartesianas del extremo final de la pierna en balanceo.

La suposición 2 considera que no existe deslizamiento ni rebote en la pierna en balanceo, esta se representa como

$$E_2(\theta_e)\dot{\theta}_e^+ = 0. \tag{3.8}$$

El conjunto de ecuaciones (3.4) y (3.8) producen

$$\begin{bmatrix} M_e & -E_2^T \\ E_2 & 0_{2\times 2} \end{bmatrix} \begin{bmatrix} \dot{\theta}_e^+ \\ F_2 \end{bmatrix} = \begin{bmatrix} M_e\dot{\theta}_e^- \\ 0_{2\times 1} \end{bmatrix}. \tag{3.9}$$

Debido a que $\theta_e^+ = \theta_e^-$ (suposición 5), las posiciones θ_e^+ y velocidades angulares $\dot{\theta}_e^+$ forman el vector x^- que es utilizado en la función $\Delta(x^-)$ la cual expresa el intercambio entre los roles de las piernas pues produce las nuevas condiciones iniciales $x^+ := [\theta^+, \dot{\theta}^+]$ (en términos de $x^- := [\theta^-, \dot{\theta}^-]$) para el modelo de la fase de soporte simple. Cabe señalar que x^- representa el límite por la izquierda y x^+ representa el límite por la derecha de las trayectorias del modelo de la fase de soporte simple. La función Δ se define como

$$x^+ = \Delta(x^-) := \begin{bmatrix} \theta_2^- & \theta_1^- & \theta_3^- & \dot{\theta}_2^+(x^-) & \dot{\theta}_1^+(x^-) & \dot{\theta}_3^+(x^-), \end{bmatrix}^T. \tag{3.10}$$

Para mayor detalle de la función véase (Grizzle *et al.* (2001)).

3.3.3 Modelo completo

El modelo en (3.11) describe el robot bípedo como un sistema que incorpora los efectos impulsivos a través de la unión del modelo de la fase de soporte simple y el modelo de impacto.

$$\Sigma : \begin{cases} \dot{x} = f(x) + g(x)u & x^- \notin \mathcal{S} \\ x^+ = \Delta(x^-) & x^- \in \mathcal{S} \end{cases}, \tag{3.11}$$

con

$$\mathcal{S} := \{x := (\theta, \dot{\theta}) \in \mathcal{X} | \theta_1 = \theta_1^d\}, \tag{3.12}$$

donde $\mathcal{S} \subset \mathcal{X}$ que se define como $\mathcal{X} := \{(\theta, \dot{\theta}) | \theta \in (-\pi, \pi)^3, \dot{\theta} \in \Re^3\}$ y θ_1^d es la posición angular deseada de la pierna de soporte.

Las trayectorias del modelo se obtienen mediante el modelo de la fase de soporte simple hasta que los estados del sistema alcanzan el conjunto $\mathcal{S}$ que representa la superficie o suelo (esto es cuando sucede el evento de impacto). El resultado del modelo de impacto proporciona la condicion inicial con la cual el modelo de la fase de soporte simple evoluciona hasta que ocurre el siguiente impacto.

Entonces, un *paso* es la solución de (3.11) donde el robot inicia en fase de soporte doble y termina en fase de soporte doble con la configuración de las piernas intercambiada y contiene solo un evento de impacto. Por tanto, la caminata es una sucesión de pasos.

Capítulo 4

Diseño de patrones de caminata del robot bípedo

En problemas de control de movimiento el esquema que frecuentemente se ha utilizado consiste en determinar una trayectoria de referencia que satisface los requerimientos del problema y después se diseña un controlador que se dedica a resolver el problema de seguimiento. Para el problema de locomoción de robots bípedos, la meta consiste en obtener un patrón de caminata (trayectoria de referencia) tal que permita que el robot bípedo ejecute pasos estables mientras satisface requisitos dados en términos de velocidad, longitud de paso, frecuencia de paso, consumo de energía entre otros. Los requerimientos del patrón de caminata a menudo llevan a formular la síntesis de patrones de caminata como un problema de optimización con restricciones que es resuelto numéricamente a través de herramientas de computo algebraico durante la etapa de diseño; o bien, utilizan algoritmos computacionales embebidos en el mecanismo que proveen la adaptación necesaria en tiempo de ejecución.

Las metodologías y/o enfoques aplicados en la síntesis de patrones de caminata son diversos. Una de ellas es el principio de Punto de Momento Cero (PMC - ZMP en inglés) propuesto por (Vukobratovic y Juricic (1969)) y utilizado como criterio de verificación de condiciones de estabilidad del robot bípedo en (Shih *et al.* (1990)), (Hirai *et al.* (1998)) y (Dasgupta y Nakamura (1999)), su estrategia consiste en calcular las trayectorias de PCM y ajustar los movimientos de las caderas y el torso del robot para que logren alcanzar dicha trayectoria. Mientras que en (Huang *et al.* (2001)) proponen un algoritmo que evita el cálculo a priori de las trayectorias de PMC, determina de forma iterativa los movimientos del pie y caderas mediante trazadores cúbicos tal que cumplen restricciones relacionadas con parámetros del robot, además, que las trayectorias satisfacen el principio de PMC y permanezcan dentro del margen de estabilidad. En (Denk y Schmidt (2003)) proponen un enfoque sistemático para diseño de una base de datos de patrones de caminata en donde utiliza técnicas de control óptimo e información de PMC para prevenir la rotación del pie y conservar la viabilidad de la caminata del robot bípedo. En (Kajita *et al.* (2003)) propone un controlador que permite el seguimiento de la trayectoria de PCM basádose en un modelo del péndulo invertido y la estrategia que le nombran control previo de PMC. En (Sato *et al.* (2011)) también utiliza PCM para planear movimientos que permitan subir las escaleras.

Si el esquema de solución elegida es a través de optimización, la formulación del problema no es única. Las diferencias suelen presentarse desde las variables elegidas, los criterios que se evaluan en la función de costo, que estan sujetas a la información disponible acerca del robot. Métodos de computación inteligente han sido utilizados en (Vundavilli y Pratihar (2010)), donde incorporan redes neuronales artificiales (RNA), lógica difusa (LD) y un algortimo genético (AG) para obtener movimientos de caminata, ascenso y descenso de escaleras. En el caso de (Choi *et al.* (1999)) utilizan un AG para determinar las trajectorias de las velocidades y aceleraciones del ZMP que proporcionan una caminata estable y suave. En (Capi *et al.* (2001)) proponen un AG para generar trayectorias de las articulaciones para ejecutar movimientos de caminata, subir y bajar escaleras, con el objetivo de obtener trayectorias con la menor energía consumida y la menor variación en los pares. En (Lee y Lee (2004)) se lleva la formulación del problema de generación de trayectorias como un problema de optimización con múltiples objetivos, aplica un algoritmo evolutivo y criterio de Optimalidad de Pareto para determinar parámetros que definen distancia y orientación de las coordenadas de la cadera y tobillos, inclinación del robot, entre otros, que cumplan con los objetivos formulados para posteriormente determinar las trayectorias a través de interpolación. En (Park y Choi (2004)) usa un AG que encuentra los coeficientes de polinomios de cuarto orden que definen las tayectorias de cada una de las articulaciones y las localizaciones óptimas de los centros de masa de cada enlace del robot que permiten eficiencia en el contexto de consumo de energía.

Todas las propuestas mencionadas hasta el momento tienen en común que garantizan estabilidad dinámica a través del uso de PCM en su metodología de solución. Sin embargo otras formulaciones para resolver problema de síntesis de patrones de caminata mediante optimización se enfocan en determinar parámetros de funciones suaves que representan el patrón de caminata e involucran en el proceso el modelo dinámico del robot. Tal es el caso de (Cabodevila y Abba (1997)) donde cada coordenada generalizada las aproxima a través de series de Fourier, la función de desempeño comprende la minimización de la suma de las pérdidas mecánicas y pérdidas de Joule, para resolver el problema de optimización utiliza un AG y anulación simulada. En (Bessonnet *et al.* (2005)) las trayectorias de las coordenadas generalizadas son aproximadas por trazadores cúbicos y utiliza programación cuadrática para encontrar los parámetros tal que minimizan las entradas de control. En (Chevallereau y Aoustin (2001)) y (Djoudi *et al.* (2005)) definen un problema de optimización no lineal con restricciones, la evolución del las coordenadas generalizadas del sistema mecánico es descrita con polinomios de cuarto grado parametrizados por otra variable de tal manera que el movimiento que diseñan debe satisfacer el modelo dinámico del robot, la función de costo considera la pérdida de energía durante la fase de soporte simple y la fase de soporte doble, el proceso de optimización resulta en un movimiento cíclico para un robot bípedo con grado de subactuación uno.

Los inconvenientes de utilizar el principio de PMC como indicador de estabilidad es que se basa en revisar que la proyección de su centro de masa no salga fuera del polígono de soporte formados por los pies del robot, el cual no puede ser cubierto por el robot bípedo que se utiliza en este trabajo. La estrategia utilizada para determinar movimientos de caminata periódica tiene como elemento primordial la verificación de estabilidad en lazo cerrado del sistema con el controlador presentado en (Grizzle *et al.* (1999)), el cual introduce el comportamiento dinámico deseado en la salida y el controlador realiza la estabilización. El comportamiento dinámico deseado lo expresan mediante una familia de funciones definidas en términos de una de las variables de configuración del robot y establecen parámetros de esas funciones que permiten obtener movimientos de caminata periódica.

Para ello consideran que durante un paso del robot bípedo $\theta_1(t)$ se comporta de forma monótona estrictamente creciente, definen el comportamiento de las coordenadas restantes en términos de la evolución de la coordenada angular $\theta_1(t)$. La función que representa la salida (Grizzle *et al.* (1999)), la definen como

$$y := \begin{bmatrix} y_1 \\ y_2 \end{bmatrix} := \begin{bmatrix} h_1(\theta, a) \\ h_2(\theta, a) \end{bmatrix} := \begin{bmatrix} \theta_3 - h_{d,1}(\theta_1, a) \\ \theta_2 - h_{d,2}(\theta_1, a) \end{bmatrix}, \tag{4.1}$$

donde

$$\begin{aligned} h_{d,1}(\theta_1, a) &:= a_1^0 + a_1^1\theta_1 + a_1^2(\theta_1)^2 + a_1^3(\theta_1)^3, \\ h_{d,2}(\theta_1, a) &:= -\theta_1 + (a_2^0 + a_2^1\theta_1 + a_2^2(\theta_1)^2 + a_2^3(\theta_1)^3) \times (\theta_1 + \theta_1^d) \times (\theta_1 - \theta_1^d), \end{aligned} \tag{4.2}$$

lo cual impone que $h_{d,2}(\theta_1^d, a) = h_{d,2}(-\theta_1, a) = 0$.

El sistema en lazo cerrado que involucra al robot bípedo (3.12) y el controlador se expresa como (Grizzle *et al.* (2001)):

$$\Sigma_{cl}: \begin{cases} \dot{x} = f_{cl}(x(t)), & x^- \notin S \\ x^+ = \Delta(x^-(t)), & x^- \in S \end{cases}, \tag{4.3}$$

con $f_{cl}(x) := f(x) + g(x)u(x)$, donde el controlador es

$$u(x) := (L_g L_f h(x))^{-1}(\Psi(h(x), L_f h(x)) - L_f^2 h(x)), \tag{4.4}$$

del cual $L_f h(x) = \frac{\partial h}{\partial x} f(x)$, $L_f^2 h(x) = \frac{\partial}{\partial x}\left(\frac{\partial h}{\partial x} f(x)\right) f(x)$ y $L_g L_f h(x) = \frac{\partial}{\partial x}\left(\frac{\partial h}{\partial x} f(x)\right) g(x)$,

$$\Psi(y, \dot{y}) := \begin{bmatrix} \frac{1}{\epsilon^2}\psi_\alpha(y_1, \epsilon\dot{y}_1) \\ \frac{1}{\epsilon^2}\psi_\alpha(y_2, \epsilon\dot{y}_2) \end{bmatrix}, \tag{4.5}$$

donde $y := [y_1, y_2]$, $\dot{y} := [\dot{y}_1, \dot{y}_2]$. $\psi_\alpha(y_i, \epsilon\dot{y}_i)$ se define como

$$\psi_\alpha(y_i, \epsilon\dot{y}_i) := -\mathrm{sign}(\epsilon\dot{y}_i)|\epsilon\dot{y}_i|^\alpha - \mathrm{sign}(\phi_\alpha(y_i, \epsilon\dot{y}_i))|\phi_\alpha(y_i, \epsilon\dot{y}_i)|^{\frac{\alpha}{2-\alpha}}, \tag{4.6}$$

y

$$\phi_\alpha(y_i, \epsilon\dot{y}_i) := y_i + \left(\frac{1}{2-\alpha}\right)\mathrm{sign}(\epsilon\dot{y}_i)|\epsilon\dot{y}_i|^{2-\alpha}, \tag{4.7}$$

con $i = 1, 2$, $\alpha \in (0, 1)$ y $\epsilon > 0$.

Es de interés determinar otro conjunto de parámetros para la función de salida tal que el sistema en lazo cerrado (4.3) produce movimientos periódicos, es por ello que se implementa un AG que evolucionará una colección codificada de conjuntos de parámetros de la forma dada en (4.2) tal que el proceso resulte en movimientos periódicos en el robot bípedo que presenten disminución en el consumo de energía.

Los resultados que se presentan en este capítulo estan publicados en (Cardenas-Maciel *et al.* (2011b)), (Cardenas-Maciel *et al.* (2009a)) y (Cardenas-Maciel *et al.* (2009b)).

4.1 Formulación de problema

El problema se describe como sigue: dado el modelo del robot bípedo (3.11), la ley de control (4.4), encuentre los parámetros de la función que describe la salida (4.2) tal que el sistema en lazo cerrado (4.3) alcance estabilización orbital en tiempo finito y con energía de control baja.

4.2 Estrategia de Solución

El problema se formula como un problema de optimización con restricciones debido a que se descartan las soluciones que no representan el ciclo de caminata normal, es decir aquellos en que las trayectorias del vector de estados no son periódicas y satisfacen las restricciones en la dinámica. El problema de optimización se lleva al contexto de AG, la metodología empleada se basa en:

- Elegir las variables de decisión del problema de optimización, para entonces representar al individuo (soluciones candidatas) dentro del algoritmo;
- Establecer la función objetivo y restricciones que deben satisfacer las soluciones durante la evolución;
- Elegir la estrategia de selección de individuos;
- Elegir las operaciones genéticas;
- Realizar implementación de algoritmo computacional y ejecutar;

Los elementos involucrados en el AG que resultan de realizar lo que menciona la lista previa, se describen a continuación.

4.2.1 Representación del individuo

La representación de cada individuo esta dada por un esquema de codificación con números reales. Su genotipo esta compuesto por números reales donde cada uno representa los parámetros a_i^j de la i-esima función de salida, donde $i = 1, 2$ y $j = 0, 1, 2, 3$.

Si consideramos un individuo (conjunto de parámetros a_i^j de la salida (4.2)) en la generación k con n números reales expresado como $s_v^k = [v_1^k, v_2^k, v_3^k, \ldots, v_n^k]$, el m-ésimo número real del individuo en la etapa inicial del algoritmo v_m^0 es obtenido mediante la siguiente expresión:

$$v_m^0 = \left(\frac{LB}{2} + \frac{UB}{2}\right) + \left(\left(\frac{UB}{2} - \frac{UL}{2}\right)(2p-1)\right), \tag{4.8}$$

donde $p \in [0, 1]$ es un número obtenido de manera aleatoria; LB denota el límite inferior y UB denota el límite superior del dominio de v_m^0. Los valores de v_m^k están forzados a permanecer dentro de un dominio para todo k.

4.2.2 Función Objetivo

Se utiliza una función de costo con meta a minimizar, la cual representa una aproximación del promedio de los pares aplicados al sistema durante el tiempo que sucede un paso

$$\hat{J}(a) = \int_0^T (u_1^2 + u_2^2)dt, \tag{4.9}$$

donde T es tal que $\theta_1(T) - \theta_1^d = 0$ y $u = [u_1, u_2]$ son los pares que se aplican al robot.

4.2.3 Restricciones

La función de costo (4.9) esta sujeta a las siguientes restricciones tomadas de (Grizzle *et al.* (1999))

$$\begin{array}{rcl} \hat{\dot{\theta}}_1^- - 0.99\lambda(\hat{\dot{\theta}}_1^-) & \leq & 0, \\ \|y(\bar{t})\| & \leq & 0, \\ |\frac{F_T}{F_N}| - \mu & \leq & 0, \\ -\dot{z}_2^+ & \leq & 0, \end{array} \tag{4.10}$$

donde $\hat{\dot{\theta}}_1^-$ es la velocidad angular de la pierna de soporte antes del impacto, μ es el coeficiente de fricción, F_T y F_N son las fuerzas tangenciales y normales (respectivamente) aplicadas en la pierna en balanceo, $\dot{z}_2^+$ es la razón de cambio de la coordenada vertical del extremo de la pierna después del impacto.

La primera restricción revisa la existencia de un punto fijo, la segunda restricción asegura que el controlador ha convergido antes de que suceda el impacto, las dos últimas verifica la validez del modelo de impacto.

Como el requisito es que la caminata del robot sea equiparable a la caminata humana típica, las trayectorias del sistema en lazo cerrado (4.3) deben ser periódicas (también llamado órbitas periódicas). Una de las herramientas que permite analizar las propiedades de estabilidad del sistema es a través del mapa de Poincaré (Khalil (2002)). El método de Poincaré determina si la trayectoria del sistema dinámico que evoluciona desde una determinada condición inicial intersecta en forma transversal en un solo punto a una superficie establecida. La trayectoria es periódica si la evolución de la trayectoria después de su previa intersección con la superficie vuelve a tocar la superficie en el mismo punto. En términos téoricos es el punto fijo que se requiere garantizar su existencia en la primera restricción de (4.10).

La superficie en cuestión es el conjunto $\mathcal{S}$ definido en (3.12) el cual describe el conjunto de puntos (estado del sistema) tal que llevan a que suceda el evento de impacto. Se utiliza la extensión del método de Poincaré que fue desarrollado y demostrado en (Grizzle *et al.* (2001)), ya que permite analizar el sistema incluyendo el modelo del impacto. Para mencionar el algoritmo computacional utilizado para la verificación de la primer restricción se define $\varphi(t, x_0)$ como la solución de $f_{cl} := f(x) + g(x)u(x)$ en el tiempo t, con condición inicial x_0 en el tiempo $t_0 = 0$.

La solución es periódica si existe un tiempo $T > 0$ tal que $\varphi(t+T, x_0) = \varphi(t, x_0); \forall t \in [t_0, \infty)$.

Un conjunto $\mathcal{O} \subset \mathcal{X}$ es una órbita periódica si $\mathcal{O} := \{\varphi(t, x_0) | t \geq t_0\}$ para algunas soluciones periódicas $\varphi(t, x_0)$.

Se le llama tiempo de asentamiento del sistema en lazo cerrado a

$$T_{set}^{cl} := T_{set}(h, L_f h), \tag{4.11}$$

donde $T_{set}(h, L_f h)$ es $T_{set}\,(y, \dot{y}) := \inf\{t > 0|\,(y(t), \dot{y}(t)) = (0,0), (y(0), \dot{y}(0)) = (y_0, \dot{y}_0)\}$.

La función de tiempo que ocurre el impacto $T_I : \mathcal{X} \to \Re \cup \{\infty\}$ se expresa como

$$T_I(x_0) := \begin{cases} \inf_{t\geq 0}\{\varphi(t, x_0) \in \mathcal{S}\}, & \text{Si } \exists\ t \text{ tal que } \varphi(t, x_0) \in \mathcal{S} \\ \infty, & \text{en otro caso} \end{cases}. \tag{4.12}$$

El conjunto $\tilde{\mathcal{S}}$ que pertenece a $\mathcal{S}$ representa los puntos que después de aplicarse el modelo de impacto produce soluciones del modelo de fase de soporte simple que llevan a una intersección que no es tangente a $\mathcal{S}$ es decir,

$$\tilde{\mathcal{S}} := \left\{x \in \mathcal{S} | 0 < T_I\left(\Delta(x)\right) < \infty, L_f h\left(\varphi^{f_{cl}}\left(T_I(\Delta(x)), \Delta(x)\right)\right) \neq 0\right\}.$$

El mapa de retorno de Poincaré es definido por $P : \tilde{\mathcal{S}} \to \mathcal{S}$ como

$$P(x) := \varphi\left(T_I(\Delta(x)), \Delta(x)\right), \tag{4.13}$$

el cual describe la evolución del robot después del impacto con la superficie hasta solo antes del siguiente impacto.

El conjunto $\hat{\mathcal{S}} := \left\{x_0 \in \tilde{\mathcal{S}} | T_{set}^{cl}(x_0) < T_I(x_0) < \infty\right\}$ define a aquellos puntos en que el tiempo de asentamiento obtenido con el controlador es menor que el tiempo en que se lleva a cabo un paso; el conjunto del espacio de estados $\mathcal{Z}$ define los puntos en que la dinámica cero evoluciona.

El mapa de Poincaré que permite identificar que las trayectorias del sistema en lazo cerrado son órbitas periódicas se define como

$$\rho : \hat{\mathcal{S}} \cap \mathcal{Z} \rightarrow \mathcal{S} \cap \mathcal{Z}; \qquad \rho(x) := P(x), \tag{4.14}$$

con $P(x)$ definida en (4.13).

El algoritmo que permite calcular numéricamente el mapa de Poincaré que se basa en evaluar la función $\lambda : \sigma^{-1} \circ \rho \circ \sigma$, donde $\sigma : \Re \rightarrow \hat{\mathcal{S}} \cap \mathcal{Z}$ se define como

$$\sigma(\dot{\theta}_1^-) := \left(\theta_1^d, -\theta_1^d, \theta_3^d, \dot{\theta}_1^-, -\dot{\theta}_1^-, 0\right),$$

y ρ es definida en (4.14).

Algoritmo

1. `Inicio`
2. `Para` $\dot{\theta}_1^- > 0$`, calcular los estados del robot antes del impacto` $x^- \leftarrow \sigma(\dot{\theta}_1^-)$
3. `Aplicar el modelo de impacto` $x^+ \leftarrow \Delta(x^-)$ `usando (3.10)`

4. `Use` x^+ `como condicion inicial para` $\dot{x}$ `en (4.3) y simular hasta que uno de los siguientes dos casos suceda:`

   (a) `Existe un tiempo` $T > 0$ `donde` $\theta_1(T) = \theta_1^d$. `Si` T `es mayor que el tiempo de asentamiento del controlador, entonces` $x^+ \in \hat{\mathcal{S}} \cap \mathcal{Z}$ `y` $\lambda(\dot{\theta}_1^-) = \dot{\theta}_1(T)$; `caso contrario` $x^+ \notin \hat{\mathcal{S}} \cap \mathcal{Z}$ `y` $\lambda(\dot{\theta}_1^-)$ `no esta definida en ese punto.`

   (b) `No existe un tiempo` $T > 0$ `tal que` $\theta_1(T) = \theta_1^d$ `entonces` $x^+ \notin \hat{\mathcal{S}} \cap \mathcal{Z}$ `y` $\lambda(\dot{\theta}_1^-)$ `no esta definida en ese punto.`

5. `Fin.`

En resumen, para conocer la aptitud del individuo dentro del proceso evolutivo del AG implica evaluar la función de costo (4.9) pero previamente debe satisfacer las resticciones (4.10), lo cual requiere que se calcule la función λ que involucra revisar las trayectorias del modelo continuo de (4.3) utilizando las condiciones iniciales $x_0 = \Delta \circ \sigma\left(\hat{\dot{\theta}}_1^-\right)$ y para ser aplicable la función λ, $\hat{\dot{\theta}}_1^-$ debe de ser un número tal que $\lambda\left(\hat{\dot{\theta}}_1^-\right) > \dot{\theta}_1^-$.

4.2.4 Operaciones Genéticas

Las operaciones genéticas comprenden el cruce de un punto (Goldberg (1989)) y la mutación no uniforme (Michalewicz (1994)).

La mutación no uniforme agrega una perturbación a un número de la definición del individuo. Si se tiene al individuo en la generación k, descrito como $s_v^k = [v_1^k, v_2^k, v_3^k, \ldots, v_n^k]$ y el número v_m^k es seleccionado para aplicar esta operación de mutación, el individuo resultante queda $s_v^k = [v_1^k, \ldots, v_m^{k'}, \ldots, v_n^t]$ donde

$$v_m^{k'} = \begin{cases} v_m^k + \delta(k, UB - v_m^k); & \mathrm{q} = 0 \\ v_m^k - \delta(k, v_m^k - LB); & \mathrm{q} = 1 \end{cases}, \tag{4.15}$$

Para determinar q se realiza lo siguiente: Sea $p \in [0,1]$ generado de forma aleatoria, if $0 \leq p \leq 0.5$, $q = 0$; Si $0.5 < p \leq 1$, $q = 1$. LB y UB son el límite inferior y superior del dominio de v_k^t.

La función $\delta(k,y) = y\left(1 - r^{\left(1-\frac{k}{T}\right)^b}\right)$ representa la perturbación agregada a v_m^k, $\delta(k,y) \in [0,y]$ por lo que no excede el dominio definido para v_m^k; $r \in [0,1]$; T es el número máximo de generación; b es un grado de dependencia del número de generación en la cual se aplica la operación de mutación al individuo, los valores pueden estar entre [1, 5].

El valor de b permite regular la rapidez de decrecimiento del valor que toma $\delta(k,y)$ conforme se va incrementando el número de generaciones desarrolladas por el algoritmo, por lo que la variación experimentada en el individuo al que se le aplica la mutación es mucho más grande en las primeras generaciones que en las del final.

4.3 Resultados de Implementación de AG

El AG con los elementos descritos en la sección 4.2 fue programado en MATLAB®. La evaluación de la función objetivo utiliza la implementación en software del modelo del robot bípedo (3.11) y el controlador (4.4), los cuales se encuentran disponibles en (Grizzle (2007)). Detalle del modelo del robot bípedo se presenta en el apéndice A. Los parámetros del modelo del robot bípedo se muestran en la Tabla 4.1, los parámetros del controlador toman los valores $\epsilon = 0.1$ and $\alpha = 0.9$. También se considera que la velocidad angular de la pierna de soporte previa al impacto es $\dot{\theta}_1^- = 1.55$, el coeficiente de fricción es $\mu = \frac{2}{3}$ y la pierna en balanceo entra al plano de movimiento cuando $\theta_1^d = \frac{\pi}{8}$. Los parámetros utilizados en la ejecución del AG se muestran en la Tabla 4.2.

La Tabla 4.3 muestra los parámetros a_i^j de las funciones en (4.1) que fueron obtenidos

Tabla 4.1. Parámetros del modelo del robot bípedo

Parámetro	**Valor**
Masa de cadera (M_H)	15 kg
Masa de Torso (M_T)	10 kg
Masa de pierna (m)	5 kg
Longitud de piernas (r)	1 m
Longitud de torso (l)	0.5 m

Tabla 4.2. Parámetros del AG

Parámetro	**Valor**
Número de individuos	100
Número máximo de generaciones	400
Tasa de cruce	0.9
Tasa de mutación	0.2
Tasa de selección	0.4
b	5
Elitismo	1

con el AG y la energía de control consumida $\hat{J}(a)$ que fue calculada al ejecutar el sistema en lazo cerrado utilizando los parámetros. En la Tabla 4.4 muestra los parámetros determinados mediante programación cuadrática secuencial (PCS - SQP en inglés) y su respectiva energía de control para el mismo robot los cuales están reportados en (Grizzle *et al.* (1999)).

A continuación se presentan las trayectorias de los estados, el comportamiento de la salida y las señales de control y la órbitas proyectadas en los estados θ_1, $\dot{\theta}_1$ and $\dot{\theta}_3$ que fueron obtenidos de la ejecución del sistema en lazo cerrado para producir en

Tabla 4.3. Parámetros a_i^j y energía de control

No.	Parámetros								$\hat{J}(a)$
	a_1^0	a_1^1	a_1^2	a_1^3	a_2^0	a_2^1	a_2^2	a_2^3	
1	0.3005	1.1474	-1.8933	-0.3126	-1.5921	3.7716	2.8948	-0.3294	468.8927
2	0.4833	0.6622	-2.276	1.2824	-0.3166	1.8917	1.2474	-0.4689	609.4312
3	0.4833	0.6622	-2.276	1.2824	-0.3166	1.8917	0.8934	0.312	639.8821
4	0.3687	1.3459	-1.6739	-1.6964	-1.5381	2.9158	1.684	2.9733	689.2893
5	0.5893	0.4644	1.5558	-0.0367	-1.2656	1.0308	1.1086	3.7436	719.3200
7	0.4857	-0.2815	1.8735	-2.5745	1.5987	4.3327	-2.2472	-2.5773	773.3510
8	0.4317	0.3851	-0.6071	-0.3504	-0.3006	2.0402	2.1131	-0.1945	883.9733
9	0.7098	0.0581	0.0536	-1.0280	-1.9803	2.5752	3.6109	2.0000	1225.4000
10	0.3992	0.7515	-2.5759	2.5365	1.8022	0.5344	0.2620	6.0033	1679.2000
11	1.0730	-0.4986	-0.4127	1.6194	2.7029	-1.4978	1.6201	-0.8384	2541.7000
12	0.2892	1.9435	-2.8760	0.4328	2.0252	4.5643	-0.5546	-4.1460	2980.5000

Tabla 4.4. Parámetros a_i^j obtenidos con PCS (Grizzle *et al.* (1999)) y energía de control

a_1^0	a_1^1	a_1^2	a_1^3	a_2^0	a_2^1	a_2^2	a_2^3	$\hat{J}(a)$
0.5120	0.0730	0.0350	-0.8190	-2.2700	3.2600	3.1100	1.8900	761.00

el robot bípedo ocho pasos. En cuanto a las ejecuciones en lazo cerrado usando los resultados obtenidos con AG, se presentan los casos extremos: de la Figura 4.1 a la Figura 4.4 muestran los resultados de simulación usando los parámetros de la primera fila de la Tabla 4.3 que presenta menor valor de energía de control con respecto a los parámetros obtenidos con PCS mostrados en Tabla 4.4. De la Figura 4.5 a la Figura 4.8 se muestra el caso para el que se obtuvo el mayor valor en energía de control. De la Figura 4.9 a la Figura 4.12 se muestran los resultados de simulación utilizando los parámetros obtenidos con PCS. Se puede observar que las trayectorias del vector de estado (Figura 4.1 y Figura 4.5) tienen convergencia a un comportamiento periódico lo cual puede también ser observado en las figuras que muestran la convergencia a una órbita periódica donde línea recta que se muestra en la órbita representa el evento de impacto. Los parámetros encontrados al resolver el problema de optimización mediante AG satisfacen las restricciones impuestas en la formulación del problema y permiten definir movimientos (patrones de caminata) que junto con el controlador llevan a estabilizar las trayectorias a una órbita periódica.

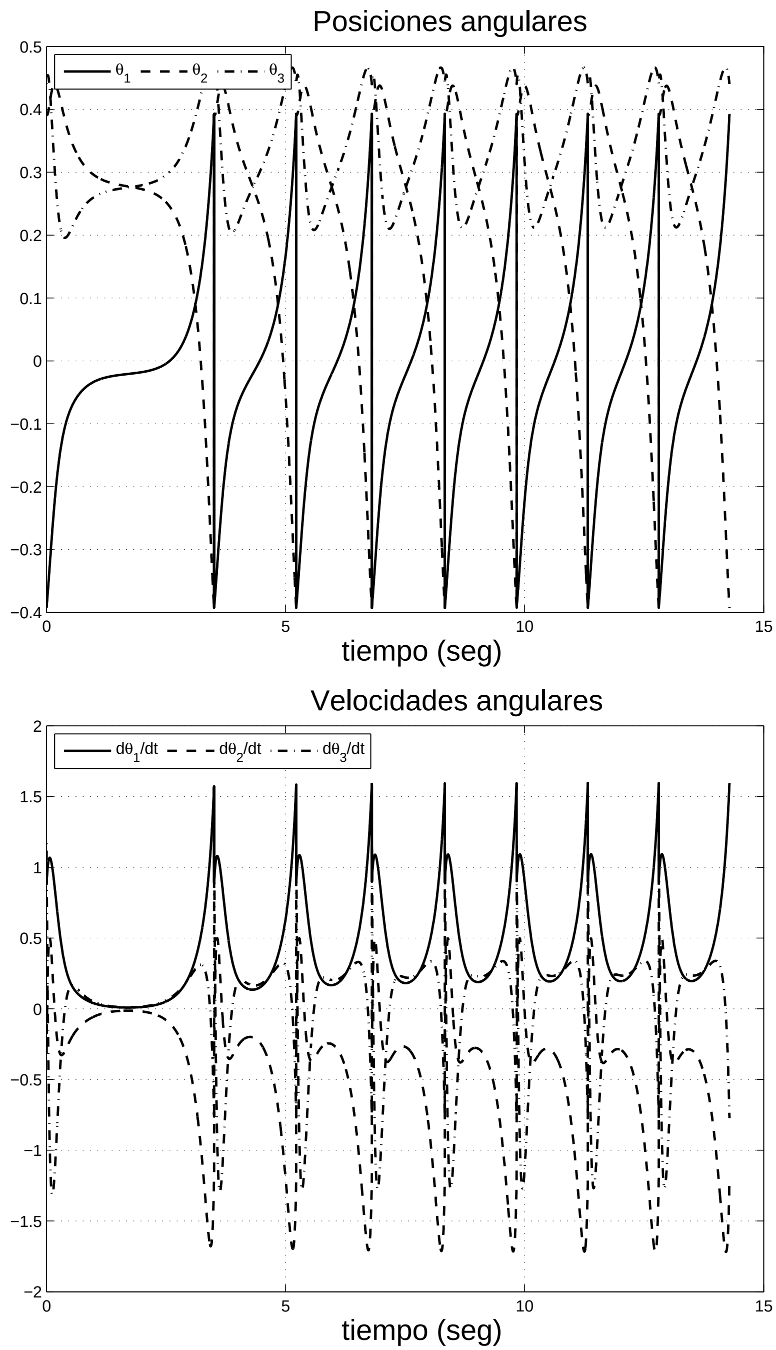

Figura 4.1. Trayectorias de las posiciones y velocidades angulares al simular el sistema en lazo cerrado con los parámetros de la primer fila de la Tabla 4.3

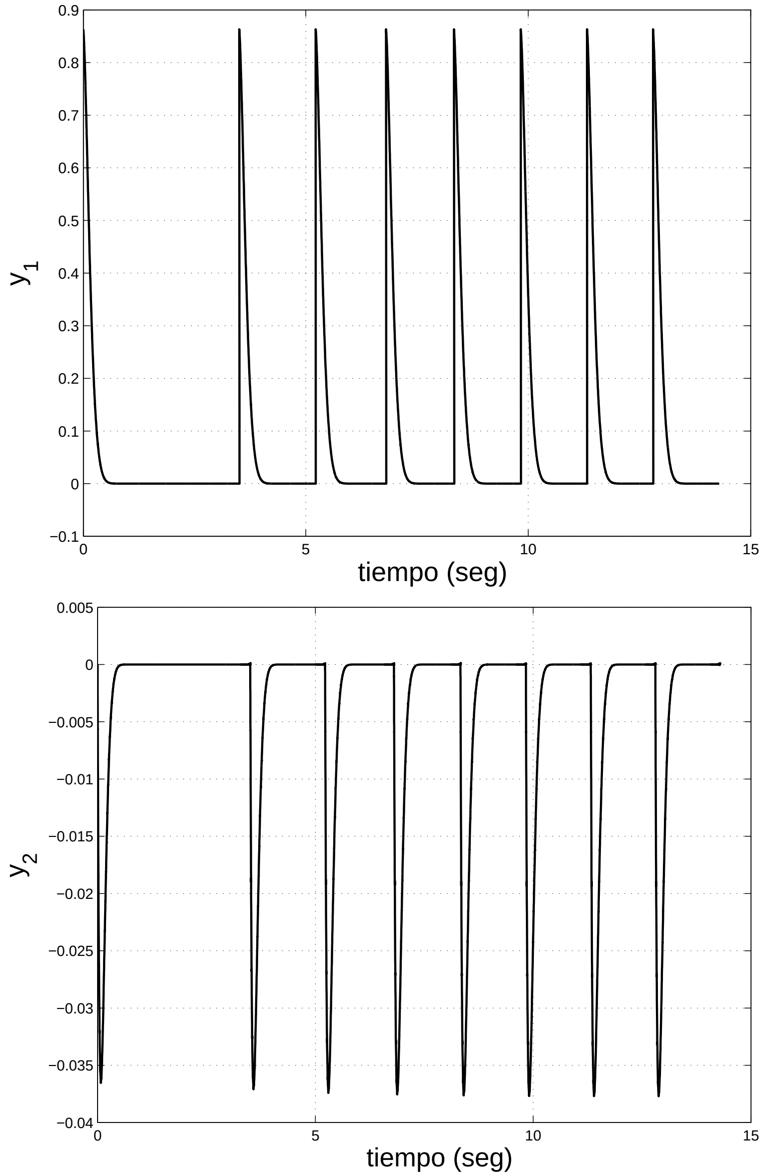

Figura 4.2. Trayectoria de la salida al simular el sistema en lazo cerrado con los parámetros de la primer fila de la Tabla 4.3

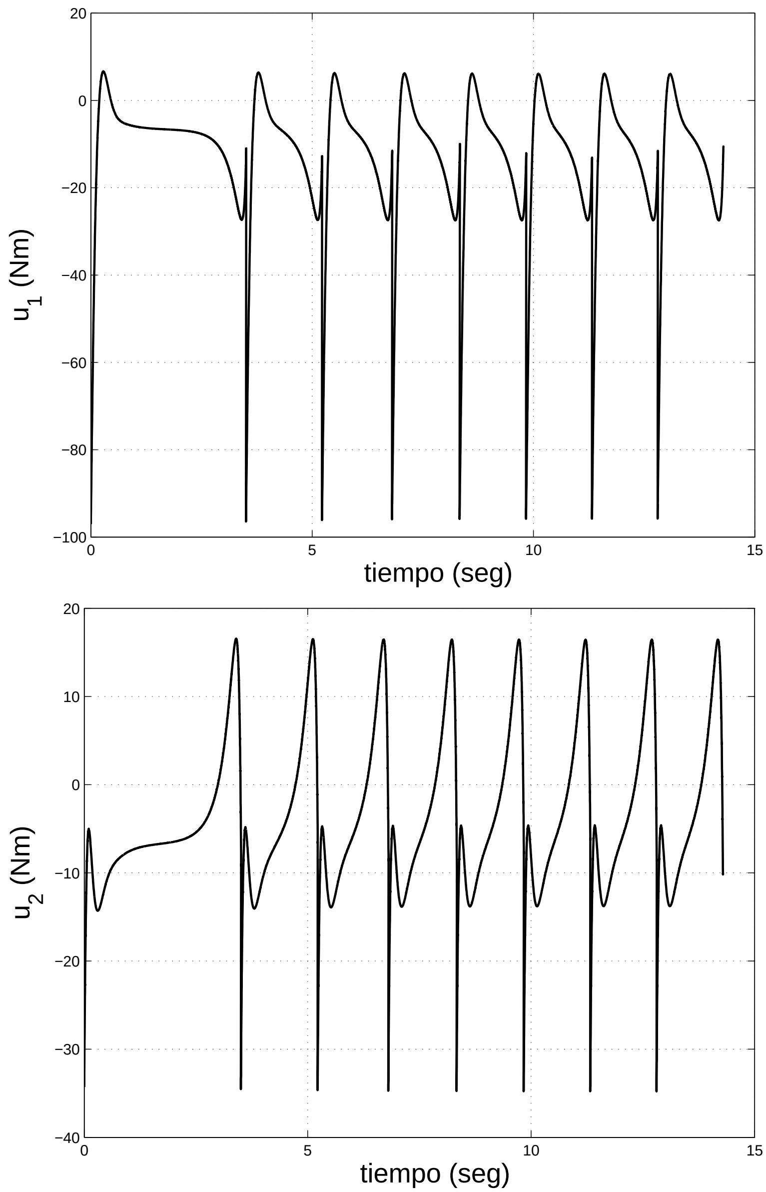

Figura 4.3. Señales de control al simular el sistema en lazo cerrado con los parámetros de la primer fila de la Tabla 4.3

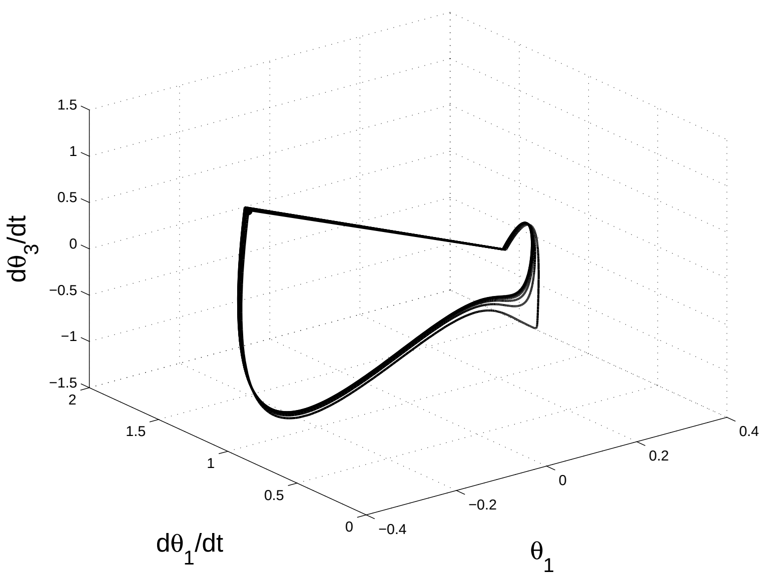

Figura 4.4. Órbita proyectada θ_1, $\dot{\theta_1}$ y $\dot{\theta}_3$ obtenida al simular el sistema en lazo cerrado utilizando los parámetros de la primer fila de la Tabla 4.3

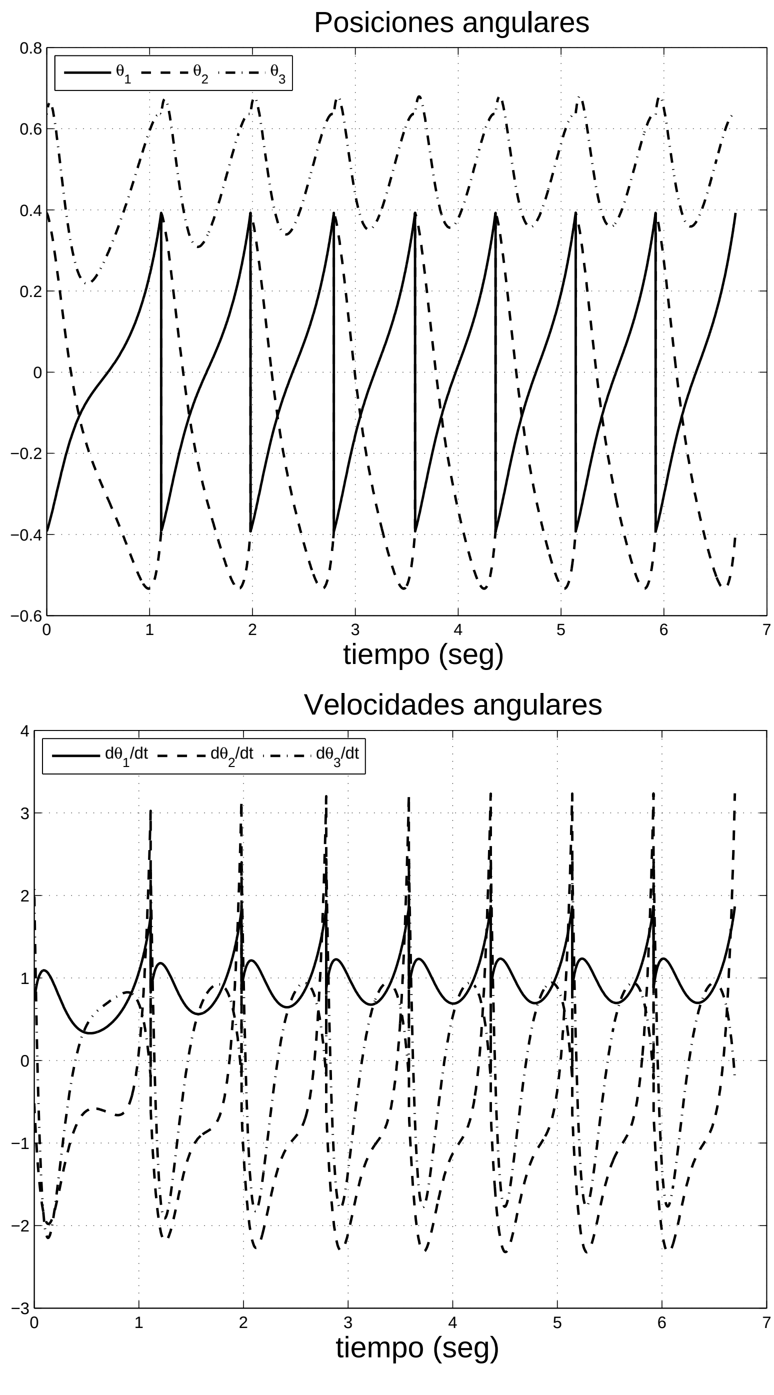

Figura 4.5. Trayectorias de las posiciones y velocidades angulares al simular el sistema en lazo cerrado utilizando los parámetros de la última fila de la Tabla 4.3

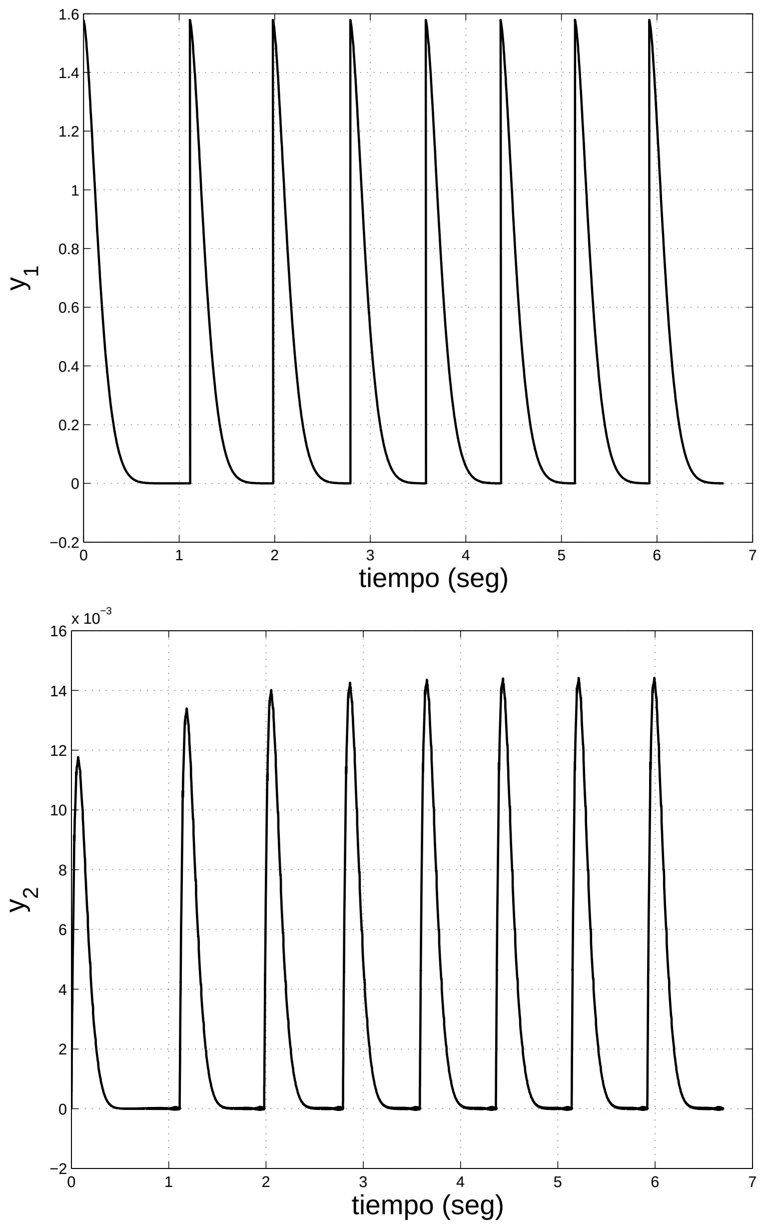

Figura 4.6. Trayectorias de la salida al simular el sistema en lazo cerrado utilizando los parámetros de la última fila de la Tabla 4.3

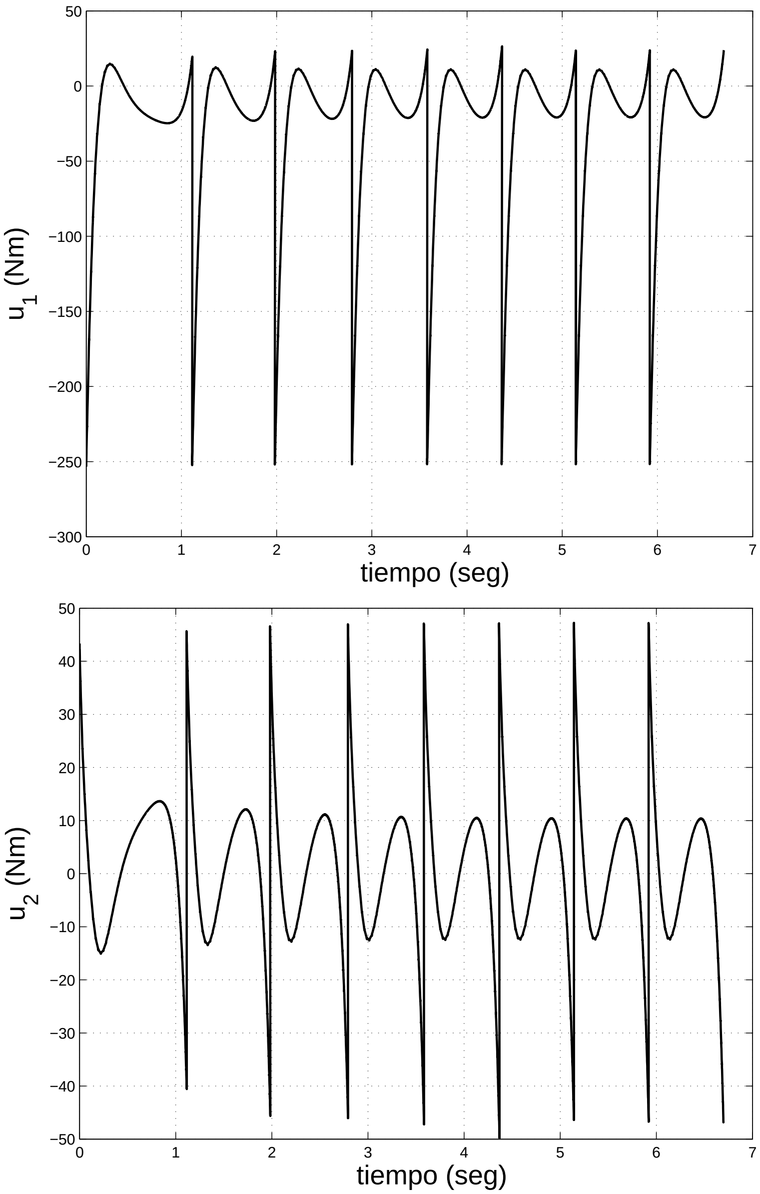

Figura 4.7. Señales de control al simular el sistema en lazo cerrado utilizando los parámetros de la última fila de la Tabla 4.3

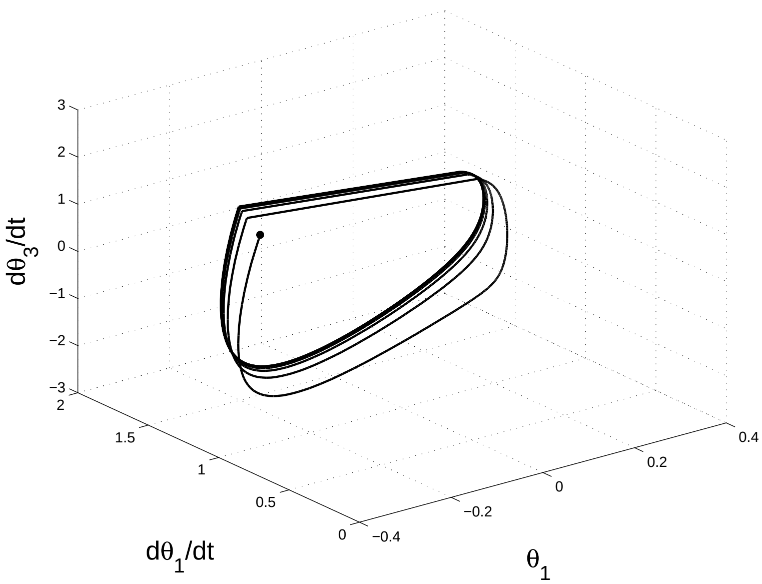

Figura 4.8. Órbita proyectada en θ_1, $\dot{\theta}_1$ y $\dot{\theta}_3$ obtenida utilizando los parámetros de la última fila de la Tabla 4.3

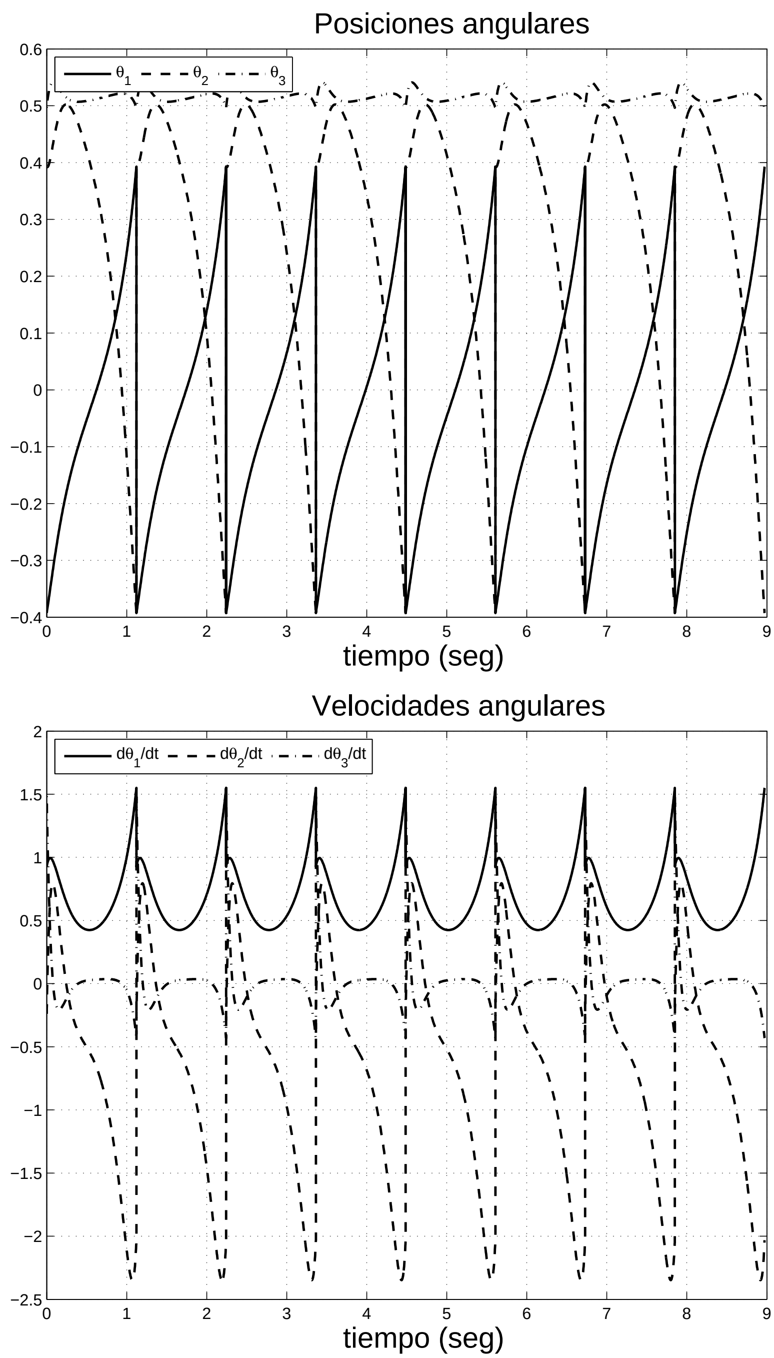

Figura 4.9. Trayectorias de las posiciones y velocidades angulares obtenidas al simular el sistema en lazo cerrado con los parámetros de la Tabla 4.3

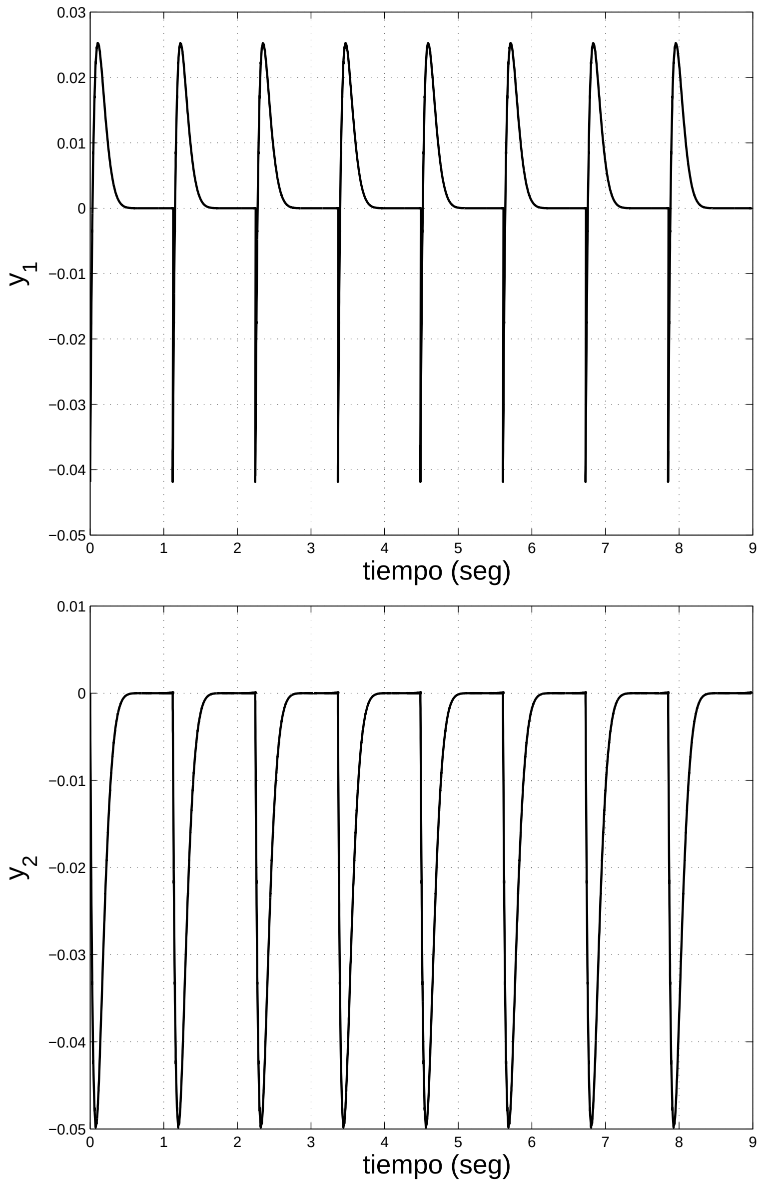

Figura 4.10. Trayectorias de la salida obtenidas al simular el sistema en lazo cerrado con los parámetros de la Tabla 4.4

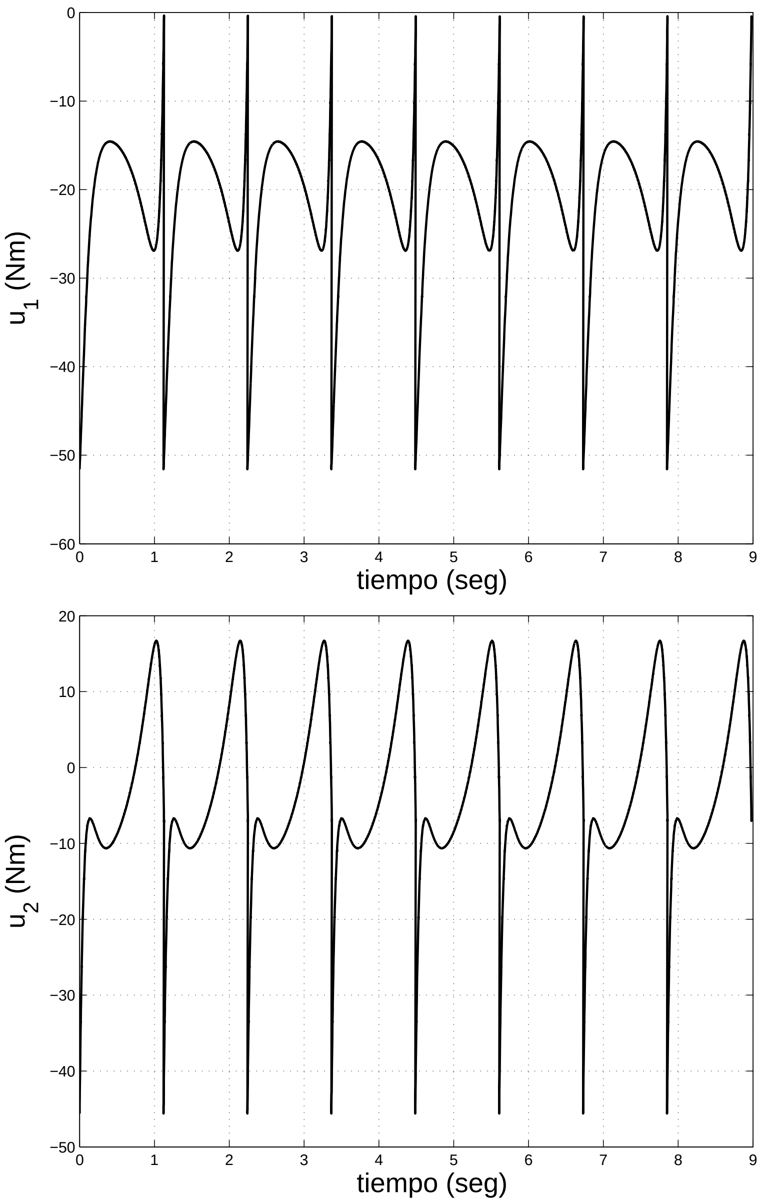

Figura 4.11. Señales de control obtenidas al simular el sistema en lazo cerrado con los parámetros de la Tabla 4.4

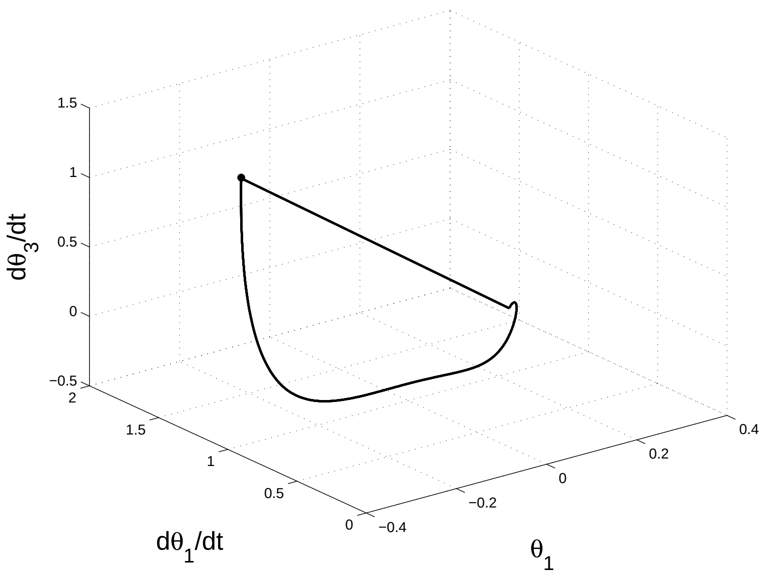

Figura 4.12. Órbita proyectada en θ_1, $\dot{\theta}_1$ y $\dot{\theta}_3$ obtenida utilizando los parámetros de la Tabla 4.4

Capítulo 5

Control de caminata de robot bípedo con métodos de computación inteligente

El control difuso como un área de aplicación de la lógica difusa ha tenido atención por parte de científicos e ingenieros debido a que mediante el uso de reglas de la forma `If-Then` es posible representar el conocimiento experto acerca de cómo controlar un sistema, lo cual ha permitido que en la etapa de diseño de controladores pueda llegar a no ser requerido el conocimiento del modelo matemático del sistema, definir de manera empírica los conjuntos difusos, la base de reglas difusas para el proceso de inferencia que caracterice el mapeo no-lineal suficiente tal que el sistema en lazo cerrado logre los objetivos de control.

Cuando la dimensión del espacio de las variables medibles que son consideradas para el diseño del controlador y la cantidad de particiones difusas aumentan, la síntesis del controlador difuso se convierte en una tarea no trivial, pues produce dificultad en caracterizar mediante las reglas difusas y conjutos difusos la relación entre las variables. Por ello, métodos basados en la combinación de lógica difusa, redes neuronales artificiales, cómputo evolutivo y otras técnicas involucradas en menor medida se han propuesto para resolver la dificultad mencionada.

Uno de los trabajos pioneros que emplean esta idea es (Jang (1993)), que propone ANFIS, un modelo neuro-difuso tal que utiliza muestras del comportamiento de las variables de entrada - salida y produce un modelo difuso. La validez de la metodología propuesta fue verificada con resultados satisfactorios en problemas de predicción en series de tiempo e identificación y control. Esta misma ha sido empleada para modelado de sistemas no lineales en (Ahtiwas *et al.* (2002)). En (Prabu *et al.* (2008)) muestra su uso para construir un controlador que resuelve el problema de seguimiento de ruta para un robot manipulador verificando su funcionamiento teniendo dinámicas no modeladas. En cuanto a control de movimiento en robots bípedos ha sido aplicada en (Shieh *et al.* (2007)) para identificar el sistema y para diseñar un controlador tal que permiten determinar los ángulos que deben tener las articulaciones. También en (Ferreira *et al.* (2004)) lo utilizan para desarrollar un controlador de seguimiento de la posición del centro de gravedad de un robot caminante. La estrategia elegida para realizar control de movimientos de robots caminantes en las publicaciones mencionadas es establecer las acciones de control en base al cómputo y verificación de PMC y uso de esa información en la etapa de diseño.

En este capítulo se presenta un controlador que permite realizar en un robot bípedo movimientos de caminata, donde el controlador se obtiene a través del modelo neuro-difuso y no utiliza información de PMC.

5.1 Descripción del problema y estrategia de solución

La meta del controlador es producir en el robot bípedo (3.2) dado en el Capítulo 3, movimiento coordinado de caminata típica, el cual es caracterizado desde el punto de vista formal como órbitas periódicas. El problema requiere determinar una ley de control expresada como un modelo difuso que produzca trayectorias del vector de estado que sean periódicas.

A diferencia de las estrategias de control empleadas para realizar el seguimiento de movimientos de referencia (patrones de caminata) que estan definidos como función del tiempo, la estrategia esta basada en (Grizzle *et al.* (1999)) que inicialmente consiste en reparametrizar el movimiento periódico deseado en base a coordenadas del vector de estado que satisfacen tener un comportamiento estrictamente monótono y definir de manera apropiada la salida usando la parametrización. Para el robot bípedo de este trabajo, las salidas controladas estan basadas en la cantidad de articulaciones que tienen actuación y el movimiento deseado definido por $h_{d,i}(\theta_1, a)$, es decir

$$y := \begin{bmatrix} y_1 \\ y_2 \end{bmatrix} := \begin{bmatrix} \theta_3 - h_{d,1}(\theta_1, a) \\ \theta_2 - h_{d,2}(\theta_1, a) \end{bmatrix}, \tag{5.1}$$

donde

$$\begin{aligned} h_{d,1}(\theta_1, a) &:= a_1^0 + a_1^1\theta_1 + a_1^2(\theta_1)^2 + a_1^3(\theta_1)^3, \\ h_{d,2}(\theta_1, a) &:= -\theta_1 + (a_2^0 + a_2^1\theta_1 + a_2^2(\theta_1)^2 + a_2^3(\theta_1)^3) \times (\theta_1 + \theta_1^d) \times (\theta_1 - \theta_1^d), \end{aligned} \tag{5.2}$$

que esta definida en términos de una variable de configuración θ_1 que debe ser estrictamente monótona y que representa la posición angular de la pierna de soporte y a_i^j son parámetros constantes escalares.

El objetivo de control es determinar las entradas de control de tal manera que $y(t)$ sea igual a cero. Esto implica que durante la convergencia de las trayectorias del sistema en lazo cerrado, el robot bípedo efectuará el movimiento deseado.

Como lo reportan (Grizzle *et al.* (1999) y Grizzle *et al.* (2001)) la elección de variables controladas, la retroalimentación y la síntesis del controlador llevaron a resolver el objetivo de control, simplificar el análisis de estabilidad del sistema en lazo cerrado y demostrar estabilidad orbital. En este trabajo, el sistema en lazo cerrado que puede observarse en el diagrama de la Figura 5.1, tiene como retroalimentación el vector de estados del sistema y la salida $y(t)$ que define en (5.1), donde las cantidades a controlar que son θ_3 y θ_2, se denotan en el diagrama como $h_0(\theta)$ y $h_d(\theta, a)$ para representar la

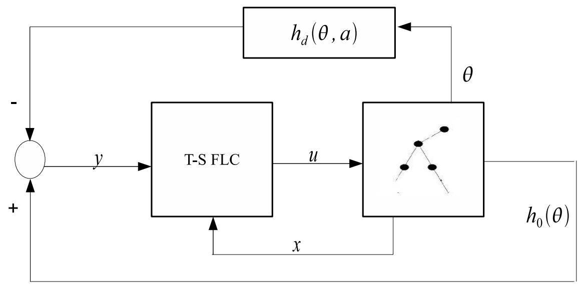

Figura 5.1. Diagrama a bloques del sistema en lazo cerrado

definición de (5.2).

La metodología para diseñar el controlador es libre del modelo matemático del robot bípedo, es decir el conocimiento experto acerca de la dinámica del sistema no esta disponible. Considerando las dimensiones del vector de estados $x(t) = [\theta, \dot{\theta}]^T \in \Re^6$ que representan las posiciones y velocidades angulares en las articulaciones del robot, la salida $y(t) \in \Re^2$ y los pares $u \in \Re^2$, el mapeo $U \subset \Re^6 \times \Re^2 \rightarrow V \subset \Re^2$ que representa el controlador difuso es difícil obtenerlo de forma manual, aún utilizando como vector de estados solo a las posiciones angulares $\theta = [\theta_1, \theta_2, \theta_3]^T$, ya que nos encontramos con el problema nombrado como la maldición de la dimensionalidad debido a que se dispone de una cantidad no despreciable de variables de entrada. Esto motiva a utilizar el método neuro-difuso ANFIS (Jang (1993)) para describir el controlador como un modelo Takagi-Sugeno-Kang (TSK) basado en datos de la dinámica deseada del sistema en lazo cerrado durante un paso, usando los parámetros del Capítulo 4.

La muestra de datos recopilados forman tuplas que representan asociaciones puntuales del mapeo no lineal que son utilizadas para obtener el controlador. Estos datos son representativos de las trayectorias de la función de salida $y = [y_1, y_2]^T$ y del vector de estados $x(t)$, las cuales constituyen las entradas; por otra parte las entradas de control $u = [u_1, u_2]^T$, constituyen a las salidas. El algoritmo usa los datos para generar la arquitectura de la red adaptativa descrita en la sección 2.2.2. Se predefine que el grupo de nodos en la primer capa de la arquitectura de red adaptativa que denotan a las funciones de membresía para el antecedente de las reglas difusas sean funciones gaussianas definidas en (2.13), lo que implica que para cada función de membresia difusa se necesitan dos parámetros. Posteriormente mediante el algoritmo de aprendizaje se actualizan los parámetros del modelo difuso tipo TSK implicitos en la arquitectura de red hasta que satisface los criterios preestablecidos de error de aprendizaje o un número máximo de iteraciones.

5.1.1 Caso de estudio 1: Controladores difusos TSK definido por tramos

Se aplica el algoritmo de aprendizaje de ANFIS con dos muestras de conjuntos de datos entradas - salidas, la particularidad de cada muestra de datos esta en los utilizados para el vector de estados. En el primer conjunto de datos, el vector de estados solo representan las posiciones angulares $\theta = [\theta_1, \theta_2, \theta_3]^T$. En el segundo conjunto de datos se considera el vector de estado completo (las posiciones y velocidades angulares) $x = [\theta, \dot{\theta}]^T = [\theta_1, \theta_2, \theta_3, \dot{\theta}_1, \dot{\theta}_2, \dot{\theta}_3]^T$. Para ambos conjuntos de datos de entrada se le asocia como datos de salida sus respectivas entradas de control.

De cada conjunto de datos se toman subconjuntos que son distribuidos en instancias diferentes de ANFIS. Esta decisión obedece solo a la restricción de recursos de memoria que no permitió hacer uso del total de datos a la vez por el algoritmo. Para este caso la configuración de los datos se realizó como sigue: para cada subconjunto de los datos de entrada se le asocia el subconjunto apropiado de datos de salida que representa a la primer entrada de control, y para el mismo subconjunto de entrada se le asocia como datos de salida el subconjunto apropiado que representa a la segunda entrada de control.

Esto significa que se determinan $2n$ subcontroladores tipo Takagi-Sugeno, donde n es el número de subconjuntos en que se dividió la muestra de datos de entrada - salida.

Para este caso de estudio se realizan $n = 4$ subconjuntos, por lo que se cuentan con 8 subcontroladores como lo muestra la Figura 5.2 donde los denota como T-S FLC. Cada par de subcontroladores se dedican a proporcionar las entradas de control en cierto intervalo de tiempo de la fase de soporte simple, por lo que la estructura de las reglas que definen cada controlador toma la forma de la ecuación (5.3) o como en la ecuación (5.4), dependiendo de la dimensión del vector de estados.

El controlador difuso que tiene como entrada $x(t)$ solo las variables de configuración (posiciones angulares) tiene 1994 reglas con la estructura dada en (5.3)

$$\begin{array}{lll} R^l: & \text{If} & \theta_1 \text{ is } A_{1,i} \text{ and } \theta_2 \text{ is } A_{2,i} \text{ and } \theta_3 \text{ is } A_{3,i} \\ & & \text{and } y_1 \text{ is } A_{4,i} \text{ and } y_2 \text{ is } A_{5,i} \\ & \text{Then} & u_k = p_{1,1}\theta_1 + p_{1,2}\theta_2 + p_{1,3}\theta_3 + p_{1,4}y_1 + \\ & & p_{1,5}y_2 + p_{1,6} \end{array} \tag{5.3}$$

Por otra parte el controlador que considera el vector de estados completo como entradas al controlador, su base de reglas difusas consta de 2048 cuya estructura esta definida en (5.4)

$$\begin{array}{lll} R^l: & \text{If} & \theta_1 \text{ is } A_{1,i} \text{ and } \theta_2 \text{ is } A_{2,i} \text{ and } \theta_3 \text{ is } A_{3,i} \text{ and} \\ & & \dot{\theta}_1 \text{ is } A_{4,i} \text{ and } \dot{\theta}_2 \text{ is } A_{5,i} \text{ and } \dot{\theta}_3 \text{ is } A_{6,i} \text{ and} \\ & & y_1 \text{ is } A_{7,i} \text{ and } y_2 \text{ is } A_{8,i} \\ & \text{Then} & u_k = p_{1,1}\theta_1 + p_{1,2}\theta_2 + p_{1,3}\theta_3 + p_{1,4}\dot{\theta}_1 + \\ & & p_{1,5}\dot{\theta}_2 + p_{1,6}\dot{\theta}_3 + p_{1,7}y_1 + p_{1,8}y_2 + p_{1,9} \end{array} \tag{5.4}$$

El algoritmo permite obtener los pares $u = [u_1^c, u_2^c]$ que se definen a través de la

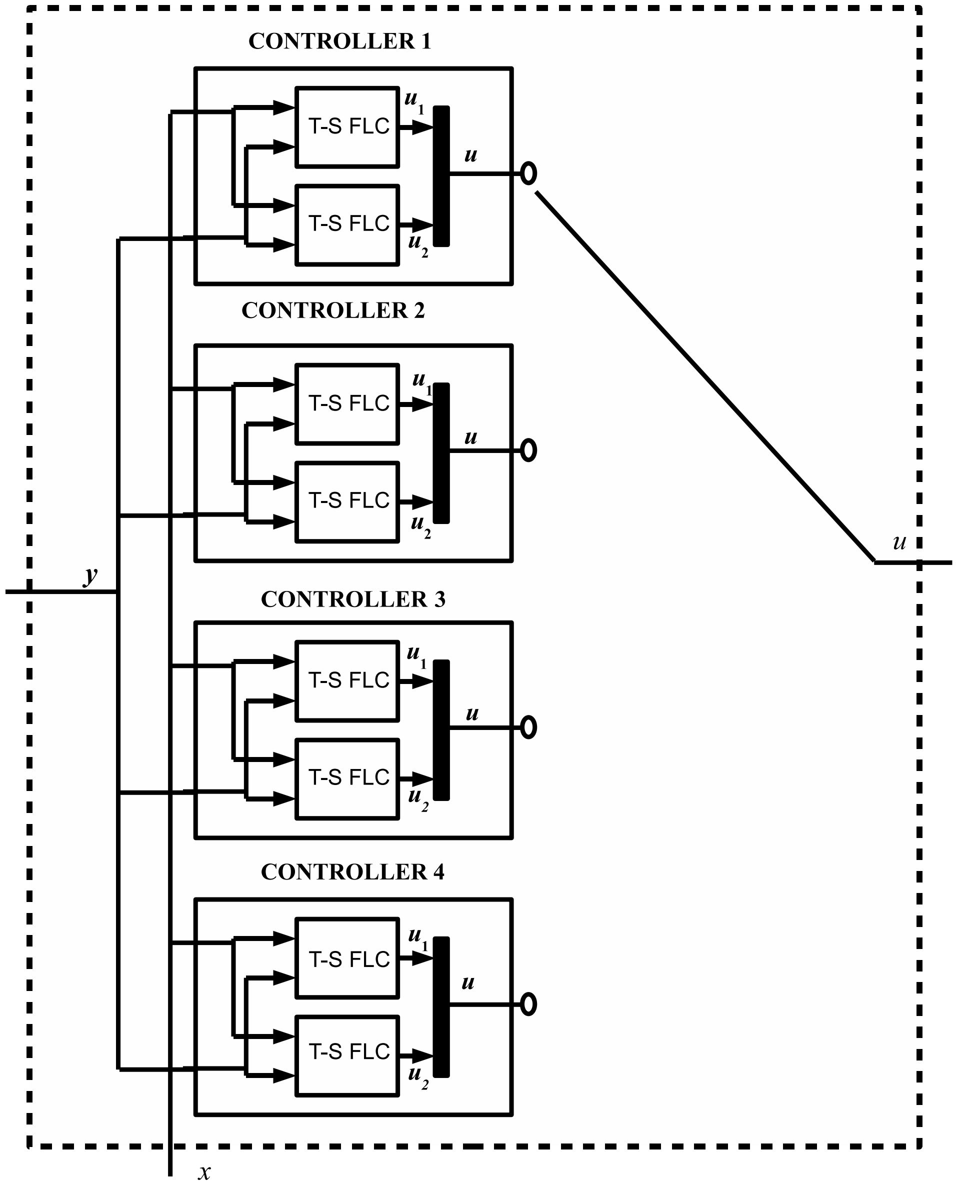

Figura 5.2. Estructura del Controlador

.

siguiente función a tramos:

$$u(x,y,t) := \begin{cases} \begin{array}{lcl} u_1^1 & = & \frac{\sum_i w_i G_i(x,y;p)}{\sum_i w_i} \\ & & \qquad , 0 \leq t < t_1 \\ u_2^1 & = & \frac{\sum_i w_i G_i(x,y;p)}{\sum_i w_i} \\ & & \\ u_1^2 & = & \frac{\sum_i w_i G_i(x,y;p)}{\sum_i w_i} \\ & & \qquad , t_1 \leq t < t_2 \\ u_2^2 & = & \frac{\sum_i w_i G_i(x,y;p)}{\sum_i w_i} \\ & & \\ u_1^3 & = & \frac{\sum_i w_i G_i(x,y;p)}{\sum_i w_i} \\ & & \qquad , t_2 \leq t < t_3 \\ u_2^3 & = & \frac{\sum_i w_i G_i(x,y;p)}{\sum_i w_i} \\ & & \\ u_1^4 & = & \frac{\sum_i w_i G_i(x,y;p)}{\sum_i w_i} \\ & & \qquad , t_3 \leq t \leq t_4 \\ u_2^4 & = & \frac{\sum_i w_i G_i(x,y;p)}{\sum_i w_i} \end{array} \end{cases} , \tag{5.5}$$

donde $i = 1, 2, ..., l_c$ es el la i-ésima regla en el c-ésimo controlador; u_k^c denota la $k-$ésima entrada de control proporcionada por el $c-$ésimo subcontrolador en el intervalo de tiempo indicado; w_i es la fuerza de disparo de cada regla mostrada en (2.14); $G_i(x, y; p)$ es el consecuente de la regla que es representado como a una combinación lineal de las variables de entrada.

5.1.2 Caso de estudio 2: Controlador difuso TSK definido en un solo tramo

El algoritmo ANFIS se aplica sin realizar particiones de la muestra de datos. Los datos que utiliza el algoritmo constan como datos de entrada el vector de estados $x(t)$ completo y la salida $y(t)$; pero utiliza como datos de salida los que representan la trayectoria de la primer entrada de control u_1, de manera similar se usa otro conjunto con los mismos datos de entrada y como dato de salida las trayectorias que representan la segunda entrada de control u_2, es decir, se utilizan dos instancias del algoritmo ANFIS, que proporcionan dos subcontroladores cada uno proporciona la entrada de control para una de las piernas del robot. La ley de control se define con la función para el intervalo en que ocurre la fase de soporte simple

$$u(x,y) := \begin{cases} u_1 = \frac{\sum_i w_i G_i(x,y;p)}{\sum_i w_i} \\ \\ u_2 = \frac{\sum_i w_i G_i(x,y;p)}{\sum_i w_i} \end{cases} , 0 \leq t \leq T \quad , \tag{5.6}$$

donde $i = 1, 2, ..., l_c$ es el la i-ésima regla en cada controlador; u_k denota la $k-$ésima entrada de control durante el tiempo que el robot realiza un paso; w_i es la fuerza de disparo de cada regla mostrada en (2.14) y $G_i(x, y; p)$ es el consecuente de la regla que se representa como a una combinación lineal de las variables de entrada. Cada regla difusa tiene la estructura dada en (5.4).

Tabla 5.1. Parámetros del robot bípedo

Parámetros	**Valor**
Masa de las caderas (M_H)	15 kg
Masa del torso (M_T)	10 kg
Masa de las piernas (m)	5 kg
longitud de las piernas (r)	1 m
Longitud del torso (l)	0.5 m

5.2 Resultados

Se realizaron verificaciones numéricas del sistema en lazo cerrado de los controladores difusos TSK obtenidos utilizando software codificado en MATLAB®. Para ello utiliza la codificación del sistema en lazo cerrado que se proporcionan en (Grizzle (2007)), la que incluye el modelo dinámico del robot bípedo, que está descrito en el Apéndice A y usa los parámetros que se muestran en la Tabla 5.1. Se asume que el evento de impacto ocurre cuando $\theta_1 = \pi/8$. Se hacen actualizaciones pertinentes al código para acoplar los controladores (especificamente para los descritos en el primer caso de estudio).

El primer grupo de resultados que se presentan y que provienen de la configuración dicha en subsección 5.1.1 están publicados en (Cardenas-Maciel *et al.* (2010)) y (Cardenas-Maciel *et al.* (2011a)).

Tabla 5.2. Parámetros de la función definida en (5.2)

a_1^0	a_1^1	a_1^2	a_1^3
0.512	0.0730	0.0350	-0.8190

a_2^0	a_2^1	a_2^2	a_2^3
-2.2700	3.2600	3.1100	1.8900

Tabla 5.3. Valores de tiempo para la entrada de control definida en (5.5)

T-S FLC	t_1	t_2	t_3	t_4
1	0.08004	0.38203	0.95253	1.12134
2	0.09775	0.38264	0.98032	1.12134

5.2.1 Resultados del caso de estudio 1

Para los controladores descritos en subsección 5.1.1, la muestra de datos obtenida y la verificación en lazo cerrado utiliza los parámetros a para la función $h_d(\theta_1, a)$ que se muestra en la Tabla 5.2. En la Tabla 5.3 se proporcionan los extremos de los intervalos de tiempo en los que opera cada subcontrolador que se encuentran definidos en (5.5), en donde el instante de tiempo t_4 indica el momento en que el robot termina de realizar el paso. El primer renglón de la Tabla 5.3 muestra los dominios en el tiempo en que los subcontroladores difusos operan y su base de reglas difusas tiene la estructura que se muestra en (5.3); el segundo renglón muestra los dominios en el tiempo en que los subcontroladores difusos operan y su base de reglas difusas tiene la estructura que se muestra en (5.4).

Los parámetros de las funciones de membresía que denotan a los conjuntos difusos usados en la base de reglas difusas, se proporcionan en Apéndice B.

De la Figura 5.3 a la Figura 5.6 se presentan las trayectorias del vector de estados, de la salida y las entradas de control obtenidas de realizar la simulación del sistema en lazo cerrado hasta ejecutar un paso. El controlador utiliza reglas difusas que tienen la forma definida en (5.4).

De la Figura 5.7 a la Figura 5.10 se presentan las trayectorias del vector de estados, de la salida y las entradas de control obtenidas de realizar la simulación del sistema en lazo cerrado hasta ejecutar un paso. El controlador utiliza reglas difusas que tienen la forma definida en (5.3).

En los controladores probados en lazo cerrado, las trayectorias obtenidas muestran correspondencia con las presentadas en la Figura 4.9 a la Figura 4.11 dentro del intervalo de tiempo que representa cuando ejecuta el primer paso. Las trayectorias del vector de estado son iguales para los dos controladores probados a pesar de que para las trayectorias que se muestran desde la Figura 5.7 a la Figura 5.10 el controlador no recibe de retroalimentación las velocidades angulares. Las trayectorias de la salida se presentan convergencia a cero y una variación pequeña en los últimos instantes de tiempo, que es más notoria en la Figura 5.9 para el controlador que no recibe de retroalimentación las velocidades angulares.

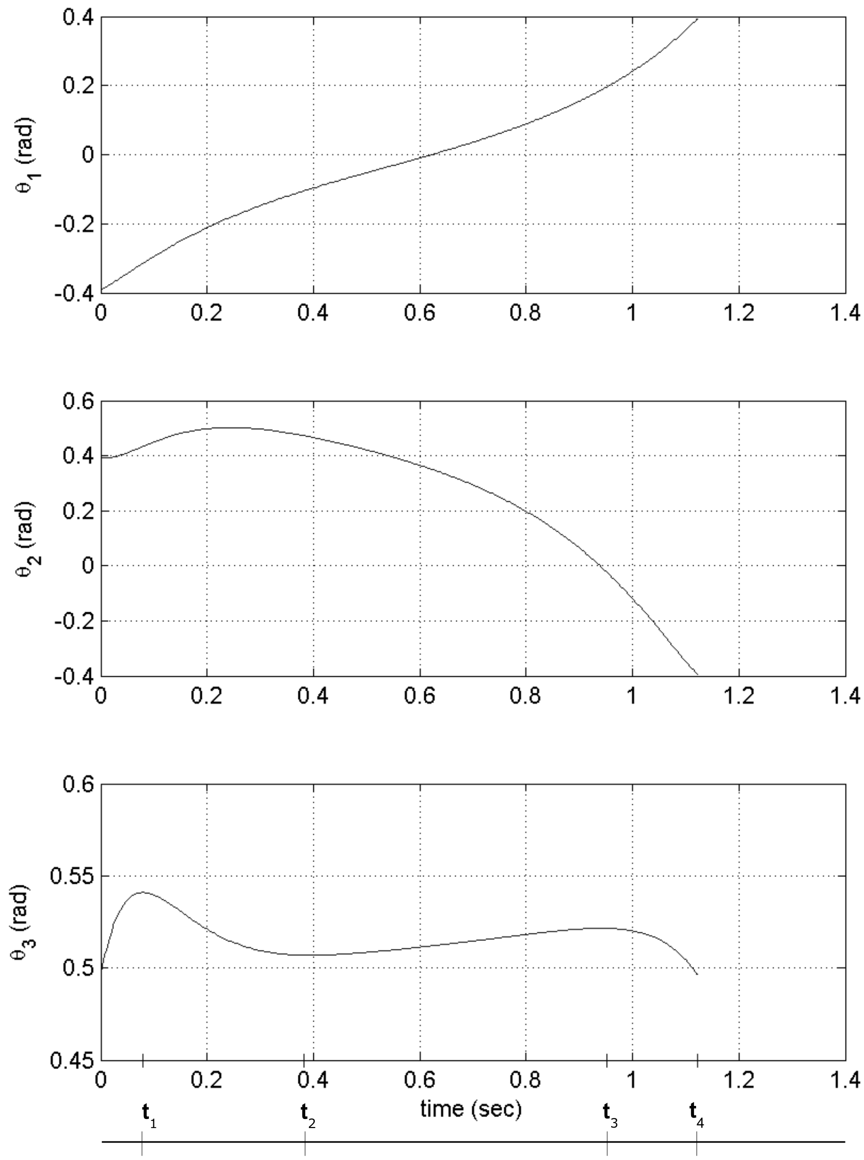

Figura 5.3. Trayectorias de las posiciones angulares usando el controlador difuso con reglas de la forma (5.4).

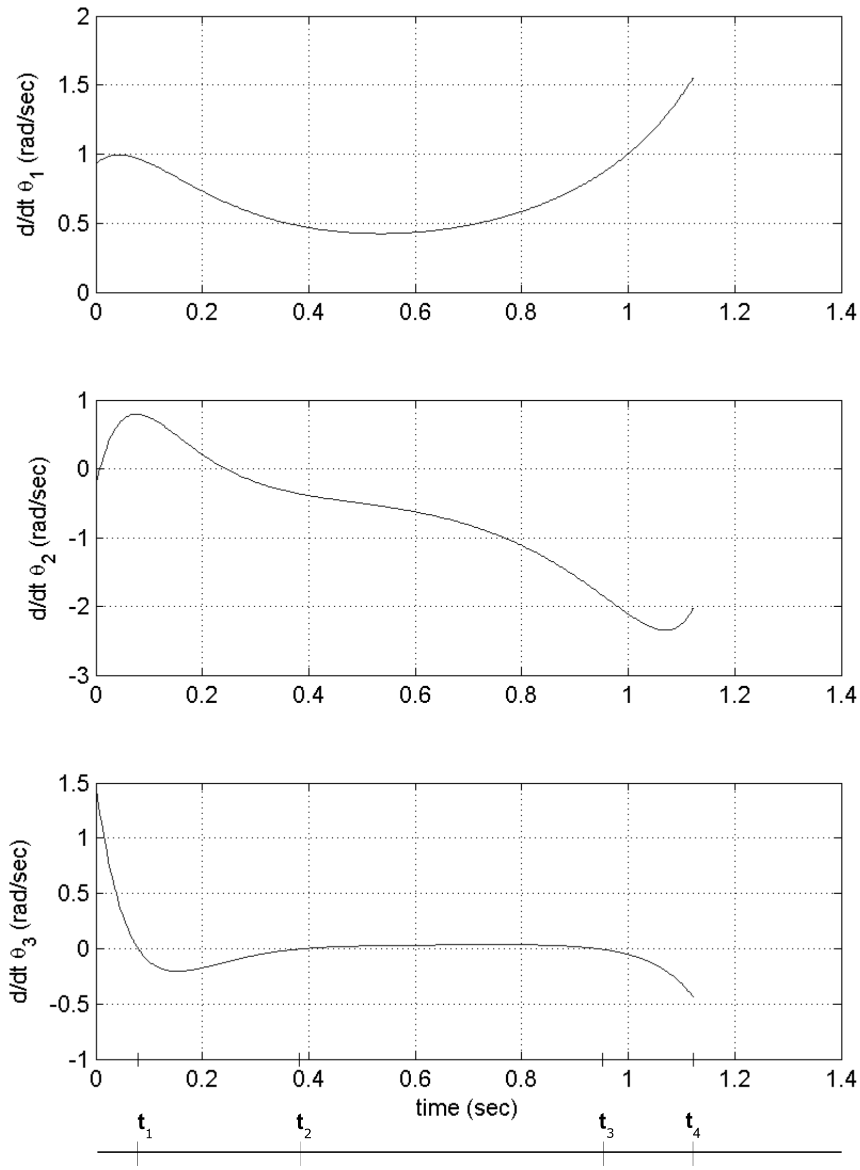

Figura 5.4. Trayectorias de las velocidades angulares usando el controlador difuso con reglas de la forma (5.4).

5.2.2 Resultados del caso de estudio 2

En el caso de controladores obtenidos mediante la configuración descrita y definición de los pares que se mencionó en la subsección 5.1.2, dos subcontroladores con 256

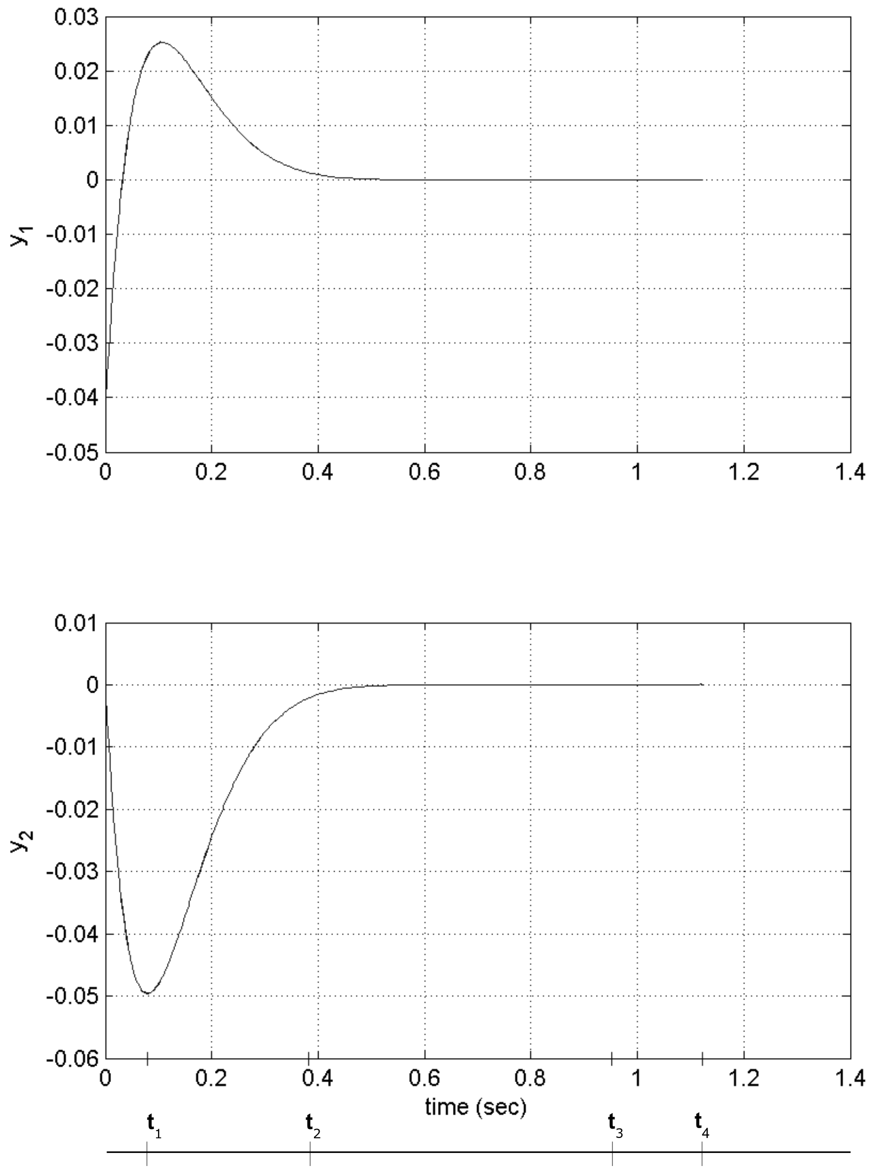

Figura 5.5. Trayectorias de la salida usando el controlador difuso con reglas de la forma (5.4).

reglas que tienen la forma (5.4) son obtenidos. Se utiliza la misma muestra de datos, por lo que debe desempeñar la misma tarea. Por ello, se realiza la simulación del sistema en lazo cerrado para realizar un paso con los mismos parámetros del robot y los

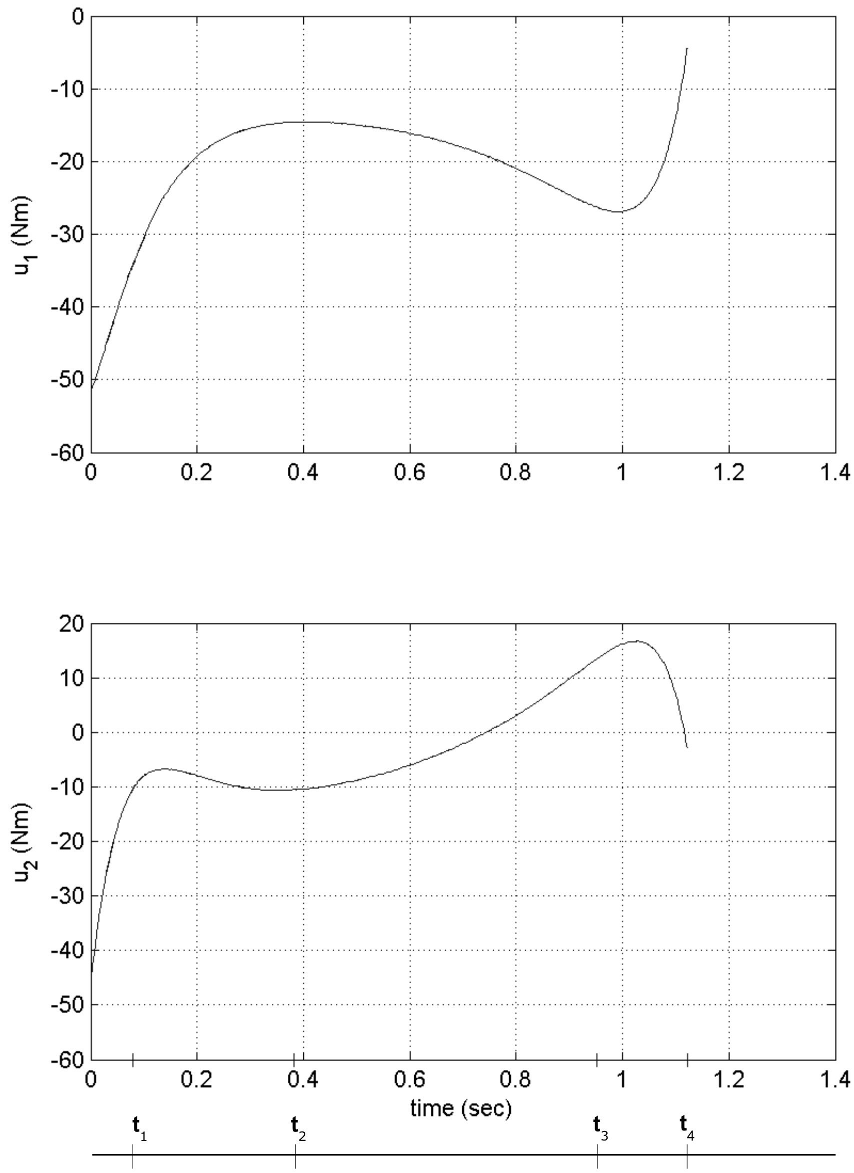

Figura 5.6. Señales de control usando el controlador difuso con reglas de la forma (5.4)

mismos parámetros en la salida que describen el movimiento deseado. Se muestran las trayectorias del vector de estados en la Figura 5.11 y la Figura 5.12; las trayectorias de las entradas de control en la Figura 5.13 y la Figura 5.14; las trayectorias de la salida

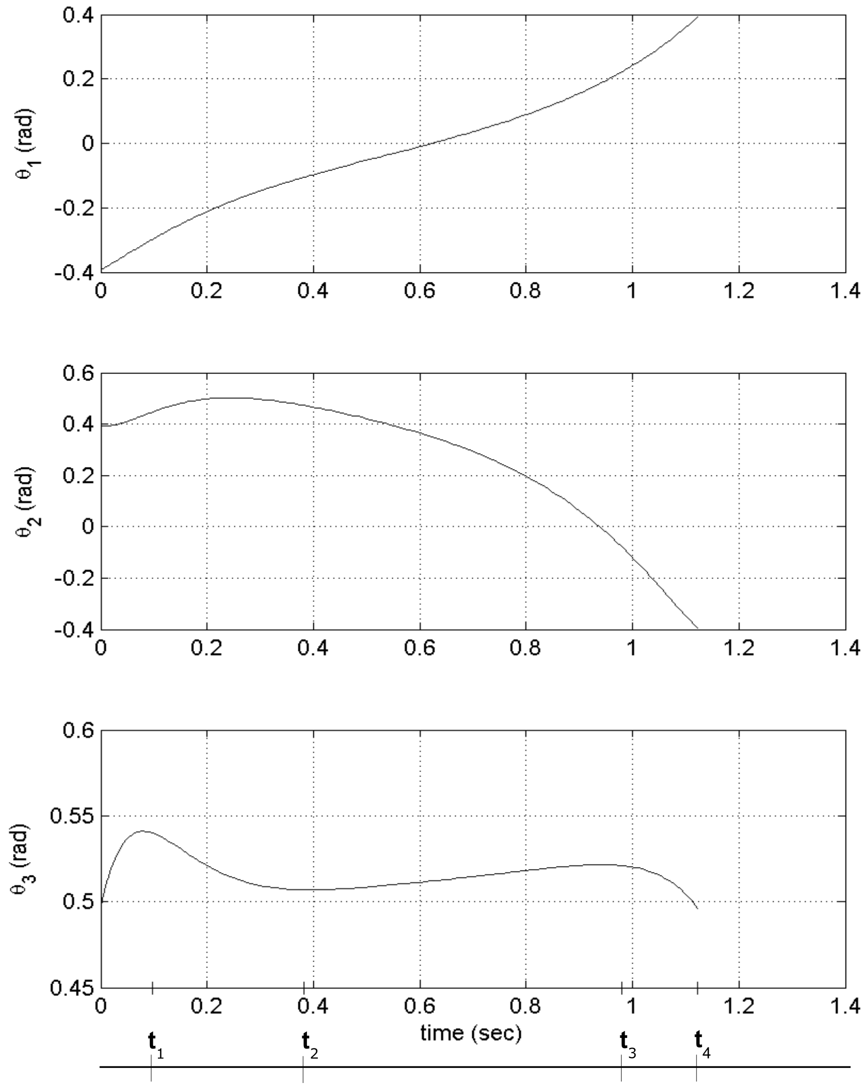

Figura 5.7. Trayectorias de las posiciones angulares usando el controlador difuso con reglas de la forma (5.3).

en la Figura 5.15 y la Figura 5.16.

En las trayectorias de la salida se presenta convergencia a cero, por lo que se afirma que el movimiento deseado fue obtenido muy a pesar de que se presentan oscilaciones de amplitud pequeña en las trayectorias de la salida durante los últimos instantes de

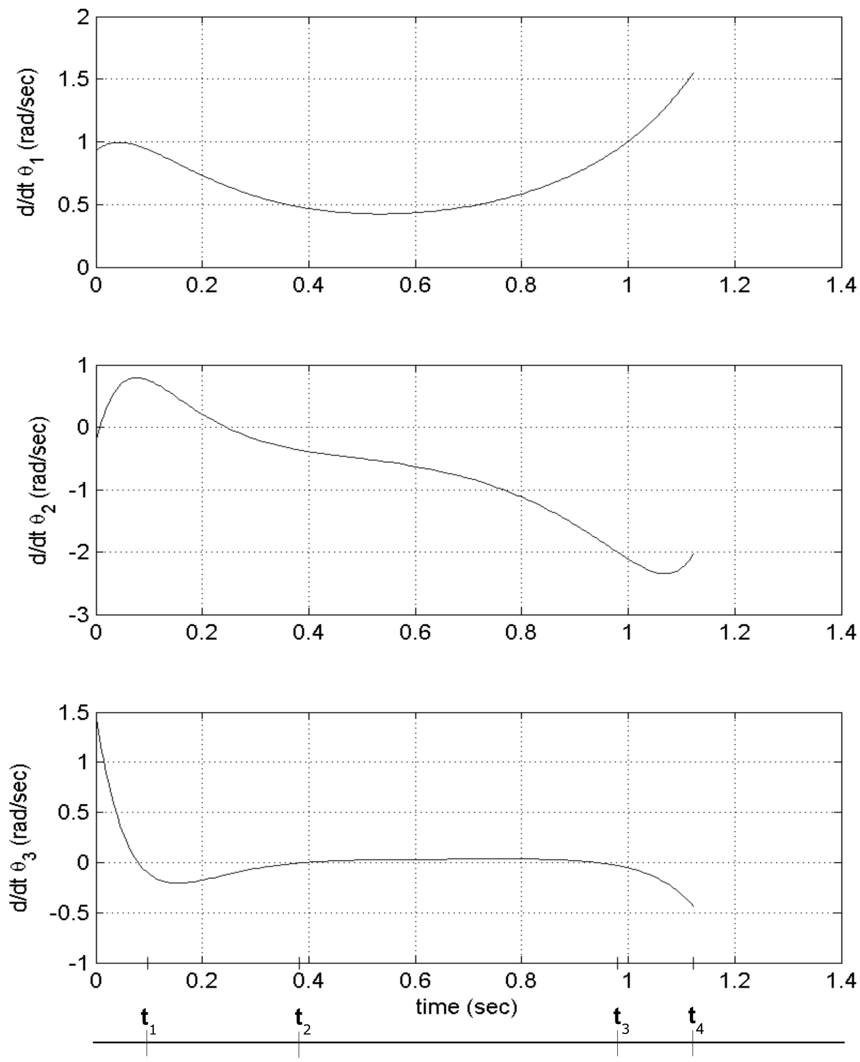

Figura 5.8. Trayectorias de las velocidades angulares usando el controlador difuso con reglas de la forma (5.3).

tiempo, comportamiento que es notorio para el controlador que no recibe de retroalimentación las velocidades angulares como lo muestran la Figura 5.16.

La Figura 5.11 y la Figura 5.12 muestran que las trayectorias de los estados obtenidas al ejecutar el sistema en lazo cerrado expresan el mismo movimiento obtenido en el caso

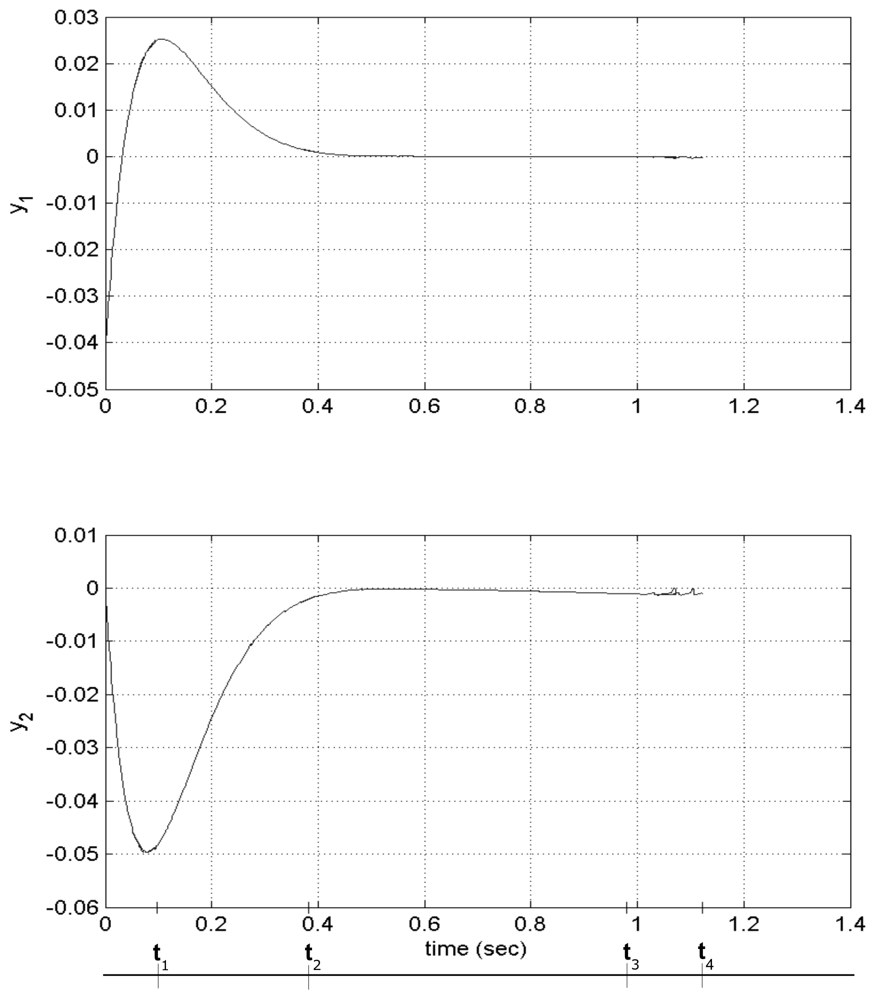

Figura 5.9. Trayectorias de la salida usando el controlador difuso con reglas de la forma (5.3).

de estudio 1. Como muestra la Figura 5.15 y la Figura 5.16 la trayectoria de la salida converge a cero por lo que satisface el objetivo de control logrando en el robot que desarrolle el movimiento deseado. Las trayectorias que corresponden a las entradas de control y a la salida presentan trazos irregulares entre 0.3 y 0.4 segundos y 0.9 y 1 segundos que son atribuidos al método numérico. El comportamiento oscilatorio con amplitud pequeña se observa en el final de la trayectoria de salida que es notorio en la

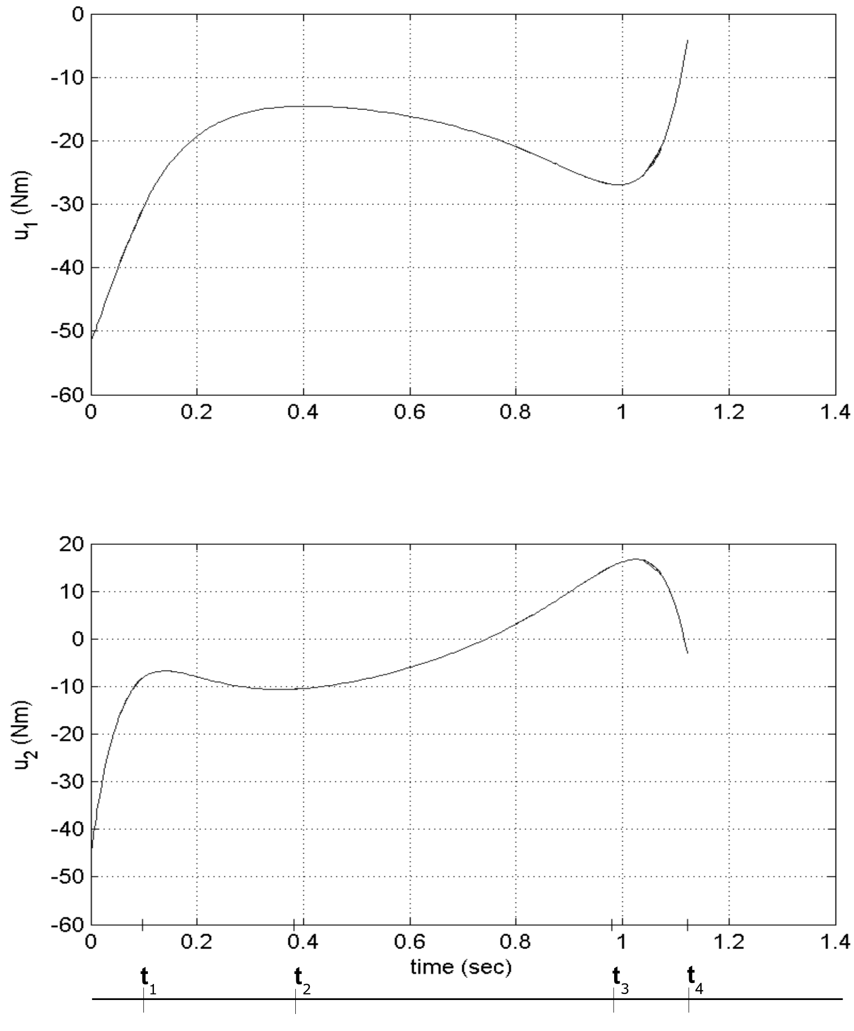

Figura 5.10. Señales de control usando el controlador difuso con reglas de la forma (5.3).

Figura 5.16. Se atribuye a una falta de reglas difusas que eviten que la amplitud tenga crecimiento.

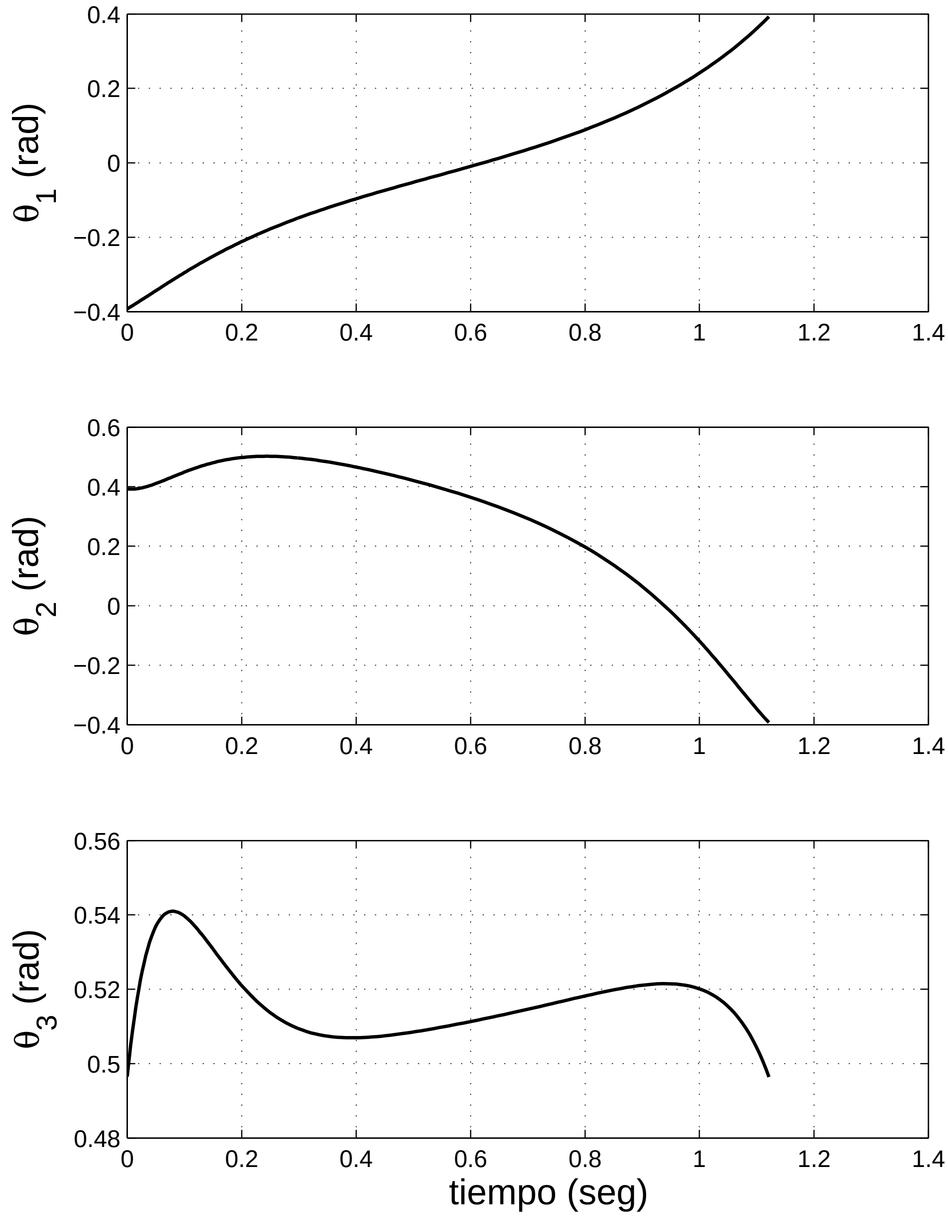

Figura 5.11. Trayectorias de las posiciones angulares usando el controlador difuso de 5.1.2.

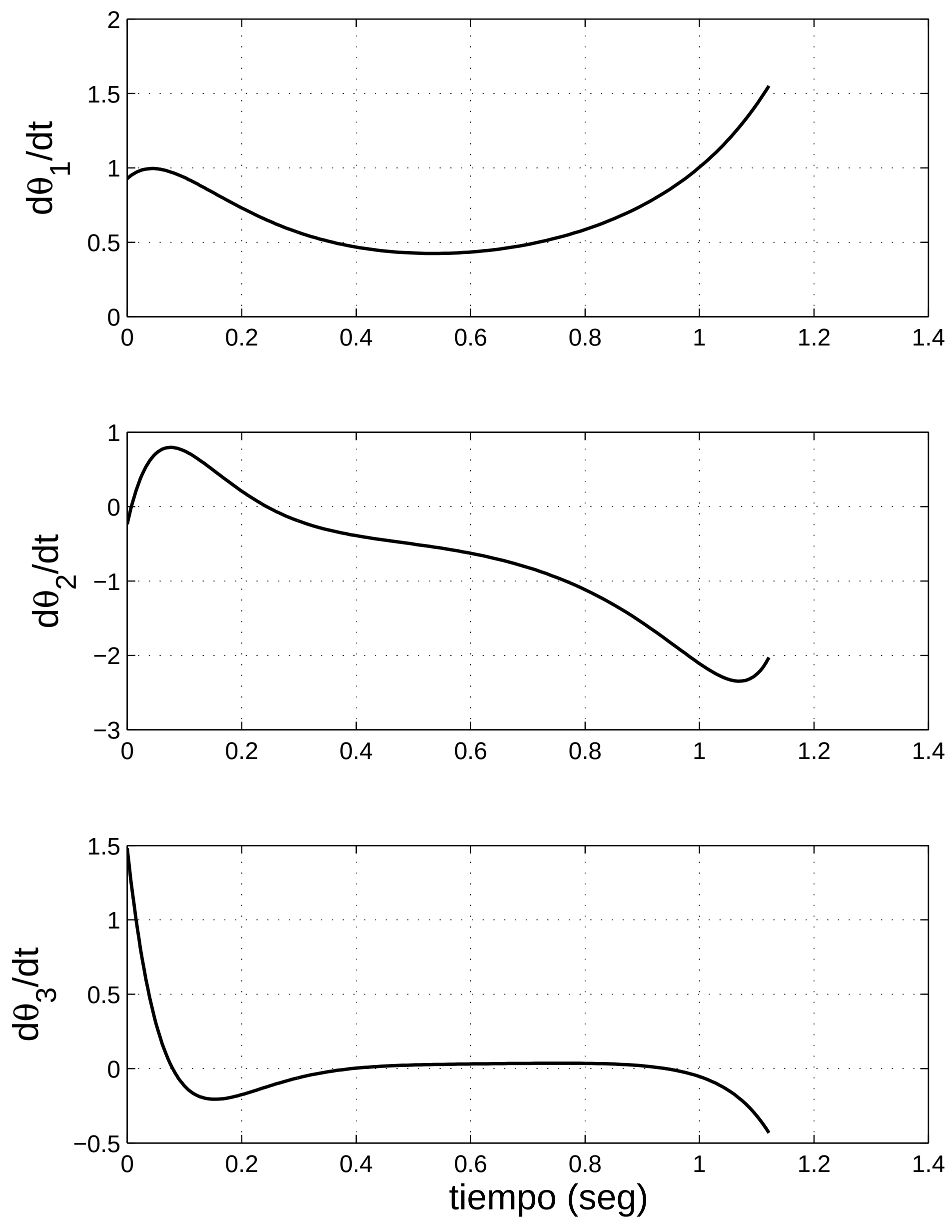

Figura 5.12. Trayectorias de las velocidades angulares usando el controlador difuso de 5.1.2.

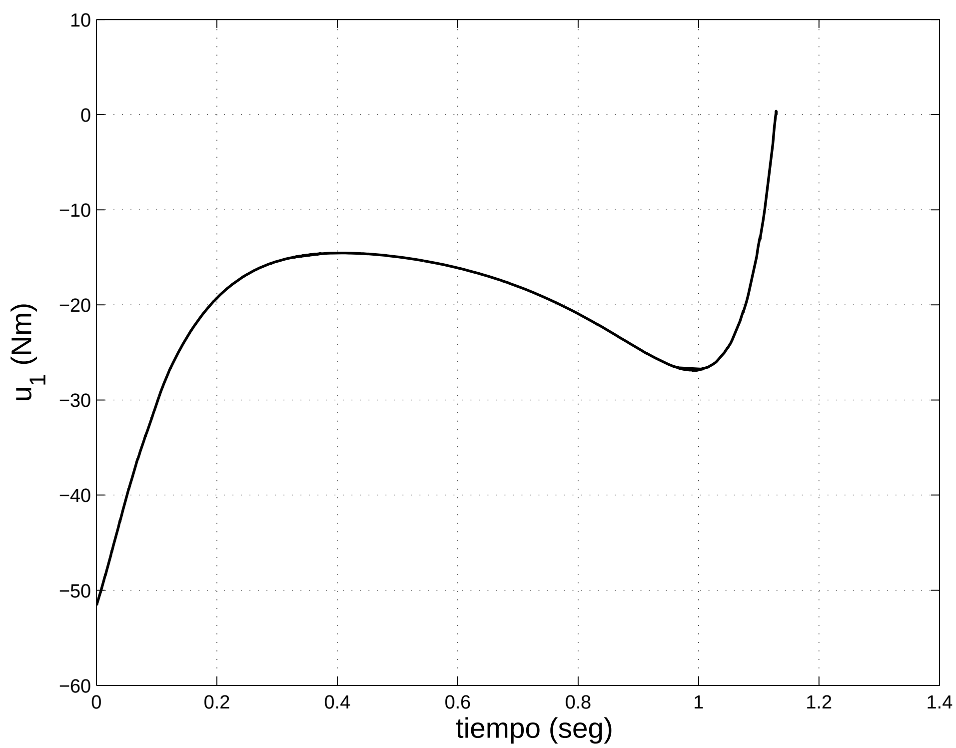

Figura 5.13. Primera señal de control usando el controlador difuso de 5.1.2.

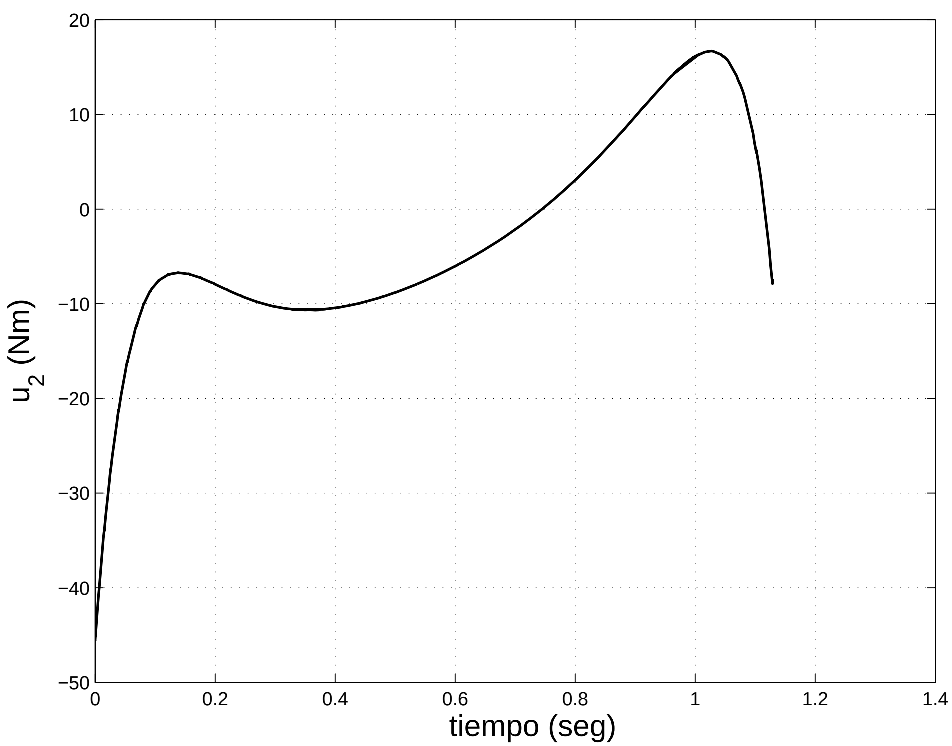

Figura 5.14. Segunda señal de control usando el controlador difuso de 5.1.2.

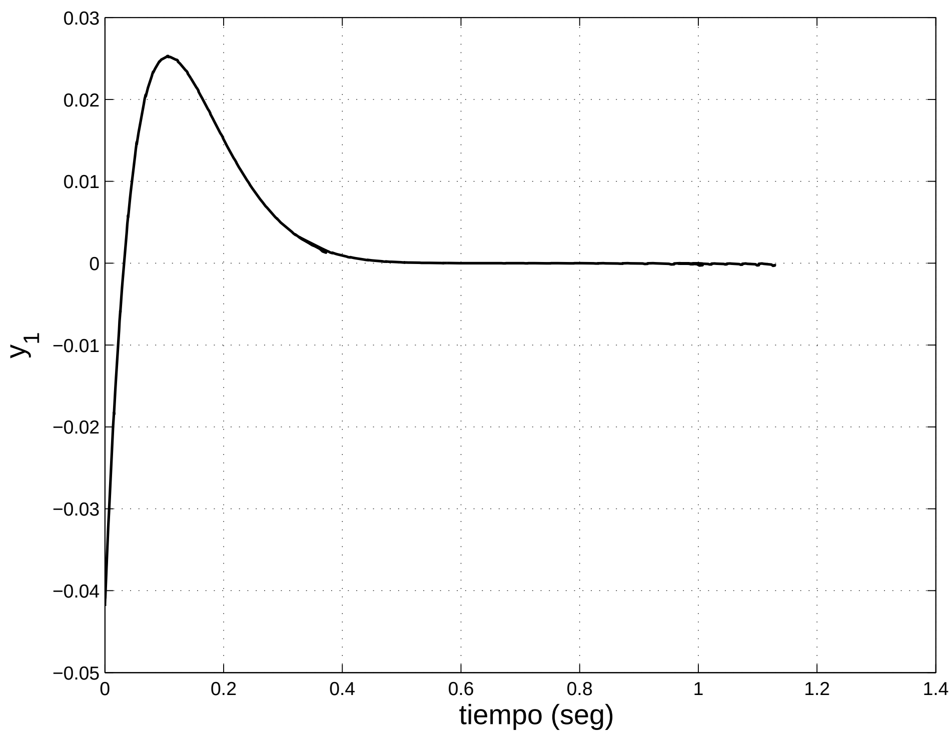

Figura 5.15. Trayectoria de la salida usando el controlador difuso de 5.1.2.

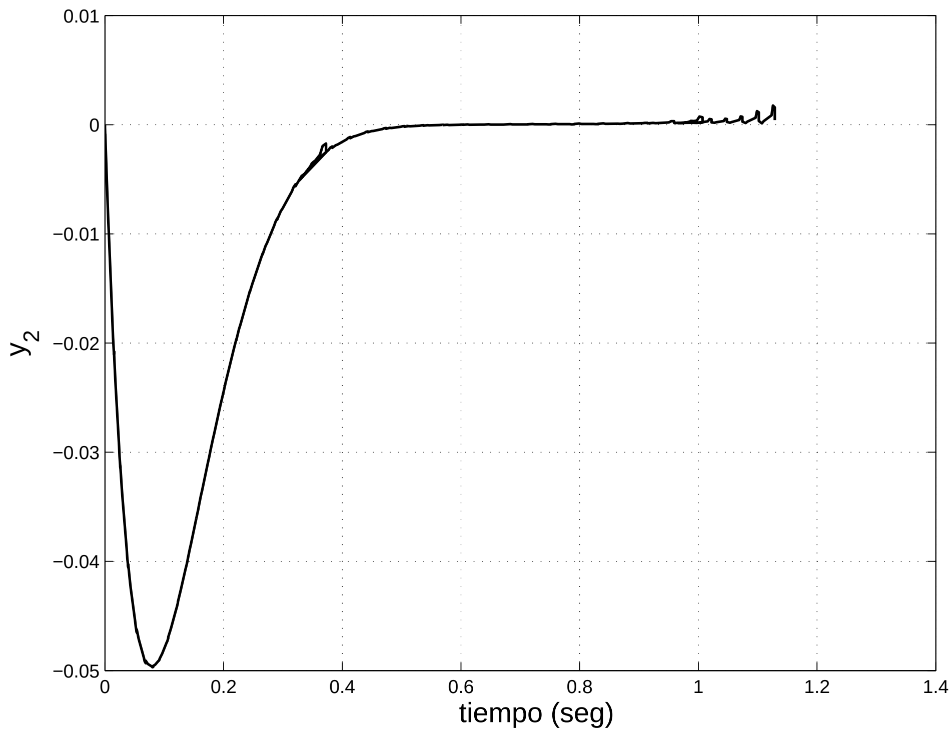

Figura 5.16. Trayectoria de la salida usando el controlador difuso de 5.1.2.

Capítulo 6

Conclusiones

En esta tesis se aborda el problema de propiciar movimientos de caminata en un robot bípedo sin pies, sistema con grado de subactuación uno, que debido a la naturaleza de la caminata, su dinámica se representa mediante un modelo matemático híbrido: un modelo continuo que representa una fase de movimiento libre, eventos discretos que describen contactos del extremo de la pierna con la superficie donde camina y que a través de reglas permite la transición entre ellos.

Los movimientos de caminata que se enfoca este trabajo son aquellos que muestran un comportamiento periódico en las trayectorias de las variables de estado. El problema de control no es trivial pues requiere determinar los movimientos viables para el mecanismo y una ley de control que realice estabilización orbital garantizando propiedades de estabilidad. Los métodos de computación inteligente se han aplicado para la síntesis de movimientos coordinados y el control de movimiento en robots humanoides cuyas trayectorias no requieren exhibir periodicidad. En este trabajo, los métodos de computación inteligente ayudan a la síntesis de controladores difusos tipo Takagi-Sugeno-Kang que induce movimientos de caminata periódica para el robot bípedo descrito en el Capítulo 3.

En el desarrollo de este trabajo se obtienen movimientos de caminata que se reportan en el Capítulo 4, donde se toma como base las contribuciones relacionadas en definir movimientos coordinados como funciones de tipo polinomial parametrizadas en una de las coordenadas de configuración del robot (posición angular de la pierna de soporte).

Para determinar los polinomios adecuados se plantea un problema de optimización cuya solución indica los parámetros de los polinomios que satisfacen minimizar la función de costo que representa la energía de control promedio ejercida durante la ejecución de un paso, restringiendo el espacio de solución a aquellos parámetros que satisfacen además las suposiciones del robot y que la dinámica del sistema en lazo cerrado de (Westervelt *et al.* (2007)), exhibe trayectorias periódicas. Se implementa un algoritmo genético para resolver el problema de optimización restringida, verificado la existencia de un punto fijo con el algoritmo de (Grizzle *et al.* (2001)) que calcula numéricamente el mapa de retorno de Poincaré que considera el modelo híbrido. Los parámetros de los polinomios que se encontraron al realizar ejecuciones independientes del algoritmo bajo las mismas condiciones de simulación, proveen movimientos en el robot bípedo cuyas trayectorias tienden a ser periódicas, es decir, se observa convergencia hacia una órbita periódica. El algoritmo logra obtener parámetros cuya energía de control es menor pero utiliza mayor tiempo para converger (en el orden de los milisegundos) al movimiento periódico. Esto lleva a revisar la viabilidad de una reformulación del problema de optimización que considere un tiempo de convergencia.

Enseguida en el Capítulo 5 se considera el diseño de un controlador para coordinar el movimiento del robot que es representado como una función parametrizada por la posición angular de la pierna de soporte del robot en lugar de ser con respecto al tiempo. Se muestra la síntesis de un controlador difuso que toma como retroalimentación la salida que tiene codificada la posición del robot durante un paso y el vector de estado del robot, el controlador difuso proporciona las entradas de control tal que al anular la salida se garantice que el robot desarrolla el movimiento deseado. A través de ANFIS se obtienen los parámetros que caracterizan tres modelos difusos tipo Takagi-Sugeno-Kang que relacionan los estados, salidas y entradas de control que se utilizan para el mismo problema de control de movimiento. El primer y segundo modelo representan una ley de control definida en cuatro tramos de la fase de movimiento libre, el primer modelo recibe como retroalimentación el vector de estado completo, el modelo dos tiene como retroalimentación posiciones; el tercer modelo representa una ley de control para toda la fase libre donde el vector de estados completo es el que recibe como retroalimentación. Las trayectorias del vector de estados obtenidas al probar los controladores en lazo cerrado son bastante similares a las producidas en (Grizzle *et al.* (1999)), las trayectorias de la función de salida muestran anularse aproximadamente a la mitad del tiempo de la fase libre, manteniendo una muy pequeña oscilación en los últimos instantes de la simulación y que es notoria en la trayectoria de la salida $y_2(t)$ cuando se utiliza el tercer modelo. Se atribuye este resultado a que puede hacer falta en este modelo reglas difusas que ayuden proporcionar la entrada de control adecuada tal que se anule la salida de una forma suave. Sin embargo la magnitud de las oscilaciones son pequeñas, por lo tanto el controlador satisface el objetivo de control.

Aunque los resultados permiten elevar un poco el nivel de confianza para alentar el uso de métodos de computación inteligente para continuar en esta línea de trabajo, todavía quedan problemas que no fueron resueltos y alternativas que pueden ser exploradas. Se puede advertir que de aumentar la amplitud en las oscilaciones en la salida se puede esperar un efecto que provocará inestabilidad en pasos a futuro lo que llevan a requerir un esquema de adaptación en línea del controlador o de los parámetros que describen el movimiento deseado en la salida tal que garantice estabilización orbital, esto motiva a buscar funciones apropiadas que caractericen a las restricciones holónomicas e involucrar otras técnicas de control, o en primera instancia, determinar si solo ajustes en los parámetros del modelo difuso es suficiente para resolver el problema. Para obtener los movimientos de referencia definidos como funciones parametrizadas en términos del estado del robot implican una tarea ardua ya que deben cumplir que el estado sea estrictamente monótono, lo que motiva a desarrollar leyes de control inteligente para seguimiento de un movimiento de referencia en términos del tiempo.

Referencias

Aguilar, L., Boiko, I., Fridman, L., y Iriarte, R. (2009). Generating self-excited oscillations for underactuated mechanical systems via two relay controller. *International Journal of Control*, **82**(9): 1678–1691.

Ahtiwas, O.-M., Abdulmuin, M.-Z., y S.-F., S. (2002). A neural-fuzzy logic approach for modeling and control of nonlinear systems. En *IEEE International Symposium on Intelligent Control, 2002.*, páginas 270–275.

Bessonnet, G., Seguin, P., y Sardain, P. (2005). A Parametric Optimization Approach to Walking Pattern Synthesis. *The International Journal of Robotics Research*, **24**(7): 523–536.

Cabodevila, G. y Abba, G. (1997). Quasi optimal gait for a biped robot using genetic algorithm. En *IEEE International Conference on Systems, Man, and Cybernetics: 'Computational Cybernetics and Simulation'.*, Vol. 4, páginas 3960–3965.

Canudas-de Wit, C. (2004). On the concept of virtual constraints as a tool for walking robot control and balancing. *Annual Reviews in Control*, **28**(2): 157–166.

Canudas-de Wit, C., Espiau, B., y Urrea, C. (2002). Orbital stabilization of underactuated mechanical systemss. En *Proceedings of IFAC '02 15th World Congress IFAC*.

Capi, G., Nasu, Y., Barolli, L., Mitobe, K., y Takeda, K. (2001). Application of genetic algorithms for biped robot gait synthesis optimization during walking and going upstairs. *Advanced Robotics*, **15**(6): 675–694.

Cardenas-Maciel, S., Castillo, O., Aguilar, L., y Rodríguez-Díaz, A. (2009a). Genetic optimization for the design of walking patterns of a biped robot. En O. Castillo, W. Pedrycz, y J. Kacprzyk, editores, *Evolutionary Design of Intelligent Systems in Modeling, Simulation and Control*, Vol. 257 de *Studies in Computational Intelligence*, páginas 259–271. Springer Berlin Heidelberg. ISBN 978-3-642-04513-4.

Cardenas-Maciel, S., Castillo, O., Aguilar, L., y Castro, J. (2010). A t-s fuzzy logic controller for biped robot walking based on adaptive network fuzzy inference system. En *The 2010 International Joint Conference on Neural Networks (IJCNN)*, páginas 1–8.

Cardenas-Maciel, S., Castillo, O., y Aguilar, L. (2011a). Neuro-fuzzy based output feedback controller design for biped robot walking. En O. Castillo, J. Kacprzyk, y W. Pedrycz, editores, *Soft Computing for Intelligent Control and Mobile Robotics*, Vol. 318 de *Studies in Computational Intelligence*, páginas 423–444. Springer Berlin Heidelberg. ISBN 978-3-642-15533-8.

Cardenas-Maciel, S.-L., Castillo, O., y Aguilar, L.-T. (2009b). *Genetic Optimization for the design of Walking Patterns of a Biped Robot*. Evolutionary Design of Intelligent Systems in Modeling, Simulation and Control (Studies in Computational Intelligence). Springer, Berlin.

Cardenas-Maciel, S. L., Castillo, O., y Aguilar, L. T. (2011b). Generation of walking periodic motions for a biped robot via genetic algorithms. *Applied Soft Computing*, **11**(8): 5306 – 5314.

Chevallereau, C. y Aoustin, Y. (2001). Optimal reference trajectories for walking and running of a biped robot. *Robotica*, **19**(5): 557–569.

Choi, S.-H., Choi, Y.-H., y Kim, J.-G. (1999). Optimal walking trajectory generation for a biped robot using genetic algorithm. *Proceedings of IROS '99. IEEE/RSJ International Conference on Intelligent Robots and Systems 1999*, **3**: 1456–1461.

Dasgupta, A. y Nakamura, Y. (1999). Making feasible walking motion of humanoid robots from human motion capture data. En *Proceedings of IEEE International Conference on Robotics and Automation,*, Vol. 2, páginas 1044–1049.

Denk, J. y Schmidt, G. (2003). Synthesis of Walking Primitive Databases for Biped Robots in 3D-Environments. En *Proceedings of the IEEE International Conference on Robotics and Automation (ICRA2003)*, Taipei, Taiwan.

Djoudi, D., Chevallereau, C., y Aoustin, Y. (2005). Optimal reference motions for walking of a biped robot. En *Proceedings of ICRA 2005, the 2005 IEEE International Conference on Robotics and Automation.*, páginas 2002–2007.

Ferreira, J., Amaral, T., Pires, V., Crisostomo, M., y Coimbra, A. (2004). A neural-fuzzy walking control of an autonomous biped robot. En *Proceedings of World Automation Congress, 2004.*, Vol. 15, páginas 253–258.

Goldberg, D. E. (1989). *Genetic Algorithms in Search, Optimization and Machine Learning*. Addison-Wesley Longman Publishing Co., Inc., Boston, MA, USA. ISBN 0201157675.

Grizzle, J. (2007). Feedback control of dynamic bipedal robot locomotion book webpage. Reporte técnico.

Grizzle, J., Abba, G., y Plestan, F. (1999). Proving asymptotic stability of a walking cycle for a 5 DOF biped robot model. En *International Conference on Climbing and Walking Robots*, Angleterre, Portsmouth.

Grizzle, J., Abba, G., y Plestan, F. (2001). Asymptotically stable walking for biped robots: analysis via systems with impulse effects. *IEEE Transactions on Automatic Control*, **46**(1): 51–64.

Grizzle, J., Moog, C., y Chevallereau, C. (2005). Nonlinear control of mechanical systems with an unactuated cyclic variable. *IEEE Transactions on Automatic Control*, **50**(5): 559–576.

Hirai, K., Hirose, M., Haikawa, Y., y Takenaka, T. (1998). The development of honda humanoid robot. En *Proceedings of 1998 IEEE International Conference on Robotics and Automation*, Vol. 2, páginas 1321–1326.

Holland, J. M. (1975). *Adaptation in Natural and Artificial Systems*. University of Michigan Press, Ann Arbor, MI.

Huang, Q., Yokoi, K., Kajita, S., Kaneko, K., Arai, H., Koyachi, N., y Tanie, K. (2001). Planning walking patterns for a biped robot. *IEEE Transactions on Robotics and Automation*, **17**(3): 280–289.

Hurmuzlu, Y. y Marghitu, D. (1994). Rigid body collisions of planar kinematic chains with multiple contact points. *Int. J. Robot Res.*, **13**(1): 82–92.

Jang, J.-S. (1993). Anfis: adaptive-network-based fuzzy inference system. *IEEE Transactions on Systems, Man and Cybernetics.*, **23**(3): 665–685.

Kajita, S., Kanehiro, F., Kaneko, K., Fujiwara, K., Harada, K., Yokoi, K., y Hirukawa, H. (2003). Biped walking pattern generation by using preview control of zero-moment point. *Proceedings of ICRA'03. IEEE International Conference on Robotics and Automation 2003*, **2**: 1620–1626.

Katic, D. y Vukobratovic, M. (2003). Survey of intelligent control techniques for humanoid robots. *Journal of Intelligent and Robotic Systems*, **37**(2): 117–141.

Kelly, R., Santibañez, R., y Loria, A. (2005). *Control of Robots Manipulators in Joint Space*. Springer-Verlag London Limited.

Khalil, H. K. (2002). *Nonlinear Systems*. Prentice Hall, tercero edición. ISBN 0-13-067389-7.

Kuo, A. (2007). Choosing your steps carefully. *IEEE Robotics & Automation Magazine*, **14**(2): 18–29.

La Hera, P., Shiriaev, A., Freidovich, L., Mettin, U., y Gusev, S. (2013). Stable walking gaits for a three-link planar biped robot with one actuator. *Robotics, IEEE Transactions on*, **29**(3): 589–601.

Lee, J.-Y. y Lee, J.-J. (2004). Optimal walking trajectory generation for a biped robot using multi-objective evolutionary algorithm. En *Control Conference, 2004. 5th Asian*, Vol. 1, páginas 357–364.

Mamdani, E. (1976). Advances in the linguistic synthesis of fuzzy controllers. *J. Man-Machine Studies*, **8**: 669–678.

Mamdani, E. y Assilian, S. (1975). An experiment in linguistic synthesis with fuzzy logic controller. *J. Man- Machine Studies*, **7**(1): 1–13.

McGeer, T. (1990). Passive dynamic walking. *Int. J. Robot Res.*, **9**(2): 62–82.

Mendel, J. (2001). *Uncertain Rule-Based Fuzzy Logic Systems: Introduction and New Directions*. Prentice Hall, Upper Saddle River, NJ.

Mettin, U., La Hera, P., Freidovich, L., y Shiriaev, A. (2007). Generating human-like motions for an underactuated three-link robot based on the virtual constraints approach. En *46th IEEE Conference on Decision and Control*, páginas 5138–5143.

Michalewicz, Z. (1994). *Genetic Algorithms + Data Structures = Evolution Programs*. Springer-Verlag New York, Inc., Secaucus, NJ, USA.

Park, J. H. y Choi, M. (2004). Generation of an optimal gait trajectory for biped robots using a genetic algorithm. *JSME International Journal Series C Mechanical Systems, Machine Elements and Manufacturing*, **47**(2): 715–721.

Prabu, D., Kumar, S., y Prasad, R. (2008). Dynamic control of three-link scara manipulator using adaptive neuro fuzzy inference system. En *ICNSC 2008. IEEE International Conference on Networking, Sensing and Control.*, páginas 1609–1614.

Rumelhart, D. E., McClelland, J. L., y PDP Research Group, C., editores (1986). *Parallel Distributed Processing: Explorations in the Microstructure of Cognition, Vol. 1: Foundations*. MIT Press, Cambridge, MA, USA. ISBN 0-262-68053-X.

Sato, T., Sakaino, S., Ohashi, E., y Ohnishi, K. (2011). Walking trajectory planning on stairs using virtual slope for biped robots. *IEEE Transactions on Industrial Electronics*, **58**(4): 1385–1396.

Shieh, M.-Y., Chang, K.-H., Chuang, C.-Y., Chiou, J.-S., y Li, J.-H. (2007). Anfis based controller design for biped robots. En *Proccedings of 4th. IEEE International Conference on Mechatronics*, páginas 1–6.

Shih, C., Li, Y. Z., Churng, S., Lee, T.-T., y Gruver, W. (1990). Trajectory synthesis and physical admissibility for a biped robot during the single-support phase. En *Proceedings of 1990 IEEE International Conference on Robotics and Automation.*, Vol. 3, páginas 1646–1652.

Shiriaev, A., Perram, J., y Canudas-de Wit, C. (2005). Constructive tool for orbital stabilization of underactuated nonlinear systems: Virtual constraints approach. *IEEE Transactions on Automatic Control*, **50**(8): 1164–1176.

Sugeno, M. y Kang, T. (1988). Structure identification of fuzzy model. *Fuzzy Sets and Systems*, **28**: 15–,3,3.

Takagi, T. y Sugeno, M. (1985). Fuzzy identification of systems and its application to modeling and control. *IEEE Trans. on Systems, Man and Cybernetics*, **15**: 116–132.

Tsukamoto, Y. (1979). *Advances in fuzzy set theory and applications*, capítulo An approach to fuzzy reasoning method, páginas 137–149. North-Holland.

Vukobratovic, M. y Juricic, D. (1969). Contribution to the synthesis of biped gait. *IEEE Transactions on Biomedical Engineering*, **16**(1): 1–6.

Vundavilli, P. y Pratihar, D. (2010). *Intelligent Autonomous Systems*, Vol. 275 de *Studies in Computational Intelligence*, capítulo Gait Planning of Biped Robots Using Soft Computing: An Attempt to Incorporate Intelligence, páginas 57–85. Springer Berlin Heidelberg.

Wang, T. y Chevallereau, C. (2011). Stability analysis and time-varying walking control for an under-actuated planar biped robot. *Robotics and Autonomous Systems*, **59**(6): 444 – 456.

Werbos, P. (1974). *Beyound regression: New tools for prediction and analysis in the behavioral sciences.*. Tesis de doctorado, Harvard.

Westervelt, E. R., Grizzle, J. W., Chevallereau, C., Choi, J.-H., y Morris, B. (2007). *Feedback Control of Dynamic Bipedal Robot Locomotion*, capítulo Systematic Design of Within-Stride Feedback Controllers for Walking, páginas 137–190. Taylor & Francis/CRC.

Zadeh, L. (1973). Outline of a new approach to the analysis of complex systems an decision processes. *IEEE Trans. on Systems, Man and Cybernetics*, **3**(1): 28–44.

Zadeh, L. (1996). Fuzzy logic = computing with words. *IEEE Trans. Fuzzy Syst.*, **4**(2): 103–111.

Zadeh, L. A. (1965). Fuzzy sets. *Information and Control*, **8**: 338–353.

Zadeh, L. A. (1975a). The concept of a linguistic variable and its application to approximate reasoning - i. *Inf. Sci.*, **8**(3): 199–249.

Zadeh, L. A. (1975b). The concept of a linguistic variable and its application to approximate reasoning - ii. *Inf. Sci.*, **8**(4): 301–357.

Apéndice A

Modelo Dinámico del robot bípedo

Este apéndice completa el modelo del robot bípedo dado en el Capítulo 3 en las ecuaciones (3.1). La notación que se da a continuación es la que se utiliza en esta sección:

$$\begin{aligned} s_{1j} &= \sin(\theta_1 - \theta_j), j \in \{2, 3\} \\ c_{1j} &= \cos(\theta_1 - \theta_j), j \in \{2, 3\} \end{aligned}$$

A.1 Modelo de fase libre

$$M = \begin{bmatrix} (\frac{5}{4}m + M_H + M_T)r^2 & -\frac{1}{2}mr^2c_{12} & M_Trlc_{13} \\ -\frac{1}{2}mr^2c_{12} & \frac{1}{4}mr^2 & 0 \\ M_Trlc_{13} & 0 & M_Tl^2 \end{bmatrix}$$

$$C = \begin{bmatrix} 0 & -\frac{1}{2}mr^2s_{12}\dot{\theta}_2 & M_Trls_{13}\dot{\theta}_3 \\ \frac{1}{2}mr^2s_{12}\dot{\theta}_1 & 0 & 0 \\ -M_Trls_{13}\dot{\theta}_1 & 0 & 0 \end{bmatrix}$$

$$G = \begin{bmatrix} -\frac{1}{2}g(2M_H + 3m + 2M_T)r\sin(\theta_1) \\ \frac{1}{2}gmr\sin(\theta_2) \\ -gM_Tl\sin(\theta_3) \end{bmatrix}$$

$$B = \begin{bmatrix} -1 & 0 \\ 0 & -1 \\ 1 & 1 \end{bmatrix}$$

A.2 Modelo de impacto

La matriz de Inercia M_e de la ecuación (3.4) tiene las entradas diferentes de cero como sigue

$$
\begin{aligned}
M_e^{11} &= (\frac{5}{4}m + M_H + M_T)r^2 \\
M_e^{12} &= -\frac{1}{2}mr^2 c_{12} \\
M_e^{13} &= M_T r l c_{13} \\
M_e^{14} &= (\frac{3}{2}m + M_H + M_T)r\cos(\theta_1) \\
M_e^{15} &= -(\frac{3}{2}m + M_H + M_T)r\sin(\theta_1) \\
M_e^{22} &= \frac{1}{4}mr^2 \\
M_e^{23} &= 0 \\
M_e^{24} &= -\frac{1}{2}mr\cos(\theta_2) \\
M_e^{25} &= \frac{1}{2}mr\sin(\theta_2) \\
M_e^{33} &= M_T l^2 \\
M_e^{34} &= M_T l\cos(\theta_3) \\
M_e^{35} &= -M_T l\sin(\theta_3) \\
M_e^{44} &= 2m + M_H + M_T \\
M_e^{45} &= 0 \\
M_e^{55} &= 2m + M_H + M_T
\end{aligned}
$$

Apéndice B

Parámetros del Controlador Difuso: Caso 1

Este apéndice presenta los parámetros de las funciones de membresía que caracteriza a los conjuntos difusos de los antecentes de las reglas difusas en los controladores descritos en el Capítulo 5 en la subsección 5.1.1.

B.0.1 Parámetros de funciones de membresia de primer Controlador Difuso TSK

De la Tabla B.1 a la Tabla B.4 muestra los parámetros de las funciones de membresía difusa de las variables de entrada del controlador difuso TSK cuyas reglas difusas tienen la estructura definida en (5.3)

Tabla B.1. Funciones de membresía del primer subcontrolador difuso con reglas de la forma (5.3)

Entrada	Conjunto Difuso	T-S FLC 1 Parámetros		T-S FLC 2 Parámetros	
		a	c	a	c
θ_1	$A_{1,1}$	0.01585	−0.39267	0.06025	−0.33105
	$A_{1,2}$	0.01964	−0.34458	0.03542	−0.28163
	$A_{1,3}$	0.01528	−0.31308	0.00833	−0.29258
θ_2	$A_{2,1}$	0.01166	0.39374	0.01430	0.39633
	$A_{2,2}$	0.00806	0.42428	0.00005	0.42013
	$A_{2,3}$	0.00454	0.43581	−0.00018	0.43636
θ_3	$A_{3,1}$	−0.00079	0.49104	0.00077	0.49111
	$A_{3,2}$	0.00724	0.51279	0.01768	0.52108
	$A_{3,3}$	0.00757	0.54053	0.00089	0.55700
y_1	$A_{4,1}$	0.01219	−0.04186	0.03426	−0.00738
	$A_{4,2}$	0.01063	−0.00821	0.02296	0.02153
	$A_{4,3}$	0.00749	0.02542	0.00766	0.03739
y_2	$A_{5,1}$	0.00242	−0.04948	0.01468	−0.07297
	$A_{5,2}$	0.00996	−0.01788	0.01895	0.02325
	$A_{5,3}$	0.01586	−0.00281	0.07741	−0.00231

Tabla B.2. Funciones de membresía del segundo subcontrolador difuso con reglas de la forma (5.3)

Entrada	Conjunto Difuso	T-S FLC 1 Parámetros a	T-S FLC 1 Parámetros c	T-S FLC 2 Parámetros a	T-S FLC 2 Parámetros c
θ_1	$A_{1,1}$	0.03956	-0.31715	0.04445	-0.31458
	$A_{1,2}$	0.04408	-0.20955	0.04613	-0.21215
	$A_{1,3}$	0.04140	-0.10424	0.04429	-0.10654
θ_2	$A_{2,1}$	0.01358	0.43586	0.00976	0.42965
	$A_{2,2}$	0.01556	0.47751	0.01613	0.46805
	$A_{2,3}$	0.00535	0.50849	0.01192	0.50415
θ_3	$A_{3,1}$	0.01131	0.51020	0.00984	0.50975
	$A_{3,2}$	-0.00561	0.51894	0.00776	0.52591
	$A_{3,3}$	-0.00468	0.54396	0.00144	0.54478
y_1	$A_{4,1}$	0.00704	-0.00016	0.00977	0.00373
	$A_{4,2}$	0.00629	0.01715	-0.00847	0.02392
	$A_{4,3}$	0.00619	0.03385	0.01094	0.02871
y_2	$A_{5,1}$	0.00242	-0.04948	0.00198	-0.05524
	$A_{5,2}$	0.00996	-0.01788	0.01403	-0.02256
	$A_{5,3}$	0.01586	-0.00281	0.00875	0.00304

Tabla B.3. Funciones de membresía del tercer subcontrolador difuso con reglas de la forma (5.3)

Entrada	Conjunto Difuso	T-S FLC 1 Parámetros a	T-S FLC 1 Parámetros c	T-S FLC 2 Parámetros a	T-S FLC 2 Parámetros c
θ_1	$A_{1,1}$	0.06333	-0.10525	0.06333	-0.10525
	$A_{1,2}$	0.06333	0.04387	0.06333	0.04387
	$A_{1,3}$	0.06333	0.19300	0.06333	0.19300
θ_2	$A_{2,1}$	0.10377	-0.01623	0.103771	-0.01623
	$A_{2,2}$	0.10377	0.22814	0.103771	0.22814
	$A_{2,3}$	0.10377	0.47250	0.103771	0.47250
θ_3	$A_{3,1}$	0.00310	0.50694	0.003096	0.50694
	$A_{3,2}$	0.00310	0.51424	0.003096	0.51423
	$A_{3,3}$	0.00310	0.52152	0.003096	0.52152
y_1	$A_{4,1}$	0.00028	-8×10^{-7}	0.000276	-9×10^{-7}
	$A_{4,2}$	0.00028	0.00065	0.000276	0.00065
	$A_{4,3}$	0.00028	0.01301	0.000276	0.00130
y_2	$A_{5,1}$	0.00046	-0.00216	0.000460	-0.00216
	$A_{5,2}$	0.00046	-0.00108	0.000459	-0.00108
	$A_{5,3}$	0.00046	1×10^{-6}	0.000461	1×10^{-6}

B.0.2 Parámetros de funciones de membresía del segundo Controlador Difuso TSK

De la Tabla B.5 a la Tabla B.8 muestra los parámetros de las funciones de membresía difusa de las variables de entrada del controlador difuso TSK cuyas reglas difusas tienen

Tabla B.4. Funciones de membresía del cuarto subcontrolador difuso con reglas de la forma (5.3)

Entrada	Conjunto Difuso	T-S FLC 1 Parámetros		T-S FLC 2 Parámetros	
		a	c	a	c
θ_1	$A_{1,1}$	0.04382	-0.10525	0.043823	0.197075
	$A_{1,2}$	0.06333	0.04387	0.043823	0.300271
	$A_{1,3}$	0.06333	0.19300	0.043823	0.403467
θ_2	$A_{2,1}$	0.10377	-0.01623	0.08097	-0.406247
	$A_{2,2}$	0.10377	0.228138	0.08097	-0.215576
	$A_{2,3}$	0.10377	0.472501	0.08097	-0.024905
θ_3	$A_{3,1}$	0.00310	0.50694	0.00597	0.493359
	$A_{3,2}$	0.00310	0.51423	0.00597	0.507418
	$A_{3,3}$	0.00310	0.52152	0.00597	0.521477
y_1	$A_{4,1}$	0.00028	-0.000001	1×10^{-6}	-5×10^{-6}
	$A_{4,2}$	0.00028	0.000650	1×10^{-6}	-3×10^{-6}
	$A_{4,3}$	0.00028	0.001301	1×10^{-6}	-5×10^{-7}
y_2	$A_{5,1}$	0.00046	-0.002164	7×10^{-6}	1×10^{-6}
	$A_{5,2}$	0.00046	-0.001081	7×10^{-6}	2×10^{-5}
	$A_{5,3}$	0.00046	1×10^{-7}	7×10^{-6}	3×10^{-5}

la estructura definida en (5.4).

Tabla B.5. Funciones de membresía del primer subcontrolador difuso con reglas de la forma (5.4)

Entrada	Conjunto Difuso	T-S FLC 1 Parámetros		T-S FLC 2 Parámetros	
		a	c	a	c
θ_1	$A_{1,1}$	0.04179	−0.38862	0.04136	−0.39037
	$A_{1,2}$	0.01850	−0.28397	0.01845	−0.28763
θ_2	$A_{2,1}$	0.02619	0.39265	0.01917	0.39171
	$A_{2,2}$	0.00797	0.45614	0.00766	0.45421
θ_3	$A_{3,1}$	0.00331	0.47294	0.02037	0.49516
	$A_{3,2}$	0.03138	0.53158	−0.00288	0.55305
$\dot{\theta}_1$	$A_{1,1}$	0.02612	0.90943	0.02432	0.92174
	$A_{1,2}$	0.04841	0.97931	0.04458	0.98509
$\dot{\theta}_2$	$A_{2,1}$	0.43232	−0.24231	0.43764	−0.23986
	$A_{2,2}$	0.43512	0.79588	0.43810	0.79484
$\dot{\theta}_3$	$A_{3,1}$	0.67073	−0.10894	0.67329	−0.10776
	$A_{3,2}$	0.67316	1.48427	0.67532	1.48346
y_1	$A_{4,1}$	0.01973	−0.04125	0.03504	−0.03530
	$A_{4,2}$	0.01592	0.03541	0.01244	0.04119
y_2	$A_{5,1}$	0.03453	−0.03573	−0.00024	−0.06683
	$A_{5,2}$	0.01242	0.02543	0.02626	−0.00515

Tabla B.6. Funciones de membresía del segundo subcontrolador difuso con reglas de la forma (5.4)

Entrada	Conjunto Difuso	T-S FLC 1 Parámetros		T-S FLC 2 Parámetros	
		a	c	a	c
θ_1	$A_{1,1}$	0.11912	−0.26805	0.04926	−0.31383
	$A_{1,2}$	0.04469	−0.05091	0.07628	−0.10665
θ_2	$A_{2,1}$	0.00209	0.43179	0.02466	0.43144
	$A_{2,2}$	0.03183	0.49398	0.02314	0.49563
θ_3	$A_{3,1}$	0.01710	0.51069	0.01704	0.50994
	$A_{3,2}$	0.00148	0.55181	−0.00160	0.54978
$\dot{\theta}_1$	$A_{1,1}$	0.15245	0.45236	0.19035	0.47829
	$A_{1,2}$	0.19932	0.92833	0.18665	0.94280
$\dot{\theta}_2$	$A_{2,1}$	0.46471	−0.36901	0.47436	−0.36670
	$A_{2,2}$	0.46829	0.76003	0.47100	0.75723
$\dot{\theta}_3$	$A_{3,1}$	0.04614	−0.23211	0.09284	−0.19973
	$A_{3,2}$	0.08043	−0.01404	0.07787	0.00310
y_1	$A_{4,1}$	−0.00075	−0.00595	0.01248	0.00329
	$A_{4,2}$	0.01384	0.02182	−0.00078	0.03306
y_2	$A_{5,1}$	0.01796	−0.08025	0.01307	−0.06672
	$A_{5,2}$	0.00909	−0.02957	0.01867	−0.00895

Tabla B.7. Funciones de membresía del tercer subcontrolador difuso con reglas de la forma (5.4)

Entrada	Conjunto Difuso	T-S FLC 1 Parámetros a	T-S FLC 1 Parámetros c	T-S FLC 2 Parámetros a	T-S FLC 2 Parámetros c
θ_1	$A_{1,1}$	0.13746	-0.10592	0.13768	-0.10662
	$A_{1,2}$	0.13887	0.22189	0.14065	0.22035
θ_2	$A_{2,1}$	0.23348	-0.07858	0.23411	-0.07802
	$A_{2,2}$	0.23356	0.47241	0.23311	0.47289
θ_3	$A_{3,1}$	0.00812	0.50028	0.00461	0.49942
	$A_{3,2}$	0.01100	0.51772	0.01351	0.51900
$\dot{\theta}_1$	$A_{1,1}$	0.22045	0.42482	0.21962	0.42427
	$A_{1,2}$	0.21908	0.94333	0.21921	0.94308
$\dot{\theta}_2$	$A_{2,1}$	0.69502	-2.00380	0.69503	-2.00372
	$A_{2,2}$	0.69512	-0.36665	0.69490	-0.36648
$\dot{\theta}_3$	$A_{3,1}$	0.02408	-0.03254	0.02631	-0.03178
	$A_{3,2}$	0.03000	0.03532	0.02974	0.03535
y_1	$A_{4,1}$	0.00061	0.00626	-0.00204	0.01551
	$A_{4,2}$	-0.00696	0.00520	-0.00870	0.00277
y_2	$A_{5,1}$	0.00253	-0.01839	-0.00363	-0.00373
	$A_{5,2}$	0.00774	0.00191	-6×10^{-5}	0.00076

Tabla B.8. Funciones de membresía del cuarto subcontrolador difuso con reglas de la forma (5.4)

Entrada	Conjunto Difuso	T-S FLC 1 Parámetros a	T-S FLC 1 Parámetros c	T-S FLC 2 Parámetros a	T-S FLC 2 Parámetros c
θ_1	$A_{1,1}$	0.07507	0.22460	0.08552	0.23442
	$A_{1,2}$	0.07136	0.39446	0.03315	0.41950
θ_2	$A_{2,1}$	0.13168	-0.39218	0.12745	-0.39340
	$A_{2,2}$	0.12964	-0.07554	0.12509	-0.07315
θ_3	$A_{3,1}$	-0.01008	0.48029	0.00837	0.48193
	$A_{3,2}$	0.01417	0.51326	0.00808	0.50781
$\dot{\theta}_1$	$A_{1,1}$	0.25863	0.94355	0.25958	0.94432
	$A_{1,2}$	0.25689	1.55087	0.25120	1.55362
$\dot{\theta}_2$	$A_{2,1}$	0.14937	-2.34638	0.15849	-2.34355
	$A_{2,2}$	0.14704	-2.00387	0.14260	-2.00340
$\dot{\theta}_3$	$A_{3,1}$	0.16569	-0.43464	0.14283	-0.44816
	$A_{3,2}$	0.17196	-0.03286	0.17654	-0.03871
y_1	$A_{4,1}$	-0.00826	-0.00474	-0.00815	-0.00371
	$A_{4,2}$	-0.00034	-0.00333	-0.00145	-0.00814
y_2	$A_{5,1}$	-0.00932	0.00284	0.00288	0.00011
	$A_{5,2}$	-0.00032	0.00309	0.00189	0.01339

Apéndice C

Parámetros del Controlador Difuso: Caso 2

Este apéndice presenta los parámetros de las funciones de membresía que caracteriza a los conjuntos difusos en los antecedentes y los parámetros de los consecuentes de las reglas difusas en los controladores descritos en el Capítulo 5, en la subsección 5.1.2.

Controlador difuso que proporciona la primer entrada de control

```
[System]
Name='TS-FLC1'
Type='sugeno'
Version=2.0
NumInputs=8
NumOutputs=1
NumRules=256
AndMethod='prod'
OrMethod='max'
ImpMethod='prod'
AggMethod='max'
DefuzzMethod='wtaver'

[Input1]
Name='th1'
Range=[-0.392699081698724 0.392699081698746]
NumMFs=2
MF1='in1mf1':'gaussmf',[0.285065250355171 -0.419901450691507]
MF2='in1mf2':'gaussmf',[0.282311590079953 0.403202759644401]

[Input2]
Name='th2'
Range=[-0.392697390114973 0.502148156859372]
NumMFs=2
MF1='in2mf1':'gaussmf',[0.324566818526267 -0.41759170776654]
MF2='in2mf2':'gaussmf',[0.382246529410536 0.498600401143803]

[Input3]
Name='th3'
Range=[0.496466035821262 0.540963680678532]
NumMFs=2
MF1='in3mf1':'gaussmf',[0.0149272838146031 0.510421786535542]
MF2='in3mf2':'gaussmf',[0.00161586128142086 0.561172915081514]

[Input4]
Name='dth1'
Range=[0.424486970733943 1.54995445913001]
NumMFs=2
MF1='in4mf1':'gaussmf',[0.12003780910287 0.320235872162028]
MF2='in4mf2':'gaussmf',[0.131300940074432 1.6189175618644]

[Input5]
Name='dth2'
Range=[-2.34795490674393 0.794466278906833]
NumMFs=2
MF1='in5mf1':'gaussmf',[1.32539204127991 -2.34541763599516]
MF2='in5mf2':'gaussmf',[1.32935493712153 0.802985935350657]

[Input6]
Name='dth3'
Range=[-0.431527515858298 1.48388744704806]
NumMFs=2
MF1='in6mf1':'gaussmf',[0.79228384028106 -0.49205245424537]
MF2='in6mf2':'gaussmf',[0.784222241760198 1.44351969196423]
```

```
[Input7]
Name='y1'
Range=[-0.0418617957952893 0.0251872360255873]
NumMFs=2
MF1='in7mf1':'gaussmf',[0.0337028184913944 -0.0321901757717731]
MF2='in7mf2':'gaussmf',[-0.00377792575867576 0.0530085622109146]

[Input8]
Name='y2'
Range=[-0.0495763435844818 1.69158377975999e-006]
NumMFs=2
MF1='in8mf1':'gaussmf',[0.00175700185484145 -0.0615848309025873]
MF2='in8mf2':'gaussmf',[0.0219987692036081 -0.00454975589594204]

[Output1]
Name='u1'
Range=[-51.5913289468066 -4.4333321225163]
NumMFs=256


 MF1='out1mf1':'linear',[8.89792691084597e-010 -1.24911667983766e-009 -1.54882697776647e-009
-2.75437981591345e-009 -2.27161265305905e-009 9.47195750643906e-011 -6.82344982625254e-011
1.42290443699112e-010 -2.86242399261793e-009]
 MF2='out1mf2':'linear',[-0.514691893374885 0.389745437289047 -1.09958745719841 -2.19520272429035
5.44985130745117 -0.00254334993129095 -0.00187578022091332 0.00397910366930243 -2.08955441454985]
 MF3='out1mf3':'linear',[-1.75213007603285e-022 2.76031588850136e-022 3.27669807665954e-022
5.61797669054212e-022 4.49961153755259e-022 -1.01885171022239e-022 1.6016490362307e-023
-2.91220500656334e-023 6.07182788727212e-022]
MF4='out1mf4':'linear',[-1.30483865922304e-011 2.27272608130953e-011 2.59423611434055e-011
4.27485415486256e-011 3.07002540926554e-011 -1.04363756676124e-011 1.22520822540694e-012
-2.10434487415381e-012 4.84116261422923e-011] MF5='out1mf5':'linear',[1.75606413703306e-010
-2.48078571740189e-010 -3.06889439827969e-010 -5.44766369305252e-010 -4.49573052737198e-010
2.40344827103145e-011 -1.36532114961949e-011 2.81894603078548e-011 -5.67172428622409e-010]
MF6='out1mf6':'linear',[0.000561224877158825 0.0277266342224732 -0.349014226506383 -0.80284056592921
1.43261954214071 -0.578494730550167 0.0207233991336486 -0.00595562837299813 -0.699392660668846]
MF7='out1mf7':'linear',[-2.05091902879815e-023 3.40642555701682e-023 3.968472230157e-023
6.69181234881515e-023 5.29931965504456e-023 -1.69375029689181e-023 2.03332531820453e-024
-3.48078776788396e-024 7.36122135954535e-023] MF8='out1mf8':'linear',[-1.4191910838738e-012
2.54095717294995e-012 2.87134346496428e-012 4.68045089934099e-012 3.26313172318873e-012
-1.23756600547115e-012 1.34955411979506e-013 -2.27452210439672e-013 5.36739211240104e-012]
MF9='out1mf9':'linear',[1.46925951474708e-008 -2.06350832990905e-008 -2.5581800327267e-008
-4.54874727978114e-008 -3.75116694413368e-008 1.59054027302087e-009 -1.12755656100142e-009
2.34994200501009e-009 -4.72787445433476e-008] MF10='out1mf10':'linear',[0.461598424168104
-0.792698395271154 -1.22274685567164 -1.85965228974363 -1.40636757748356 0.0355438447408107
-0.0527079925185729 0.103689654469539 -2.24240182596918]
MF11='out1mf11':'linear',[-2.61570174701654e-021 4.14984405158278e-021 4.91370958590471e-021
8.40606881275207e-021 6.72257598433583e-021 -1.6038919994055e-021 2.41725032458634e-022
-4.35940256340891e-022 9.10651756181298e-021] MF12='out1mf12':'linear',[-1.55615472034391e-010
2.78407958529072e-010 3.1470943466121e-010 5.13161057399719e-010 3.58236285385779e-010
-1.35608630289141e-010 1.48028423605329e-011 -2.49539030565764e-011 5.88241587430599e-010]
MF13='out1mf13':'linear',[2.89492114087158e-009 -4.09133151130386e-009 -5.06044355418035e-009
-8.98176360308841e-009 -7.41180608464705e-009 4.01178732975765e-010 -2.25236923051522e-010
4.64787437391363e-010 -9.35243874580362e-009] MF14='out1mf14':'linear',[0.270047250196158
-0.386985369234714 -0.500746060059032 -0.770023564049894 0.0770022228406563 -0.832985308942261
0.0186512955696945 0.00957609061114553 -0.982808810396718]
MF15='out1mf15':'linear',[-2.91453172833597e-022 4.92981661734012e-022 5.70702012840225e-022
9.56838111686713e-022 7.54711993668997e-022 -2.66112985928063e-022 2.96991943234087e-023
-4.98296112970255e-023 1.05897915110837e-021] MF16='out1mf16':'linear',[-1.58393382947759e-011
2.95223924527042e-011 3.28860986671134e-011 5.27627249666154e-011 3.51575015910338e-011
-1.55575324126197e-011 1.53567755005661e-012 -2.51536975359553e-012 6.16232781559788e-011]
MF17='out1mf17':'linear',[3.01890671278717e-009 -4.54437409394374e-009 -5.4958807327049e-009
-9.58060633511355e-009 -7.98812978344752e-009 1.40335474772113e-009 -2.69845330387649e-010
5.05447093228072e-010 -1.01551610064522e-008] MF18='out1mf18':'linear',[-0.185652735502993
-0.0303623433099208 -0.664966458467007 -1.08808821665709 2.36246946320035 0.0186933813546012
-0.000875774379232427 0.00283471652562103 -1.28548247517475]
MF19='out1mf19':'linear',[9.72036243245141e-022 -1.30112113663143e-021 -1.64323965348699e-021
-2.964661311121e-021 -2.45356141522706e-021 -9.2822865663214e-023 -6.80330890006377e-023
1.52105099964559e-022 -3.03512962177677e-021] MF20='out1mf20':'linear',[7.6924209283762e-013
-1.93254490286038e-012 -1.96982749678795e-012 -2.88411969593026e-012 -1.7220963367557e-012
2.13834005948455e-012 -1.15979847892375e-013 1.39105627895578e-013 -3.71065496776431e-012]
MF21='out1mf21':'linear',[3.47880873816799e-010 -5.73233456304489e-010 -6.72459386686323e-010
-1.14270185697961e-009 -9.69933967050631e-010 3.40429716010535e-010 -3.74866067641755e-011
6.20933984458692e-011 -1.24197402734024e-009] MF22='out1mf22':'linear',[0.0845095112656784
-0.143268793936918 -0.195709268596443 -0.325535534208399 0.0321697396836001 -0.292876689082063
0.00940028583213636 0.000460986916225445 -0.397089382759774]
MF23='out1mf23':'linear',[2.30750396358321e-022 -3.12599114554377e-022 -3.92914631085784e-022
```

```
-7.0624359854439e-022 -5.83172786022078e-022 -1.13512747040909e-023 -1.64889489622834e-023
3.62625992239809e-023 -7.2590313704388e-022] MF24='out1mf24':'linear',[-1.35999534796045e-013
7.78219043008646e-014 1.53540413180466e-013 3.56702266712393e-013 3.94334440324041e-013
2.42633053002938e-013 3.65130072116099e-015 -2.0344684630197e-014 2.73282071028896e-013]
MF25='out1mf25':'linear',[4.92056502042817e-008 -7.41587254069307e-008 -8.96482345626758e-008
-1.56223659196185e-007 -1.30276275791707e-007 2.31837693248867e-008 -4.40916639485179e-009
8.24472883595606e-009 -1.65649784419469e-007] MF26='out1mf26':'linear',[0.424704763347066
-0.481521585218779 -0.890557262448282 -1.56843194481352 -0.351254047829029 -0.839431408738674
-0.00905613245387358 0.0620221023772651 -1.65026629052015]
MF27='out1mf27':'linear',[1.64431586869694e-020 -2.2071121632892e-020 -2.78436921321035e-020
-5.01911118293187e-020 -4.15160217265917e-020 -1.39582639580067e-021 -1.15637459965594e-021
2.57553803950125e-021 -5.14313267201349e-020] MF28='out1mf28':'linear',[2.24349295288963e-012
-1.60572616427061e-011 -1.34356768998834e-011 -1.44445603185224e-011 -1.38352202123562e-012
3.06292323338027e-011 -9.99162812077983e-013 5.69096498594525e-013 -2.59461517645661e-011]
MF29='out1mf29':'linear',[5.60032160326715e-009 -9.26768299133357e-009 -1.08566598109748e-008
-1.84262041356501e-008 -1.56516127680116e-008 5.62095375441227e-009 -6.08469596875045e-010
1.00257555531534e-009 -2.00510280764682e-008] MF30='out1mf30':'linear',[0.213767086223023
-0.26767285366519 -0.374247561543148 -0.643605722540955 0.407020839665096 -0.864766855951723
0.0254651605069082 -0.00193025763983489 -0.750255043003094]
MF31='out1mf31':'linear',[3.87245932672756e-021 -5.2552772620411e-021 -6.60090194474069e-021
-1.1858287684732e-020 -9.78848727893671e-021 -1.64160361504183e-022 -2.77550484116322e-022
6.08936864568224e-022 -1.21954918449478e-020] MF32='out1mf32':'linear',[-3.72825997681714e-012
3.57516709716385e-012 5.27305406680017e-012 1.06168861891515e-011 1.03242888558632e-011
3.2515728121377e-012 1.92474835196351e-013 -5.81203644849899e-013 9.58263214970837e-012]
MF33='out1mf33':'linear',[8.96795938450272e-043 -1.25857604120127e-042 -1.56033710013521e-042
-2.77428753990955e-042 -2.27914267239962e-042 8.49064712230996e-044 -6.82489467200229e-044
1.42930777949439e-043 -2.88442143234753e-042] MF34='out1mf34':'linear',[1.64771590611268e-033
-2.31437537645704e-033 -2.86848971875695e-033 -5.09915882185407e-033 -4.19175088308855e-033
1.65140878173021e-034 -1.25756201234844e-034 2.6286631078234e-034 -5.30246829363158e-033]
MF35='out1mf35':'linear',[1.88426784829311e-055 -2.62771602916361e-055 -3.26532754150165e-055
-5.8163201840851e-055 -4.77379282805945e-055 1.1985941305345e-056 -1.41330990988888e-056
2.99097913411191e-056 -6.03632508673791e-055] MF36='out1mf36':'linear',[2.55054499368461e-046
-3.46677177777672e-046 -4.35163677226541e-046 -7.81354194724786e-046 -6.44557263126516e-046
-9.48087327739482e-048 -1.83181174307463e-047 4.01181184414146e-047 -8.04029687970765e-046]
MF37='out1mf37':'linear',[1.81400269445256e-043 -2.54990459935809e-043 -3.1594205125536e-043
-5.61488603186613e-043 -4.61399987100121e-043 1.86327006530531e-044 -1.38568953696526e-044
2.89422106212426e-044 -5.84043627451092e-043] MF38='out1mf38':'linear',[3.3073855846177e-034
-4.65691075520853e-034 -5.76671410938988e-034 -1.02439803513209e-033 -8.4238609269037e-034
3.71202777648054e-035 -2.5382507816231e-035 5.28459859720022e-035 -1.06598618016342e-033]
MF39='out1mf39':'linear',[3.94453364242833e-056 -5.50169359898914e-056 -6.83626888850083e-056
-1.21764313321818e-055 -9.99351423162428e-056 2.53141329177835e-057 -2.95930974244157e-057
6.26160663161638e-057 -1.26376590544759e-055] MF40='out1mf40':'linear',[5.79540216064378e-047
-7.92893111094098e-047 -9.92706439984584e-047 -1.77882398276022e-046 -1.46555702184543e-046
-6.76023120992874e-049 -4.2090937878381e-048 9.13703049946435e-048 -1.83441358039e-046]
MF41='out1mf41':'linear',[1.47232550024666e-041 -2.06638109977209e-041 -2.56178001885477e-041
-4.55479641461485e-041 -3.74190484271593e-041 1.39748837866214e-042 -1.12061081815911e-042
2.34665815238536e-042 -4.73567648805467e-041] MF42='out1mf42':'linear',[2.70678722489374e-032
-3.8023743673666e-032 -4.71254800965775e-032 -8.3769569012945e-032 -6.88623832228386e-032
2.72660752221271e-033 -2.06632486081748e-033 4.31848604505611e-033 -8.71126068439007e-032]
MF43='out1mf43':'linear',[3.09731465383279e-054 -4.31954481023646e-054 -5.36759409457494e-054
-9.5608361781584e-054 -7.84705694253364e-054 1.97480512794063e-055 -2.32330619904628e-055
4.91655914385919e-055 -9.92261052689722e-054] MF44='out1mf44':'linear',[4.26848033451768e-045
-5.81031065057489e-045 -7.28913455859749e-045 -1.30819979447849e-044 -1.0788607358663e-044
-1.34445955509837e-046 -3.07330538316444e-046 6.71747509989427e-046 -1.34681580509157e-044]
MF45='out1mf45':'linear',[2.977347862459e-042 -4.18545543095676e-042 -5.18580692190428e-042
-9.21599305155429e-042 -7.57327225325446e-042 3.06753837745095e-043 -2.2746834141341e-043
4.75052323103065e-043 -9.58636784851793e-042] MF46='out1mf46':'linear',[5.43039131522224e-033
-7.64712058974009e-033 -9.46909266184377e-033 -1.6820262823168e-032 -1.38317225816048e-032
6.12569906748161e-034 -4.16860581988874e-034 8.67735290955526e-034 -1.75037801183471e-032]
MF47='out1mf47':'linear',[6.48315859154797e-055 -9.04274403937803e-055 -1.12361596160771e-054
-2.00131151595827e-054 -1.6425151521284e-054 4.16780410626289e-056 -4.86408401492132e-056
1.02915439129766e-055 -2.07713979193174e-054] MF48='out1mf48':'linear',[9.65582105837956e-046
-1.32239516267769e-045 -1.65498335267862e-045 -2.96461613634438e-045 -2.44203987961156e-045
-7.42741866409511e-048 -7.02498353344225e-047 1.52288801525162e-046 -3.05829192884864e-045]
MF49='out1mf49':'linear',[4.59162638356448e-042 -6.53333547044022e-042 -8.05933148090772e-042
-1.42733738070199e-041 -1.17526555938195e-041 7.51830403985174e-043 -3.60693020893561e-043
7.3849209671462e-043 -1.48976944602609e-041] MF50='out1mf50':'linear',[7.74717689893285e-033
-1.11197238417418e-032 -1.36741777180149e-032 -2.41578873514589e-032 -1.99256952037647e-032
1.61629110921801e-033 -6.21014284469107e-034 1.25350573809732e-033 -2.52755575732976e-032]
MF51='out1mf51':'linear',[1.25253899938565e-054 -1.74767393642886e-054 -2.1712856973655e-054
-3.86691168218302e-054 -3.17336997568052e-054 8.22222640107625e-056 -9.402579864848e-056
1.98853172823281e-055 -4.01391921078956e-054] MF52='out1mf52':'linear',[2.29084485434217e-045
-3.18206316894494e-045 -3.96034649525354e-045 -7.06311416018197e-045 -5.80241465151429e-045
1.10395312408103e-046 -1.70725174855524e-046 3.63156422205354e-046 -7.32049806967412e-045]
MF53='out1mf53':'linear',[8.56303413537712e-043 -1.22703371455845e-042 -1.50978484228367e-042
-2.66851620943228e-042 -2.19978923882147e-042 1.70756006841424e-043 -6.83503754252144e-044
```

```
1.38366126383782e-043 -2.79077655513025e-042] MF54='out1mf54':'linear',[1.36353949776812e-033
-1.98217915212673e-033 -2.42645905837762e-033 -4.27128394041908e-033 -3.53080682514148e-033
3.73737298182423e-034 -1.1247624542149e-034 2.22514841304487e-034 -4.48488267200669e-033]
MF55='out1mf55':'linear',[2.61761070679756e-055 -3.65250527664367e-055 -4.53775943161186e-055
-8.08135324039261e-055 -6.63201725846036e-055 1.72352742234549e-056 -1.96518186484701e-056
4.15583836649715e-056 -8.38866708589784e-055] MF56='out1mf56':'linear',[4.85619377630364e-046
-6.75253418857622e-046 -8.4006575694413e-046 -1.49773354112188e-045 -1.23018607792037e-045
2.54726025704627e-047 -3.62570605598279e-047 7.70139446419991e-047 -1.552848517976e-045]
MF57='out1mf57':'linear',[7.52045051212266e-041 -1.07028636111197e-040 -1.32017742689082e-040
-2.3379483938159e-040 -1.92512453936801e-040 1.23906403486518e-041 -5.91037649958164e-042
1.20970977221275e-041 -2.44034961533891e-040] MF58='out1mf58':'linear',[1.26751091007345e-031
-1.81987195686469e-031 -2.23768001958394e-031 -3.95290137317057e-031 -3.26054769996367e-031
2.66477450399066e-032 -1.01675710459006e-032 2.05127597023718e-032 -4.13615907121477e-031]
MF59='out1mf59':'linear',[2.05804032529187e-053 -2.87159740381129e-053 -3.56763049417581e-053
-6.35370321003267e-053 -5.21413870272614e-053 1.35098809142087e-054 -1.54493105362204e-054
3.26734281200398e-054 -6.59525487645856e-053] MF60='out1mf60':'linear',[3.77703470995202e-044
-5.2475328625849e-044 -6.53046294249317e-044 -1.16460487418396e-043 -9.5669436879624e-044
1.85155979533248e-045 -2.81582795636368e-045 5.98799868216974e-045 -1.20712780848923e-043]
MF61='out1mf61':'linear',[1.40075596429666e-041 -2.00781465848922e-041 -2.47021350022298e-041
-4.36567633405668e-041 -3.59902111649329e-041 2.81493303140101e-042 -1.11885632393707e-042
2.26387310455446e-042 -4.56608579775706e-041] MF62='out1mf62':'linear',[2.22626824571347e-032
-3.23804041032044e-032 -3.96305611467677e-032 -6.975093707243e-032 -5.76635262226978e-032
6.16242806804323e-033 -1.83855150884514e-033 3.63429077249792e-033 -7.32500171714922e-032]
MF63='out1mf63':'linear',[4.30099935940733e-054 -6.00143355860959e-054 -7.45599574150466e-054
-1.32784773438328e-053 -1.08970600559522e-053 2.83170072641478e-055 -3.22898240063362e-055
6.82845446729647e-055 -1.37834259720185e-053] MF64='out1mf64':'linear',[8.00107261612401e-045
-1.11273512346692e-044 -1.38423511566018e-044 -2.46779129725887e-044 -2.0268910265444e-044
4.25014234165629e-046 -5.97540419393258e-046 1.26895943793821e-045 -2.55874578014666e-044]
MF65='out1mf65':'linear',[2.79734676432091e-008 -3.92026544250989e-008 -4.86399999783317e-008
-8.65433979617456e-008 -7.13700983166484e-008 2.75522571697095e-009 -2.13752559184661e-009
4.46911110612982e-009 -8.98919753982604e-008] MF66='out1mf66':'linear',[-0.382059858133356
1.55331618579781 -1.65481172429475 -4.86707568614542 -7.0313088610158 4.61689592575881
-0.377028574076267 0.562129240992584 -2.20331242305637] MF67='out1mf67':'linear',[-6.434748811698e-021
1.00309245597113e-020 1.1953080115229e-020 2.05619522560026e-020 1.65054950986401e-020
-3.43791021662973e-021 5.7860105244942e-022 -1.06515893375708e-021 2.21448714924185e-020]
MF68='out1mf68':'linear',[-5.4508776457517e-010 9.35132144906503e-010 1.07340754591765e-009
1.77933347317213e-009 1.2979312124267e-009 -4.1449396537691e-010 5.08182969107591e-011
-8.81903860086965e-011 2.00124669156492e-009] MF69='out1mf69':'linear',[5.56842198737667e-009
-7.85046823830586e-009 -9.7188419698733e-009 -1.7262360417106e-008 -1.42432368953136e-008
7.07484829281175e-010 -4.31034149722223e-010 8.927876945991e-010 -1.79616576192055e-008]
MF70='out1mf70':'linear',[2.05368851047596 -0.887470365539178 -2.75027996871211 -5.18786411518535
3.70003562913775 -14.2136035013189 0.401669843711004 -0.0337495272565888 -5.5415085543103]
MF71='out1mf71':'linear',[-8.0720375451981e-022 1.30807516146684e-021 1.53717367655279e-021
2.61223039125419e-021 2.07969981202979e-021 -5.73406223984975e-022 7.7078899744804e-023
-1.35659069785221e-022 2.84999110889835e-021] MF72='out1mf72':'linear',[-6.13548551732705e-011
1.07617135534143e-010 1.22523056943433e-010 2.0134335491437e-010 1.43526059285246e-010
-5.01846681067488e-011 5.77938564655272e-012 -9.87925093350351e-012 2.28742604961728e-010]
MF73='out1mf73':'linear',[4.6219154435723e-007 -6.48029742478655e-007 -8.03884887211289e-007
-1.43011423762544e-006 -1.17927143321027e-006 4.63947351368158e-008 -3.53448884878676e-008
7.3853488671798e-008 -1.48568006276012e-006] MF74='out1mf74':'linear',[4.94701927575228 2.51446253791901
-4.64955364417825 -15.9294418052835 -12.1207048461276 -22.4113341365054 0.181440550032821
0.742118257732023 -7.65172629280105] MF75='out1mf75':'linear',[-9.69567443461488e-020
1.51967874445509e-019 1.80730719362077e-019 3.10364916248989e-019 2.4884693051463e-019
-5.41535882235479e-020 8.79250011235701e-021 -1.60830864840777e-020 3.34866707000413e-019]
MF76='out1mf76':'linear',[-6.7203894896943e-009 1.17809449257182e-008 1.34160017444615e-008
2.20512139395242e-008 1.57295067036099e-008 -5.48811038708082e-009 6.32922474588611e-010
-1.08228723360022e-009 2.50457875955102e-008] MF77='out1mf77':'linear',[9.18488869750495e-008
-1.29545070545625e-007 -1.60350049974549e-007 -2.84772393214014e-007 -2.34950193441846e-007
1.18294499091284e-008 -7.11485595809956e-009 1.472858393767e-008 -2.96349600527382e-007]
MF78='out1mf78':'linear',[6.07246952088366 -5.02341284539775 -7.858265677585 -16.9308391004126
-3.39281221610129 -17.0710846499139 0.29690315016721 0.416677021537602 -15.1005431194842]
MF79='out1mf79':'linear',[-1.17450270262959e-020 1.92684789880395e-020 2.25449532338277e-020
3.81641446766177e-020 3.0303212279014e-020 -9.01597548069592e-021 1.14279310531508e-021
-1.98351969708929e-021 4.18093381585034e-020] MF80='out1mf80':'linear',[-7.19536228231576e-010
1.30050503079819e-009 1.46463476201543e-009 2.37858759343299e-009 1.64144374984903e-009
-6.46111958877431e-010 6.8746965216093e-011 -1.15088642408302e-010 2.73938361466428e-009]
MF81='out1mf81':'linear',[1.04278335996408e-007 -1.55162482399891e-007 -1.88410135814237e-007
-3.29522668982131e-007 -2.74141839937408e-007 4.19740698886155e-008 -9.08877299701004e-009
1.73195753078366e-008 -3.48159563259776e-007] MF82='out1mf82':'linear',[-0.0926286974104182
-0.750552165022504 -2.46632726618307 -3.68597881257057 4.53113103458127 -0.755141601650044
-0.00536795137318752 0.0481004463886542 -4.69061689072199]
MF83='out1mf83':'linear',[2.86101224981618e-020 -3.80710222928546e-020 -4.81950339069768e-020
-8.71106574127193e-020 -7.21736347464652e-020 -3.37609124658139e-021 -1.9820393885534e-021
4.46766084514757e-021 -8.90075601166167e-020] MF84='out1mf84':'linear',[5.05416054264497e-011
-1.01493997385774e-010 -1.10619748162744e-010 -1.74731354802201e-010 -1.21981645916557e-010
8.07635143544291e-011 -6.00088580370188e-012 8.73702431281259e-012 -2.06827419052232e-010]
```

MF85='out1mf85':'linear',[1.35312260350136e-008 -2.14429604200012e-008 -2.54819448070249e-008
-4.37805180618263e-008 -3.6876199985075e-008 1.01643498847569e-008 -1.34805367537283e-009
2.34894792466918e-009 -4.70723034033946e-008] MF86='out1mf86':'linear',[1.89610459448097
-2.12199957237839 -3.07287137000565 -5.50052133886153 2.40037559959158 -7.42988400193711
0.202715678251454 0.0125012785302742 -6.1176969156342] MF87='out1mf87':'linear',[6.90646618670927e-021
-9.32207194104876e-021 -1.1734198743886e-020 -2.11155987998489e-020 -1.74480345500529e-020
-4.37622011796357e-022 -4.90420297570256e-022 1.0839419033001e-021 -2.16771467406937e-020]
MF88='out1mf88':'linear',[-7.85605864668008e-013 -3.08199545619356e-012 -1.71958285916771e-012
6.79961400323935e-015 3.46376313403771e-012 9.73031995060036e-012 -2.05383645894852e-013
-5.98198049311653e-014 -3.54355087522783e-012] MF89='out1mf89':'linear',[1.70238059966053e-006
-2.5355005014511e-006 -3.07775553994078e-006 -5.38140019017824e-006 -4.4774596655573e-006
6.9358120104376e-007 -1.4866965503475e-007 2.82917303210681e-007 -5.68732808072122e-006]
MF90='out1mf90':'linear',[6.35468289786369 -3.66843670696095 -7.27475218474899 -15.6441961880381
-2.60024203850164 -24.5186952739723 0.514936167746663 0.299694757781202 -13.9784543263257]
MF91='out1mf91':'linear',[4.85855489051237e-019 -6.48683369462982e-019 -8.2008563660062e-019
-1.48073575506234e-018 -1.22604192033709e-018 -5.11571200592518e-020 -3.38541379018588e-020
7.59580449959946e-020 -1.51465401131088e-018] MF92='out1mf92':'linear',[4.69004413598656e-010
-1.12729566507445e-009 -1.16334571990468e-009 -1.72835898800892e-009 -1.06468956123663e-009
1.1805944819606e-009 -6.7319034507667e-011 8.38630476032936e-011 -2.18856926619582e-009]
MF93='out1mf93':'linear',[2.19040298872303e-007 -3.48051656304243e-007 -4.13233710018416e-007
-7.09430191086759e-007 -5.97805909507854e-007 1.67853819260265e-007 -2.19394950763622e-008
3.80937797197351e-008 -7.63353231187687e-007] MF94='out1mf94':'linear',[5.72039704184363
-6.30220253739961 -7.86854201534543 -14.4452163541237 1.8396308902281 -17.8260639061146
0.447882366047004 0.130060352253331 -15.6065937741373] MF95='out1mf95':'linear',[1.16188675822157e-019
-1.57148308197028e-019 -1.97650186217712e-019 -3.55443441062737e-019 -2.9358940836351e-019
-6.44485290173123e-021 -8.2794236853306e-021 1.82484744819199e-020 -3.65143895837264e-019]
MF96='out1mf96':'linear',[-6.60984383992352e-011 3.03484460556872e-011 6.91039435692465e-011
1.69054259510345e-010 1.94327768353814e-010 1.35295986122969e-010 1.30416215117102e-012
-9.7740192737934e-012 1.2196135094277e-010] MF97='out1mf97':'linear',[2.81849602380223e-041
-3.95397123563452e-041 -4.90269010582234e-041 -8.71797940085071e-041 -7.16155616626682e-041
2.6135823463877e-042 -2.14301287320075e-042 4.49094280043081e-042 -9.06306971955322e-041]
MF98='out1mf98':'linear',[5.18442505648747e-032 -7.27749353555762e-032 -9.02195960455199e-032
-1.60407342171756e-031 -1.31853273204377e-031 5.03995426049967e-033 -3.95136519557597e-033
8.26774640075746e-033 -1.66772958912734e-031] MF99='out1mf99':'linear',[5.87091499108363e-054
-8.1867669091228e-054 -1.01735431316528e-053 -1.81218714900128e-053 -1.48739354326628e-053
3.71957504865747e-055 -4.40306748274767e-055 9.31896556780515e-055 -1.8806907109161e-053]
MF100='out1mf100':'linear',[7.66946971096589e-045 -1.03933482712941e-044 -1.30616692571547e-044
-2.34746409415997e-044 -1.93759122455376e-044 -3.74352962867541e-046 -5.47998445141119e-046
1.20506359971558e-045 -2.41319219692429e-044] MF101='out1mf101':'linear',[5.71370608105266e-042
-8.02758678454898e-042 -9.94828795698236e-042 -1.76825231279848e-041 -1.45292898751356e-041
5.72521690177958e-043 -4.35951337337861e-043 9.11312447843596e-043 -1.83902215991285e-041]
MF102='out1mf102':'linear',[1.04412558300195e-032 -1.4690255336933e-032 -1.81963029352978e-032
-3.23310803925184e-032 -2.65838468768028e-032 1.13217267563319e-033 -7.99915393548182e-034
1.66750482241131e-033 -3.36361858919329e-032] MF103='out1mf103':'linear',[1.2292727474202e-054
-1.71445730541817e-054 -2.13038550487132e-054 -3.7946015598932e-054 -3.11436995662111e-054
7.86497934427051e-056 -9.22164766375953e-056 1.95133420269582e-055 -3.93826686627765e-054]
MF104='out1mf104':'linear',[1.75857549397204e-045 -2.40103137709105e-045 -3.00854662069648e-045
-5.39444988280281e-045 -4.44619586492518e-045 -3.46737511948594e-047 -1.27273702573867e-046
2.77052943943043e-046 -5.55923736164322e-045] MF105='out1mf105':'linear',[4.62760169832614e-040
-6.49219169815807e-040 -8.04980288778909e-040 -1.43140048549133e-039 -1.17586154070805e-039
4.30144969391576e-041 -3.51891305301411e-041 7.37375913093793e-041 -1.4880791928119e-039]
MF106='out1mf106':'linear',[8.51804464974693e-031 -1.19583204145657e-030 -1.48241804691048e-030
-2.63559899084972e-030 -2.16642757270193e-030 8.32336270023402e-032 -6.4935509460984e-032
1.35847164823616e-031 -2.74028624746431e-030] MF107='out1mf107':'linear',[9.65098698675103e-053
-1.34585063951369e-052 -1.67243556103677e-052 -2.97902641544663e-052 -2.445077026971e-052
6.13021264940347e-054 -7.23853028896119e-054 1.53193180399811e-053 -3.09168318881903e-052]
MF108='out1mf108':'linear',[1.2861373010091e-043 -1.745854601296e-043 -2.19261158819312e-043
-3.93853522790549e-043 -3.24980492308536e-043 -5.43886267255342e-045 -9.21624832504374e-045
2.02204637509684e-044 -4.05106942351452e-043] MF109='out1mf109':'linear',[9.37878509560895e-041
-1.31776754216789e-040 -1.63302563282694e-040 -2.90256363616599e-040 -2.38498887745105e-040
9.42485493499097e-042 -7.15690729630896e-042 1.49593505177015e-041 -3.01878035115629e-040]
MF110='out1mf110':'linear',[1.71463829933214e-031 -2.41268965649753e-031 -2.98837891179895e-031
-5.30954342190692e-031 -4.36571205276201e-031 1.86865611112842e-032 -1.31392268593099e-032
2.73851104484996e-032 -5.524075631552e-031] MF111='out1mf111':'linear',[2.02049118147334e-053
-2.81805569766539e-053 -3.50167230311262e-053 -6.2370463796399e-053 -5.11893015772847e-053
1.29522320048692e-054 -1.51579031756806e-054 3.20733711008912e-054 -6.47325624243297e-053]
MF112='out1mf112':'linear',[2.93412490570286e-044 -4.01064736148275e-044 -5.02315339805519e-044
-9.00350287985337e-044 -7.41918776043586e-044 -4.46861449915252e-046 -2.12768592594122e-045
4.62442909391041e-045 -9.28207296072548e-044] MF113='out1mf113':'linear',[1.47042393596599e-040
-2.08898188557027e-040 -2.57836088477071e-040 -4.56840077168821e-040 -3.76064783441855e-040
2.29224639687836e-041 -1.15098898143404e-041 2.36251994024159e-041 -4.76613097162998e-040]
MF114='out1mf114':'linear',[2.51042705286163e-031 -3.59390904443486e-031 -4.42365559244394e-031
-7.82097999378389e-031 -6.44796473503252e-031 4.90415601059759e-032 -2.00051304181523e-032
4.0548616125236e-032 -8.17683052223802e-031] MF115='out1mf115':'linear',[3.90548849894086e-053
-5.44929521332331e-053 -6.77015237238062e-053 -1.20572138011874e-052 -9.89470715277654e-053
2.5619930368594e-054 -2.93171793338219e-054 6.20032190836374e-054 -1.25155541669548e-052]

MF116='out1mf116':'linear',[7.09874527699478e-044 -9.85621533792841e-044 -1.22689241973387e-043
-2.18840073467725e-043 -1.79792888530074e-043 3.29992522451935e-045 -5.28648702957649e-045
1.12515124444259e-044 -2.26782952234574e-043] MF117='out1mf117':'linear',[2.76858891776499e-041
-3.95801724171438e-041 -4.87416686780914e-041 -8.62071177428007e-041 -7.10376694306515e-041
5.19428404509026e-042 -2.19830702208129e-042 4.46676094336543e-042 -9.00977011702396e-041]
MF118='out1mf118':'linear',[4.49509246833653e-032 -6.50616221697305e-032 -7.97680881954372e-032
-1.40589302021612e-031 -1.16128744479574e-031 1.13106079525584e-032 -3.67200648465385e-033
7.3140976292412e-033 -1.47439744364767e-031] MF119='out1mf119':'linear',[8.16228457596281e-054
-1.13891759334523e-053 -1.4149620665562e-053 -2.51993243828406e-053 -2.06799293472342e-053
5.36933617433231e-055 -6.12768777476636e-055 1.29587054161417e-054 -2.61575055919978e-053]
MF120='out1mf120':'linear',[1.50699897667525e-044 -2.09475466777106e-044 -2.60638279731495e-044
-4.64735820236916e-044 -3.81740219981867e-044 7.69367160199162e-046 -1.12447264953843e-045
2.38962064435393e-045 -4.81782734496985e-044] MF121='out1mf121':'linear',[2.40901283153444e-039
-3.42302458739232e-039 -4.22464776845179e-039 -7.48494377998421e-039 -6.16169418157378e-039
3.77745799027987e-040 -1.88646143003346e-040 3.87100896739499e-040 -7.80930711278908e-039]
MF122='out1mf122':'linear',[4.10907148627411e-030 -5.88417945338063e-030 -7.24195282481228e-030
-1.28026635644463e-029 -1.05555063326605e-029 8.08533187577953e-031 -3.27649668500726e-031
6.63820926692646e-031 -1.33862572798854e-029] MF123='out1mf123':'linear',[6.41709842472439e-052
-8.95374137069129e-052 -1.11240329270432e-051 -1.98111846943365e-051 -1.62579400357893e-051
4.20978997951515e-053 -4.81709801785803e-053 1.01877252119309e-052 -2.05643022002367e-051]
MF124='out1mf124':'linear',[1.17074566799434e-042 -1.62588566455942e-042 -2.02370715304429e-042
-3.60941819425041e-042 -2.96526431679759e-042 5.54798361789258e-044 -8.72196891085987e-044
1.85578356243057e-043 -3.74070607401768e-042] MF125='out1mf125':'linear',[4.53077710754651e-040
-6.4790104068233e-040 -7.97791194775758e-040 -1.4109079124644e-039 -1.16268856991142e-039
8.56216055132693e-041 -3.59970565227956e-041 7.31112376346451e-041 -1.47469488311414e-039]
MF126='out1mf126':'linear',[7.34443055843509e-031 -1.06350710231033e-030 -1.30369007915603e-030
-2.29742510914208e-030 -1.89783596730794e-030 1.86491784714416e-031 -6.00558952608484e-032
1.19538678488975e-031 -2.40967938150852e-030] MF127='out1mf127':'linear',[1.34114524191673e-052
-1.87135618569638e-052 -2.3249246756223e-052 -4.14050115669317e-052 -3.39791470540605e-052
8.82189918439005e-054 -1.00683807879551e-053 2.12924282668992e-053 -4.29794111111156e-052]
MF128='out1mf128':'linear',[2.48350806955799e-043 -3.45274548275094e-043 -4.2957483511466e-043
-7.65917876786261e-043 -6.29112777659433e-043 1.28578885649668e-044 -1.85367703463783e-044
3.93830980361219e-044 -7.94060244122596e-043] MF129='out1mf129':'linear',[3.90353223223246e-011
-5.46610326407501e-011 -6.78401297149679e-011 -1.20734169523925e-010 -9.95643216403523e-011
3.70043477319984e-012 -2.9778530095128e-012 6.23366130598046e-012 -1.25375307094216e-010]
MF130='out1mf130':'linear',[2.00224389320459 -7.8787927445499 -5.82293531565094 5.86043524404819
7.32768551793838 -8.72445736409274 0.000360438566205561 -0.000399761961835286 -10.1153544087551]
MF131='out1mf131':'linear',[-9.62510725268812e-024 1.49414631295698e-023 1.78318133099169e-023
3.07151593133878e-023 2.46775303731072e-023 -4.96316338553138e-024 8.59804380646398e-025
-1.59069826887318e-024 3.30333820493708e-023] MF132='out1mf132':'linear',[-8.70629332247672e-013
1.48244803912091e-012 1.70640317620185e-012 2.83699592051468e-012 2.08547270918929e-012
-6.45590111449371e-013 8.08995720356257e-014 -1.41096201456166e-013 3.17990189275199e-012]
MF133='out1mf133':'linear',[7.80107130917212e-012 -1.0987858651385e-011 -1.36075999198895e-011
-2.41760357468368e-011 -1.99462268099271e-011 9.56432864950349e-013 -6.02649861889276e-013
1.25006237787655e-012 -2.51485274051204e-011] MF134='out1mf134':'linear',[-1.27465274634736
0.0533681620028822 -3.75705031758523 -5.27040056312582 15.3441387685367 -1.11467608701635
0.000685740662444464 -0.000561855693383416 -7.01647904410543]
MF135='out1mf135':'linear',[-1.23926585058101e-024 1.99027099167393e-024 2.34633814227542e-024
3.99859025129927e-024 3.18957420811719e-024 -8.29022090054238e-025 1.1671318755455e-025
-2.07535440361991e-025 4.34946257877545e-024] MF136='out1mf136':'linear',[-9.95803583222243e-014
1.72984391118235e-013 1.97644479541046e-013 3.26033116014063e-013 2.34812081228545e-013
-7.8978589004859e-014 9.33975963771426e-015 -1.60698752875707e-014 3.68767484941325e-013]
MF137='out1mf137':'linear',[6.45155618168675e-010 -9.03844810414707e-010 -1.121556877437e-009
-1.99571971521045e-009 -1.64562951678423e-009 6.24048866177471e-011 -4.92558609751498e-011
1.03044670765738e-010 -2.07276883195362e-009] MF138='out1mf138':'linear',[0.0375577422617759
-0.269498854625396 -0.412827762376971 -0.290080118391873 0.994067324047388 -0.0999265323733158
0.000797933378533873 7.329437847478e-005 -0.806554038681718]
MF139='out1mf139':'linear',[-1.45556354994361e-022 2.2705709236061e-022 2.70499586929782e-022
4.65219652426807e-022 3.73383704108924e-022 -7.82013265693507e-023 1.31018196906537e-023
-2.41003537838231e-023 5.01148036582675e-022] MF140='out1mf140':'linear',[-1.09047630056607e-011
1.89359149813429e-011 2.16390514751439e-011 3.56996172003402e-011 2.57183641670768e-011
-8.63420805844286e-012 1.02241486403139e-012 -1.75973492696434e-012 4.03736384801502e-011]
MF141='out1mf141':'linear',[1.28710669238775e-010 -1.81367612258467e-010 -2.24572341702421e-010
-3.98934881808592e-010 -3.29113430224796e-010 1.60065594740739e-011 -9.9504174657743e-012
2.06282905080204e-011 -4.15040775268246e-010] MF142='out1mf142':'linear',[0.00336248755374731
-0.0265133999795874 -0.072934250420821 -0.122946043370763 0.200844860577384 0.0246619919429492
0.00044741184740631 9.9236753436046e-005 -0.152170086170486]
MF143='out1mf143':'linear',[-1.81825079654336e-023 2.9508234658686e-023 3.4658230123712e-023
5.88698708521886e-023 4.68533280090339e-023 -1.30396781005862e-023 1.74012295925336e-024
-3.05751627974146e-024 6.42598345047827e-023] MF144='out1mf144':'linear',[-1.19378578847036e-012
2.1289211831087e-012 2.40923298681459e-012 3.93338924764388e-012 2.75476559731775e-012
-1.02911516817419e-012 1.13343198911147e-013 -1.91529422018012e-013 4.50242511899043e-012]
MF145='out1mf145':'linear',[1.51463208018486e-010 -2.24336204282031e-010 -2.72846388581845e-010
-4.77822045523482e-010 -3.97170202829 66e-010 5.72462174865923e-011 -1.30685050988298e-011
2.50767537854667e-011 -5.0419889032376e-010] MF146='out1mf146':'linear',[4.09291575331963
-6.86152520831412 -1.40773897213664 16.2360144579721 17.410835510085 -14.374745872696

```
-8.11644388234784e-005 0.000303937722212001 -0.790788062903561]
MF147=’out1mf147’:’linear’,[3.8616187321415e-023 -5.12203024733138e-023 -6.49250812611966e-023
-1.17467181038759e-022 -9.73843885807855e-023 -5.03057127909728e-024 -2.66023769964386e-024
6.02335401876528e-024 -1.19897112651455e-022] MF148=’out1mf148’:’linear’,[8.98193258819266e-014
-1.71090402882062e-013 -1.89741618134079e-013 -3.05168049106287e-013 -2.20124012180611e-013
1.21928368676145e-013 -1.00814347608431e-014 1.53865299818393e-014 -3.54091595145757e-013]
MF149=’out1mf149’:’linear’,[2.05204535068224e-011 -3.2085141254966e-011 -3.83015653558707e-011
-6.6055918978443e-011 -5.54921365571516e-011 1.38517245236951e-011 -1.98848302392594e-012
3.52860785563663e-012 -7.0758588365696e-011] MF150=’out1mf150’:’linear’,[-1.65310502534878
1.99696244345415 -2.45313496281814 -6.27361212880682 17.7438818933046 0.176212587268816
0.000167519677359142 3.79618476982559e-005 -4.65810675175968]
MF151=’out1mf151’:’linear’,[9.40630176323671e-024 -1.26715422700985e-023 -1.59627172707593e-023
-2.87421731687273e-023 -2.3758711370002e-023 -6.66776824349235e-025 -6.65689111327298e-025
1.4752593615323e-024 -2.94875388919247e-023] MF152=’out1mf152’:’linear’,[1.54294780582272e-015
-8.42480442649939e-015 -7.30859729332984e-015 -8.43520600289201e-015 -1.95491103318888e-015
1.50505146739798e-014 -5.25794539594791e-016 3.54707231678979e-016 -1.40386368868888e-014]
MF153=’out1mf153’:’linear’,[2.47427896714894e-009 -3.6678907852848e-009 -4.45965580776553e-009
-7.8080121403067e-009 -6.49067828031524e-009 9.46051879666983e-010 -2.13865755878614e-010
4.09869347725749e-010 -8.24110192551363e-009] MF154=’out1mf154’:’linear’,[2.06093813562432
-2.57056002329107 1.41488360332693 7.73068034730832 -3.5911943024386 -3.57516076574121
0.00105420721913076 -0.000195571875688229 3.12409953789097]
MF155=’out1mf155’:’linear’,[6.57162787788841e-022 -8.74862798556683e-022 -1.10731294423238e-021
-2.00114894398919e-021 -1.65785196915881e-021 -7.64583115259483e-023 -4.55607554736028e-023
1.02635400025871e-022 -2.04502757649871e-021] MF156=’out1mf156’:’linear’,[9.51002863489296e-013
-2.03099129176404e-012 -2.17088120420985e-012 -3.35728993961926e-012 -2.24909680745114e-012
1.79883975580144e-012 -1.20405582824378e-013 1.66113810745388e-013 -4.06788566769633e-012]
MF157=’out1mf157’:’linear’,[3.32799038330503e-010 -5.2152325922496e-010 -6.22090850459788e-010
-1.07218665542468e-009 -9.01028619987928e-010 2.28766027114994e-010 -3.23948786817404e-011
5.73127636879036e-011 -1.14924924394393e-009] MF158=’out1mf158’:’linear’,[0.025100782138069
-0.161580621073989 -0.175757691424327 -0.0385066315872473 0.262314091662383 -0.110016077374639
0.000285470104780581 0.000241503826121865 -0.330945138294352]
MF159=’out1mf159’:’linear’,[1.58449624651079e-022 -2.13924886478654e-022 -2.69250715563181e-022
-4.84474800257331e-022 -4.00302080852105e-022 -9.88462701794721e-024 -1.12561562458718e-023
2.48701069534623e-023 -4.9740270796643e-022] MF160=’out1mf160’:’linear’,[-5.28369485083055e-014
-1.99845139666353e-014 2.25830723129711e-014 1.09430276916368e-013 1.70303788946274e-013
2.12335401176178e-013 -1.78904586981378e-015 -7.0955014507897e-015 3.33094517639488e-014]
MF161=’out1mf161’:’linear’,[3.93485276380998e-044 -5.51909444837543e-044 -6.84379165804059e-044
-1.2170265086861e-043 -9.99720793104966e-044 3.61413595402237e-045 -2.99059234360973e-045
6.26899528436795e-045 -1.26513808312601e-043] MF162=’out1mf162’:’linear’,[7.24101287285375e-035
-1.01614736254803e-034 -1.25985750596332e-034 -2.24016830720463e-034 -1.84134070763545e-034
6.93967365511235e-036 -5.51533352022678e-036 1.15454362789787e-035 -2.32887471679466e-034]
MF163=’out1mf163’:’linear’,[8.16377143724361e-057 -1.13836761580205e-056 -1.4146474390909e-056
-2.51990270356478e-056 -2.06828531994794e-056 5.16155488725106e-058 -6.12233522130401e-058
1.29583043892321e-057 -2.61512830644091e-056] MF164=’out1mf164’:’linear’,[1.04717869779494e-047
-1.416845640052e-047 -1.78171740691947e-047 -3.20370964575252e-047 -2.6451371870395e-047
-5.75420895113176e-049 -7.46194331655691e-049 1.6444515740081e-048 -3.29168434356256e-047]
MF165=’out1mf165’:’linear’,[7.98473368713954e-045 -1.12157648032385e-044 -1.39004295985582e-044
-2.47088323070814e-044 -2.03018644898814e-044 7.91035872247645e-046 -6.08907775953801e-046
1.2733411600145e-045 -2.5696097994006e-044] MF166=’out1mf166’:’linear’,[1.46052785151064e-035
-2.05415768780525e-035 -2.54474109026886e-035 -4.52193800402559e-035 -3.71794103718697e-035
1.55856474262459e-036 -1.11804156410442e-036 2.3319980359528e-036 -4.70400032764549e-035]
MF167=’out1mf167’:’linear’,[1.70954034334053e-057 -2.38421989486713e-057 -2.96266362860005e-057
-5.27708355698232e-057 -4.33112728699623e-057 1.09206404319553e-058 -1.28239504073116e-058
2.71368401492753e-058 -5.47682679085498e-057] MF168=’out1mf168’:’linear’,[2.41258588705562e-048
-3.29043802077745e-048 -4.12473984249366e-048 -7.39830002243469e-048 -6.09905840298712e-048
-5.76729471168454e-050 -1.74286579994558e-049 3.79942759554278e-049 -7.62159165190041e-048]
MF169=’out1mf169’:’linear’,[6.46070382303236e-043 -9.06228675214227e-043 -1.12372480103125e-042
-1.99828729972788e-042 -1.64149648403852e-042 5.94798533547297e-044 -4.91079988688369e-044
1.02934681302268e-043 -2.07730869038463e-042] MF170=’out1mf170’:’linear’,[1.1897908156592e-033
-1.66984832506178e-033 -2.07025191821193e-033 -3.6810157001875e-033 -3.02565235053498e-033
1.14621296048516e-034 -9.0643837368378e-035 1.89716670113567e-034 -3.8269113015967e-033]
MF171=’out1mf171’:’linear’,[1.34204975625423e-055 -1.87145605225511e-055 -2.32561447609498e-055
-4.14254435256815e-055 -3.40007917363961e-055 8.50801825996433e-057 -1.00652689025034e-056
2.13025719872051e-056 -4.29915362642484e-055] MF172=’out1mf172’:’linear’,[1.75795286089203e-046
-2.38282867973196e-046 -2.99431951080412e-046 -5.38107063398402e-046 -4.44132956257688e-046
-8.43154481031697e-048 -1.25656234063034e-047 2.76239188365691e-047 -5.53214213739913e-046]
MF173=’out1mf173’:’linear’,[1.31070751793917e-043 -1.84118935925663e-043 -2.28185986312099e-043
-4.05607601965334e-043 -3.33268363164718e-043 1.3021597675881e-044 -9.99662686422172e-045
2.0902887371291e-044 -4.21820641823637e-043] MF174=’out1mf174’:’linear’,[2.39863351094865e-034
-3.37395774210336e-034 -4.17955477261548e-034 -7.42669534593962e-034 -6.10623426230176e-034
2.5726421143139e-035 -1.8366074348958e-035 3.8300927165203e-035 -7.72599010566453e-034]
MF175=’out1mf175’:’linear’,[2.80994059665978e-056 -3.91903328577169e-056 -4.86977767689839e-056
-8.67393256170916e-056 -7.11900166878728e-056 1.79865143450439e-057 -2.10796129250343e-057
4.46047949271691e-057 -9.00235558202655e-056] MF176=’out1mf176’:’linear’,[4.02826875028772e-047
-5.50072172613555e-047 -6.89212450249597e-047 -1.23572955505298e-046 -1.01847821437215e-046
-7.71084039194013e-049 -2.91611634698551e-048 6.34662175634839e-048 -1.27354098504844e-046]
```

```
MF177='out1mf177':'linear',[2.07008956158183e-043 -2.93888976423636e-043 -3.62827607006456e-043
-6.42992317477056e-043 -5.2924330704124e-043 3.15555858482281e-044 -1.61784576487688e-044
3.32449319936609e-044 -6.70692692724317e-043] MF178='out1mf178':'linear',[3.55238201892386e-034
-5.0798258165205e-034 -6.25517863016349e-034 -1.10626520414926e-033 -9.11879299416882e-034
6.73559580766399e-035 -2.82357724755622e-035 5.73352214569937e-035 -1.15623255292691e-033]
MF179='out1mf179':'linear',[5.43283708612243e-056 -7.58035523707491e-056 -9.41777798316569e-056
-1.67724920805228e-055 -1.37642788087262e-055 3.56275054846785e-057 -4.07820652835967e-057
8.62510614711877e-057 -1.74100522458114e-055] MF180='out1mf180':'linear',[9.84385582965087e-047
-1.36647302652387e-046 -1.70111444957474e-046 -3.03446919613934e-046 -2.49313150818439e-046
4.49181174128915e-048 -7.32811071068814e-048 1.56012760597867e-047 -3.14438469412415e-046]
MF181='out1mf181':'linear',[3.91400198542692e-044 -5.5898642013163e-044 -6.88624501004828e-044
-1.21828922086249e-043 -1.00374628023137e-043 7.14283283075436e-045 -3.10067292561767e-045
6.31051822393873e-045 -1.27290862635044e-043] MF182='out1mf182':'linear',[6.40766993135085e-035
-9.25735354207781e-035 -1.13573529364095e-034 -2.00275487561841e-034 -1.65377622855901e-034
1.55155674018212e-035 -5.21277327247919e-036 1.04132394046996e-035 -2.0992567915058e-034]
MF183='out1mf183':'linear',[1.13546479687656e-056 -1.58435231115081e-056 -1.96836283550981e-056
-3.50549995848081e-056 -2.87679925152166e-056 7.46611252984732e-058 -8.52418136766066e-058
1.80269346404992e-057 -3.63878753152641e-056] MF184='out1mf184':'linear',[2.09128194487643e-047
-2.90641365071615e-047 -3.61652756777739e-047 -6.4488622945006e-047 -5.29733984859872e-047
1.05302280260692e-048 -1.55997762089993e-048 3.31588940102088e-048 -6.68503074691718e-047]
MF185='out1mf185':'linear',[3.39186142250547e-042 -4.8162302181699e-042 -5.9456192800227e-042
-1.05361317193795e-041 -8.67247996322881e-042 5.19993214328114e-043 -2.6519038258145e-043
5.44783625740078e-043 -1.09905667017551e-041] MF186='out1mf186':'linear',[5.81563940128761e-033
-8.31845750353369e-033 -1.02421606829624e-032 -1.8112473399291e-032 -1.4930417731223e-032
1.11047011294324e-033 -4.62524908566388e-034 9.38801277757169e-034 -1.893201653369e-032]
MF187='out1mf187':'linear',[8.92669232124194e-055 -1.24553086842709e-054 -1.54743682010381e-054
-2.75588872677745e-054 -2.26160406532072e-054 5.8543496718722e-056 -6.70090298576135e-056
1.41718983684171e-055 -2.86064936174403e-054] MF188='out1mf188':'linear',[1.62371417818746e-045
-2.25448949639601e-045 -2.80634136447199e-045 -5.00561714983319e-045 -4.11244267904836e-045
7.56148024807789e-047 -1.20923151571833e-046 2.57360167322021e-046 -5.18733999972543e-045]
MF189='out1mf189':'linear',[6.40638578283836e-043 -9.15173777825067e-043 -1.12731414626037e-042
-1.99425847053101e-042 -1.64313448449026e-042 1.1773665913565e-043 -5.07806271814829e-044
1.0330705281937e-043 -2.08381592520084e-042] MF190='out1mf190':'linear',[1.04725088863523e-033
-1.51363108409994e-033 -1.85671267350778e-033 -3.27373190356959e-033 -2.70345779855619e-033
2.55821109903825e-034 -8.52752454417281e-035 1.70237636577494e-034 -3.43188488664674e-033]
MF191='out1mf191':'linear',[1.86568276044746e-055 -2.60325126511717e-055 -3.23421856828958e-055
-5.75988825134255e-055 -4.72686292464319e-055 1.22671259535283e-056 -1.40060573147194e-056
2.96200324015541e-056 -5.97889540109051e-055] MF192='out1mf192':'linear',[3.44679723343768e-046
-4.79117891916421e-046 -5.96135229202862e-046 -1.06294450492107e-045 -8.73110576130916e-046
1.76133854024007e-047 -2.57193024184743e-047 5.46553353711732e-047 -1.10194030328488e-045]
MF193='out1mf193':'linear',[1.22297292376846e-009 -1.70966261096191e-009 -2.12320644638325e-009
-3.78051685817892e-009 -3.11757467895428e-009 1.06615449085055e-010 -9.29783833127761e-011
1.95126797636304e-010 -3.92385256061307e-009] MF194='out1mf194':'linear',[-1.23387688894293
-1.63910277305363 -5.61055354474161 -6.00331895175887 12.3063281673726 0.406971006286952
-0.0270262340109926 0.0335254891901978 -10.9760256746925]
MF195='out1mf195':'linear',[-3.46651026281887e-022 5.34082622724356e-022 6.39155947912028e-022
1.10355103936694e-021 8.8803583620412e-022 -1.67224705434914e-022 3.06017383978806e-023
-5.71244023973957e-023 1.18385884645985e-021] MF196='out1mf196':'linear',[-3.53574047801171e-011
5.94886382724882e-011 6.87821523603947e-011 1.14892456611976e-010 8.54800098051738e-011
-2.51567315148394e-011 3.26786315064562e-012 -5.74488848714516e-012 1.280807349031e-010]
MF197='out1mf197':'linear',[2.46368410844976e-010 -3.46357183783431e-010 -4.29236350831703e-010
-7.63026570128892e-010 -6.29447316108685e-010 2.80035997488836e-011 -1.89562373239392e-011
3.94355612807165e-011 -7.93277393005024e-010] MF198='out1mf198':'linear',[0.00542126546217777
-1.02053043705152 -1.26490911811343 -0.658644308819186 1.45172842745313 -0.363276439353263
0.0248188963034278 -0.0287762216387371 -2.60261996394897]
MF199='out1mf199':'linear',[-4.66799667001227e-023 7.38433542355484e-023 8.75274539348528e-023
1.498739968263e-022 1.19936450577496e-022 -2.80137757595219e-023 4.29464809854461e-024
-7.77122181127252e-024 1.62204019038095e-022] MF200='out1mf200':'linear',[-4.14668697170823e-012
7.09692281942358e-012 8.15340488865007e-012 1.35287973388719e-011 9.89524462481848e-012
-3.13125418926051e-012 3.86324430114185e-013 -6.71388631945455e-013 1.51986472814451e-011]
MF201='out1mf201':'linear',[2.02260736918117e-008 -2.828966343428e-008 -3.51255268126865e-008
-6.25334347415813e-008 -5.15623974616396e-008 1.80457048295211e-009 -1.53902294426041e-009
3.22768369257896e-009 -6.49154213875496e-008] MF202='out1mf202':'linear',[-1.76120489415243
-2.9042670463126 -7.77108090986747 -7.71024432113424 16.5545349542227 -2.04966171291673
0.0568103093451421 -0.0696187204550603 -14.9822673980866]
MF203='out1mf203':'linear',[-5.27623108829946e-021 8.16103883504775e-021 9.75257466931349e-021
1.68177631213449e-020 1.35220242964282e-020 -2.63633745781178e-021 4.68652035717089e-022
-8.70764395451455e-022 1.80653494318624e-020] MF204='out1mf204':'linear',[-4.53793819542309e-010
7.76588942852782e-010 8.92245290307927e-010 1.4804379111871e-009 1.08251687645335e-009
-3.4205122445539e-010 4.22520722652877e-011 -7.34522383871059e-011 1.66324472942268e-009]
MF205='out1mf205':'linear',[4.06725224824456e-009 -5.72049996720694e-009 -7.08812395740931e-009
-1.25983666595234e-008 -1.03919889054145e-008 4.69673740986632e-010 -3.13179763287034e-010
6.51143138012825e-010 -1.30997685775226e-008] MF206='out1mf206':'linear',[-0.395491752723911
-0.90120939510707 -2.3728750555457 -2.20374749653048 3.88548938875083 -0.747866221842293
-0.00524700460457684 0.0222165459624055 -4.51825273351097]
MF207='out1mf207':'linear',[-6.94338655104885e-022 1.1068755873684e-021 1.30836431411959e-021
```

2.23489718058126e-021 1.78552363040665e-021 -4.40930460603621e-022 6.464678314127e-023
-1.1593958851535e-022 2.42499865648169e-021] MF208='out1mf208':'linear',[-5.13550402772078e-011
8.97960995620528e-011 1.02352167815748e-010 1.68403228929712e-010 1.20449739064799e-010
-4.15952754974029e-011 4.83085549127586e-012 -8.27519276674322e-012 1.91047324287047e-010]
MF209='out1mf209':'linear',[5.1198744491946e-009 -7.52126120168354e-009 -9.17410085686254e-009
-1.61035367338149e-008 -1.33648251118494e-008 1.71284994454426e-009 -4.33820480986611e-010
8.42906172719506e-010 -1.6953676167889e-008] MF210='out1mf210':'linear',[-1.19506421826645
-2.48563804323001 -6.66315189979903 -7.46729695345782 14.8126097729347 -0.599411804379854
0.000333756652164409 0.000595606234172164 -12.8294594769165]
MF211='out1mf211':'linear',[1.12214497245816e-021 -1.47661285329803e-021 -1.87770838732823e-021
-3.40567849618702e-021 -2.82767585507722e-021 -1.79909391453249e-022 -7.62360930433016e-023
1.74546907488921e-022 -3.46700337857428e-021] MF212='out1mf212':'linear',[4.21733493857408e-012
-7.49879637742452e-012 -8.51470156056496e-012 -1.40202420442957e-011 -1.05278140135948e-011
4.48018378648624e-012 -4.39748713734924e-013 7.14340840075748e-013 -1.58499288612173e-011]
MF213='out1mf213':'linear',[7.45350844085935e-010 -1.14061964456949e-009 -1.37162938127998e-009
-2.37997129599871e-009 -1.99098070759901e-009 4.13841253791501e-010 -6.90346960541592e-011
1.26246912233712e-010 -2.53423439340544e-009] MF214='out1mf214':'linear',[-0.199836661986626
-0.808735637294723 -1.68120498922337 -1.76490534846576 2.71920205003657 -0.251422818996087
0.00378062201368957 0.000395737443047039 -3.25121218962969]
MF215='out1mf215':'linear',[2.7934205059548e-022 -3.74568099117315e-022 -4.72728056142758e-022
-8.52413566593407e-022 -7.05238109342641e-022 -2.4790492524943e-023 -1.96111678826406e-023
4.37392995904871e-023 -8.73177480334567e-022] MF216='out1mf216':'linear',[2.4197905129036e-013
-5.65627628213616e-013 -5.88479078194016e-013 -8.83310135008194e-013 -5.59448118032717e-013
5.77277156369051e-013 -3.39564808178261e-014 4.32397025068352e-014 -1.10573291575574e-012]
MF217='out1mf217':'linear',[8.3734523010774e-008 -1.23097213724626e-007 -1.50109704332645e-007
-2.63436294398294e-007 -2.1864765478818e-007 2.83143646497709e-008 -7.10552816141053e-009
1.37915488427107e-008 -2.77402075684838e-007] MF218='out1mf218':'linear',[-0.63320903925308
-0.272965179446953 -2.18190177074967 -2.86512208983476 7.69193358277495 -1.04381227165592
0.0370474340115662 -0.0337943219085029 -4.20204912732138]
MF219='out1mf219':'linear',[1.91951346548188e-020 -2.53735346084211e-020 -3.22067797421092e-020
-5.83325574087272e-020 -4.83904831979145e-020 -2.74927587322669e-021 -1.31445421339639e-021
2.99046064378704e-021 -5.94721657169634e-020] MF220='out1mf220':'linear',[5.14175732218862e-011
-9.69463068060428e-011 -1.07880517676156e-010 -1.74080349005602e-010 -1.26144517318711e-010
6.72119592208936e-011 -5.69687315233201e-012 8.78206605263321e-012 -2.01266966011323e-010]
MF221='out1mf221':'linear',[1.21238006727041e-008 -1.85830700128542e-008 -2.23342365229409e-008
-3.87351750195106e-008 -3.24114301433472e-008 6.83603682203681e-009 -1.1265997767201e-009
2.05568355967293e-009 -4.12648312038758e-008] MF222='out1mf222':'linear',[-0.0463367964903251
-0.202218987159037 -0.775677104949315 -1.20671596809787 1.76805058866411 -0.352798976652474
0.00505153548738783 0.00845881744767805 -1.48719596422561]
MF223='out1mf223':'linear',[4.72006577508415e-021 -6.34567880611414e-021 -8.00028845560967e-021
-1.44142348544726e-020 -1.19194691204686e-020 -3.71595681161415e-022 -3.3286660171857e-022
7.39743816020289e-022 -1.47781466007501e-020] MF224='out1mf224':'linear',[1.24538593032757e-012
-5.19982350767474e-012 -4.71782300549716e-012 -5.87369400622575e-012 -2.09318976983812e-012
8.34589641320756e-012 -3.206107345399e-013 2.59073082566386e-013 -9.01155123109768e-012]
MF225='out1mf225':'linear',[1.23570713547937e-042 -1.73261410444064e-042 -2.14875392099448e-042
-3.82149714220803e-042 -3.13896517263954e-042 1.11329543841917e-043 -9.38399665613876e-044
1.96826690788532e-043 -3.97217500197132e-042] MF226='out1mf226':'linear',[2.27551060894289e-033
-3.19143007923682e-033 -3.95769886125487e-033 -7.03841268909256e-033 -5.7849978773906e-033
2.11768987358729e-034 -1.73100654848587e-034 3.62692256401934e-034 -7.31589090206345e-033]
MF227='out1mf227':'linear',[2.54327445064057e-055 -3.54610267534516e-055 -4.40686983724789e-055
-7.85012260063314e-055 -6.44334990288283e-055 1.60049415138917e-056 -1.90707174999463e-056
4.03682798470895e-056 -8.14655864245711e-055] MF228='out1mf228':'linear',[3.12882192400332e-046
-4.21751422085093e-046 -5.31152114800294e-046 -9.56177898619441e-046 -7.90032264069472e-046
-2.1717262089294e-047 -2.21520015591535e-047 4.90687613147393e-047 -9.81217944096768e-046]
MF229='out1mf229':'linear',[2.51250439196785e-043 -3.5275975858387e-043 -4.3727029184446e-043
-7.7737378387221e-043 -6.3867631702237e-043 2.43248967154304e-044 -1.91400036905827e-044
4.00554594024558e-044 -8.08331706386654e-043] MF230='out1mf230':'linear',[4.60373076438247e-034
-6.47035118943362e-034 -8.01770495697556e-034 -1.42501441212128e-033 -1.17154544598573e-033
4.75453691039147e-035 -3.51862010636765e-035 7.34745716248486e-035 -1.48208811640873e-033]
MF231='out1mf231':'linear',[5.32703333549143e-056 -7.42893524254383e-056 -9.23151049341083e-056
-1.64434365409165e-055 -1.34960364453256e-055 3.39093885418869e-057 -3.99565411830591e-057
8.45585486574972e-057 -1.70654911130403e-055] MF232='out1mf232':'linear',[7.28905597958186e-047
-9.91654061535029e-047 -1.2443160615216e-046 -2.23358614461673e-046 -1.84221876043084e-046
-2.45010894223172e-048 -5.24324987463225e-048 1.14688765311135e-047 -2.2991011074193e-046]
MF233='out1mf233':'linear',[2.02904807962712e-041 -2.8450897244835e-041 -3.52837294909366e-041
-6.27503872704145e-041 -5.15433293908182e-041 1.83209789890195e-042 -1.54100933186374e-042
3.23200731298376e-042 -6.52253029432663e-041] MF234='out1mf234':'linear',[3.7395331406485e-032
-5.2453335531598e-032 -6.50446870226026e-032 -1.1567218752688e-031 -9.50724316470756e-032
3.4987486331131e-033 -2.84532399036714e-033 5.96074045177025e-033 -1.20236645329792e-031]
MF235='out1mf235':'linear',[4.18116824598689e-054 -5.83011150095869e-054 -7.24515151931419e-054
-1.29058618478063e-053 -1.05929548748824e-053 2.63905905888011e-055 -3.13548707832395e-055
6.63668803273488e-055 -1.33934336940933e-053] MF236='out1mf236':'linear',[5.26574225650586e-045
-7.11296487214665e-045 -8.95053728630612e-045 -1.61021671941532e-044 -1.32988728465962e-044
-3.22684131764956e-046 -3.74168536885842e-046 8.26432694716511e-046 -1.65353797361319e-044]
MF237='out1mf237':'linear',[4.12463221720166e-042 -5.79135087465186e-042 -7.17864768003913e-042
-1.27619246693674e-041 -1.04850641285494e-041 4.00395194191896e-043 -3.14248292649889e-043

```
6.57589827192476e-043 -1.32703442580771e-041] MF238='out1mf238':'linear',[7.56196884871156e-033
-1.06292785998158e-032 -1.31706383985323e-032 -2.34078106003953e-032 -1.92442029540248e-032
7.84964820627475e-034 -5.78094459091444e-034 1.20694660252665e-033 -2.43462011809863e-032]
MF239='out1mf239':'linear',[8.7563615405948e-055 -1.22118423019978e-054 -1.51747291255851e-054
-2.70293489540239e-054 -2.21842639328468e-054 5.58643947494784e-056 -6.56828014475241e-056
1.38995522426903e-055 -2.80522285704165e-054] MF240='out1mf240':'linear',[1.21911231555257e-045
-1.66087936251588e-045 -2.08290359552282e-045 -3.73725531206701e-045 -3.08158665149349e-045
-3.43645433090979e-047 -8.79039410511393e-047 1.91914834051279e-046 -3.84865295446598e-045]
MF241='out1mf241':'linear',[6.60906924374567e-042 -9.37030524805824e-042 -1.15739445441782e-041
-2.05188236706556e-041 -1.68852214294688e-041 9.6300584735454e-043 -5.14943908489174e-043
1.06045813049662e-042 -2.13947178503408e-041] MF242='out1mf242':'linear',[1.14531752819951e-032
-1.63423641601659e-032 -2.01393270687682e-032 -3.56395623599618e-032 -2.93664507234493e-032
2.0457410114729e-033 -9.05872839711898e-034 1.84587595133503e-033 -3.72266370530295e-032]
MF243='out1mf243':'linear',[1.69395652813922e-054 -2.36352839959468e-054 -2.93644140256375e-054
-5.22964003822711e-054 -4.2916830992821e-054 1.11013178071947e-055 -1.27155867091084e-055
2.68929186873049e-055 -5.42841347596747e-054] MF244='out1mf244':'linear',[3.04767453800971e-045
-4.22860734993466e-045 -5.26514813945968e-045 -9.39342912349015e-045 -7.71834987978147e-045
1.33257605405609e-046 -2.26694785069469e-046 4.82933045774388e-046 -9.73214869365961e-045]
MF245='out1mf245':'linear',[1.25975628578815e-042 -1.79564785126938e-042 -2.2136450237548e-042
-3.91847487133839e-042 -3.22739341379824e-042 2.17491849931082e-043 -9.93576715043006e-044
2.02848470110964e-043 -4.09190475144716e-042] MF246='out1mf246':'linear',[2.09479541450354e-033
-3.01597166268571e-033 -3.70472011150285e-033 -6.53933245568471e-033 -5.39663860862493e-033
4.70059694767923e-034 -1.69094186525294e-034 3.39642415073626e-034 -6.84777583841094e-033]
MF247='out1mf247':'linear',[3.5405431254314e-055 -4.94018368400738e-055 -6.13759559126118e-055
-1.09306122158315e-054 -8.97022041748847e-055 2.3260956174392e-056 -2.65789373838097e-056
5.62101748339252e-056 -1.13461840194612e-054] MF248='out1mf248':'linear',[6.48511984892888e-046
-9.0093907573822e-046 -1.12123061859125e-045 -1.99957743785035e-045 -1.64263926002078e-045
3.16482945536835e-047 -4.834320469735e-047 1.02811667884133e-046 -2.07254244411257e-045]
MF249='out1mf249':'linear',[1.08315663127646e-040 -1.53593353243635e-040 -1.89703578045246e-040
-3.36300328878593e-040 -2.76753402892868e-040 1.58677215231112e-041 -8.44240808834303e-042
1.73815838197486e-041 -3.50671482612777e-040] MF250='out1mf250':'linear',[1.8756914815486e-031
-2.67703777381518e-031 -3.29872980510971e-031 -5.8371952091439e-031 -4.80991324077152e-031
3.37269761120274e-032 -1.48434006561427e-032 3.02345985462855e-032 -6.09755125811435e-031]
MF251='out1mf251':'linear',[2.78334855380788e-053 -3.88353858619636e-053 -4.82489111312418e-053
-8.5928543013908e-053 -7.05167371615113e-053 1.82428516136235e-054 -2.08930859306722e-054
4.41878719577565e-054 -8.91947277688455e-053] MF252='out1mf252':'linear',[5.02868962784434e-044
-6.97903530695026e-044 -8.68890243492201e-044 -1.55004256426236e-043 -1.2735674214927e-043
2.25005105723346e-045 -3.742105794115e-045 7.9691729638583e-045 -1.6060731404289e-043]
MF253='out1mf253':'linear',[2.06266294839226e-041 -2.94076986222403e-041 -3.62503633794394e-041
-6.41643017206125e-041 -5.28499407365725e-041 3.58467075094638e-042 -1.62766999345986e-042
3.32183732751038e-042 -6.7008450184137e-041] MF254='out1mf254':'linear',[3.42561926459308e-032
-4.93382068241327e-032 -6.05974496203594e-032 -1.0695150797865e-031 -8.82673761549433e-032
7.75018638728451e-033 -2.76743450818227e-033 5.55548954141885e-033 -1.12007765906347e-031]
MF255='out1mf255':'linear',[5.81747181226611e-054 -8.11723266767402e-054 -1.00846987910838e-053
-1.79601076301289e-053 -1.47389591570182e-053 3.82201282853771e-055 -4.36718425744429e-055
9.23589364228837e-055 -1.86429460276276e-053] MF256='out1mf256':'linear',[1.06913864437666e-044
-1.48559392265856e-044 -1.84869385338423e-044 -3.29670904181463e-044 -2.70811535637522e-044
5.30414907907596e-046 -7.97261298571146e-046 1.69508019938285e-045 -3.41723834852323e-044]

[Rules]
1 1 1 1 1 1 1 1, 1 (1) :  1
1 1 1 1 1 1 1 2, 2 (1) :  1
1 1 1 1 1 1 2 1, 3 (1) :  1
1 1 1 1 1 1 2 2, 4 (1) :  1
1 1 1 1 1 2 1 1, 5 (1) :  1
1 1 1 1 1 2 1 2, 6 (1) :  1
1 1 1 1 1 2 2 1, 7 (1) :  1
1 1 1 1 1 2 2 2, 8 (1) :  1
1 1 1 1 2 1 1 1, 9 (1) :  1
1 1 1 1 2 1 1 2, 10 (1) :  1
1 1 1 1 2 1 2 1, 11 (1) :  1
1 1 1 1 2 1 2 2, 12 (1) :  1
1 1 1 1 2 2 1 1, 13 (1) :  1
1 1 1 1 2 2 1 2, 14 (1) :  1
1 1 1 1 2 2 2 1, 15 (1) :  1
1 1 1 1 2 2 2 2, 16 (1) :  1
1 1 1 2 1 1 1 1, 17 (1) :  1
1 1 1 2 1 1 1 2, 18 (1) :  1
1 1 1 2 1 1 2 1, 19 (1) :  1
1 1 1 2 1 1 2 2, 20 (1) :  1
1 1 1 2 1 2 1 1, 21 (1) :  1
1 1 1 2 1 2 1 2, 22 (1) :  1
1 1 1 2 1 2 2 1, 23 (1) :  1
1 1 1 2 1 2 2 2, 24 (1) :  1
1 1 1 2 2 1 1 1, 25 (1) :  1
1 1 1 2 2 1 1 2, 26 (1) :  1
```

```
1 1 1 2 2 1 2 1, 27 (1) :  1
1 1 1 2 2 1 2 2, 28 (1) :  1
1 1 1 2 2 2 1 1, 29 (1) :  1
1 1 1 2 2 2 1 2, 30 (1) :  1
1 1 1 2 2 2 2 1, 31 (1) :  1
1 1 1 2 2 2 2 2, 32 (1) :  1
1 1 2 1 1 1 1 1, 33 (1) :  1
1 1 2 1 1 1 1 2, 34 (1) :  1
1 1 2 1 1 1 2 1, 35 (1) :  1
1 1 2 1 1 1 2 2, 36 (1) :  1
1 1 2 1 1 2 1 1, 37 (1) :  1
1 1 2 1 1 2 1 2, 38 (1) :  1
1 1 2 1 1 2 2 1, 39 (1) :  1
1 1 2 1 1 2 2 2, 40 (1) :  1
1 1 2 1 2 1 1 1, 41 (1) :  1
1 1 2 1 2 1 1 2, 42 (1) :  1
1 1 2 1 2 1 2 1, 43 (1) :  1
1 1 2 1 2 1 2 2, 44 (1) :  1
1 1 2 1 2 2 1 1, 45 (1) :  1
1 1 2 1 2 2 1 2, 46 (1) :  1
1 1 2 1 2 2 2 1, 47 (1) :  1
1 1 2 1 2 2 2 2, 48 (1) :  1
1 1 2 2 1 1 1 1, 49 (1) :  1
1 1 2 2 1 1 1 2, 50 (1) :  1
1 1 2 2 1 1 2 1, 51 (1) :  1
1 1 2 2 1 1 2 2, 52 (1) :  1
1 1 2 2 1 2 1 1, 53 (1) :  1
1 1 2 2 1 2 1 2, 54 (1) :  1
1 1 2 2 1 2 2 1, 55 (1) :  1
1 1 2 2 1 2 2 2, 56 (1) :  1
1 1 2 2 2 1 1 1, 57 (1) :  1
1 1 2 2 2 1 1 2, 58 (1) :  1
1 1 2 2 2 1 2 1, 59 (1) :  1
1 1 2 2 2 1 2 2, 60 (1) :  1
1 1 2 2 2 2 1 1, 61 (1) :  1
1 1 2 2 2 2 1 2, 62 (1) :  1
1 1 2 2 2 2 2 1, 63 (1) :  1
1 1 2 2 2 2 2 2, 64 (1) :  1
1 2 1 1 1 1 1 1, 65 (1) :  1
1 2 1 1 1 1 1 2, 66 (1) :  1
1 2 1 1 1 1 2 1, 67 (1) :  1
1 2 1 1 1 1 2 2, 68 (1) :  1
1 2 1 1 1 2 1 1, 69 (1) :  1
1 2 1 1 1 2 1 2, 70 (1) :  1
1 2 1 1 1 2 2 1, 71 (1) :  1
1 2 1 1 1 2 2 2, 72 (1) :  1
1 2 1 1 2 1 1 1, 73 (1) :  1
1 2 1 1 2 1 1 2, 74 (1) :  1
1 2 1 1 2 1 2 1, 75 (1) :  1
1 2 1 1 2 1 2 2, 76 (1) :  1
1 2 1 1 2 2 1 1, 77 (1) :  1
1 2 1 1 2 2 1 2, 78 (1) :  1
1 2 1 1 2 2 2 1, 79 (1) :  1
1 2 1 1 2 2 2 2, 80 (1) :  1
1 2 1 2 1 1 1 1, 81 (1) :  1
1 2 1 2 1 1 1 2, 82 (1) :  1
1 2 1 2 1 1 2 1, 83 (1) :  1
1 2 1 2 1 1 2 2, 84 (1) :  1
1 2 1 2 1 2 1 1, 85 (1) :  1
1 2 1 2 1 2 1 2, 86 (1) :  1
1 2 1 2 1 2 2 1, 87 (1) :  1
1 2 1 2 1 2 2 2, 88 (1) :  1
1 2 1 2 2 1 1 1, 89 (1) :  1
1 2 1 2 2 1 1 2, 90 (1) :  1
1 2 1 2 2 1 2 1, 91 (1) :  1
1 2 1 2 2 1 2 2, 92 (1) :  1
1 2 1 2 2 2 1 1, 93 (1) :  1
1 2 1 2 2 2 1 2, 94 (1) :  1
1 2 1 2 2 2 2 1, 95 (1) :  1
1 2 1 2 2 2 2 2, 96 (1) :  1
1 2 2 1 1 1 1 1, 97 (1) :  1
1 2 2 1 1 1 1 2, 98 (1) :  1
1 2 2 1 1 1 2 1, 99 (1) :  1
1 2 2 1 1 1 2 2, 100 (1) :  1
1 2 2 1 1 2 1 1, 101 (1) :  1
1 2 2 1 1 2 1 2, 102 (1) :  1
```

```
1 2 2 1 1 2 2 1, 103 (1) :  1
1 2 2 1 1 2 2 2, 104 (1) :  1
1 2 2 1 2 1 1 1, 105 (1) :  1
1 2 2 1 2 1 1 2, 106 (1) :  1
1 2 2 1 2 1 2 1, 107 (1) :  1
1 2 2 1 2 1 2 2, 108 (1) :  1
1 2 2 1 2 2 1 1, 109 (1) :  1
1 2 2 1 2 2 1 2, 110 (1) :  1
1 2 2 1 2 2 2 1, 111 (1) :  1
1 2 2 1 2 2 2 2, 112 (1) :  1
1 2 2 2 1 1 1 1, 113 (1) :  1
1 2 2 2 1 1 1 2, 114 (1) :  1
1 2 2 2 1 1 2 1, 115 (1) :  1
1 2 2 2 1 1 2 2, 116 (1) :  1
1 2 2 2 1 2 1 1, 117 (1) :  1
1 2 2 2 1 2 1 2, 118 (1) :  1
1 2 2 2 1 2 2 1, 119 (1) :  1
1 2 2 2 1 2 2 2, 120 (1) :  1
1 2 2 2 2 1 1 1, 121 (1) :  1
1 2 2 2 2 1 1 2, 122 (1) :  1
1 2 2 2 2 1 2 1, 123 (1) :  1
1 2 2 2 2 1 2 2, 124 (1) :  1
1 2 2 2 2 2 1 1, 125 (1) :  1
1 2 2 2 2 2 1 2, 126 (1) :  1
1 2 2 2 2 2 2 1, 127 (1) :  1
1 2 2 2 2 2 2 2, 128 (1) :  1
2 1 1 1 1 1 1 1, 129 (1) :  1
2 1 1 1 1 1 1 2, 130 (1) :  1
2 1 1 1 1 1 2 1, 131 (1) :  1
2 1 1 1 1 1 2 2, 132 (1) :  1
2 1 1 1 1 2 1 1, 133 (1) :  1
2 1 1 1 1 2 1 2, 134 (1) :  1
2 1 1 1 1 2 2 1, 135 (1) :  1
2 1 1 1 1 2 2 2, 136 (1) :  1
2 1 1 1 2 1 1 1, 137 (1) :  1
2 1 1 1 2 1 1 2, 138 (1) :  1
2 1 1 1 2 1 2 1, 139 (1) :  1
2 1 1 1 2 1 2 2, 140 (1) :  1
2 1 1 1 2 2 1 1, 141 (1) :  1
2 1 1 1 2 2 1 2, 142 (1) :  1
2 1 1 1 2 2 2 1, 143 (1) :  1
2 1 1 1 2 2 2 2, 144 (1) :  1
2 1 1 2 1 1 1 1, 145 (1) :  1
2 1 1 2 1 1 1 2, 146 (1) :  1
2 1 1 2 1 1 2 1, 147 (1) :  1
2 1 1 2 1 1 2 2, 148 (1) :  1
2 1 1 2 1 2 1 1, 149 (1) :  1
2 1 1 2 1 2 1 2, 150 (1) :  1
2 1 1 2 1 2 2 1, 151 (1) :  1
2 1 1 2 1 2 2 2, 152 (1) :  1
2 1 1 2 2 1 1 1, 153 (1) :  1
2 1 1 2 2 1 1 2, 154 (1) :  1
2 1 1 2 2 1 2 1, 155 (1) :  1
2 1 1 2 2 1 2 2, 156 (1) :  1
2 1 1 2 2 2 1 1, 157 (1) :  1
2 1 1 2 2 2 1 2, 158 (1) :  1
2 1 1 2 2 2 2 1, 159 (1) :  1
2 1 1 2 2 2 2 2, 160 (1) :  1
2 1 2 1 1 1 1 1, 161 (1) :  1
2 1 2 1 1 1 1 2, 162 (1) :  1
2 1 2 1 1 1 2 1, 163 (1) :  1
2 1 2 1 1 1 2 2, 164 (1) :  1
2 1 2 1 1 2 1 1, 165 (1) :  1
2 1 2 1 1 2 1 2, 166 (1) :  1
2 1 2 1 1 2 2 1, 167 (1) :  1
2 1 2 1 1 2 2 2, 168 (1) :  1
2 1 2 1 2 1 1 1, 169 (1) :  1
2 1 2 1 2 1 1 2, 170 (1) :  1
2 1 2 1 2 1 2 1, 171 (1) :  1
2 1 2 1 2 1 2 2, 172 (1) :  1
2 1 2 1 2 2 1 1, 173 (1) :  1
2 1 2 1 2 2 1 2, 174 (1) :  1
2 1 2 1 2 2 2 1, 175 (1) :  1
2 1 2 1 2 2 2 2, 176 (1) :  1
2 1 2 2 1 1 1 1, 177 (1) :  1
2 1 2 2 1 1 1 2, 178 (1) :  1
```

```
2 1 2 2 1 1 2 1, 179 (1) :  1
2 1 2 2 1 1 2 2, 180 (1) :  1
2 1 2 2 1 2 1 1, 181 (1) :  1
2 1 2 2 1 2 1 2, 182 (1) :  1
2 1 2 2 1 2 2 1, 183 (1) :  1
2 1 2 2 1 2 2 2, 184 (1) :  1
2 1 2 2 2 1 1 1, 185 (1) :  1
2 1 2 2 2 1 1 2, 186 (1) :  1
2 1 2 2 2 1 2 1, 187 (1) :  1
2 1 2 2 2 1 2 2, 188 (1) :  1
2 1 2 2 2 2 1 1, 189 (1) :  1
2 1 2 2 2 2 1 2, 190 (1) :  1
2 1 2 2 2 2 2 1, 191 (1) :  1
2 1 2 2 2 2 2 2, 192 (1) :  1
2 2 1 1 1 1 1 1, 193 (1) :  1
2 2 1 1 1 1 1 2, 194 (1) :  1
2 2 1 1 1 1 2 1, 195 (1) :  1
2 2 1 1 1 1 2 2, 196 (1) :  1
2 2 1 1 1 2 1 1, 197 (1) :  1
2 2 1 1 1 2 1 2, 198 (1) :  1
2 2 1 1 1 2 2 1, 199 (1) :  1
2 2 1 1 1 2 2 2, 200 (1) :  1
2 2 1 1 2 1 1 1, 201 (1) :  1
2 2 1 1 2 1 1 2, 202 (1) :  1
2 2 1 1 2 1 2 1, 203 (1) :  1
2 2 1 1 2 1 2 2, 204 (1) :  1
2 2 1 1 2 2 1 1, 205 (1) :  1
2 2 1 1 2 2 1 2, 206 (1) :  1
2 2 1 1 2 2 2 1, 207 (1) :  1
2 2 1 1 2 2 2 2, 208 (1) :  1
2 2 1 2 1 1 1 1, 209 (1) :  1
2 2 1 2 1 1 1 2, 210 (1) :  1
2 2 1 2 1 1 2 1, 211 (1) :  1
2 2 1 2 1 1 2 2, 212 (1) :  1
2 2 1 2 1 2 1 1, 213 (1) :  1
2 2 1 2 1 2 1 2, 214 (1) :  1
2 2 1 2 1 2 2 1, 215 (1) :  1
2 2 1 2 1 2 2 2, 216 (1) :  1
2 2 1 2 2 1 1 1, 217 (1) :  1
2 2 1 2 2 1 1 2, 218 (1) :  1
2 2 1 2 2 1 2 1, 219 (1) :  1
2 2 1 2 2 1 2 2, 220 (1) :  1
2 2 1 2 2 2 1 1, 221 (1) :  1
2 2 1 2 2 2 1 2, 222 (1) :  1
2 2 1 2 2 2 2 1, 223 (1) :  1
2 2 1 2 2 2 2 2, 224 (1) :  1
2 2 2 1 1 1 1 1, 225 (1) :  1
2 2 2 1 1 1 1 2, 226 (1) :  1
2 2 2 1 1 1 2 1, 227 (1) :  1
2 2 2 1 1 1 2 2, 228 (1) :  1
2 2 2 1 1 2 1 1, 229 (1) :  1
2 2 2 1 1 2 1 2, 230 (1) :  1
2 2 2 1 1 2 2 1, 231 (1) :  1
2 2 2 1 1 2 2 2, 232 (1) :  1
2 2 2 1 2 1 1 1, 233 (1) :  1
2 2 2 1 2 1 1 2, 234 (1) :  1
2 2 2 1 2 1 2 1, 235 (1) :  1
2 2 2 1 2 1 2 2, 236 (1) :  1
2 2 2 1 2 2 1 1, 237 (1) :  1
2 2 2 1 2 2 1 2, 238 (1) :  1
2 2 2 1 2 2 2 1, 239 (1) :  1
2 2 2 1 2 2 2 2, 240 (1) :  1
2 2 2 2 1 1 1 1, 241 (1) :  1
2 2 2 2 1 1 1 2, 242 (1) :  1
2 2 2 2 1 1 2 1, 243 (1) :  1
2 2 2 2 1 1 2 2, 244 (1) :  1
2 2 2 2 1 2 1 1, 245 (1) :  1
2 2 2 2 1 2 1 2, 246 (1) :  1
2 2 2 2 1 2 2 1, 247 (1) :  1
2 2 2 2 1 2 2 2, 248 (1) :  1
2 2 2 2 2 1 1 1, 249 (1) :  1
2 2 2 2 2 1 1 2, 250 (1) :  1
2 2 2 2 2 1 2 1, 251 (1) :  1
2 2 2 2 2 1 2 2, 252 (1) :  1
2 2 2 2 2 2 1 1, 253 (1) :  1
2 2 2 2 2 2 1 2, 254 (1) :  1
```

```
2 2 2 2 2 2 2 1, 255 (1) :  1
2 2 2 2 2 2 2 2, 256 (1) :  1
```

Controlador difuso que proporciona la segunda entrada de control

```
[System]
Name='TS_FLC2'
Type='sugeno'
Version=2.0
NumInputs=8
NumOutputs=1
NumRules=256
AndMethod='prod'
OrMethod='max'
ImpMethod='prod'
AggMethod='max'
DefuzzMethod='wtaver'

[Input1]
Name='th1'
Range=[-0.392699081698724 0.392699081698746]
NumMFs=2
MF1='in1mf1':'gaussmf',[0.331299584051453 -0.393065826255094]
MF2='in1mf2':'gaussmf',[0.324849983857585 0.396917461349916]

[Input2]
Name='th2'
Range=[-0.392697390114973 0.502148156859372]
NumMFs=2
MF1='in2mf1':'gaussmf',[0.372978239152141 -0.39573675456062]
MF2='in2mf2':'gaussmf',[0.379039500054973 0.502470875196113]

[Input3]
Name='th3'
Range=[0.496466035821262 0.540963680678532]
NumMFs=2
MF1='in3mf1':'gaussmf',[0.00744136558452192 0.511239137307385]
MF2='in3mf2':'gaussmf',[0.006355082909772 0.570000175889325]

[Input4]
Name='dth1'
Range=[0.424486970733943 1.54995445913001]
NumMFs=2
MF1='in4mf1':'gaussmf',[0.475532541842261 0.423450309044259]
MF2='in4mf2':'gaussmf',[0.475898144273864 1.55080362272399]

[Input5]
Name='dth2'
Range=[-2.34795490674393 0.794466278906833]
NumMFs=2
MF1='in5mf1':'gaussmf',[1.33353528652899 -2.34836989388601]
MF2='in5mf2':'gaussmf',[1.33450126695065 0.794429194762057]

[Input6]
Name='dth3'
Range=[-0.431527515858298 1.48388744704806]
NumMFs=2
MF1='in6mf1':'gaussmf',[0.811697531172577 -0.433184777516154]
MF2='in6mf2':'gaussmf',[0.811785089889789 1.48363940722818]

[Input7]
Name='y1'
Range=[-0.0418617957952893 0.0251872360255873]
NumMFs=2
MF1='in7mf1':'gaussmf',[0.0304982618213313 -0.0356913977556446]
MF2='in7mf2':'gaussmf',[-0.00219856094990668 0.0415957950869002]

[Input8]
Name='y2'
Range=[-0.0495763435844818 1.69158377975999e-006]
NumMFs=2
MF1='in8mf1':'gaussmf',[-0.00107434795710089 -0.0613342628586224]
MF2='in8mf2':'gaussmf',[0.0223965611086808 -0.00259035764994451]
```

```
[Output1]
Name='u2'
Range=[-45.6018507805194 16.6918110223817]
NumMFs=256
 MF1='out1mf1':'linear',[-1.9956573848036e-025 3.12832348748178e-025 3.72946559546218e-025
6.42409721290867e-025 5.36190647895933e-025 -1.3377653404961e-025 1.92432151117413e-026
-3.41885410443395e-026 6.89276778077796e-025] MF2='out1mf2':'linear',[0.238612285330695
0.315962637673722 1.11697082813427 1.38417919693378 -0.530818600620937 -0.549848492711427
0.0151217879189102 -0.0257452303288515 2.11839102975973] MF3='out1mf3':'linear',[-7.33448326945184e-039
1.01772063841966e-038 1.26712935138669e-038 2.26054755776014e-038 1.85679520939212e-038
-3.16032045066117e-040 5.45282014508105e-040 -1.16192442342176e-039 2.34222876265289e-038]
MF4='out1mf4':'linear',[-7.83761531823611e-011 1.22334677146547e-010 1.45546000706463e-010
2.4976489487714e-010 1.96128194920176e-010 -3.72664670936078e-011 6.81009228744291e-012
-1.27442388945843e-011 2.70031167636969e-010] MF5='out1mf5':'linear',[-1.62456722719559e-026
3.08811909525333e-026 3.46117764731509e-026 5.64355678534696e-026 4.84487059134214e-026
-2.98840342684743e-026 2.2371059296932e-027 -3.17705810935779e-027 6.39460952177712e-026]
MF6='out1mf6':'linear',[0.439774655417843 -0.434881224657361 -0.407662723226876 -0.716999323502361
1.23645094951158 -2.24257076020725 0.0778239324246623 -0.0377030451366847 -0.895722135447028]
MF7='out1mf7':'linear',[-1.52720765501518e-039 2.12098720208903e-039 2.63986595251118e-039
4.70821499567067e-039 3.8666745554134e-039 -7.1173487057973e-041 1.13711116974921e-040
-2.42018265017455e-040 4.87974939867625e-039] MF8='out1mf8':'linear',[-1.13727477085704e-011
1.7762903051022e-011 2.11279087084993e-011 3.62480587629081e-011 2.84510609658013e-011
-5.42984595034851e-012 9.88699764497711e-013 -1.8492333602417e-012 3.91998164154019e-011]
MF9='out1mf9':'linear',[-3.10671176930506e-024 4.88768518922649e-024 5.81969860512916e-024
1.00141573087604e-023 8.36271977172516e-024 -2.14462504700877e-024 3.01757013722519e-025
-5.33511445961429e-025 1.07558474835895e-023] MF10='out1mf10':'linear',[1.09569509999756
-0.331634802974232 0.917798990864969 0.931930913511522 -3.94907354375732 -1.96664109134646
-0.011008513335717 0.0788032331335651 1.77342559422866] MF11='out1mf11':'linear',[-1.17512790376708e-037
1.63089283731738e-037 2.03042116472245e-037 3.62204328066289e-037 2.97501799473661e-037
-5.15178694874854e-039 8.73930327544923e-039 -1.86176135515207e-038 3.75315084819563e-037]
MF12='out1mf12':'linear',[-1.11603316586616e-009 1.74280847044941e-009 2.07310092298676e-009
3.55690290952496e-009 2.79192757003657e-009 -5.31971258070271e-010 9.69964820570516e-011
-1.81457594253748e-010 3.84632867895523e-009] MF13='out1mf13':'linear',[-2.40291784971812e-025
4.67361919106413e-025 5.20265566645303e-025 8.4284385732195e-025 7.25989836072092e-025
-4.79168777819325e-025 3.44007809896508e-026 -4.77624498898007e-026 9.61164433295795e-025]
MF14='out1mf14':'linear',[0.674269750875036 -0.762861089363547 -0.52801506234569 -0.756928690917794
0.369166913787684 -2.55666764269841 0.0783031275366859 -0.025465057015876 -1.14417175119278]
MF15='out1mf15':'linear',[-2.44543174668847e-038 3.39673774035802e-038 4.2274640349448e-038
7.5393462922501e-038 6.19160317745881e-038 -1.15470821015869e-039 1.82127170821416e-039
-3.87552459185886e-039 7.81442137995178e-038] MF16='out1mf16':'linear',[-1.61797297173078e-010
2.52827909913024e-010 3.00668984400898e-010 5.15750162444646e-010 4.04658824733871e-010
-7.74520546589047e-011 1.4070136338504e-011 -2.63072513683588e-011 5.57863146838744e-010]
MF17='out1mf17':'linear',[-1.46164960142848e-025 2.36043148206648e-025 2.78585316320398e-025
4.75800880919039e-025 3.9884494157967e-025 -1.22249886509373e-025 1.49508591468443e-026
-2.55434786898635e-026 5.14849803070918e-025] MF18='out1mf18':'linear',[0.204837994610529
-0.0766354821231092 0.658269865374541 0.986790467895943 -4.09722805091398 0.274386110019186
-0.00270179922630778 0.0040546011389743 1.22541342277526]
MF19='out1mf19':'linear',[-6.57642653223241e-039 9.12903733543284e-039 1.13644584290408e-038
2.02715440889369e-038 1.66496690047794e-038 -2.94059059472568e-040 4.89264889316042e-040
-1.04199121660756e-039 2.10068263895083e-038] MF20='out1mf20':'linear',[-5.75028246071599e-011
8.98087517586953e-011 1.06823730459581e-010 1.83273153840875e-010 1.43844654654763e-010
-2.74329891060191e-011 4.99824710962309e-012 -9.34949573013317e-012 1.9819667298369e-010]
MF21='out1mf21':'linear',[-6.96399511769735e-027 1.73831259479644e-026 1.80919770531768e-026
2.73614574186203e-026 2.44427600390313e-026 -2.7350517599128e-026 1.47233576304938e-027
-1.6634619925882e-027 3.34098639004202e-026] MF22='out1mf22':'linear',[0.261615743932057
-0.237843088789668 -0.13745568460518 -0.203813835837748 -0.0274509197663509 -1.05527281679566
0.0342687400404213 -0.0116542088906105 -0.304751316874626]
MF23='out1mf23':'linear',[-1.36760542803604e-039 1.89996088698268e-039 2.36446232773117e-039
4.21659734605516e-039 3.46272064864975e-039 -6.55533418616921e-041 1.01885517801885e-040
-2.16752685099174e-040 4.37069790022832e-039] MF24='out1mf24':'linear',[-8.33355578837467e-012
1.30241559542809e-011 1.54877480792394e-011 2.65653638844481e-011 2.08412900247787e-011
-3.99331773928071e-012 7.24799917326637e-013 -1.35499431756029e-012 2.87362609435056e-011]
MF25='out1mf25':'linear',[-2.25925817975591e-024 3.66856401583135e-024 4.32182232549469e-024
7.36974510896138e-024 6.18264663553824e-024 -1.95994824577479e-024 2.33576856623364e-025
-3.9628077806507e-025 7.98702170943902e-024] MF26='out1mf26':'linear',[0.668983106108254
-0.216551935240462 -0.788186594449612 -1.98115968292719 -1.18222338602332 -2.97543998272554
0.0358313294052618 0.07377689494242 -1.48821354832471] MF27='out1mf27':'linear',[-1.05338409683368e-037
1.46250127197636e-037 1.82050125418072e-037 3.2471769894234e-037 2.66692912284888e-037
-4.78271418717261e-039 7.83915206196915e-039 -1.6691246964802e-038 3.36514738895268e-037]
MF28='out1mf28':'linear',[-8.18096057946279e-010 1.27825693291399e-009 1.52018467335222e-009
2.60770143826194e-009 2.04600106190526e-009 -3.91215600696028e-010 7.11293358166907e-011
-1.33009875015072e-010 2.82055962409364e-009] MF29='out1mf29':'linear',[-9.33499249417692e-026
2.53528857672968e-025 2.58624335472108e-025 3.82453407711632e-025 3.45819209269325e-025
-4.38569739626911e-025 2.22761211071678e-026 -2.37899808239584e-026 4.77530964825553e-025]
MF30='out1mf30':'linear',[0.196779135379697 -0.185093337797684 -0.157171765389214 -0.2712033602218
1.14281100547525 -1.74957707023454 0.0733014224502656 -0.0512196556222614 -0.414312920618968]
```

MF31='out1mf31':'linear',[-2.18937795773286e-038 3.04204537964467e-038 3.78555548014586e-038
6.75056900241147e-038 5.54350837605978e-038 -1.06180471887694e-039 1.63146329593659e-039
-3.47014197116933e-039 6.99760086491776e-038] MF32='out1mf32':'linear',[-1.18455449389011e-010
1.85210920687637e-010 2.20207252222014e-010 3.77648616706097e-010 2.96178964361134e-010
-5.69114826103836e-011 1.03058141494542e-011 -1.925977523016e-011 4.08586179004907e-010]
MF33='out1mf33':'linear',[-1.94148768924638e-026 2.98312049127985e-026 3.58087352547902e-026
6.20355909406429e-026 5.16244429072635e-026 -1.08955912133206e-026 1.79720385846295e-027
-3.28198042538156e-027 6.61843225203279e-026] MF34='out1mf34':'linear',[0.0159742827172847
0.015049376175342 0.00126572546660954 -0.0222998947188255 -0.0172449397043963 -0.120236776762029
0.00293502902242954 0.000284219157451987 0.0029076862388312]
MF35='out1mf35':'linear',[-6.37640535640959e-040 8.87026077289952e-040 1.1033154448032e-039
1.96675716151444e-039 1.61475000601947e-039 -3.39812630267635e-041 4.76128522386316e-041
-1.011109395461e-040 2.03952392230063e-039] MF36='out1mf36':'linear',[-4.58015915103198e-013
7.28957095483589e-013 8.6092050165468e-013 1.46745108972456e-012 1.13982924101819e-012
-2.48828831751844e-013 4.06140948232806e-014 -7.46260593076922e-014 1.59852383022438e-012]
MF37='out1mf37':'linear',[-2.01263513856831e-027 3.46283129197208e-027 4.00290134940693e-027
6.71395421777002e-027 5.67906711962728e-027 -2.42791075204148e-027 2.32136119093735e-028
-3.67131642601995e-028 7.39691244495499e-027] MF38='out1mf38':'linear',[0.0264897111199458
-0.0289490968353368 -0.0396884876169256 -0.0758991123885791 -0.0616057001466112 -0.0248273187386399
-0.00107440427134426 0.00369698908840743 -0.0732884261572896]
MF39='out1mf39':'linear',[-1.31701233912855e-040 1.83289632371577e-040 2.27943886970971e-040
4.06275335135278e-040 3.33532186442631e-040 -7.2443482837867e-042 9.84130981098649e-042
-2.08871472638923e-041 4.21367336546223e-040] MF40='out1mf40':'linear',[-6.24449762310312e-014
1.00019032681622e-013 1.17843624296953e-013 2.00422671293316e-013 1.55105406371546e-013
-3.53157222046949e-014 5.57354320975139e-015 -1.01806405531954e-014 2.18864619327363e-013]
MF41='out1mf41':'linear',[-3.03599390560527e-025 4.67708304611182e-025 5.60918584752711e-025
9.71014172502402e-025 8.08354617015846e-025 -1.7466776661756e-025 2.82550303847568e-026
-5.14106375042377e-026 1.0367258290931e-024] MF42='out1mf42':'linear',[0.41406000238181
0.00628039864306773 -0.264142180098875 -0.852647774878143 -0.665581566258462 -1.88945482481054
0.0345707061758837 0.0295831453480138 -0.480914988249868]
MF43='out1mf43':'linear',[-1.01987872640186e-038 1.41889669984458e-038 1.76480937286421e-038
3.14583435312024e-038 2.58275119134288e-038 -5.47440963838661e-040 7.6167182816576e-040
-1.61728336952161e-039 3.26232874099091e-038] MF44='out1mf44':'linear',[-6.35413949192557e-012
1.0140149038054e-011 1.19637666980943e-011 2.03734971811359e-011 1.58011701247151e-011
-3.51253272886696e-012 5.65044654108385e-013 -1.03560941240273e-012 2.22162444075434e-011]
MF45='out1mf45':'linear',[-3.06019688571718e-026 5.32264849477257e-026 6.13147578337325e-026
1.02524037589395e-025 8.68568751907618e-026 -3.89291377340011e-026 3.60065145155081e-027
-5.62390402059184e-027 1.13300622072304e-025] MF46='out1mf46':'linear',[0.453793321500618
-0.506421880078892 -0.687993012890642 -1.30756636471631 -1.06024282877749 -0.392841115151191
-0.0194870462623764 0.063890843461561 -1.27073925559713]
MF47='out1mf47':'linear',[-2.10586406589364e-039 2.93097946553904e-039 3.64493186096508e-039
6.49637691770352e-039 5.33312688363882e-039 -1.16500438481561e-040 1.57380748468867e-040
-3.33988983688444e-040 6.737875957526e-039] MF48='out1mf48':'linear',[-8.58552499279652e-013
1.38024810692449e-012 1.62397937743277e-012 2.75844965716248e-012 2.13024051809668e-012
-4.96807249400821e-013 7.69260352935233e-014 -1.400275095488e-013 3.01657968283975e-012]
MF49='out1mf49':'linear',[-1.47686999382278e-026 2.31664092749443e-026 2.7611572856186e-026
4.75521465117784e-026 3.96891491778847e-026 -9.95003803727505e-027 1.4257702697829e-027
-2.53100263003685e-027 5.10317656175041e-026] MF50='out1mf50':'linear',[0.0484800853790787
-0.0346170452996411 -0.0583737375856736 -0.125530150524149 -0.100725643621679 -0.105652219447596
9.54900271399153e-005 0.00563173388519868 -0.107526982272826]
MF51='out1mf51':'linear',[-5.69613198243061e-040 7.92553733492108e-040 9.85729161481512e-040
1.757038040014e-039 1.44250933170107e-039 -3.08166261679512e-041 4.25478139287008e-041
-9.03304553423264e-041 1.82216823235074e-039] MF52='out1mf52':'linear',[-3.22936013835388e-013
5.16075481175879e-013 6.08566621361818e-013 1.03584355504315e-012 8.02722661447095e-013
-1.80101889095572e-013 2.87585601592344e-014 -5.26398131144886e-014 1.13014940755509e-012]
MF53='out1mf53':'linear',[-1.19338238231516e-027 2.27601456548879e-027 2.54838354010065e-027
4.15123166466423e-027 3.56428017496905e-027 -2.22045127195897e-027 1.65204463930817e-028
-2.33869431259903e-028 4.70826731844974e-027] MF54='out1mf54':'linear',[0.0309162336910823
-0.0359385503628406 -0.0479875566193304 -0.0901300140356659 -0.0731794299770827 -0.0220448275489655
-0.00148925862064959 0.00444179109565867 -0.0886539929360242]
MF55='out1mf55':'linear',[-1.1757565548664e-040 1.63658158122917e-040 2.03516453619062e-040
3.62718340464488e-040 2.97764266533567e-040 -6.54502192022739e-042 8.78823834251068e-042
-1.8648015026288e-041 3.76213089588386e-040] MF56='out1mf56':'linear',[-4.34337345719078e-014
6.99602189281916e-014 8.22550874852391e-014 1.39623009146079e-013 1.0770338468439e-013
-2.54255961325949e-014 3.89923933975328e-015 -7.08516677750282e-015 1.52802886095448e-013]
MF57='out1mf57':'linear',[-2.29829051450774e-025 3.61848380609927e-025 4.30736602924025e-025
7.41021664632427e-025 6.1881615807582e-025 -1.59519090560057e-025 2.23527582524071e-026
-3.94840739578704e-026 7.96082975365995e-025] MF58='out1mf58':'linear',[0.904082256137323
-0.740908526204796 -1.16217358375741 -2.40836249252036 -1.92729742766303 -1.67058445752892
-0.00826887191280677 0.110296241446202 -2.1434762326865]
MF59='out1mf59':'linear',[-9.10942804590969e-039 1.26758826115196e-038 1.57649324262093e-038
2.80998314897515e-038 2.30692729315715e-038 -4.96050319821745e-040 6.80539842237604e-040
-1.44463900575536e-039 2.91422938941871e-038] MF60='out1mf60':'linear',[-4.45462866095783e-012
7.14260137887137e-012 8.41219447042147e-012 1.43019134595434e-011 1.1062305934002e-011
-2.53705282873983e-012 3.9808813017036e-013 -7.26382781466984e-013 1.56241088838855e-011]
MF61='out1mf61':'linear',[-1.76216703884301e-026 3.44118078445861e-026 3.82608997419408e-026

```
6.19119312622535e-026 5.33406373358602e-026 -3.56047592720227e-026 2.53886279204006e-027
-3.51171440545947e-027 7.06861015399141e-026] MF62='out1mf62':'linear',[0.520050972878399
-0.611179595215119 -0.812349338435785 -1.52078613193931 -1.23428096624794 -0.350070601076866
-0.0257464132105071 0.075080206211584 -1.50093204863662]
MF63='out1mf63':'linear',[-1.87978062936186e-039 2.61673069459073e-039 3.25393268725296e-039
5.79920827591608e-039 4.76064330891615e-039 -1.05186041043988e-040 1.40522207271238e-040
-2.98149322831613e-040 6.01510994907471e-039] MF64='out1mf64':'linear',[-5.92391736926822e-013
9.58681294705138e-013 1.12518863800649e-012 1.9068260526235e-012 1.46690913496762e-012
-3.56683301869339e-013 5.34412195634878e-014 -9.66811203261721e-014 2.09062850743734e-012]
MF65='out1mf65':'linear',[-2.65527386373029e-024 4.09549757954205e-024 4.90968472828598e-024
8.49634536356693e-024 7.074953490154e-024 -1.54558322964812e-024 2.47762351038995e-025
-4.50027705837557e-025 9.07432232274377e-024] MF66='out1mf66':'linear',[-1.07428775490374
-7.25965500124881 -5.61549996831881 14.1391397697547 4.07659510283246 -4.6733524126986
-0.00349388911847813 -0.0632223976278663 -11.3273544386805]
MF67='out1mf67':'linear',[-8.59755701246276e-038 1.19264169002957e-037 1.48508315248278e-037
2.64961026868527e-037 2.17647983986898e-037 -3.60599827939113e-039 6.38871216270089e-039
-1.36187445385627e-038 2.74509115508173e-037] MF68='out1mf68':'linear',[-1.03526819147756e-009
1.61541083089137e-009 1.9221439596265e-009 3.29889472802576e-009 2.59111890843551e-009
-4.91410693591445e-010 8.99375242259585e-011 -1.68344593406517e-010 3.56608580670246e-009]
MF69='out1mf69':'linear',[-2.63801839996814e-025 4.61429514247942e-025 5.30604905435234e-025
8.85812989981394e-025 7.51242607168186e-025 -3.44862623034392e-025 3.13696392354504e-026
-4.86780253792192e-026 9.80455180582378e-025] MF70='out1mf70':'linear',[3.32796198040197
-6.40569502958998 -7.23323490992256 -4.83822939263957 11.2599364319065 -21.5394330229908
0.694988521239865 -0.294304495992367 -14.9803476848003] MF71='out1mf71':'linear',[-1.7918287695923e-038
2.48791294980419e-038 3.09683804681873e-038 5.52362713156186e-038 4.53653219228005e-038
-8.18298594341451e-040 1.33360616644563e-039 -2.83928395078009e-039 5.72442941846792e-038]
MF72='out1mf72':'linear',[-1.50317338378151e-010 2.34703379392428e-010 2.79199736615938e-010
4.79065367978404e-010 3.76108955919624e-010 -7.16350449278111e-011 1.30650992074747e-011
-2.4442504082488e-011 5.18006369469926e-010] MF73='out1mf73':'linear',[-4.14914521128391e-023
6.41749208144377e-023 7.68590999804029e-023 1.32900702288072e-022 1.10711191166242e-022
-2.47767882951533e-023 3.89362029520823e-024 -7.04511269890424e-024 1.42054065656742e-022]
MF74='out1mf74':'linear',[-0.0934221238415629 -7.87313413989558 -10.8718812254751 19.9083918322102
-6.79811679833768 -22.8554265957282 -0.211133878403991 0.922034857266432 -20.3684671815918]
MF75='out1mf75':'linear',[-1.37776289988971e-036 1.91159310366316e-036 2.38014105210043e-036
4.24626639989383e-036 3.48790523995046e-036 -5.88834685098556e-038 1.02414436221427e-037
-2.18257334843055e-037 4.39957080842082e-036] MF76='out1mf76':'linear',[-1.47482462668043e-008
2.30244604618114e-008 2.73909854074136e-008 4.70008125263227e-008 3.69004983926027e-008
-7.01837933487336e-009 1.28154977845292e-009 -2.39799536691006e-009 5.08190945688273e-008]
MF77='out1mf77':'linear',[-3.99514955410614e-024 7.07557243883325e-024 8.10441219101402e-024
1.34820432917209e-023 1.14545787127458e-023 -5.52938996439327e-024 4.85901232734915e-025
-7.43560426036172e-025 1.49750484044886e-023] MF78='out1mf78':'linear',[3.93110782907055
-8.75152441857898 -10.7945740904418 -6.52111817086076 8.72253854478105 -22.3792698501364
0.555117798218862 -0.0223568236582771 -21.598037953019] MF79='out1mf79':'linear',[-2.869608022306e-037
3.98503023643706e-037 4.96006661854612e-037 8.84650110493538e-037 7.26538473617705e-037
-1.32918545388788e-038 2.13636152513278e-038 -4.54738025338507e-038 9.16858997218993e-037]
MF80='out1mf80':'linear',[-2.13948787912889e-009 3.34219983909287e-009 3.97508321575968e-009
6.81938324613455e-009 5.35166043303628e-009 -1.02227564553383e-009 1.86009875845333e-010
-3.4787132353728e-010 7.37528161193336e-009] MF81='out1mf81':'linear',[-2.00565440087139e-024
3.16322733868778e-024 3.76324926611656e-024 6.47097999793188e-024 5.40579623535524e-024
-1.41191193526326e-024 1.95777094508623e-025 -3.44996377929438e-025 6.95512573252465e-024]
MF82='out1mf82':'linear',[-0.520987593636656 2.1349080347937 2.1363171836636 2.60817557554923
-2.17901550637499 -0.567477804480906 -0.00972853829562586 0.0280370803047863 4.27378533826421]
MF83='out1mf83':'linear',[-7.71217757856779e-038 1.07028252880053e-037 1.33249778248908e-037
2.37705837255861e-037 1.95244631540176e-037 -3.36753546105763e-039 5.73503464927688e-039
-1.22182428364377e-038 2.46306590245314e-037] MF84='out1mf84':'linear',[-7.59990407501954e-010
1.18662290936389e-009 1.41159371745408e-009 2.42207345019838e-009 1.90141350152815e-009
-3.61959733700583e-010 6.60464522645177e-011 -1.23570818052612e-010 2.61897691467475e-009]
MF85='out1mf85':'linear',[-1.49559887346777e-025 2.95814444777317e-025 3.2768482155812e-025
5.28359336981625e-025 4.56232267379919e-025 -3.15514601693417e-025 2.20213746172319e-026
-3.00862140002122e-026 6.05362744154614e-025] MF86='out1mf86':'linear',[1.87031264279008
-1.55960218630622 -1.93558274669671 -3.80142068393325 3.48768608254268 -9.83073215595555
0.333978591260042 -0.117315941838551 -4.12945057603423] MF87='out1mf87':'linear',[-1.60512051098878e-038
2.22945453076356e-038 2.77474170345516e-038 4.94858617127272e-038 4.06399638365185e-038
-7.55617167109025e-040 1.19536389778859e-039 -2.54376370921122e-039 5.1290764783669e-038]
MF88='out1mf88':'linear',[-1.10213154950565e-010 1.72194348524682e-010 2.04789999915948e-010
3.51305669397565e-010 2.75669281646822e-010 -5.27119645413029e-011 9.58332226228676e-012
-1.79202520177309e-011 3.79965373026648e-010] MF89='out1mf89':'linear',[-3.11777898397195e-023
4.93682419542703e-023 5.86534215734852e-023 1.00740840875809e-022 8.42060221407646e-023
-2.26352381432632e-023 3.06759656317166e-024 -5.37718672325217e-024 1.08400721766872e-022]
MF90='out1mf90':'linear',[3.54465766342011 -0.577610772420593 -1.61273672166256 -4.29547716435339
2.91770236161232 -29.2728507937444 0.705174253808066 -0.0369797162631035 -3.72472130861784]
MF91='out1mf91':'linear',[-1.23552247742423e-036 1.71494785794674e-036 2.13495262541164e-036
3.80835245551411e-036 3.12796864935885e-036 -5.485087878079e-038 9.19063574529589e-038
-1.95754606428292e-037 3.94638330911802e-036] MF92='out1mf92':'linear',[-1.08167871128553e-008
1.68963777591581e-008 2.00963469367356e-008 3.44764111799878e-008 2.70554035872343e-008
-5.16390618765561e-009 9.40264923470631e-010 -1.75865780461023e-009 3.728636864745e-008]
```

MF93='out1mf93':'linear',[-2.18530938904738e-024 4.45034617202364e-024 4.88852151277354e-024 7.8180385170647e-024 6.77963446672452e-024 -5.05911557955383e-024 3.37616146461139e-025 -4.48915399306915e-025 9.0305651803844e-024] MF94='out1mf94':'linear',[2.23151312211498 -2.14425519429948 -2.29832622106392 -4.11996958797188 5.7401943725007 -13.7192243818879 0.486052363985984 -0.230466818922158 -5.10488958144151] MF95='out1mf95':'linear',[-2.56998507828494e-037 3.57014775288003e-037 4.44308837772107e-037 7.92361698729315e-037 6.50704872397114e-037 -1.22519111044947e-038 1.91440639905126e-038 -4.07308897691724e-038 8.21301830171376e-037] MF96='out1mf96':'linear',[-1.5672666127576e-009 2.44975407409005e-009 2.91298215854261e-009 4.9962211628323e-009 3.91918322751649e-009 -7.51511593294068e-010 1.36319171721011e-010 -2.54822509454778e-010 5.40484963291789e-009] MF97='out1mf97':'linear',[-2.53014910610102e-025 3.84183773265545e-025 4.63066536740388e-025 8.04951066549521e-025 6.68725710022082e-025 -1.25948420189613e-025 2.28549416261555e-026 -4.24383957519031e-026 8.55892386309453e-025] MF98='out1mf98':'linear',[-0.137936537119332 0.633877466814076 0.580967237523117 0.743037030109953 0.609965703410397 -1.42881207176253 0.0585223714346521 -0.0478574408134963 1.08177480906749] MF99='out1mf99':'linear',[-7.49407160373546e-039 1.04235723626584e-038 1.29659393816798e-038 2.31139549767415e-038 1.89775783245137e-038 -3.95135920951254e-040 5.59450841656596e-040 -1.18827714578074e-039 2.39680035105263e-038] MF100='out1mf100':'linear',[-6.16878644017585e-012 9.7989102533386e-012 1.15812629931082e-011 1.97536959081687e-011 1.53603283563742e-011 -3.30920851393722e-012 5.45902485877586e-013 -1.00489512021385e-012 2.15019529551974e-011] MF101='out1mf101':'linear',[-2.94878949689325e-026 4.85849428603077e-026 5.69597740416596e-026 9.67254143140667e-026 8.13052603884029e-026 -2.8034196976286e-026 3.13504981007759e-027 -5.2227814428064e-027 1.05263571791331e-025] MF102='out1mf102':'linear',[0.24210844290225 -0.244130360643922 -0.346896773056737 -0.678980996883184 -0.550891158861064 -0.292815506446051 -0.00758240864954504 0.0325817196547227 -0.640191463943311] MF103='out1mf103':'linear',[-1.5485494389994e-039 2.15487797145588e-039 2.67998539746721e-039 4.77683974777308e-039 3.9216417695499e-039 -8.44648350596508e-041 1.15692004979026e-040 -2.45581847514904e-040 4.95409493760904e-039] MF104='out1mf104':'linear',[-8.4641909715715e-013 1.3521781312824e-012 1.59471631917904e-012 2.71467974886635e-012 2.1040314790716e-012 -4.70898640532584e-013 7.53434426274817e-014 -1.3795876190257e-013 2.96146464524113e-012] MF105='out1mf105':'linear',[-3.96728126292837e-024 6.03660569403924e-024 7.27078259947483e-024 1.26312759017422e-023 1.04967423159008e-023 -2.01899385151961e-024 3.59922959636144e-025 -6.66348775794993e-025 1.34386388481157e-023] MF106='out1mf106':'linear',[-0.226732106658859 7.18468152596036 5.72152087923929 5.67565191595338 4.89122486678937 -22.3610135192366 0.779406857857773 -0.45206082572162 10.6785374648005] MF107='out1mf107':'linear',[-1.19876356599131e-037 1.66754062827443e-037 2.07418083601783e-037 3.69745730869164e-037 3.03571829164204e-037 -6.36943666972884e-039 8.95061406945727e-039 -1.90085815369014e-038 3.83420516325503e-037] MF108='out1mf108':'linear',[-8.58116430294982e-011 1.36635722261819e-010 1.61343645289242e-010 2.74970014711209e-010 2.13530336181323e-010 -4.6761749024038e-011 7.61312536080915e-012 -1.39824945044754e-011 2.99581710464437e-010] MF109='out1mf109':'linear',[-4.53415540728392e-025 7.52313939143848e-025 8.79958383793596e-025 1.49129723641811e-024 1.25481495827823e-024 -4.49481032144981e-025 4.88555275622748e-026 -8.06886611200348e-026 1.62617223892567e-024] MF110='out1mf110':'linear',[4.23865155578917 -4.43687273309047 -6.19864624463078 -12.0009222201671 -9.71969800199374 -4.62297458152116 -0.14949768934025 0.579041326640774 -11.4442778063555] MF111='out1mf111':'linear',[-2.47628723235701e-038 3.44615627070764e-038 4.28578658119738e-038 7.638841040335e-038 6.27115883312109e-038 -1.35895492183038e-039 1.85029472679773e-039 -3.92722226073962e-039 7.92251652493039e-038] MF112='out1mf112':'linear',[-1.16805787136419e-011 1.8721016051821e-011 2.20520287268587e-011 3.74967239467046e-011 2.90084004624093e-011 -6.63340741010754e-012 1.04329261015988e-012 -1.90449437807021e-012 4.09570538742114e-011] MF113='out1mf113':'linear',[-1.96637778218227e-025 3.03456325330062e-025 3.63714303797346e-025 6.29317484765212e-025 5.24028624776208e-025 -1.14978808324022e-025 1.83657116945721e-026 -3.33363963447925e-026 6.72237937825971e-025] MF114='out1mf114':'linear',[0.282484501496975 -0.00666131392648725 -0.188874584414133 -0.590390968730529 -0.465974249338521 -1.24863143308758 0.0221268846907523 0.0210749263260566 -0.343914482640902] MF115='out1mf115':'linear',[-6.69596057200013e-039 9.31547511969733e-039 1.15865989517115e-038 2.06536667535773e-038 1.69568706757985e-038 -3.58791304832101e-040 5.00051646017128e-040 -1.06180968356151e-039 2.14183348467542e-038] MF116='out1mf116':'linear',[-4.36733151437094e-012 6.96271541104524e-012 8.21791418051978e-012 1.39992924987971e-011 1.08634357768423e-011 -2.39905171092782e-012 3.87965333747057e-013 -7.11717639137909e-013 1.52597475767182e-011] MF117='out1mf117':'linear',[-1.94447215714719e-026 3.40755019272521e-026 3.91600717155005e-026 6.53394559883159e-026 5.54152151149806e-026 -2.56299970694658e-026 2.31944479854731e-027 -3.59200681484702e-027 7.23610351323109e-026] MF118='out1mf118':'linear',[0.301350408759045 -0.336692774277128 -0.45719310809791 -0.868673331387148 -0.704803570116184 -0.259116537826336 -0.0130079625683759 0.0424735551354203 -0.844417608329585] MF119='out1mf119':'linear',[-1.38269707537854e-039 1.92442546503806e-039 2.39321106925486e-039 4.26545545873896e-039 3.50168983002655e-039 -7.63863103562568e-041 1.03331801720482e-040 -2.19293494631238e-040 4.42399307308416e-039] MF120='out1mf120':'linear',[-5.9205128460578e-013 9.5051800112417e-013 1.11893225835118e-012 1.90148314521593e-012 1.46957586747493e-012 -3.39738651208983e-013 5.29724825825689e-014 -9.65479382207266e-014 2.07832926888732e-012] MF121='out1mf121':'linear',[-3.07180493117841e-024 4.75392939130884e-024 5.69236803534001e-024 9.84124180953758e-024 8.1980429779916e-024 -1.84325863728814e-024 2.8856462664124e-025 -5.21744521319642e-025 1.05209120071248e-023] MF122='out1mf122':'linear',[6.09846423950662 -2.42897858466667 -5.84464297443999 -14.3767089515566 -11.3338402607802 -19.6763741662586 0.2318947500227 0.585997850473895 -10.7370221072497] MF123='out1mf123':'linear',[-1.07093614813463e-037 1.49003443682187e-037 1.85323903345733e-037 3.30339112692003e-037 2.71207003497277e-037 -5.77847149236372e-039 7.99897957016637e-039 -1.69829167505876e-038 3.42579965512991e-037] MF124='out1mf124':'linear',[-6.04454730249257e-011 9.66515525173968e-011 1.13949156241935e-010

1.93915329350263e-010 1.50228432665027e-010 -3.38367692938065e-011 5.38628514573299e-012
-9.85362306982391e-012 2.11615887639864e-010] MF125='out1mf125':'linear',[-2.94196909435585e-025
5.22173007531875e-025 5.97680649210318e-025 9.93633368442576e-025 8.44266359328962e-025
-4.1095744145213e-025 3.59109752548961e-026 -5.48268451830389e-026 1.10438571016489e-024]
MF126='out1mf126':'linear',[5.12672971633828 -5.82470739993191 -7.85259712279334 -14.8460634144831
-12.0359589013761 -4.10859153083249 -0.231286748692803 0.727746937669382 -14.5061096065782]
MF127='out1mf127':'linear',[-2.21079967466364e-038 3.07720803825759e-038 3.82669396923518e-038
6.82020978592339e-038 5.59891103921057e-038 -1.22812937166165e-039 1.65239118708386e-039
-3.50639021577684e-039 7.07388230919967e-038] MF128='out1mf128':'linear',[-8.11310727912169e-012
1.3078903325685e-011 1.53726635183191e-011 2.60867232715601e-011 2.01138755514222e-011
-4.77385320402714e-012 7.29007316176233e-013 -1.32360012808188e-012 2.85582632899223e-011]
MF129='out1mf129':'linear',[-2.24278891232113e-026 3.44003036830035e-026 4.13187194091764e-026
7.16175946198906e-026 5.95883568358543e-026 -1.23796957441773e-026 2.06890008770002e-027
-3.78717876869452e-027 7.63681265550463e-026] MF130='out1mf130':'linear',[1.11244969006651
-0.271742000212591 2.8629122969958 4.87831120869548 -9.15199603737049 -0.877342969252646
0.0125750687876991 -0.0202595744505316 5.56423390482588]
MF131='out1mf131':'linear',[-6.92656098884213e-040 9.6072481539332e-040 1.19635671062303e-039
2.13456086850114e-039 1.75343951876726e-039 -2.87087254659581e-041 5.14592866163463e-041
-1.09713393814301e-040 2.21139168544725e-039] MF132='out1mf132':'linear',[-8.77879961637208e-012
1.36959498356768e-011 1.62975888150367e-011 2.79726814351557e-011 2.19743560969651e-011
-4.16343004890889e-012 7.62580868108565e-013 -1.42755698091891e-012 3.02360337228776e-011]
MF133='out1mf133':'linear',[-2.36548640851125e-027 4.0431070371086e-027 4.683690202924e-027
7.87076053613229e-027 6.65256803913168e-027 -2.76092390087735e-027 2.6958713386046e-028
-4.29617552437104e-028 8.65492748185266e-027] MF134='out1mf134':'linear',[0.221754227753245
-0.21652952438317 0.326630500066078 0.673042583338378 -1.56411318802697 -0.285214406981968
0.00715221483537952 -0.0072962832292139 0.625929415630174]
MF135='out1mf135':'linear',[-1.44413776674034e-040 2.00495037770526e-040 2.49576660296699e-040
4.45167435862049e-040 3.65620809036504e-040 -6.53688395266068e-042 1.07464431735207e-041
-2.28825627970365e-041 4.61335470791946e-040] MF136='out1mf136':'linear',[-1.27503938216352e-012
1.99050161927866e-012 2.36802178189885e-012 4.06342765798424e-012 3.19057947374858e-012
-6.07086376234324e-013 1.1081147157375e-013 -2.07333215649571e-013 4.39340974808023e-012]
MF137='out1mf137':'linear',[-3.50908431215369e-025 5.39587421020297e-025 6.47541671566132e-025
1.12157159119902e-024 9.335226149952e-025 -1.984516873414e-025 3.25380839661221e-026
-5.93530394344462e-026 1.1968259471345e-024] MF138='out1mf138':'linear',[0.411335691660379
1.89532479642472 3.52759837907266 2.58154443880045 -4.10742816002748 -0.249068296462244
0.0209068530872279 -0.0283139929140264 6.77027673392751]
MF139='out1mf139':'linear',[-1.11007726650401e-038 1.5400069853146e-038 1.91756463438892e-038
3.42113753561264e-038 2.81019992609879e-038 -4.69151649498747e-040 8.24995139754086e-040
-1.75844320095153e-039 3.54451362110004e-038] MF140='out1mf140':'linear',[-1.25092065710177e-010
1.95260563979361e-010 2.32304448779395e-010 3.98638939237511e-010 3.13010961032384e-010
-5.94810295217805e-011 1.08689475819221e-011 -2.03397690527623e-011 4.30995842826316e-010]
MF141='out1mf141':'linear',[-3.60442007766843e-026 6.22336707107013e-026 7.185994803666e-026
1.20410006717892e-025 1.01923164242183e-025 -4.42667848773502e-026 4.18540055943307e-027
-6.59185483094672e-027 1.32786575715027e-025] MF142='out1mf142':'linear',[0.165648853147186
0.26521775144686 0.680872703329863 0.502948683725254 -0.868056815749957 -0.161453834226975
0.00835433702514238 -0.00859575467289187 1.29123039543852]
MF143='out1mf143':'linear',[-2.31293938932843e-039 3.2116727604272e-039 3.99763882496346e-039
7.13018214718666e-039 5.85592220683956e-039 -1.06236698613467e-040 1.72164798403319e-040
-3.6651123907493e-040 7.3895466306898e-039] MF144='out1mf144':'linear',[-1.81521102299887e-011
2.83520536516415e-011 3.37227801985986e-011 5.78557619105787e-011 4.54088280336047e-011
-8.66583016429312e-012 1.57800870072715e-012 -2.95149000059297e-012 6.25679916657252e-011]
MF145='out1mf145':'linear',[-1.71162760313591e-026 2.67834863979651e-026 3.19495145644247e-026
5.50616962879324e-026 4.59456950462023e-026 -1.13073738939087e-026 1.64457115659645e-027
-2.92881778037466e-027 5.90490392445231e-026] MF146='out1mf146':'linear',[-5.16718288554357
6.11912412171503 -1.54219214445243 -20.3704307375906 -21.5424618343359 15.0946674891824
0.000483588295358589 -0.000915883970722334 -4.93929145627689]
MF147='out1mf147':'linear',[-6.21438153210845e-040 8.62323698554243e-040 1.07363705456733e-039
1.91534078097965e-039 1.57323689432721e-039 -2.68539410335647e-041 4.62032720123022e-041
-9.84490103025223e-041 1.98456851367551e-039] MF148='out1mf148':'linear',[-6.44649290120179e-012
1.00638403518438e-011 1.19725189336696e-011 2.05441202107587e-011 1.61298055785624e-011
-3.0677701060781e-012 5.60178249080022e-013 -1.04818757698633e-012 2.22128260052173e-011]
MF149='out1mf149':'linear',[-1.427194390999e-027 2.68450803936323e-027 3.01834724383457e-027
4.93616831629034e-027 4.23103034957504e-027 -2.52559887475387e-027 1.93009719726272e-028
-2.77037727701976e-028 5.57657781594978e-027] MF150='out1mf150':'linear',[0.596023019416732
-0.586974898248416 0.925309975581777 2.34413925364117 -5.4644067083423 -0.325667906920295
0.0017059881953177 -0.000685607349463494 1.79276779431231]
MF151='out1mf151':'linear',[-1.29384941787039e-040 1.7969445443971e-040 2.23652740419121e-040
3.98882728544771e-040 3.27585486515089e-040 -6.04301102130588e-042 9.63402061407006e-042
-2.05039695771671e-041 4.13418657544561e-040] MF152='out1mf152':'linear',[-9.35146973766063e-013
1.46082929814852e-012 1.73745915948744e-012 2.9806813659679e-012 2.33920786729875e-012
-4.46860591587702e-013 8.13049433372981e-014 -1.52053139873577e-013 3.22363860391397e-012]
MF153='out1mf153':'linear',[-2.66564891881597e-025 4.18595955560986e-025 4.98733237133129e-025
8.58645998927823e-025 7.16851566757208e-025 -1.81272311819964e-025 2.57947730960855e-026
-4.57199147115744e-026 9.21751943873065e-025] MF154='out1mf154':'linear',[-2.40919669225146
2.62244500676508 -2.47661308162573 -9.43939740353768 8.20972304162397 3.19407831953911
0.00797893291063836 -0.00333816789423284 -5.16253704604929]

```
MF155='out1mf155':'linear',[-9.95645314184761e-039 1.38184015336009e-038 1.72033689570534e-038
3.06885961910139e-038 2.52063970412405e-038 -4.3768380300965e-040 7.40489070009538e-040
-1.57742393205946e-039 3.17997443905665e-038] MF156='out1mf156':'linear',[-9.17711307656034e-011
1.43331816004767e-010 1.70485986232781e-010 2.92493072578653e-010 2.29558092470362e-010
-4.37769812267841e-011 7.97660326082462e-012 -1.49208580236297e-011 3.16314047186365e-010]
MF157='out1mf157':'linear',[-2.11757861698312e-026 4.06930339285858e-026 4.54611341149431e-026
7.38986007001666e-026 6.35403681493243e-026 -4.04959926557605e-026 2.9704617777318e-027
-4.17317189044229e-027 8.39889989868962e-026] MF158='out1mf158':'linear',[-0.0651600104792297
0.08587150979227 -0.0519113770362735 -0.282241168371021 0.151734006255554 0.052938980416417
0.00259885695975862 -0.00161200786483048 -0.117496229001991]
MF159='out1mf159':'linear',[-2.07173323429017e-039 2.87773568483371e-039 3.58149772892901e-039
6.38726839571614e-039 5.24544984447016e-039 -9.80290539169121e-041 1.54301929707662e-040
-3.28331687697624e-040 6.6203626783375e-039] MF160='out1mf160':'linear',[-1.3300936506572e-011
2.07873541982403e-011 2.47194330412061e-011 4.23999458813238e-011 3.32631942687728e-011
-6.37223448923941e-012 1.15677266230112e-012 -2.16261526166058e-012 4.58649709621776e-011]
MF161='out1mf161':'linear',[-2.12182162033675e-027 3.20836090002561e-027 3.87277679670627e-027
6.74015448137643e-027 5.59613846471188e-027 -1.00903206255415e-027 1.89999430986151e-028
-3.54917068200816e-028 7.15816396161601e-027] MF162='out1mf162':'linear',[-0.00221753796000503
0.00667239247731178 0.00661341820081366 0.00940890705258935 0.00767547075024058 -0.0116006088254204
0.000554213650580544 -0.000559934721262099 0.0122929509775606]
MF163='out1mf163':'linear',[-6.04434606031259e-041 8.40662036142483e-041 1.04572918917673e-040
1.86422274907039e-040 1.53062735119427e-040 -3.17220435029743e-042 4.51178497668862e-042
-9.58384032063156e-042 1.93306551510329e-040] MF164='out1mf164':'linear',[-5.2737142034048e-014
8.37050795835038e-014 9.8959820419049e-014 1.68837855043459e-013 1.3134510861626e-013
-2.81437955624985e-014 4.66306762049839e-015 -8.59014325229779e-015 1.83724512151171e-013]
MF165='out1mf165':'linear',[-2.56876909201921e-028 4.17610296759644e-028 4.91774595540157e-028
8.38301310392226e-028 7.03298225959282e-028 -2.2449099470743e-028 2.6614126870512e-029
-4.50883483591321e-029 9.0883830028407e-028] MF166='out1mf166':'linear',[0.00172115108099704
-0.00164622200952573 -0.00239696833082416 -0.00476282969899078 -0.00386442496652427 -0.00236814170047244
-4.41965865142196e-005 0.000226408646070152 -0.00442171003458724]
MF167='out1mf167':'linear',[-1.24922330692589e-041 1.73826467285227e-041 2.16189278642236e-041
3.85344520941992e-041 3.16359373588888e-041 -6.788917278949e-043 9.33214954461435e-043
-1.98108645494078e-042 3.99636927311668e-041] MF168='out1mf168':'linear',[-7.25484172615896e-015
1.15775472253315e-014 1.36596192944998e-014 2.32612543104411e-014 1.80396929314546e-014
-4.00912512165379e-015 6.45075532543175e-016 -1.18234593899408e-015 2.53654773966946e-014]
MF169='out1mf169':'linear',[-3.33019069491166e-026 5.04515991033926e-026 6.08588348753236e-026
1.05860174463801e-025 8.79162566824181e-026 -1.61748055780838e-026 2.99396342947372e-027
-5.5774093742426e-027 1.12486732671211e-025] MF170='out1mf170':'linear',[-0.0190130878283291
0.0820759432443898 0.0760270482496166 0.0988198704009981 0.0823219261067531 -0.181211277337001
0.00755490486808828 -0.00634766412580321 0.141424863359483]
MF171='out1mf171':'linear',[-9.66904458897932e-040 1.3449335758909e-039 1.67294255030981e-039
2.98226039004656e-039 2.44854915027065e-039 -5.11478644402277e-041 7.21871028958112e-041
-1.53317055812546e-040 3.09249670872911e-039] MF172='out1mf172':'linear',[-7.34405503008282e-013
1.16831718581377e-012 1.3800540100978e-012 2.35269475370985e-012 1.82793779430174e-012
-3.97858902037768e-013 6.50940249489926e-014 -1.19655427069631e-013 2.56238075144848e-012]
MF173='out1mf173':'linear',[-3.96304770447642e-027 6.48158429943473e-027 7.61744293390857e-027
1.29627738503298e-026 1.08845651145688e-026 -3.59926937782892e-027 4.15392287611724e-028
-6.98428237667985e-028 1.4077485042259e-026] MF174='out1mf174':'linear',[0.0305402181023418
-0.0307202782910321 -0.0436948930694478 -0.0855679630617267 -0.0692706271573188 -0.0373487028062868
-0.000939717033500069 0.00409753400389325 -0.0806494527528409]
MF175='out1mf175':'linear',[-1.9977046925993e-040 2.77999681315907e-040 3.45738741627639e-040
6.16242306955709e-040 5.05913150581119e-040 -1.09248836111485e-041 1.49257438707485e-041
-3.16816825629623e-041 6.39116804466896e-040] MF176='out1mf176':'linear',[-1.00265948115054e-013
1.60503495791774e-013 1.8914880842823e-013 3.21761170403996e-013 2.49098327096524e-013
-5.65062899273592e-014 8.94422275706973e-015 -1.63461198406583e-014 3.5128697259541e-013]
MF177='out1mf177':'linear',[-1.66130604829833e-027 2.54939447085506e-027 3.06157650950533e-027
5.30584181469597e-027 4.414583733046e-027 -9.2101864447952e-028 1.53385405827139e-028
-2.80600513837368e-028 5.65864323872114e-027] MF178='out1mf178':'linear',[0.00131239318328602
0.00129879096835457 0.000153503467244803 -0.00178216003568716 -0.00134625720792815 -0.0101110871575856
0.000249573749432209 1.81410236834709e-005 0.00032905146681756]
MF179='out1mf179':'linear',[-5.40111708568631e-041 7.51365598450217e-041 9.34569919499559e-041
1.66594475768975e-040 1.36777256835082e-040 -2.88201515025484e-042 4.03315023304e-042
-8.564629333941e-042 1.72759142096413e-040] MF180='out1mf180':'linear',[-3.73984828198392e-014
5.9565868312904e-014 7.03295348691837e-014 1.19847028993765e-013 9.30519544520451e-014
-2.04164626404754e-014 3.31889380629351e-015 -6.0939849941827e-015 1.305889903692e-013]
MF181='out1mf181':'linear',[-1.74516287265357e-028 2.98747422069192e-028 3.45902745039025e-028
5.81010616734941e-028 4.91092316502748e-028 -2.05209742202403e-028 1.9940972298324e-029
-3.17239285144475e-029 6.39195408303241e-028] MF182='out1mf182':'linear',[0.00222436073778842
-0.00242973926525995 -0.00333168340209959 -0.00637193549837933 -0.00516876573835788 -0.00209199047589038
-8.99169617600036e-005 0.000310207052582013 -0.00615250223011792]
MF183='out1mf183':'linear',[-1.11551178150201e-041 1.55248802538374e-041 1.93070515984022e-041
3.44117366556798e-041 2.82502829785753e-041 -6.14222995800387e-043 8.33580623787701e-043
-1.76915432271317e-042 3.56902005512246e-041] MF184='out1mf184':'linear',[-5.08610325756059e-015
8.1548094191298e-015 9.60442624701484e-015 1.63289697761738e-014 1.26295694952309e-014
-2.89492836734053e-015 4.54449237604441e-016 -8.29299737769e-016 1.78385131876101e-014]
MF185='out1mf185':'linear',[-2.59861498268278e-026 3.99798867356711e-026 4.79694559083617e-026
```

8.30720939641424e-026 6.91430936799528e-026 -1.47648426374667e-026 2.41189677165168e-027
-4.39657154801618e-027 8.86604598929157e-026] MF186='out1mf186':'linear',[0.0340410596685825
0.00151592398616332 -0.0209219014571489 -0.0692963431814455 -0.0535742764933366 -0.159082987744883
0.00297816525973795 0.00234792633848475 -0.0380927095498907]
MF187='out1mf187':'linear',[-8.63875866378732e-040 1.20187858728503e-039 1.49487505077621e-039
2.66465366608765e-039 2.18769244367458e-039 -4.64266692268116e-041 6.45182853833082e-041
-1.36990859399134e-040 2.76334394970413e-039] MF188='out1mf188':'linear',[-5.18305983688235e-013
8.27840821733919e-013 9.76406616667561e-013 1.66226243385156e-012 1.28859223690209e-012
-2.88102347254633e-013 4.61325825077945e-014 -8.44827437148214e-014 1.813210610167e-012]
MF189='out1mf189':'linear',[-2.65705673722323e-027 4.59586327854196e-027 5.303637648368e-027
8.88222122851012e-027 7.51881340985002e-027 -3.29032324696155e-027 3.09463148425316e-028
-4.86442537402666e-028 9.80043918278815e-027] MF190='out1mf190':'linear',[0.0380851153555406
-0.0424658526493295 -0.0577106663591401 -0.109703618351682 -0.0888989266528957 -0.0331461697783732
-0.00162851541795344 0.00535717459405257 -0.106596789573236]
MF191='out1mf191':'linear',[-1.78365373289341e-040 2.48255475236568e-040 3.0872599428532e-040
5.50241300229201e-040 4.51713256602991e-040 -9.87718916226463e-042 1.33303596647119e-041
-2.82888016781862e-041 5.70698729724624e-040] MF192='out1mf192':'linear',[-6.98279985121159e-014
1.1239346985813e-013 1.32181282339368e-013 2.24426454069366e-013 1.73197270408996e-013
-4.07051855163929e-014 6.26443532099419e-015 -1.13902305418503e-014 2.45541653890494e-013]
MF193='out1mf193':'linear',[-2.91748814875497e-025 4.42369911239096e-025 5.33466475240343e-025
9.27709541724513e-025 7.70607940016225e-025 -1.43083176923886e-025 2.62789706963218e-026
-4.88924436114237e-026 9.86011753474786e-025] MF194='out1mf194':'linear',[3.76516636981704
-4.25738066206621 3.36197918334352 7.02054107937422 -4.7417234013652 -3.24002068369723 0.113647406882143
-0.211584151365348 5.57891999738682] MF195='out1mf195':'linear',[-8.11595964109216e-039
1.12534653208906e-038 1.40152419223599e-038 2.50086546210607e-038 2.05445544213631e-038
-3.26270208762306e-040 6.02634195431705e-040 -1.28537966041202e-039 2.5906158669729e-038]
MF196='out1mf196':'linear',[-1.15906337741193e-010 1.80766624858986e-010 2.15132422002833e-010
3.69294378097599e-010 2.90187756380975e-010 -5.48732431361556e-011 1.00665460852926e-011
-1.88489849967151e-011 3.99115534400029e-010] MF197='out1mf197':'linear',[-3.4421662544669e-026
5.64667098772141e-026 6.6296627535438e-026 1.12722598510508e-025 9.47076286900056e-026
-3.18733545076496e-026 3.62979829226546e-027 -6.07944129122726e-027 1.22518155898062e-025]
MF198='out1mf198':'linear',[1.2101209821627 -2.44139741061575 -0.781405165306418 0.486048719596209
1.20637229441645 -2.09352964117224 0.0773337299243052 -0.0898341903161383 -1.87465620995804]
MF199='out1mf199':'linear',[-1.69378204282251e-039 2.35094607365743e-039 2.92675146533307e-039
5.22082780948758e-039 4.28811758202575e-039 -7.49504262373878e-041 1.25986790919183e-040
-2.68356791812514e-040 5.40999208915147e-039] MF200='out1mf200':'linear',[-1.68448549994008e-011
2.62882885163138e-011 3.12781379374312e-011 5.36787121176227e-011 4.21593932099815e-011
-8.00559613694586e-012 1.46365655669388e-012 -2.73922877328058e-012 5.80294969922146e-011]
MF201='out1mf201':'linear',[-4.57667053712785e-024 6.9534602072133e-024 8.37948653612664e-024
1.45636920401568e-023 1.21008944672369e-023 -2.29358291445915e-024 4.1396923023495e-025
-7.67992455653298e-025 1.54878368180405e-023] MF202='out1mf202':'linear',[5.2084464590183
-8.44300148740174 1.91102568351516 9.5210390044675 1.80192601794834 -8.54929722312243 0.247504713183852
-0.375913038201975 2.26287580079179] MF203='out1mf203':'linear',[-1.30096724275972e-037
1.80428936377846e-037 2.246901748179e-037 4.00908111837433e-037 3.29332647672238e-037
-5.34251456100025e-039 9.66365866053272e-039 -2.06059704663923e-038 4.15325175598761e-037]
MF204='out1mf204':'linear',[-1.65239663034033e-009 2.57851571473292e-009 3.06805096616162e-009
5.26542899770848e-009 4.13540646609957e-009 -7.8442365540795e-010 1.4354687668513e-010
-2.68686376967165e-010 5.69207714369642e-009] MF205='out1mf205':'linear',[-5.30015699586711e-025
8.75232032159406e-025 1.02535019856338e-024 1.74008450310981e-024 1.46338740581345e-024
-5.11014125534404e-025 5.6604974476144e-026 -9.40290164659561e-026 1.89485490702483e-024]
MF206='out1mf206':'linear',[1.70617816522072 -4.41381470192842 -2.41504121092842 -0.182664935291259
2.64702663174546 -2.83511439288021 0.0672163840937054 -0.0754875156110218 -5.0939706248108]
MF207='out1mf207':'linear',[-2.71323534410249e-038 3.76659436004701e-038 4.688806514002e-038
8.36357942692678e-038 6.86919662360996e-038 -1.21975845550006e-039 2.01876740558482e-039
-4.29903664531161e-039 8.66711452722218e-038] MF208='out1mf208':'linear',[-2.39925640193544e-010
3.74629069982047e-010 4.45647225931257e-010 7.6465191670234e-010 6.00285136547745e-010
-1.14335800042044e-010 2.08528876692256e-011 -3.9012170305866e-011 8.26823815817314e-010]
MF209='out1mf209':'linear',[-2.27319431463465e-025 3.50140482440679e-025 4.19945955437382e-025
7.27011680651035e-025 6.05266623775062e-025 -1.3064329363166e-025 2.11519197620294e-026
-3.84923537205486e-026 7.76167022170741e-025] MF210='out1mf210':'linear',[0.0797183820446854
0.412775626412871 1.2916679131917 1.89924801781922 -4.12264918685735 -0.0280037393417402
0.00755893519194322 -0.0110921098893395 2.46810291177398]
MF211='out1mf211':'linear',[-7.2847932868059e-039 1.01056970026986e-038 1.25835030459677e-038
2.24506238929721e-038 1.84416021198106e-038 -3.06495455681804e-040 5.41352328517506e-040
-1.15394370301513e-039 2.32598986165331e-038] MF212='out1mf212':'linear',[-8.51651404695804e-011
1.32914489149123e-010 1.58140848779439e-010 2.71390769476753e-010 2.13127843887984e-010
-4.04609918817182e-011 7.39917795754145e-012 -1.38481334111685e-011 2.9339659436764e-010]
MF213='out1mf213':'linear',[-2.29250424763529e-026 3.98648046129249e-026 4.5926690275461e-026
7.67999835185666e-026 6.50766549146192e-026 -2.9146367252557e-026 2.69703691936424e-027
-4.21316511844733e-027 8.48645851597908e-026] MF214='out1mf214':'linear',[0.120841495463215
-0.0592601881456231 0.0751220296081667 0.186806290112394 -0.335211745451511 -0.541978747306311
0.0152890460092969 -0.00508833352011507 0.13696251911311]
MF215='out1mf215':'linear',[-1.51807589199227e-039 2.10786969728539e-039 2.62375062969254e-039
4.67977337060974e-039 3.84346076294659e-039 -6.94916085953938e-041 1.12991210970679e-040
-2.40552685059367e-040 4.84994129422602e-039] MF216='out1mf216':'linear',[-1.23620454398122e-011
1.93052590103003e-011 2.29637215302602e-011 3.93997075907893e-011 3.09276029470789e-011

```
-5.89638390277766e-012 1.07456082044931e-012 -2.01008297355148e-012 4.26056251708414e-011]
MF217='out1mf217':'linear',[-3.55320921301133e-024 5.48791492772542e-024 6.5758353579847e-024
1.13752384154943e-023 9.47402502774624e-024 -2.09429566577506e-024 3.32466746829221e-025
-6.02752217542357e-025 1.21537568902831e-023] MF218='out1mf218':'linear',[-0.0609423104719399
1.25302760783855 1.44577516502233 1.35165548012011 -1.345037444932 -1.56686583545198 0.0282291735133636
0.0148052743867336 2.78838035874137] MF219='out1mf219':'linear',[-1.16736664928368e-037
1.61972712237623e-037 2.01671160002612e-037 3.59785889258463e-037 2.95528408947902e-037
-5.00390504926778e-039 8.67795900723964e-039 -1.84929768822464e-038 3.727791926406e-037]
MF220='out1mf220':'linear',[-1.21291200419891e-009 1.89385302539552e-009 2.25288069580881e-009
3.8655341419958e-009 3.03442371465655e-009 -5.77648676559177e-010 1.05403875719291e-010
-1.97208146443155e-010 4.17985915869649e-009] MF221='out1mf221':'linear',[-3.47732348087852e-025
6.1187181474516e-025 7.02274467916366e-025 1.17041786119455e-024 9.93462064838821e-025
-4.67319482221775e-025 4.1799554904149e-026 -6.4429030086435e-026 1.29765403338022e-024]
MF222='out1mf222':'linear',[0.119760516498208 0.0305473260830689 0.0993177203506095 0.060873327832691
-0.3147367625405 -0.589880538341282 0.0137915059389424 0.00159345196582209 0.178660348929656]
MF223='out1mf223':'linear',[-2.43115026470148e-038 3.37623009989379e-038 4.2022662759278e-038
7.49487039315122e-038 6.15530055065669e-038 -1.12862170113264e-039 1.8100198836443e-039
-3.85260729133539e-039 7.76781398514891e-038] MF224='out1mf224':'linear',[-1.75906031480807e-010
2.74833025051872e-010 3.26856737071299e-010 5.60700892637778e-010 4.39966883151826e-010
-8.41177935035796e-011 1.52948051252028e-011 -2.8600953827193e-011 6.06448114404418e-010]
MF225='out1mf225':'linear',[-2.71954025500222e-026 4.07608437627875e-026 4.93541873611406e-026
8.61129430894924e-026 7.14069795150281e-026 -1.16683060080522e-026 2.39059506884326e-027
-4.52277550185072e-027 9.12242620618565e-026] MF226='out1mf226':'linear',[-0.0573599982532347
0.122655483812155 0.132363360555007 0.20735862209715 0.168204372687943 -0.138599192693081
0.00884347889963812 -0.0115065433639832 0.24561352522832]
MF227='out1mf227':'linear',[-7.10231876462802e-040 9.87655143956722e-040 1.22865301669851e-039
2.19042645350522e-039 1.79851153377716e-039 -3.68383201398857e-041 5.30012372787897e-041
-1.12607187016939e-040 2.27119939459321e-039] MF228='out1mf228':'linear',[-7.08346884366904e-013
1.12242904832287e-012 1.32781592176056e-012 2.26672296250266e-012 1.76500786978127e-012
-3.73871418008174e-013 6.25233809315243e-014 -1.15359062086432e-013 2.46500055197983e-012]
MF229='out1mf229':'linear',[-3.54926604908952e-027 5.62499768700781e-027 6.68090840763819e-027
1.1471899949969e-026 9.58918441632259e-027 -2.59307477812501e-027 3.49771486212045e-028
-6.12443783068421e-028 1.23474279711043e-026] MF230='out1mf230':'linear',[0.0136816154593075
-0.0102146185579944 -0.0168311953000312 -0.0358014146346277 -0.0290553388884855 -0.0280322534962858
-3.94317515135501e-005 0.00163225095260439 -0.0309871610994809]
MF231='out1mf231':'linear',[-1.46859101803043e-040 2.04325215498399e-040 2.54133301016047e-040
4.52995280052073e-040 3.71908334322426e-040 -7.90748788061847e-042 1.09685777812099e-041
-2.3288660613889e-041 4.6977720086766e-040] MF232='out1mf232':'linear',[-9.79750953090675e-014
1.5600661243432e-013 1.84215445628036e-013 3.13945102897323e-013 2.43779681213908e-013
-5.33800942533267e-014 8.69161665032664e-015 -1.5963712822102e-014 3.42051444764142e-013]
MF233='out1mf233':'linear',[-4.27679924523902e-025 6.42022062910848e-025 7.76945545698034e-025
1.35499917380669e-024 1.1238493293845e-024 -1.87034608511017e-025 3.77197341649499e-026
-7.11992256081503e-026 1.43607028405462e-024] MF234='out1mf234':'linear',[-0.709265499849856
1.64739220172489 1.73871979829118 2.66121622459467 2.17849530049306 -2.15479334188199 0.124659076236625
-0.150951673816433 3.22638671306897] MF235='out1mf235':'linear',[-1.13626852163559e-038
1.58027933606972e-038 1.9657993329944e-038 3.50448154225308e-038 2.87739510612052e-038
-5.94362042623093e-040 8.48102337681055e-040 -1.8016256964586e-039 3.63384265268914e-038]
MF236='out1mf236':'linear',[-9.88687080944255e-012 1.56984947441247e-011 1.85568300899566e-011
3.16562108428609e-011 2.46217892241228e-011 -5.28997796324448e-012 8.74581109544335e-013
-1.6105251240234e-012 3.4452287138138e-011] MF237='out1mf237':'linear',[-5.5098571637881e-026
8.76983175700233e-026 1.040093350121e-025 1.78376437137081e-025 1.4919378322407e-025
-4.15729979903072e-026 5.47634971407063e-027 -9.53483683816086e-027 1.92225032393065e-025]
MF238='out1mf238':'linear',[0.255888859666439 -0.217856981331201 -0.335462562820861 -0.688431347197015
-0.556369570947542 -0.44080355151734 -0.00352421532290521 0.0319743228957602 -0.618443886841574]
MF239='out1mf239':'linear',[-2.34871553061911e-039 3.26806593368052e-039 4.06457462492487e-039
7.24494304878691e-039 5.94798405211352e-039 -1.27313976682211e-040 1.75447276372398e-040
-3.72467576031483e-040 7.51356813431169e-039] MF240='out1mf240':'linear',[-1.35827528536424e-012
2.16873937364032e-012 2.55825124468606e-012 4.35570765981982e-012 3.37701670268535e-012
-7.53240986442946e-013 1.20844515255123e-013 -2.2137914082048e-013 4.75068655536301e-012]
MF241='out1mf241':'linear',[-2.16217970110542e-026 3.27978924490967e-026 3.9546067750067e-026
6.87630502454954e-026 5.71176863001571e-026 -1.06468768104531e-026 1.94900210812375e-027
-3.62423148506816e-027 7.30936946635468e-026] MF242='out1mf242':'linear',[-0.0118842720783132
0.0535309626188625 0.0492310673735322 0.0633013514078707 0.0523183652175017 -0.120005299663594
0.00494355669731739 -0.00407805259362355 0.0916318424573188]
MF243='out1mf243':'linear',[-6.34794258158169e-040 8.82956607526135e-040 1.09830711385562e-039
1.95790543123185e-039 1.60752198313314e-039 -3.35155132610919e-041 4.73903895745895e-041
-1.00655102900109e-040 2.03026071001923e-039] MF244='out1mf244':'linear',[-5.04076681883352e-013
8.01238397178936e-013 9.46743019814652e-013 1.61445399259485e-012 1.25493263228006e-012
-2.71596557376779e-013 4.46395009434181e-014 -8.21205198360854e-014 1.75778362513601e-012]
MF245='out1mf245':'linear',[-2.54356684248833e-027 4.17697279555043e-027 4.9023480484784e-027
8.33274098805113e-027 7.00095463484623e-027 -2.36954824927564e-027 2.6870658966877e-028
-4.4949863929992e-028 9.05975974429347e-027] MF246='out1mf246':'linear',[0.0203187704889811
-0.0204781783452364 -0.029103441606934 -0.0569677371235893 -0.0461751877618097 -0.0246576494357979
-0.00063270440950925 0.00273143466791941 -0.0537134339921851]
MF247='out1mf247':'linear',[-1.31164294304601e-040 1.82523837841629e-040 2.27000526021214e-040
4.04606761431241e-040 3.32169118956105e-040 -7.16203526638568e-042 9.79952108462407e-042
```

```
-2.08012393880749e-041 4.19622609338873e-040] MF248='out1mf248':'linear',[-6.90109642204927e-014
1.10346396322706e-013 1.30095135030638e-013 2.21391487000432e-013 1.71504356746511e-013
-3.86151017462779e-014 6.14881797987034e-015 -1.12493067740487e-014 2.41601594845838e-013]
MF249='out1mf249':'linear',[-3.39107961097609e-025 5.1544299358813e-025 6.21052316965547e-025
1.07925797830848e-024 8.96740686633353e-025 -1.70672249441063e-025 3.06976327989029e-026
-5.69174702600153e-026 1.14789770346456e-024] MF250='out1mf250':'linear',[-0.0274856793701205
0.613947418965756 0.494423233217743 0.502778926072468 0.437635878788443 -1.88043179518193
0.0662560323225583 -0.039516253668058 0.922061311871107]
MF251='out1mf251':'linear',[-1.01541500998097e-038 1.4125175226115e-038 1.75695714424004e-038
3.1319544276776e-038 2.57141666143489e-038 -5.40221583621304e-040 7.58185784895517e-040
-1.6101359964048e-039 3.24780566506049e-038] MF252='out1mf252':'linear',[-7.00567784567905e-012
1.11634731711547e-011 1.31784026336592e-011 2.24533971721978e-011 1.74290315350756e-011
-3.83666733015655e-012 6.22041874096757e-013 -1.14163450488705e-012 2.44703012907252e-011]
MF253='out1mf253':'linear',[-3.91431697958933e-026 6.47153849668483e-026 7.57846211344829e-026
1.28566060445268e-025 1.081227048263e-025 -3.79915757491356e-026 4.18901515590887e-027
-6.94898643037322e-027 1.40051700159228e-025] MF254='out1mf254':'linear',[0.355397389006747
-0.37159420573094 -0.51938076991289 -1.00580484339249 -0.813857776681192 -0.389812795297663
-0.01244699696261 0.0484867887704466 -0.958963491576385]
MF255='out1mf255':'linear',[-2.09742898229069e-039 2.91895478022792e-039 3.63011635690187e-039
6.47016817787884e-039 5.31171544054313e-039 -1.15224072157156e-040 1.5672480918708e-040
-3.32639673123412e-040 6.7104751796854e-039] MF256='out1mf256':'linear',[-9.51151866517791e-013
1.52606224609577e-012 1.79688570139154e-012 3.05426726691524e-012 2.36145249632385e-012
-5.43726872482111e-013 8.50496468945949e-014 -1.55101329118548e-013 3.33748190375778e-012]


[Rules]
1 1 1 1 1 1 1 1, 1 (1) :  1
1 1 1 1 1 1 1 2, 2 (1) :  1
1 1 1 1 1 1 2 1, 3 (1) :  1
1 1 1 1 1 1 2 2, 4 (1) :  1
1 1 1 1 1 2 1 1, 5 (1) :  1
1 1 1 1 1 2 1 2, 6 (1) :  1
1 1 1 1 1 2 2 1, 7 (1) :  1
1 1 1 1 1 2 2 2, 8 (1) :  1
1 1 1 1 2 1 1 1, 9 (1) :  1
1 1 1 1 2 1 1 2, 10 (1) :  1
1 1 1 1 2 1 2 1, 11 (1) :  1
1 1 1 1 2 1 2 2, 12 (1) :  1
1 1 1 1 2 2 1 1, 13 (1) :  1
1 1 1 1 2 2 1 2, 14 (1) :  1
1 1 1 1 2 2 2 1, 15 (1) :  1
1 1 1 1 2 2 2 2, 16 (1) :  1
1 1 1 2 1 1 1 1, 17 (1) :  1
1 1 1 2 1 1 1 2, 18 (1) :  1
1 1 1 2 1 1 2 1, 19 (1) :  1
1 1 1 2 1 1 2 2, 20 (1) :  1
1 1 1 2 1 2 1 1, 21 (1) :  1
1 1 1 2 1 2 1 2, 22 (1) :  1
1 1 1 2 1 2 2 1, 23 (1) :  1
1 1 1 2 1 2 2 2, 24 (1) :  1
1 1 1 2 2 1 1 1, 25 (1) :  1
1 1 1 2 2 1 1 2, 26 (1) :  1
1 1 1 2 2 1 2 1, 27 (1) :  1
1 1 1 2 2 1 2 2, 28 (1) :  1
1 1 1 2 2 2 1 1, 29 (1) :  1
1 1 1 2 2 2 1 2, 30 (1) :  1
1 1 1 2 2 2 2 1, 31 (1) :  1
1 1 1 2 2 2 2 2, 32 (1) :  1
1 1 2 1 1 1 1 1, 33 (1) :  1
1 1 2 1 1 1 1 2, 34 (1) :  1
1 1 2 1 1 1 2 1, 35 (1) :  1
1 1 2 1 1 1 2 2, 36 (1) :  1
1 1 2 1 1 2 1 1, 37 (1) :  1
1 1 2 1 1 2 1 2, 38 (1) :  1
1 1 2 1 1 2 2 1, 39 (1) :  1
1 1 2 1 1 2 2 2, 40 (1) :  1
1 1 2 1 2 1 1 1, 41 (1) :  1
1 1 2 1 2 1 1 2, 42 (1) :  1
1 1 2 1 2 1 2 1, 43 (1) :  1
1 1 2 1 2 1 2 2, 44 (1) :  1
1 1 2 1 2 2 1 1, 45 (1) :  1
1 1 2 1 2 2 1 2, 46 (1) :  1
1 1 2 1 2 2 2 1, 47 (1) :  1
1 1 2 1 2 2 2 2, 48 (1) :  1
1 1 2 2 1 1 1 1, 49 (1) :  1
1 1 2 2 1 1 1 2, 50 (1) :  1
1 1 2 2 1 1 2 1, 51 (1) :  1
```

```
1 1 2 2 1 1 2 2, 52 (1) :  1
1 1 2 2 1 2 1 1, 53 (1) :  1
1 1 2 2 1 2 1 2, 54 (1) :  1
1 1 2 2 1 2 2 1, 55 (1) :  1
1 1 2 2 1 2 2 2, 56 (1) :  1
1 1 2 2 2 1 1 1, 57 (1) :  1
1 1 2 2 2 1 1 2, 58 (1) :  1
1 1 2 2 2 1 2 1, 59 (1) :  1
1 1 2 2 2 1 2 2, 60 (1) :  1
1 1 2 2 2 2 1 1, 61 (1) :  1
1 1 2 2 2 2 1 2, 62 (1) :  1
1 1 2 2 2 2 2 1, 63 (1) :  1
1 1 2 2 2 2 2 2, 64 (1) :  1
1 2 1 1 1 1 1 1, 65 (1) :  1
1 2 1 1 1 1 1 2, 66 (1) :  1
1 2 1 1 1 1 2 1, 67 (1) :  1
1 2 1 1 1 1 2 2, 68 (1) :  1
1 2 1 1 1 2 1 1, 69 (1) :  1
1 2 1 1 1 2 1 2, 70 (1) :  1
1 2 1 1 1 2 2 1, 71 (1) :  1
1 2 1 1 1 2 2 2, 72 (1) :  1
1 2 1 1 2 1 1 1, 73 (1) :  1
1 2 1 1 2 1 1 2, 74 (1) :  1
1 2 1 1 2 1 2 1, 75 (1) :  1
1 2 1 1 2 1 2 2, 76 (1) :  1
1 2 1 1 2 2 1 1, 77 (1) :  1
1 2 1 1 2 2 1 2, 78 (1) :  1
1 2 1 1 2 2 2 1, 79 (1) :  1
1 2 1 1 2 2 2 2, 80 (1) :  1
1 2 1 2 1 1 1 1, 81 (1) :  1
1 2 1 2 1 1 1 2, 82 (1) :  1
1 2 1 2 1 1 2 1, 83 (1) :  1
1 2 1 2 1 1 2 2, 84 (1) :  1
1 2 1 2 1 2 1 1, 85 (1) :  1
1 2 1 2 1 2 1 2, 86 (1) :  1
1 2 1 2 1 2 2 1, 87 (1) :  1
1 2 1 2 1 2 2 2, 88 (1) :  1
1 2 1 2 2 1 1 1, 89 (1) :  1
1 2 1 2 2 1 1 2, 90 (1) :  1
1 2 1 2 2 1 2 1, 91 (1) :  1
1 2 1 2 2 1 2 2, 92 (1) :  1
1 2 1 2 2 2 1 1, 93 (1) :  1
1 2 1 2 2 2 1 2, 94 (1) :  1
1 2 1 2 2 2 2 1, 95 (1) :  1
1 2 1 2 2 2 2 2, 96 (1) :  1
1 2 2 1 1 1 1 1, 97 (1) :  1
1 2 2 1 1 1 1 2, 98 (1) :  1
1 2 2 1 1 1 2 1, 99 (1) :  1
1 2 2 1 1 1 2 2, 100 (1) :  1
1 2 2 1 1 2 1 1, 101 (1) :  1
1 2 2 1 1 2 1 2, 102 (1) :  1
1 2 2 1 1 2 2 1, 103 (1) :  1
1 2 2 1 1 2 2 2, 104 (1) :  1
1 2 2 1 2 1 1 1, 105 (1) :  1
1 2 2 1 2 1 1 2, 106 (1) :  1
1 2 2 1 2 1 2 1, 107 (1) :  1
1 2 2 1 2 1 2 2, 108 (1) :  1
1 2 2 1 2 2 1 1, 109 (1) :  1
1 2 2 1 2 2 1 2, 110 (1) :  1
1 2 2 1 2 2 2 1, 111 (1) :  1
1 2 2 1 2 2 2 2, 112 (1) :  1
1 2 2 2 1 1 1 1, 113 (1) :  1
1 2 2 2 1 1 1 2, 114 (1) :  1
1 2 2 2 1 1 2 1, 115 (1) :  1
1 2 2 2 1 1 2 2, 116 (1) :  1
1 2 2 2 1 2 1 1, 117 (1) :  1
1 2 2 2 1 2 1 2, 118 (1) :  1
1 2 2 2 1 2 2 1, 119 (1) :  1
1 2 2 2 1 2 2 2, 120 (1) :  1
1 2 2 2 2 1 1 1, 121 (1) :  1
1 2 2 2 2 1 1 2, 122 (1) :  1
1 2 2 2 2 1 2 1, 123 (1) :  1
1 2 2 2 2 1 2 2, 124 (1) :  1
1 2 2 2 2 2 1 1, 125 (1) :  1
1 2 2 2 2 2 1 2, 126 (1) :  1
1 2 2 2 2 2 2 1, 127 (1) :  1
```

```
1 2 2 2 2 2 2 2, 128 (1) :  1
2 1 1 1 1 1 1 1, 129 (1) :  1
2 1 1 1 1 1 1 2, 130 (1) :  1
2 1 1 1 1 1 2 1, 131 (1) :  1
2 1 1 1 1 1 2 2, 132 (1) :  1
2 1 1 1 1 2 1 1, 133 (1) :  1
2 1 1 1 1 2 1 2, 134 (1) :  1
2 1 1 1 1 2 2 1, 135 (1) :  1
2 1 1 1 1 2 2 2, 136 (1) :  1
2 1 1 1 2 1 1 1, 137 (1) :  1
2 1 1 1 2 1 1 2, 138 (1) :  1
2 1 1 1 2 1 2 1, 139 (1) :  1
2 1 1 1 2 1 2 2, 140 (1) :  1
2 1 1 1 2 2 1 1, 141 (1) :  1
2 1 1 1 2 2 1 2, 142 (1) :  1
2 1 1 1 2 2 2 1, 143 (1) :  1
2 1 1 1 2 2 2 2, 144 (1) :  1
2 1 1 2 1 1 1 1, 145 (1) :  1
2 1 1 2 1 1 1 2, 146 (1) :  1
2 1 1 2 1 1 2 1, 147 (1) :  1
2 1 1 2 1 1 2 2, 148 (1) :  1
2 1 1 2 1 2 1 1, 149 (1) :  1
2 1 1 2 1 2 1 2, 150 (1) :  1
2 1 1 2 1 2 2 1, 151 (1) :  1
2 1 1 2 1 2 2 2, 152 (1) :  1
2 1 1 2 2 1 1 1, 153 (1) :  1
2 1 1 2 2 1 1 2, 154 (1) :  1
2 1 1 2 2 1 2 1, 155 (1) :  1
2 1 1 2 2 1 2 2, 156 (1) :  1
2 1 1 2 2 2 1 1, 157 (1) :  1
2 1 1 2 2 2 1 2, 158 (1) :  1
2 1 1 2 2 2 2 1, 159 (1) :  1
2 1 1 2 2 2 2 2, 160 (1) :  1
2 1 2 1 1 1 1 1, 161 (1) :  1
2 1 2 1 1 1 1 2, 162 (1) :  1
2 1 2 1 1 1 2 1, 163 (1) :  1
2 1 2 1 1 1 2 2, 164 (1) :  1
2 1 2 1 1 2 1 1, 165 (1) :  1
2 1 2 1 1 2 1 2, 166 (1) :  1
2 1 2 1 1 2 2 1, 167 (1) :  1
2 1 2 1 1 2 2 2, 168 (1) :  1
2 1 2 1 2 1 1 1, 169 (1) :  1
2 1 2 1 2 1 1 2, 170 (1) :  1
2 1 2 1 2 1 2 1, 171 (1) :  1
2 1 2 1 2 1 2 2, 172 (1) :  1
2 1 2 1 2 2 1 1, 173 (1) :  1
2 1 2 1 2 2 1 2, 174 (1) :  1
2 1 2 1 2 2 2 1, 175 (1) :  1
2 1 2 1 2 2 2 2, 176 (1) :  1
2 1 2 2 1 1 1 1, 177 (1) :  1
2 1 2 2 1 1 1 2, 178 (1) :  1
2 1 2 2 1 1 2 1, 179 (1) :  1
2 1 2 2 1 1 2 2, 180 (1) :  1
2 1 2 2 1 2 1 1, 181 (1) :  1
2 1 2 2 1 2 1 2, 182 (1) :  1
2 1 2 2 1 2 2 1, 183 (1) :  1
2 1 2 2 1 2 2 2, 184 (1) :  1
2 1 2 2 2 1 1 1, 185 (1) :  1
2 1 2 2 2 1 1 2, 186 (1) :  1
2 1 2 2 2 1 2 1, 187 (1) :  1
2 1 2 2 2 1 2 2, 188 (1) :  1
2 1 2 2 2 2 1 1, 189 (1) :  1
2 1 2 2 2 2 1 2, 190 (1) :  1
2 1 2 2 2 2 2 1, 191 (1) :  1
2 1 2 2 2 2 2 2, 192 (1) :  1
2 2 1 1 1 1 1 1, 193 (1) :  1
2 2 1 1 1 1 1 2, 194 (1) :  1
2 2 1 1 1 1 2 1, 195 (1) :  1
2 2 1 1 1 1 2 2, 196 (1) :  1
2 2 1 1 1 2 1 1, 197 (1) :  1
2 2 1 1 1 2 1 2, 198 (1) :  1
2 2 1 1 1 2 2 1, 199 (1) :  1
2 2 1 1 1 2 2 2, 200 (1) :  1
2 2 1 1 2 1 1 1, 201 (1) :  1
2 2 1 1 2 1 1 2, 202 (1) :  1
2 2 1 1 2 1 2 1, 203 (1) :  1
```

```
2 2 1 1 2 1 2 2, 204 (1) :  1
2 2 1 1 2 2 1 1, 205 (1) :  1
2 2 1 1 2 2 1 2, 206 (1) :  1
2 2 1 1 2 2 2 1, 207 (1) :  1
2 2 1 1 2 2 2 2, 208 (1) :  1
2 2 1 2 1 1 1 1, 209 (1) :  1
2 2 1 2 1 1 1 2, 210 (1) :  1
2 2 1 2 1 1 2 1, 211 (1) :  1
2 2 1 2 1 1 2 2, 212 (1) :  1
2 2 1 2 1 2 1 1, 213 (1) :  1
2 2 1 2 1 2 1 2, 214 (1) :  1
2 2 1 2 1 2 2 1, 215 (1) :  1
2 2 1 2 1 2 2 2, 216 (1) :  1
2 2 1 2 2 1 1 1, 217 (1) :  1
2 2 1 2 2 1 1 2, 218 (1) :  1
2 2 1 2 2 1 2 1, 219 (1) :  1
2 2 1 2 2 1 2 2, 220 (1) :  1
2 2 1 2 2 2 1 1, 221 (1) :  1
2 2 1 2 2 2 1 2, 222 (1) :  1
2 2 1 2 2 2 2 1, 223 (1) :  1
2 2 1 2 2 2 2 2, 224 (1) :  1
2 2 2 1 1 1 1 1, 225 (1) :  1
2 2 2 1 1 1 1 2, 226 (1) :  1
2 2 2 1 1 1 2 1, 227 (1) :  1
2 2 2 1 1 1 2 2, 228 (1) :  1
2 2 2 1 1 2 1 1, 229 (1) :  1
2 2 2 1 1 2 1 2, 230 (1) :  1
2 2 2 1 1 2 2 1, 231 (1) :  1
2 2 2 1 1 2 2 2, 232 (1) :  1
2 2 2 1 2 1 1 1, 233 (1) :  1
2 2 2 1 2 1 1 2, 234 (1) :  1
2 2 2 1 2 1 2 1, 235 (1) :  1
2 2 2 1 2 1 2 2, 236 (1) :  1
2 2 2 1 2 2 1 1, 237 (1) :  1
2 2 2 1 2 2 1 2, 238 (1) :  1
2 2 2 1 2 2 2 1, 239 (1) :  1
2 2 2 1 2 2 2 2, 240 (1) :  1
2 2 2 2 1 1 1 1, 241 (1) :  1
2 2 2 2 1 1 1 2, 242 (1) :  1
2 2 2 2 1 1 2 1, 243 (1) :  1
2 2 2 2 1 1 2 2, 244 (1) :  1
2 2 2 2 1 2 1 1, 245 (1) :  1
2 2 2 2 1 2 1 2, 246 (1) :  1
2 2 2 2 1 2 2 1, 247 (1) :  1
2 2 2 2 1 2 2 2, 248 (1) :  1
2 2 2 2 2 1 1 1, 249 (1) :  1
2 2 2 2 2 1 1 2, 250 (1) :  1
2 2 2 2 2 1 2 1, 251 (1) :  1
2 2 2 2 2 1 2 2, 252 (1) :  1
2 2 2 2 2 2 1 1, 253 (1) :  1
2 2 2 2 2 2 1 2, 254 (1) :  1
2 2 2 2 2 2 2 1, 255 (1) :  1
2 2 2 2 2 2 2 2, 256 (1) :  1
```

Apéndice D

Publicaciones

Parte de los resultados presentados en esta tesis han sido publicados en conferencias internacionales y en revistas indizadas de alto impacto. A continuación se adjuntan dichas contribuciones.

Genetic Optimization for the Design of Walking Patterns of a Biped Robot

Selene L. Cardenas-Maciel[1], Oscar Castillo[2], Luis T. Aguilar[3], and Antonio Rodríguez-Díaz[1]

[1] Universidad Autonoma de Baja California, Tijuana, BC, Mexico
lilettecardenas@ieee.org, ardiaz@uabc.mx
[2] Instituto Tecnologico de Tijuana, Mexico
ocastillo@hafsamx.org
[3] Instituto Politecnico Nacional
Mexico luis.aguilar@ieee.org

Abstract. This paper presents an Genetic Algorithm (GA) for the design of walking patterns of a 3-DOF biped robot formulated as a system with impulse effects. The GA optimizes the coefficients of a polynomial which represents the desired behavior of the walking which is included into the dynamics of the biped robot to obtain periodic motions while fulfills a minimal energy consumption over a complete walking cycle assumed as single support and instantaneous double support phases. Optimization results are presented showing walking patterns with low energy consumption and periodic motions.

1 Introduction

In the last years several results has been provided for the stabilization of the biped locomotion, which usually are based on find a suitable reference trajectory i. e. walking pattern such that guarantee to perform stable steps while obey a certain criteria such as walking velocity, step length, step frequency, including energy minimization [16], [17]. Recent methods proposed for the walking pattern synthesis incorporate the zero moment point approach (ZMP) [18] as stability criteria. Qiang et. al. in [9] considering the ground condition and walking patterns with small torque and velocity of the joint actuators are obtained. Capi et. al. in [3] generate the joint trajectories for walking and going up-stairs based on consumed energy and torque change using evolutionary computation methods. Denk et. al. in [5] propose a systematic approach for the design of a walking pattern database using optimal control techniques and ZMP for prevention of the foot rotation and ensure the feasibility of the walking; Kajita et. al. in [11] introduce a method for a walking pattern generation by using a preview control of ZMP that uses reference future.

On the other hand the formulation for the walking pattern synthesis is done as a optimal control problem and optimization techniques are used. Bessonnet et al. in [2], by quadratic programming define the generalized coordinates as spline functions such that fulfill the minimization of the amount of the driving torques.

O. Castillo et al. (Eds.): Evolutionary Design of Intelligent Systems, SCI 257, pp. 259–271.
springerlink.com

A Genetic Algorithm is used as optimization method by Sang-Ho et. al. [4] to determine the shape of velocities and accelerations trajectories that minimizes the sum of deviation of each one through the search of suitable via points for obtain smooth and stable walking. Likewise, Park et. al. in [15] obtain an optimal locomotion pattern with minimal energy consumption and optimal locations of the center of mass of the links.

This paper is concerned in the energy optimal walking pattern design for a biped robot modeled as a system with impulse effects. The joint trajectories are parameterized as an polynomial (as are reported in [15]), which are included into the dynamics of the biped robot. A real coded Genetic Algorithm (GA) is used as optimization method to find the compatible polynomial coefficients which minimize the required input energy during the walking cycle while holding a stable walking motions. The optimization process is based on the evaluation of the biped robot in closed-loop, considering a set of constraints which guarantee no violation of the biped model assumptions and reach periodic walking motions. The difference with related publications is the generation of walking patterns whose motions are restricted to be described as periodic orbits and the design is not based on the ZMP approach, thus the reported walking patterns, allow more maneuvers than in this work is so far of our goal.

The paper is organized as follows: Section 2 presents the mathematical model of an 3-DOF biped robot. In Section 3, the problem formulation is summarized. Section 4, presents the GA implementation details used for the problem optimization established in previous section. Section 5, presents the results of numerical simulations. Section 6 provide the conclusions.

2 Biped Robot Model

In this section the dynamical model of a planar biped robot is introduced. The biped robot consists of a torso, hips, and two legs of equal length without ankles and knees. Two torques are applied between the legs and torso, so the system is under actuated. The definition of the angular coordinates and the disposition of the masses of the torso, hips and legs of the biped robot are shown in Figure 1, note that positive angles are computed in clockwise with respect to the indicated vertical lines and all masses of the links are lumped.

The walking cycle takes place in sagittal plane and on a level of surface, and it is assumed as successive phases where only one leg (stance leg) touching the walking surface (swing phase), with the transition from one leg to another taking place in a smaller length of time. During swing phase, the stance leg is modeled like a pivot and the swing leg is assumed move into the frontal plane [13] and to renter the plane of the motion when the angle of the stance leg attains a given desired value. The assumptions concerning to the walking cycle, define the biped robot model in two parts: the model that describe the swing phase and another one that describe the contact event of the swing leg with the walking surface; which are presented below.

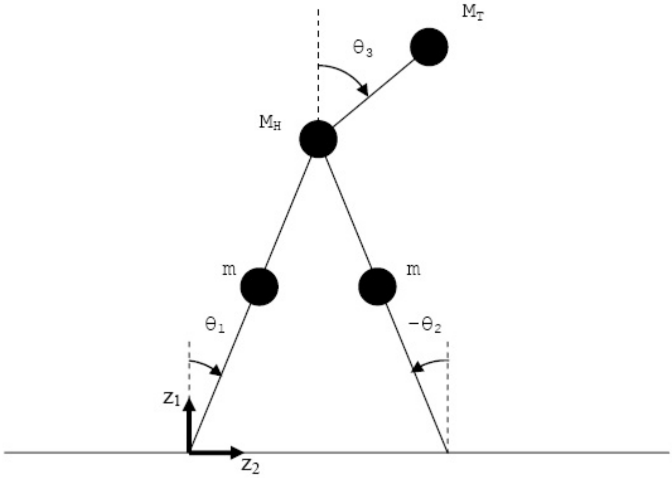

Fig. 1. 3-linkbiped robot.

2.1 Dynamic Model

The dynamical model of the robot during the swing phase is a second order system derived of Lagrange method [12]:

$$M(\theta)\ddot{\theta} + C(\theta,\dot{\theta})\dot{\theta} + G(\theta) = Bu, \tag{1}$$

where $\theta = [\theta_1, \theta_2, \theta_3]^T$ are the generalized coordinates, θ_1 parameterizes the stance leg, θ_2 the swing leg and θ_3 the torso; $u = [u_1, u_2]^T$ are the input; $M(\theta)$ is a positive-definite inertia matrix, $C(\theta,\dot{\theta})\dot{\theta}$ is the vector of the centripetal and Coriolis forces; and $G(\theta)$ is the vector of the conservative forces and B is the input matrix.

Transforming the second order equation (1) to state-space form by defining

$$\begin{aligned} \dot{x} :&= \frac{d}{dt}\begin{bmatrix}\theta\\ \dot{\theta}\end{bmatrix} = \begin{bmatrix}\dot{\theta}\\ M^{-1}(\theta)[-C(\theta,\dot{\theta})\dot{\theta} - G(\theta) + Bu]\end{bmatrix} \\ :&= f(x) + g(x)u. \end{aligned} \tag{2}$$

2.2 Impact Model

The impact between the swing leg and the ground is modeled like a contact between two rigid bodies. The main objective is to obtain the velocity of the generalized coordinates after the impact of the swing leg with the walking surface in terms of the velocity and position before the impact. The impact model for the biped robot is based in the rigid impact model of [10] and assume the case where the contact of the swing leg with de walking surface produce either no rebound nor slipping of the swing leg, and the stance leg lifting the walking surface without interaction. The conditions in [10] for these assumptions to be valid are that:

1. the impact takes place over an infinitesimally small period of time;
2. the external forces during impact can be represented by impulses;
3. impulsive forces may results in instantaneous change in the velocities of the generalized coordinates, but positions remain continuous;
4. the torques supplied by the actuators are not impulsional.

Taking into account the previous assumptions, the impact model is expressed with the equation [19]:

$$\begin{bmatrix} M_e & -E^T \\ E & 0 \end{bmatrix} \begin{bmatrix} \dot{\theta}_e^+ \\ F \end{bmatrix} = \begin{bmatrix} M_e \dot{\theta}_e^- \\ 0 \end{bmatrix}, \tag{3}$$

where $\theta_e = [\theta_1, \theta_2, \theta_3, z_1, z_2]^T$ are the generalized coordinates resulting of the add the Cartesian coordinates $[z_1, z_2]^T$ of the end of the stance leg as shown in Figure 1; M_e is the positive-definite inertia matrix of the biped model with the new generalized coordinates; $F = [F_T, F_N]^T$ is the tangential and normal forces applied at the end of the swing leg; $\dot{\theta}_e^+$ is the velocity after the impact; $\dot{\theta}_e^-$ is the velocity before the impact and

$$E := \frac{\partial Y}{\partial \theta_e} = \begin{bmatrix} r\cos(\theta_1) & -r\cos(\theta_2) & 0 & 1 & 0 \\ -r\sin(\theta_1) & r\sin(\theta_2) & 0 & 0 & 1 \end{bmatrix}, \tag{4}$$

obtaining $\dot{\theta}_e^+$ of the equation (3) must be done a change of coordinates and re-initialize the model (2). The change of coordinates is an expression for $x^+ := (\theta^+, \dot{\theta}^+)$ in terms of $x^- := (\theta^-, \dot{\theta}^-)$, which is given for the mapping function:

$$x^+ = \Delta(x^-) := \left[\, \theta_2^- \ \theta_1^- \ \theta_3^- \ \dot{\theta}_2^+(x^-) \ \dot{\theta}_1^+(x^-) \ \dot{\theta}_3^+(x^-) \,\right]. \tag{5}$$

Thus, the overall model of the biped walking is the combination of the swing phase model and impact model, as follows:

$$\Sigma : \begin{cases} \dot{x} = f(x) + g(x)u \ x^- \notin S \\ \quad x^= \Delta(x^-) \qquad x^- \in S \end{cases} \tag{6}$$

where

$$S := \{(\theta, \dot{\theta}) | z_1 > 0, z_2 = 0, \theta_1 = \theta_1^d\} \tag{7}$$

3 Problem Formulation

This paper is based on the feedback controller for walking proposed by Grizzle et al. in [19] which designs a feedback for posture control and swing leg advancement of the biped robot (6), where the posture control means maintaining the torso angle at a constant value θ_3^d and swing leg advancement consists in driving the swing leg to behave as mirror image of the stance leg ($\theta_2 = \theta_1$). Thus, the behavior is encoded into the dynamics of the robot by defining the following output function:

$$y := \begin{bmatrix} y_1 \\ y_2 \end{bmatrix} := \begin{bmatrix} h_1(\theta, a) \\ h_2(\theta, a) \end{bmatrix} := \begin{bmatrix} \theta_3 - h_{d,1}(\theta_1, a) \\ \theta_2 - h_{d,2}(\theta_1, a) \end{bmatrix} \tag{8}$$

where

$$\begin{aligned} h_{d,1}(\theta_1,a) &:= \qquad\qquad a_1^0+\cdots+a_1^3(\theta_1)^3 \\ h_{d,2}(\theta_1,a) &:= -\theta_1+(a_2^0+\cdots+a_2^3(\theta_1)^3)\times(\theta_1+\theta_1^d)\times(\theta_1-\theta_1^d) \end{aligned} \tag{9}$$

with the control objective being to zeroing the outputs (8), they define the feedback

$$u(x) := (L_g L_f h(x))^{-1}(\Psi(h(x), L_f h(x)) - L_f^2 h(x)) \tag{10}$$

and

$$\Psi(y,\dot{y}) := \begin{bmatrix} \frac{1}{\varepsilon^2}\psi_\alpha(y_1,\varepsilon\dot{y}_1) \\ \frac{1}{\varepsilon^2}\psi_\alpha(y_2,\varepsilon\dot{y}_2) \end{bmatrix} \tag{11}$$

$$\psi_\alpha(x_1,x_2) := -sign(x_2)|x_2|^\alpha - sign(\phi_\alpha(x_1,x_2))|\phi(x_1,x_2)|^{\frac{\alpha}{2-\alpha}} \tag{12}$$

$$\phi_\alpha := x_1 + \left(\frac{1}{2-\alpha}\right) sign(x_2)|x_2|^{2-\alpha} \tag{13}$$

The problem statement is described as follows: Given the biped robot model (6) and the feedback (10), find the parameters a_i^j of the function in (9) such that it obtains a walking pattern which produce periodic walking motions with low energy consumption.

4 Optimization Strategy

According to the problem, a Genetic Algorithm (GA) is proposed to solve the optimization problem. GA are search algorithms based on natural selection and natural genetic principles [8], apply them to optimization problems differ from traditional optimization methods that they use: payoff information (based on a objective function), no derivatives or other auxiliary knowledge; a coding of the parameters, not the parameters themselves and probabilistic rules as a tool to guide the search [14].

The implementation of the GA begins with the election of consistent decision variables which to solve the problem continuing with the coding of them into a string called individual, as well as an objective function which provide a numerical value that indicate the goodness degree or fitness of the individual to solve the problem. The GA operation consist of several stages, that to imitate the natural principles in which are based: The *initialization* stage where a set of individuals called population is created randomly; the *selection* stage in which each individual is evaluated through the objective function, the values of the evaluation are used by a selection algorithm that identifies and choose the fittest individuals that to serve as the parents for the creation of new individuals; The new individuals are created by applying the genetic operations to the individuals selected in the previous stage. This operations are: crossover, which with certain probability, combine the parameters encoded between pairs of individuals producing two individuals with information of both parents and the mutation, which is the alteration of the value of one parameter encoded in the individual, its function is to introduce diversity in the population, this stage is called *reproduction*; the last stage is the *replacement*, it consist in the creation of the new population with the new individuals and the parents. The overall stages is performed of iterative manner, each iteration is called generation. The GA operation explained above is expressed through an algorithm as shown below:

1. Begin
2. $i \leftarrow 0$
3. Create a population P_i of N individuals
4. Evaluate fitness of all individuals of the population: $P_i^e \leftarrow Fitness(P_i)$
5. Repeat the steps until the conditions are reached
   a) Select the parents for matting: $P_i^s \leftarrow Select(P_i, P_i^e)$
   b) Apply crossover and mutation: $P_i^g \leftarrow Genetic\_Operation(P_i^s)$
   c) $i \leftarrow i+1$
   d) Create the new population: $P_i \leftarrow New\_Pop(P_i^g, P_{i-1})$
   e) Evaluate fitness of new individuals: $P_i^e \leftarrow Fitness(P_i)$
6. Print out the best solution
7. End

Thus, the details of our implementation of the each stage are provided below.

4.1 Individual Representation

The individual representation selected is the real coding scheme, whose genotype is composed by eight real numbers such that represent to each parameter a_i^j (decision variables) of the function in (9).

4.2 Objective Function

The goal of the GA is the minimization of the cost function which represents the approximation to the average energy consumed over the walking cycle:

$$\hat{J}(a) = \int_0^T (u_1^2 + u_2^2)dt \tag{14}$$

where T is such that $\theta_1(T) - \theta_1^d = 0$, and $u(t)$ is obtained of applying (10) into the closed loop with the biped robot model (2) and (8).

This cost function is subject to the following constraints taking of [7]:

$$\begin{array}{cc} \hat{\dot{\theta}}_1^- - 0.99\lambda(\hat{\dot{\theta}}_1^-) & \leq 0 \\ \|y(\bar{t})\| & \leq 0 \\ |\frac{F_T}{F_N}| - \mu & \leq 0 \\ -\dot{z}_2^+ & \leq 0 \end{array} \tag{15}$$

The first constraint assures the existence of the one fixed point, the second one assures that the controller has converged before the impact and the last two constraints verify the validity of the impact model.

4.3 Genetic Operations

The genetic operations comprise the classical one point crossover and non-uniform mutation [6][14]. Non-uniform mutation is defined as follows: if $s_v^t = [v_1, ..., v_m]$ is a individual (with t, which means the generation number) and the element v_k was selected for this mutation, the result is a vector $s_v^t = [v_1, ..., v_k^{'}, ..., v_m]$ where:

$$v_k^{'} = \begin{cases} v_k + \Delta(t, UB - v_k) & \text{if a random digits is 0} \\ v_k - \Delta(t, v_k - LB) & \text{if a random digit is 1} \end{cases} \tag{16}$$

and LB and UB are the lower an upper domains bounds of the variable v_k the function $\Delta(t,y) = y\left(1 - r\left(1 - \frac{t}{T}\right)^b\right)$ return a value in the range $[0, y]$; r is a random number, T is the maxima generation number and b is the dependency degree on the iteration number.

5 Simulation Results

The GA was developed in MatLab with the characteristics described in Section III, the individual evaluation is during one walking cycle and uses the implementation in software of 3-DOF model (6) with the controller (10) available in [1]. The physical parameters of the biped model are shown in the Table 1, pre-impact angular velocity is taken as $\dot{\theta}_1^- = 1.55$, the friction coefficient $\mu \geq \frac{2}{3}$, and the controller parameters for equations (11) and (12) are $\varepsilon = 0.1$ and $\alpha = 0.9$ respectively. Details of the biped model can be found in [19].

In the Table 3 presents the parameters for the function (9) and the energy consumption as results of five independent GA executions using the GA parameters

Table 1. Biped model parameters

Parameter	Value
Mass of Hips (M_H)	15 kg
Mass of Torso (M_T)	10 kg
Mass of Legs (m)	5 kg
Length of legs (r)	1 m
Length of torso (l)	0.5 m

Table 2. Genetic algorithm parameters

Parameter	Value
Number of individuals	100
Number Maximum of Generations	400
Crossover Rate	0.9
Mutation Rate	0.2
Selection Rate	0.4

Table 3. Parameter a_i^j and energy magnitude results with the GA

Number	Parameters								$\hat{J}(a)$
	a_1^0	a_1^1	a_1^2	a_1^3	a_2^0	a_2^1	a_2^2	a_2^3	
1	0.5893	0.4644	1.5558	-0.0367	-1.2656	1.0308	1.1086	3.7436	719.32
2*	0.5120	0.0730	0.0350	-0.8190	-2.2700	3.2600	3.1100	1.8900	761.00
3	0.7098	0.0581	0.0536	-1.0280	-1.9803	2.5752	3.6109	2.0000	1225.40
4	0.3992	0.7515	-2.5759	2.5365	1.8022	0.5344	0.2620	6.0033	1679.20
5	1.0730	-0.4986	-0.4127	1.6194	2.7029	-1.4978	1.6201	-0.8384	2541.70
6	0.2892	1.9435	-2.8760	0.4328	2.0252	4.5643	-0.5546	-4.1460	2980.50

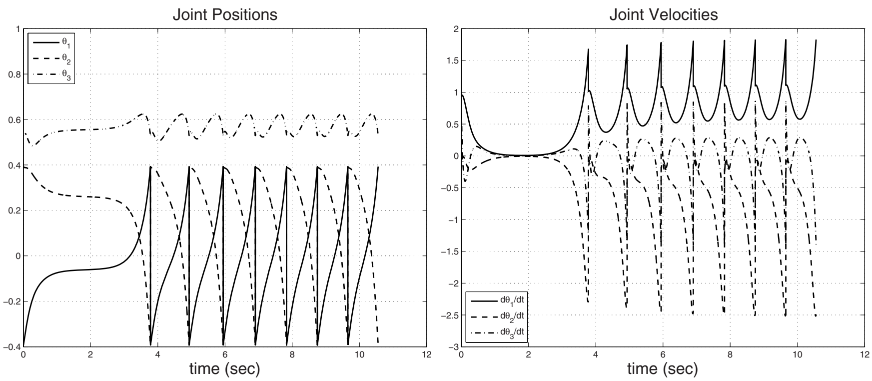

Fig. 2. Joint positions and velocities trajectories corresponding to closed-loop system execution with the parameters of the first entry of the Table 3

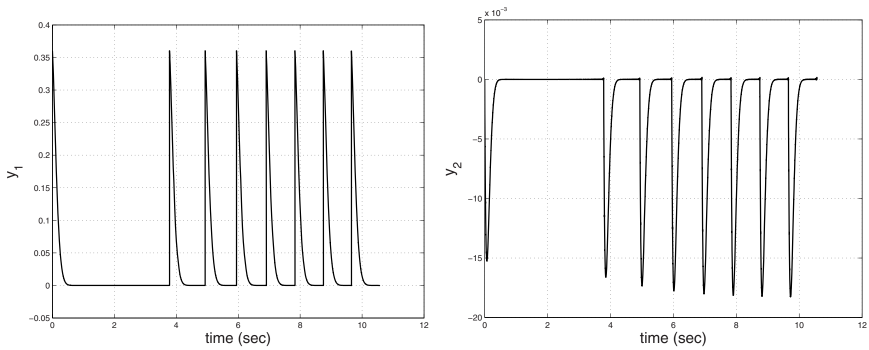

Fig. 3. Output function trajectories corresponding to closed-loop system execution with the parameters of the first entry of the Table 3

showed in the Table 2. The second entry on the table 3 include the parameters obtained by Grizzle et. al. in [19] with the same biped robot model using a traditional optimization method.

The results summarized in the Figures 2 to 5, corresponds to the closed-loop system simulations using the walking patterns defined by parameters of the first entry of the Table 3, and Figure 6 shows the fitness values of the best individual in each generation, finishing the optimization process about 140^{th} generation. Overall results depict the execution of the closed-loop system performing eight steps. Note that the energy magnitude obtained with GA is slightly lower than the reported in [19]. The joint trajectories in the Figure 2 shows that the time needed to execute the first step is longer due that minimal change in the input torques succeeded, hence

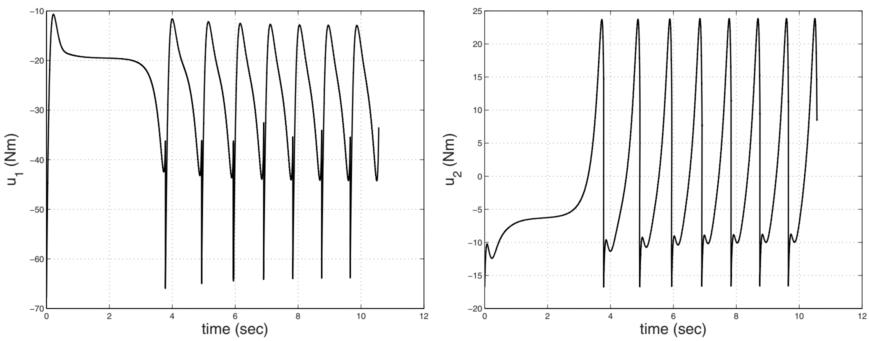

Fig. 4. Control signals corresponding to closed-loop system execution with the parameters of the first entry of the Table 3

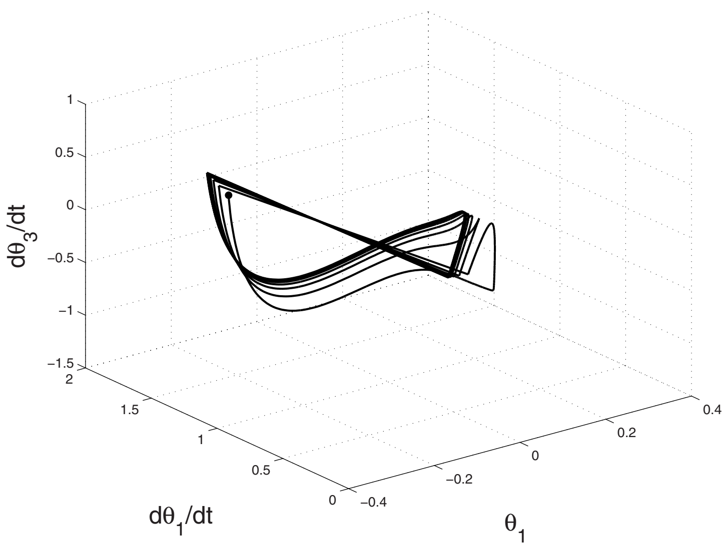

Fig. 5. Orbits obtained corresponding to closed-loop system execution with the parameters of the first entry of the Table 3

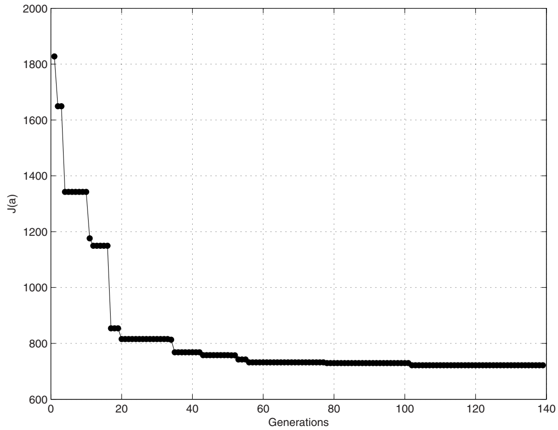

Fig. 6. Fitness values obtained through the optimization process for the first execution of the Table 3

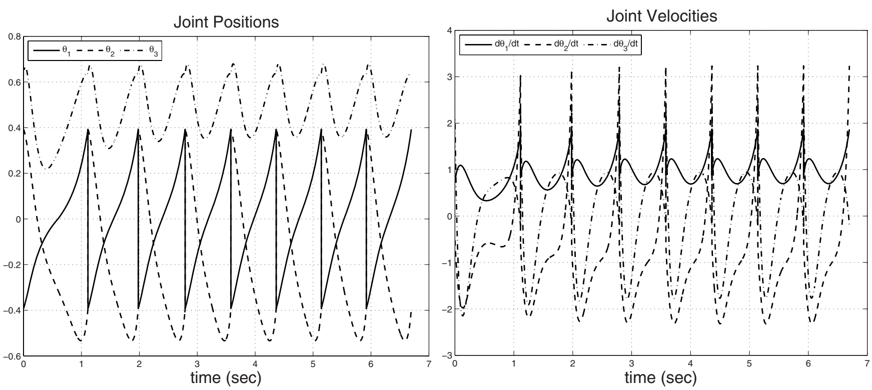

Fig. 7. Joint positions and velocities trajectories corresponding to closed-loop system execution with the parameters of the sixth entry of the Table 3

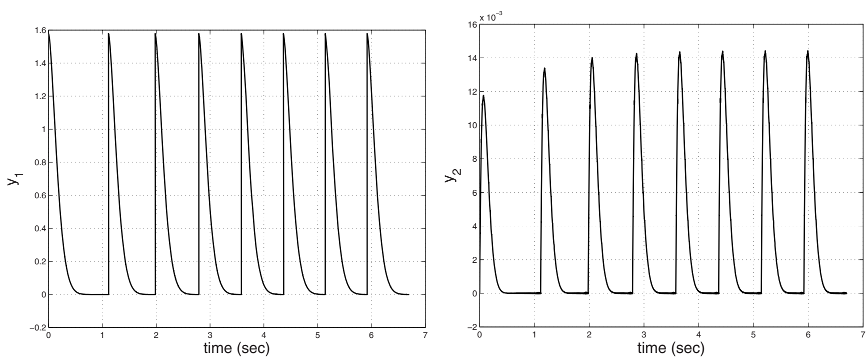

Fig. 8. Output function trajectories corresponding to closed-loop system execution with the parameters of the sixth entry of the Table 3

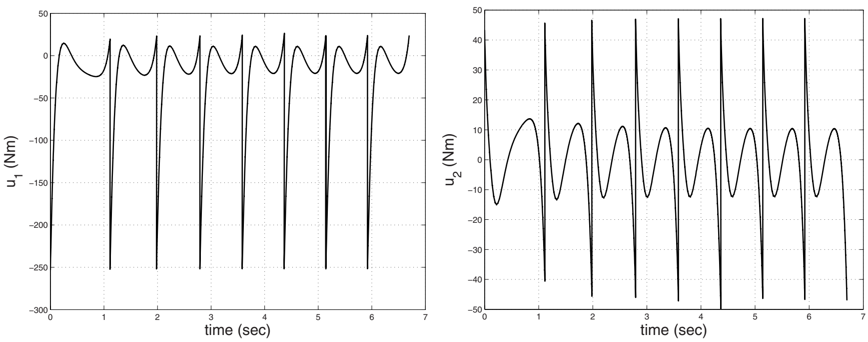

Fig. 9. Control signals corresponding to closed-loop system execution with the parameters of the sixth entry of the Table 3

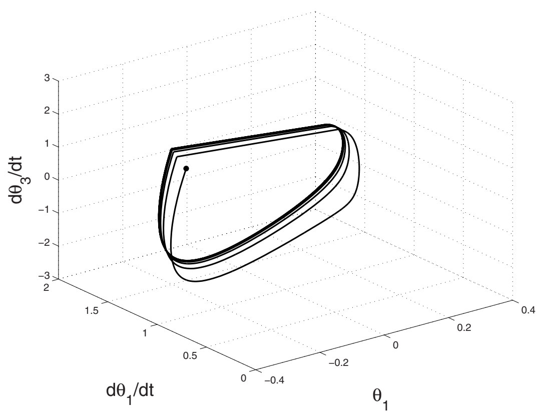

Fig. 10. Orbits corresponding to closed-loop system execution with the parameters of the sixth entry of the Table 3

the motion turning slow, after these, the step time tend to be the same through the following steps. In the Figures 7 to 10 demonstrate the results whose parameters are not optimal in energy magnitude, but still produce periodic walking motions. Moreover, in the Figures 5 and 10 present the orbits for both simulations cases, which shown the periodic nature of the walking.

6 Conclusions

In this paper a GA for the design of walking patterns of a biped robot was presented. The design approach consists in the search of suitable coefficients of a function, which describe the desired behavior of the joint trajectories such that produce periodic walking motion while keeping a minimal energy consumption. The numerical results with the function obtained by GA in the closed-loop system shows that this approach can provide a set of different walking patterns whose motions are described as periodic orbits and was able to obtain near optimal energy magnitudes.

References

1. Feedback control of dynamic bipedal robot locomotion book webpage (2007), http://www.dynamicbipedcontrol.org
2. Bessonnet, G., Seguin, P., Sardain, P.: A Parametric Optimization Approach to Walking Pattern Synthesis. The International Journal of Robotics Research 24(7), 523–536 (2005)
3. Capi, G.: Application of genetic algorithms for biped robot gait synthesis optimization during walking and going upstairs. Advanced Robotics 15(20), 675–694 (2001)
4. Choi, S.H., Choi, Y.H., Kim, J.G.: Optimal walking trajectory generation for a biped robot using genetic algorithm. In: Proceedings of IROS 1999 IEEE/RSJ International Conference on Intelligent Robots and Systems 1999, vol. 3, pp. 1456–1461 (1999)
5. Denk, J., Schmidt, G.: Synthesis of Walking Primitive Databases for Biped Robots in 3D-Environments. In: Proceedings of the IEEE International Conference on Robotics and Automation, ICRA 2003, Taipei, Taiwan (2003)
6. Goldberg, D.E.: Genetic Algorithms in Search. In: Optimization and Machine Learning. Addison-Wesley Longman Publishing Co., Boston (1989)
7. Grizzle, J., Abba, G., Plestan, F.: Proving asymptotic stability of a walking cycle for a 5 DOF biped robot model. In: International Conference on Climbing and Walking Robots. Angleterre, Portsmouth (1999)
8. Holland, J.M.: Adaptation in Natural and Artificial Systems. University of Michigan Press, Ann Arbor (1975)
9. Huang, Q., Yokoi, K., Kajita, S., Kaneko, K., Arai, H., Koyachi, N., Tanie, K.: Planning walking patterns for a biped robot. IEEE Transactions on Robotics and Automation 17(3), 280–289 (2001)
10. Hurmuzlu, Y., Marghitu, D.: Rigid body collisions of planar kinematic chains with multiple contact points. Int. J. Robot Res. 13(1), 82–92 (1994)
11. Kajita, S., Kanehiro, F., Kaneko, K., Fujiwara, K., Harada, K., Yokoi, K., Hirukawa, H.: Biped walking pattern generation by using preview control of zero-moment point. In: Proceedings of ICRA 2003. IEEE International Conference on Robotics and Automation 2003, vol. 2, pp. 1620–1626 (2003)
12. Kelly, R.: Control de Movimiento de Robots Manipuladores. Prentice Hall, Madrid (2003)
13. McGeer, T.: Passive dynamic walking. Int. J. Robot Res. 9(2), 62–82 (1990)
14. Michalewicz, Z.: Genetic Algorithms + Data Structures = Evolution Programs. Springer-Verlag New York, Inc., Secaucus (1994)
15. Park, J.H., Choi, M.: Generation of an optimal gait trajectory for biped robots using a genetic algorithm. JSME International Journal Series C Mechanical Systems, Machine Elements and Manufacturing 47(2), 715–721 (2004)
16. Roussel, L., de Wit, C.C., Goswami, A.: Generation of energy optimal complete gait cycles for biped robots. In: Proceedings of the IEEE International Conference on Robotics and Automation, pp. 2036–2041 (1998)

17. Shiriaev, A.S., Freidovich, L.B., Manchester, I.R.: Can we make a robot ballerina perform a pirouette? orbital stabilization of periodic motions of underactuated mechanical systems. Annual Reviews in Control 32(2), 200–211 (2008)
18. Vukobratovic, M., Juricic, D.: Contribution to the synthesis of biped gait. IEEE Transactions on Biomedical Engineering 16(1), 1–6 (1969)
19. Westervelt, E.R., Grizzle, J.W., Chevallereau, C., Choi, J.H., Morris, B.: Systematic Design of Within-Stride Feedback Controllers for Walking. In: Feedback Control of Dynamic Bipedal Robot Locomotion, pp. 137–11891. Taylor & Francis/CRC, Boca Raton (2007)

WCCI 2010 IEEE World Congress on Computational Intelligence
July, 18-23, 2010 - CCIB, Barcelona, Spain IJCNN

A T-S Fuzzy Logic Controller for Biped Robot Walking based on Adaptive Network Fuzzy Inference System

Selene L. Cardenas-Maciel, *Student, IEEE*; Oscar Castillo, *Senior, IEEE*; Luis T. Aguilar, *Member, IEEE* and Juan R. Castro

***Abstract*— A neuro-fuzzy learning algorithm is applied to design a Takagi-Sugeno type Fuzzy Logic Controller (T-S FLC) for a biped robot walking problem. The control design considers an output function imposed on the feedback and several TS-FLC models are determined each by ANFIS, which represent a piece-wise control inputs that together to perform a walking cycle. Two simulations of the closed-loop system for generation of walking motions are given, where we assume that the joint positions and the whole state of the system are available for controller feedback respectively.**

I. Introduction

Fuzzy logic control as an application area of Fuzzy Logic has attracted attention from scientist and engineers due to the fact that through if-then rules can express knowledge of how to control a system incorporating uncertainty. The existence of a large number of variables in the measurable variables space (system or external variables) and the partition needed in these variables, are factors that have influence in the size of the rule base, which implies a nontrivial task into the modeling. In order to overcome this difficulties, Clustering and Neuro-fuzzy approaches have been proposed and applied in the control of nonlinear systems [1] [2], identification in control systems and time series prediction [3] to name a few.

On the other hand, for the scientists community, biped robotics represents novel challenges in mathematical modeling as well as in the development of control strategies. Neuro-Fuzzy and neural network methods based biped locomotion control has been reported. To mention some of them, several Adaptive-Network-based Fuzzy Inference System (ANFIS) [3] are proposed in [4] to design a locomotion controller and another one as systems identifier to determine the model of the system; a learning algorithm and a grid partition method are proposed in [5] to obtain a walking controller; neuro-fuzzy approaches applied in Zero Moment Point [6] control trajectories are proposed in [7].

This paper is concerned with the application of ANFIS into the design of a Takagi-Sugeno Fuzzy Logic Controller (T-S FLC) such that it produces walking motions in a biped robot. The controller design is based on the learning of data-pairs which correspond a close-loop system simulation performing a walking cycle using a controller proposed in [8], which are designed by mathematical-based control methods. Due the non-linear relations between the variables, piece-wise control laws are designed through ANFIS, each one is associated to a part of the walking cycle. This work uses the output form of [8] and two T-S FLCs to produce walking motions, which are applied to a 3-DOF biped robot.

The content of the paper is organized as follows: Section II introduces the mathematical model of the biped robot. In Section III, describes some aspects of the neuro-fuzzy approach. Section IV explains the control strategy used for controller design. Section V, illustrates simulation results of the closed-loop system using two T-S FLCs. Section VI provides some conclusions.

Selene L. Cardenas-Maciel is with the Facultad de Ciencias Quimicas e Ingenieria, Universidad Autonoma de Baja California, Tijuana, BC, 22390, Mexico (email: lilettecardenas@ieee.org).

Oscar Castillo is with the Division de Estudios de Posgrado e Investigacion, Instituto Tecnologico de Tijuana, BC, 22414 Mexico (e-mail: ocastillo@hafsamx.org).

L. Aguilar is with Centro de Investigacion y Desarrollo de Tecnologia Digital, Instituto Politecnico Nacional (CITEDI-IPN), Tijuana, BC, 22510, Mexico (e-mail: luis.aguilar@ieee.org).

Juan R. Castro is with the Division de Estudios de Posgrado e Investigacion, Universidad Autonoma de Baja California, Tijuana, BC, 22390, Mexico (email: jrcastror@uabc.edu.mx).

II. Biped Robot Model

In this section the dynamical model of a planar biped robot is introduced. The biped robot consists of a torso, hips, and two legs of equal length without ankles and knees. Two torques are applied between the legs and torso. The definition of the angular coordinates and the disposition of the masses of the torso, hips and legs of the biped robot are shown in Fig. 1, the positive angles are computed in a clockwise manner with respect to the indicated vertical lines and all masses of the links are lumped.

The walking cycle takes place in the sagittal plane and on a surface level, and it is assumed as successive phases where only one leg (stance leg) touching the walking surface (swing phase), with the transition from one leg to another taking place in a smaller length of time. During the swing phase, the stance leg is modeled like a pivot and the swing leg is assumed to move into the frontal plane [9] and to renter the plane of the motion when the angle of the stance leg attains a given desired value. The assumptions concerning the walking cycle, define the biped robot model in two parts: the model that describes the swing phase and another one that describes the contact event of the swing leg with the walking surface; which are presented below.

A. Swing phase Model

The dynamical model of the robot during the swing phase is a second order system derived from the Lagrange method [10]:

$$M(\theta)\ddot{\theta} + C(\theta,\dot{\theta})\dot{\theta} + G(\theta) = Bu, \tag{1}$$

978-1-4244-8126-2/10/$26.00

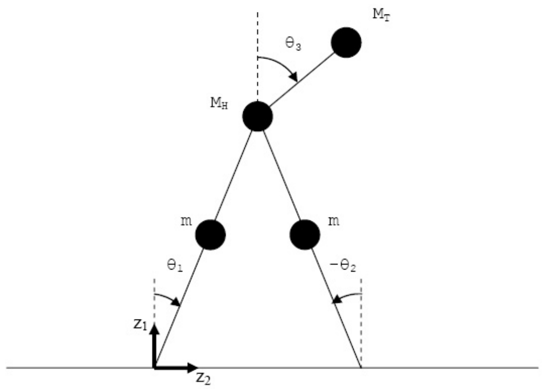

Fig. 1. 3-link biped robot.

where $\theta = [\theta_1, \theta_2, \theta_3]^T$ are the generalized coordinates, θ_1 parameterizes the stance leg, θ_2 the swing leg and θ_3 the torso; $u = [u_1, u_2]^T$ are the input; $M(\theta)$ is a positive-definite inertia matrix, $C(\theta,\dot{\theta})\dot{\theta}$ is the vector of the centripetal and Coriolis forces; and $G(\theta)$ is the vector of the conservative forces and B is the input matrix.

Transforming the second order equation (1) to state-space form by defining

$$\begin{aligned} \dot{x} &:= \frac{d}{dt}\begin{bmatrix} \theta \\ \dot{\theta} \end{bmatrix} \\ &= \begin{bmatrix} \dot{\theta} \\ M^{-1}(\theta)[-C(\theta,\dot{\theta})\dot{\theta} - G(\theta) + Bu] \end{bmatrix} \\ &:= f(x) + g(x)u. \end{aligned} \tag{2}$$

B. Impact Model

The impact between the swing leg and the ground is modeled as the contact between two rigid bodies. The main objective is to obtain the velocity of the generalized coordinates after the impact of the swing leg with the walking surface in terms of the velocity and position before the impact. The impact model for the biped robot is based on the rigid impact model of [11] and assuming the case where the contact of the swing leg with the walking surface produce either no rebound nor slipping of the swing leg, and the stance leg lifting the walking surface without interaction. the impact model is expressed with equation [8]:

$$\begin{bmatrix} M_e & -E^T \\ E & 0 \end{bmatrix}\begin{bmatrix} \dot{\theta}_e^+ \\ F \end{bmatrix} = \begin{bmatrix} M_e\dot{\theta}_e^- \\ 0 \end{bmatrix}, \tag{3}$$

where $\theta_e = [\theta_1, \theta_2, \theta_3, z_1, z_2]^T$ are the generalized coordinates resulting of the add the cartesian coordinates $[z_1, z_2]^T$ of the end of the stance leg as shown in Figure 1; M_e is the positive-definite inertia matrix of the biped model with the new generalized coordinates; $F = [F_T, F_N]^T$ represent the tangential and normal forces applied at the end of the swing leg; $\dot{\theta}_e^+$ is the velocity after the impact; $\dot{\theta}_e^-$ is the velocity before the impact and

$$E := \frac{\partial Y}{\partial \theta_e} = \begin{bmatrix} r\cos(\theta_1) & -r\cos(\theta_2) & 0 & 1 & 0 \\ -r\sin(\theta_1) & r\sin(\theta_2) & 0 & 0 & 1 \end{bmatrix}, \tag{4}$$

solving for $\dot{\theta}_e^+$ of equation (3) and a change of coordinates must be done and also a re-initialization of the model (2). The change of coordinates is an expression for $x^+ := (\theta^+, \dot{\theta}^+)$ in terms of $x^- := (\theta^-, \dot{\theta}^-)$, which is given for the mapping function [8]:

$$x^+ := \Delta(x^-) := \begin{bmatrix} \theta_2^- \\ \theta_1^- \\ \theta_3^- \\ \dot{\theta}_2^+(x^-) \\ \dot{\theta}_1^+(x^-) \\ \dot{\theta}_3^+(x^-) \end{bmatrix}. \tag{5}$$

Thus, the overall model of biped walking is the combination of the swing phase model and impact model, as follows:

$$\Sigma_{cl} : \begin{cases} \dot{x} = f(x) + g(x)u(x) & x^- \notin S \\ x^+ = \Delta(x^-) & x^- \in S \end{cases} \tag{6}$$

where

$$S := \{(\theta,\dot{\theta}) | z_1 > 0, z_2 = 0, \theta_1 = \theta_1^d\} \tag{7}$$

III. ANFIS AND FUZZY MODELS

ANFIS [3] is a class of adaptive neural network whose functionally is equivalent to the T-S fuzzy reasoning mechanism [12]. The ANFIS architecture consist on five layers and the node function for each node of same layer corresponds to the same family functions. The architecture is detailed as follows:

1) Layer 1: Every node i in this layer is an adaptive node with a node function

$$O_i^1 = \mu_{A_i}(x) \tag{8}$$

where x is the input to node i and A_i is the linguistic label associated with this node, O_i^1 is the membership function of the fuzzy set A_i, it specifies the grade that the given value x satisfies the quantifier A. The membership function $\mu_{A_i}(x)$ can be parameterized for

$$\mu_{A_i}(x) = \exp\{-\frac{1}{2}(\frac{x - c_i}{a_i})^2\} \tag{9}$$

where a_i and c_i are referred as premise parameters

2) Layer 2: Every node i in this layer is a fixed node labeled Π, whose output is the product of all the incoming signals. For example, consider two linguistic variables A and B characterized by two fuzzy sets each. Then the output of a node i of this layer is obtained by:

$$O_i^2 = w_i = \mu_{A_i}(x)\mu_{B_i}(y) \quad , \quad i = 1, 2. \tag{10}$$

each node represents the firing strength of a rule.

3) Layer 3: Every node in this layer is a fixed node labeled N. The ith node calculate the ratio of firing strength of the ith rule to the sum of the all firing strengths of the rules. The outputs of this layer are called normalized firing strengths ($\bar{w}_1$).

$$O_i^3 = \bar{w}_i = \frac{w_i}{\sum i w_i} \quad , \quad i = 1, 2. \tag{11}$$

4) Layer 4: Every node i in this layer is an adaptive node with node function

$$O_i^4 = \bar{w}_i f_i = \bar{w}_i (p_i x + q_i y + r_i), \quad i = 1, 2. \tag{12}$$

where p_i, q_i, r_i are the parameter set of this node, these are the consequent parameters.

5) Layer 5: The single node in this layer is a fixed node labeled Σ, which computes the overall output as the summation of all incoming signals:

$$O_i^5 = \sum_i \bar{w}_i f_i = \frac{\sum_i w_i f_i}{\sum_i w_i} \tag{13}$$

The learning rule combines gradient method and least squares estimate to identify and update the parameters of the network, these parameters are the premise and consequent parameters which describe a Fuzzy Model.

Thus, ANFIS can serve as basis for constructing a set of T-S type fuzzy model [12] with appropriate membership functions starting from a set of input-output data pairs. Consider a T-S fuzzy model with input variables x_1, x_2,..., x_j and output variables u_1, u_2,...,u_k, the lth rule of T-S fuzzy model takes the form:

$$\begin{array}{lll} R^l: & \text{If} & x_1 \text{ is } A_{1,i} \text{ and } x_2 \text{ is } A_{2,i} \text{ and ... } x_j \text{ is } A_{j,i} \\ & \text{Then} & u_1 = G(x_1, ..., x_j; p_{1,1}, p_{1,2}, ..., p_{1,j}, p_{1,j+1}) \\ & & \text{and ... and} \\ & & u_k = G(x_1, ..., x_j; p_{k,1}, p_{k,2}, ..., p_{k,j}, p_{k,j+1}) \end{array} \tag{14}$$

where $A_{j,i}$ with $i = 1, 2, ..., m_1$ and $j = 1, 2, ...m_2$, are the ith fuzzy set of the jth input variable; u_k (consequent) with $k = 1, 2, ..., m_3$, is represented as crisp continuous function in terms of the inputs with $k(j + 1)$ parameters p.

IV. CONTROL STRATEGY

The proposed controller uses an output function in [8]. The output was used to design, through of modern control methods, an controller that generate exponential stable walking motions for the model defined in (6). The output function is defined as follows:

$$y := \begin{bmatrix} y_1 \\ y_2 \end{bmatrix} := \begin{bmatrix} h_1(\theta, a) \\ h_2(\theta, a) \end{bmatrix} := \begin{bmatrix} \theta_3 - h_{d,1}(\theta_1, a) \\ \theta_2 - h_{d,2}(\theta_1, a) \end{bmatrix} \tag{15}$$

where

$$\begin{aligned} h_{d,1}(\theta_1, a) :=& \quad a_1^0 + \cdots + a_1^3(\theta_1)^3 \\ h_{d,2}(\theta_1, a) :=& \quad -\theta_1 + (a_2^0 + \cdots + a_2^3(\theta_1)^3) \times \cdots \\ & \quad (\theta_1 + \theta_1^d) \times (\theta_1 - \theta_1^d). \end{aligned} \tag{16}$$

The control objective is to find a control input u such that the output y is driving to zero.

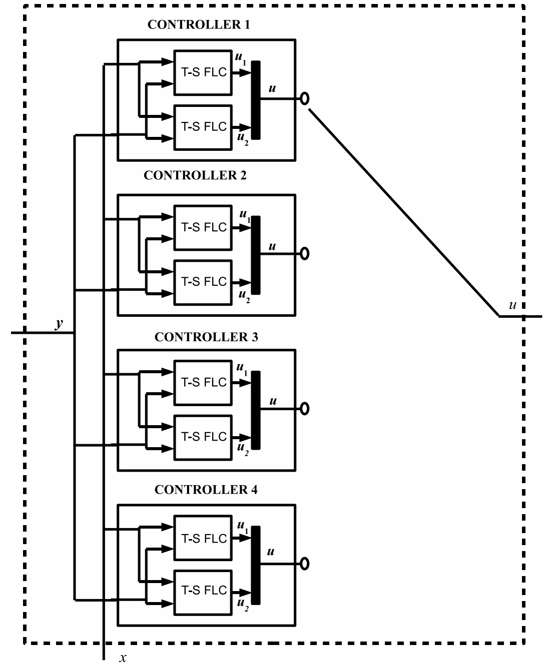

Fig. 2. Controller Structure

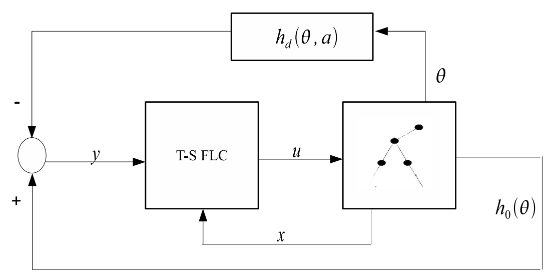

Fig. 3. Closed-loop system block diagram

In order to accomplish the control objective, ANFIS is used for the controller design. The output trajectories $y = [y_1, y_2]^T$, the control inputs $u = [u_1, u_2]^T$ and state variables trajectories x corresponding to closed-loop system simulation of the work proposed in [8] during a walking cycle, are considered to built the data set (input-output data pairs). This paper presents two T-S FLC obtained of two data set, the difference between them are the number of the state variables involved: the first one consider the joint position $\theta = [\theta_1, \theta_2, \theta_3]^T$ of the state variables and the second one contains the full state variables $x = [\theta, \dot{\theta}]^T = [\theta_1, \theta_2, \theta_3, \dot{\theta}_1, \dot{\theta}_2, \dot{\theta}_3]^T$.

The data set is partitioned to diminish the computational load and time, each data partition is distributed in two different ANFIS instances. The data distribution of one partition to each ANFIS is performed as follows: the state variables and output trajectories are taken as input data, and as output data, one of the control input. The overall controller consist of four controllers due the partition of the data set, each one contains two first order T-S FLC which provide one control input each. The scheme of proposed controller is presented in Fig. 2 and the closed-loop system is shown in Fig. 3, note into the block diagram that the loop back to the controller denoted as x, is replaced with θ when use the first T-S FLC; with the second T-S FLC, the diagram remains unchanged.

The rule set of the fuzzy controller whose data set consider the joint positions of the state variables (first T-S FLC), comprises 1944 if-then rules; 2048 if-then rules when the data set consider the whole state variables (second T-S FLC). The lth rule of the first controller has the form as:

$$\begin{aligned} R^l\text{:} \quad & \text{If} \quad && \theta_1 \text{ is } A_{1,i} \text{ and } \theta_2 \text{ is } A_{2,i} \text{ and } \theta_3 \text{ is } A_{3,i} \\ & && \text{and } y_1 \text{ is } A_{4,i} \text{ and } y_2 \text{ is } A_{5,i} \\ & \text{Then} && u_k = p_{1,1}\theta_1 + p_{1,2}\theta_2 + p_{1,3}\theta_3 + p_{1,4}y_1 + \\ & && p_{1,5}y_2 + p_{1,6} \end{aligned} \tag{17}$$

and the lth rule of the second controller has the form:

$$\begin{aligned} R^l\text{:} \quad & \text{If} \quad && \theta_1 \text{ is } A_{1,i} \text{ and } \theta_2 \text{ is } A_{2,i} \text{ and } \theta_3 \text{ is } A_{3,i} \text{ and} \\ & && \dot{\theta}_1 \text{ is } A_{4,i} \text{ and } \dot{\theta}_2 \text{ is } A_{5,i} \text{ and } \dot{\theta}_3 \text{ is } A_{6,i} \text{ and} \\ & && y_1 \text{ is } A_{7,i} \text{ and } y_2 \text{ is } A_{8,i} \\ & \text{Then} && u_k = p_{1,1}\theta_1 + p_{1,2}\theta_2 + p_{1,3}\theta_3 + p_{1,4}\dot{\theta}_1 + \\ & && p_{1,5}\dot{\theta}_2 + p_{1,6}\dot{\theta}_3 + p_{1,7}y_1 + p_{1,8}y_2 + p_{1,9} \end{aligned} \tag{18}$$

where $A_{j,i}$ is the ith fuzzy set of the jth input variable, $i = 1, 2, 3$ for the rules as in 17 and $i = 1, 2$ for the rules as in 18; u_k with $k = 1, 2$ is the kth control input, which implies that the rule consequents of each first order T-S FLC corresponds to the same control input. The fuzzy sets are parameterized as in (9). The parameters which describe the fuzzy sets for each controller are provided in Appendix II.

The control input $u = [u_1^c, u_2^c]$ defined through this function:

$$u(x,y,t) := \begin{cases} u_1^1 = \frac{\sum_i w_i G_i(x,y;p)}{\sum_i w_i} & \\ & , 0 \le t < t_1 \\ u_2^1 = \frac{\sum_i w_i G_i(x,y;p)}{\sum_i w_i} & \\ u_1^2 = \frac{\sum_i w_i G_i(x,y;p)}{\sum_i w_i} & \\ & , t_1 \le t < t_2 \\ u_2^2 = \frac{\sum_i w_i G_i(x,y;p)}{\sum_i w_i} & \\ u_1^3 = \frac{\sum_i w_i G_i(x,y;p)}{\sum_i w_i} & \\ & , t_2 \le t < t_3 \\ u_2^3 = \frac{\sum_i w_i G_i(x,y;p)}{\sum_i w_i} & \\ u_1^4 = \frac{\sum_i w_i G_i(x,y;p)}{\sum_i w_i} & \\ & , t_3 \le t \le t_4 \\ u_2^4 = \frac{\sum_i w_i G_i(x,y;p)}{\sum_i w_i} & \end{cases} \tag{19}$$

where $i = 1, 2, ..., l_c$ is the rule number in the cth controller; u_k^c denote the kth control input provided by cth controller through a time interval; w_i is the firing strength of each rule as in (10); $G_i(x, y; p)$ is the rule consequent, which take the form as in (17) or (18), based on the number of state variables considered in the data set.

V. Simulation Results

This section presents the numerical verification of closed-loop system using the two T-S FLCs described in the Section IV. The simulation study is performed in MatLab, in a Pentium IV computer with 512 MB of RAM, using the software implementation of the biped robot available in [13]. The parameters that remain unchanged throughout the simulation are provided below.

The physical parameters of the biped model are shown in Table I, and the impact occurs when $\theta_1^d = \pi/8$. The parameters a of the output in (16) are in Table II. The Table III shows the time values of the time interval of the control law in (19), the first row correspond to the first controller and the second row to the second controller. The matrices of the equations (2)-(3) which describe the mathematical model of the biped robot are given at Appendix II.

The results of closed-loop simulation with the first T-S FLC shown from Fig. 4 to 6, which correspond to joint positions trajectories, output trajectories and input control signals. From Fig. 7 to Fig. 10 the closed loop simulation with the second T-S FLC which refer to the joint positions and velocities, the output trajectories and the input control signals.

TABLE I

Biped model parameters

Parameter	**Value**
Mass of Hips (M_H)	15 kg
Mass of Torso (M_T)	10 kg
Mass of Legs (m)	5 kg
Length of legs (r)	1 m
Length of torso (l)	0.5 m

TABLE II

Parameters of the function in (16)

a_1^0	a_1^1	a_1^2	a_1^3
0.512	0.0730	0.0350	-0.8190

a_2^0	a_2^1	a_2^2	a_2^3
-2.2700	3.2600	3.1100	1.8900

TABLE III

Time values of the control law definition in (19)

T-S FLC	t_1	t_2	t_3	t_4
1	0.08004	0.38203	0.95253	1.12134
2	0.09775	0.38264	0.98032	1.12134

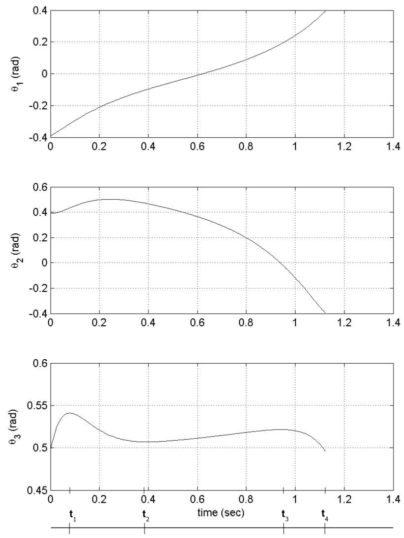

Fig. 4. Joint position trajectories of first T-S FLC.

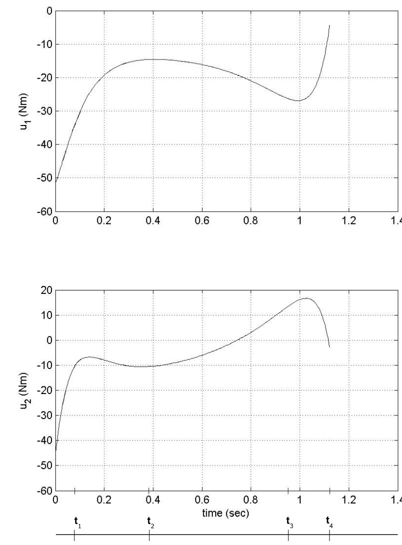

Fig. 6. Control signals of first T-S FLC

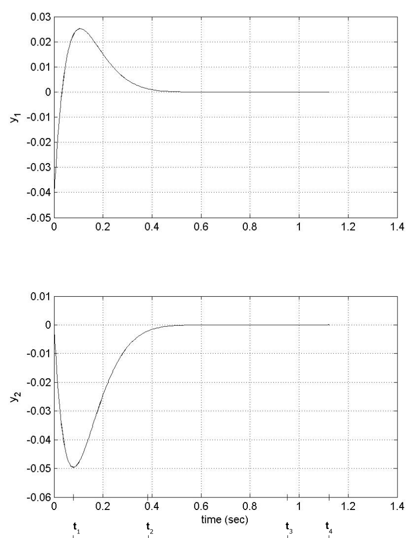

Fig. 5. Output trajectories of first T-S FLC

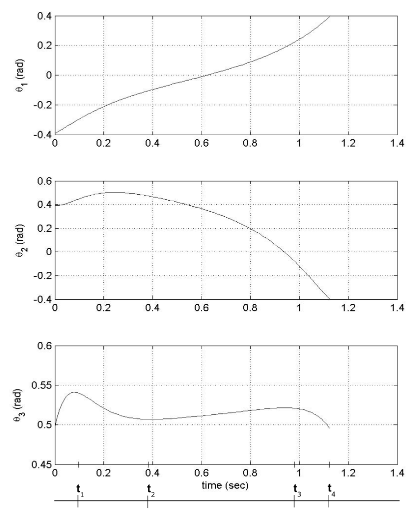

Fig. 7. Joint position trajectories of second T-S FLC.

VI. Conclusions

This paper presented a T-S Fuzzy Logic Controller for generation of walking motions. The control strategy consider an output function imposed on the feedback such that include a walking motion task and eight ANFIS, which adapt first order T-S Fuzzy models parameters taking data of a walking cycle. The objective is zeroing the output, which implies that the task is reached. The closed-loop simulations results have shown that the T-S FLCs with first order functions in the consequents have been sufficient to reach the control objective. In the second T-S FLC the output trajectories is close to zero, due to conservative result in the ANFIS data fitting, notwithstanding allows to perform a walking cycle. Further studies aim to provide evidence that this approach can be used to perform periodic walking motions.

References

[1] O.-M. Ahtiwas, M.-Z. Abdulmuin, and S. S.-F., "A neural-fuzzy logic approach for modeling and control of nonlinear systems," in *IEEE International Symposium on Intelligent Control, 2002.*, October 2002, pp. 270–275.

[2] D. Prabu, S. Kumar, and R. Prasad, "Dynamic control of three-link scara manipulator using adaptive neuro fuzzy inference system," in *ICNSC 2008. IEEE International Conference on Networking, Sensing and Control, 2008*, April 2008, pp. 1609–1614.

[3] J.-S. Jang, "Anfis: adaptive-network-based fuzzy inference system," *IEEE Transactions on Systems, Man and Cybernetics*, vol. 23, no. 3, pp. 665–685, May/Jun 1993.

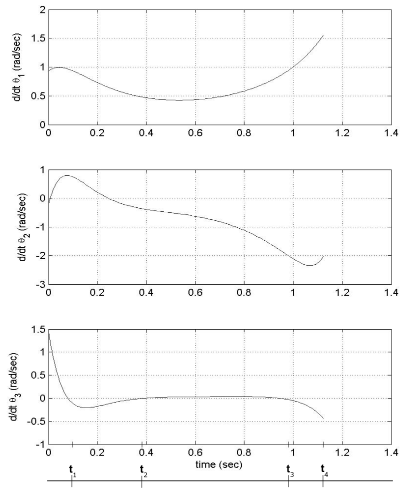

Fig. 8. Joint velocities trajectories of second T-S FLC.

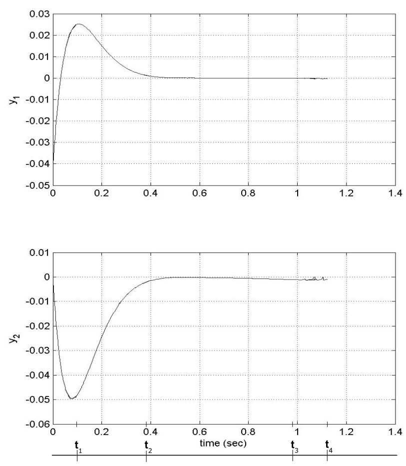

Fig. 9. Output trajectories of second T-S FLC.

[4] M.-Y. Shieh, K.-H. Chang, C.-Y. Chuang, J.-S. Chiou, and J.-H. Li, "Anfis based controller design for biped robots," in *Proccedings of 4th. IEEE International Conference on Mechatronics*, May 2007, pp. 1–6.

[5] J. Ferreira, T. Amaral, V. Pires, M. Crisostomo, and A. Coimbra, "A neural-fuzzy walking control of an autonomous biped robot," in *Proceedings of World Automation Congress, 2004.*, vol. 15, July 2004, pp. 253–258.

[6] M. Vukobratovic and D. Juricic, "Contribution to the synthesis of biped gait," *IEEE Transactions on Biomedical Engineering*, vol. 16, no. 1, pp. 1–6, Jan. 1969.

[7] J. Ferreira, M. Crisóstomo, and A. P. Coimbra, "Neuro-fuzzy zmp control of a biped robot," in *SMO'06: Proceedings of the 6th WSEAS International Conference on Simulation, Modelling and Optimization*. Stevens Point, Wisconsin, USA: World Scientific and Engineering Academy and Society (WSEAS), 2006, pp. 331–337.

[8] E. R. Westervelt, J. W. Grizzle, C. Chevallereau, J.-H. Choi, and B. Morris, *Feedback Control of Dynamic Bipedal Robot Locomotion*. Taylor & Francis/CRC, 2007, ch. Systematic Design of Within-Stride Feedback Controllers for Walking, pp. 137–190.

[9] T. McGeer, "Passive dynamic walking," *Int. J. Robot Res.*, vol. 9, no. 2, pp. 62–82, 1990.

[10] R. Kelly, R. Santibañez, and A. Loria, *Control of Robots Manipulators in Joint Space*. Springer-Verlag London Limited, 2005.

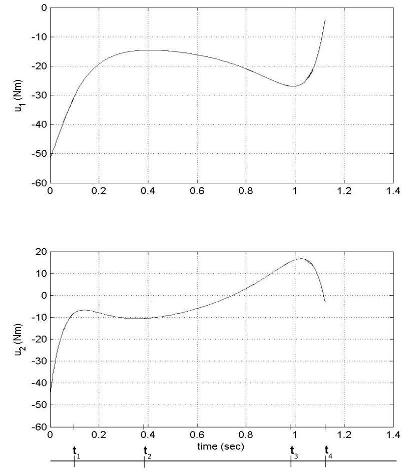

Fig. 10. Control signals of second T-S FLC.

[11] Y. Hurmuzlu and D. Marghitu, "Rigid body collisions of planar kinematic chains with multiple contact points," *Int. J. Robot Res.*, vol. 13, no. 1, pp. 82–92, 1994.

[12] M. Sugeno and T. Kang, "Structure identification of fuzzy model." *Fuzzy Sets and Systems*, vol. 28, pp. 15–,3,3, May/Jun 1988.

[13] "Feedback control of dynamic bipedal robot locomotion book webpage," 2007. [Online]. Available: http://www.dynamicbipedcontrol.org

APPENDIX I
MODEL DETAILS

This appendix section completes the equations of the biped model in (2), (3). In the following, this is the notation used:

$$\begin{aligned} s_{1j} &= \sin(\theta_1 - \theta_j), j \in \{2,3\} \\ c_{1j} &= \cos(\theta_1 - \theta_j), j \in \{2,3\} \end{aligned}$$

A. Swing phase Model

$$M = \begin{bmatrix} (\frac{5}{4}m + M_H + M_T)r^2 & -\frac{1}{2}mr^2 c_{12} & M_T rlc_{13} \\ -\frac{1}{2}mr^2 c_{12} & \frac{1}{4}mr^2 & 0 \\ M_T rlc_{13} & 0 & M_T l^2 \end{bmatrix}$$

$$C = \begin{bmatrix} 0 & -\frac{1}{2}mr^2 s_{12}\dot{\theta}_2 & M_T rls_{13}\dot{\theta}_3 \\ \frac{1}{2}mr^2 s_{12}\dot{\theta}_1 & 0 & 0 \\ -M_T rls_{13}\dot{\theta}_1 & 0 & 0 \end{bmatrix}$$

$$G = \begin{bmatrix} -\frac{1}{2}g(2M_H + 3m + 2M_T)r\sin(\theta_1) \\ \frac{1}{2}gmr\sin(\theta_2) \\ -gM_T l\sin(\theta_3) \end{bmatrix}$$

$$B = \begin{bmatrix} -1 & 0 \\ 0 & -1 \\ 1 & 1 \end{bmatrix}$$

B. Impact model

The inertia matrix M_e has the entries:

$$
\begin{aligned}
M_e^{11} &= (\frac{5}{4}m + M_H + M_T)r^2 \\
M_e^{12} &= -\frac{1}{2}mr^2 c_{12} \\
M_e^{13} &= M_T r l c_{13} \\
M_e^{14} &= (\frac{3}{2}m + M_H + M_T)r\cos(\theta_1) \\
M_e^{15} &= -(\frac{3}{2}m + M_H + M_T)r\sin(\theta_1) \\
M_e^{22} &= \frac{1}{4}mr^2 \\
M_e^{23} &= 0 \\
M_e^{24} &= -\frac{1}{2}mr\cos(\theta_2) \\
M_e^{25} &= \frac{1}{2}mr\sin(\theta_2) \\
M_e^{33} &= M_T l^2 \\
M_e^{34} &= M_T l\cos(\theta_3) \\
M_e^{35} &= -M_T l\sin(\theta_3) \\
M_e^{44} &= 2m + M_H + M_T \\
M_e^{45} &= 0 \\
M_e^{55} &= 2m + M_H + M_T
\end{aligned}
$$

APPENDIX II
T-S FLC FUZZY SET PARAMETERS

This appendix presents the membership function parameters which characterize the fuzzy sets of the controllers described in Section IV. In Table IV to Table VII show the the membership function parameters of the T-S FLC obtained with the first data set. From Table VIII to Table XI show the membership function parameters of the T-S FLC obtained with the second data set.

TABLE IV
MEMBERSHIP FUNCTION OF FIRST CONTROLLER

Input	Fuzzy Set	T-S FLC 1 Parameters		T-S FLC 2 Parameters	
		a	c	a	c
θ_1	$A_{1,1}$	0.0159	−0.39267	0.06025	−0.33105
	$A_{1,2}$	0.0196	−0.34458	0.03542	−0.28163
	$A_{1,3}$	0.0153	−0.31308	0.00833	−0.29258
θ_2	$A_{2,1}$	0.0117	0.39374	0.01430	0.39633
	$A_{2,2}$	0.0081	0.42428	0.00005	0.42013
	$A_{2,3}$	0.0045	0.43581	−0.00018	0.43636
θ_3	$A_{3,1}$	−0.0008	0.49104	0.00077	0.49111
	$A_{3,2}$	0.0072	0.51279	0.01768	0.52108
	$A_{3,3}$	0.0076	0.54053	0.00089	0.55700
y_1	$A_{4,1}$	0.0122	−0.04186	0.03426	−0.00738
	$A_{4,2}$	0.0106	−0.00821	0.02296	0.02153
	$A_{4,3}$	0.0075	0.02542	0.00766	0.03739
y_2	$A_{5,1}$	0.0024	−0.04948	0.01468	−0.07297
	$A_{5,2}$	0.0010	−0.01788	0.01895	0.02325
	$A_{5,3}$	0.0159	−0.00281	0.07741	−0.00231

TABLE V
MEMBERSHIP FUNCTION PARAMETERS OF SECOND CONTROLLER

Input	Fuzzy Set	T-S FLC 1 Parameters		T-S FLC 2 Parameters	
		a	c	a	c
θ_1	$A_{1,1}$	0.0396	−0.3172	0.0445	−0.3146
	$A_{1,2}$	0.0441	−0.2096	0.0461	−0.2122
	$A_{1,3}$	0.0414	−0.1042	0.0443	−0.1065
θ_2	$A_{2,1}$	0.0136	0.4359	0.0098	0.4297
	$A_{2,2}$	0.0156	0.4775	0.0161	0.4681
	$A_{2,3}$	0.0054	0.5085	0.0119	0.5042
θ_3	$A_{3,1}$	0.0113	0.5102	0.0098	0.5098
	$A_{3,2}$	−0.0056	0.5189	0.0078	0.5259
	$A_{3,3}$	−0.0047	0.5440	0.0014	0.5448
y_1	$A_{4,1}$	0.0070	−0.0002	0.0098	0.0037
	$A_{4,2}$	0.0063	0.0172	−0.0085	0.0239
	$A_{4,3}$	0.0062	0.0339	0.0109	0.0287
y_2	$A_{5,1}$	0.0024	−0.0495	0.0020	−0.0552
	$A_{5,2}$	0.0099	−0.0179	0.0140	−0.0226
	$A_{5,3}$	0.0159	−0.0028	0.0088	0.0030

TABLE VI
MEMBERSHIP FUNCTION PARAMETERS OF THIRD CONTROLLER

Input	Fuzzy Set	T-S FLC 1 Parameters		T-S FLC 2 Parameters	
		a	c	a	c
θ_1	$A_{1,1}$	0.0633	−0.10525	0.0633	−0.10525
	$A_{1,2}$	0.0633	0.04387	0.0633	0.04387
	$A_{1,3}$	0.0633	0.19300	0.0633	0.19300
θ_2	$A_{2,1}$	0.1038	−0.01623	0.1038	−0.01623
	$A_{2,2}$	0.1038	0.22814	0.1037	0.22814
	$A_{2,3}$	0.1038	0.47250	0.1037	0.47250
θ_3	$A_{3,1}$	0.0031	0.50694	0.0031	0.50694
	$A_{3,2}$	0.0031	0.51424	0.0031	0.51423
	$A_{3,3}$	0.0031	0.52152	0.0031	0.52152
y_1	$A_{4,1}$	0.0003	-8×10^{-7}	0.0003	-9×10^{-7}
	$A_{4,2}$	0.0003	0.00065	0.0003	0.00065
	$A_{4,3}$	0.0003	0.01301	0.0003	0.00130
y_2	$A_{5,1}$	0.0005	−0.00216	0.0005	−0.00216
	$A_{5,2}$	0.0005	−0.00108	0.0005	−0.00108
	$A_{5,3}$	0.0005	-1×10^{-6}	0.0005	1×10^{-6}

TABLE VII
MEMBERSHIP FUNCTION PARAMETERS OF FOURTH CONTROLLER

Input	Fuzzy Set	T-S FLC 1 Parameters		T-S FLC 2 Parameters	
		a	c	a	c
θ_1	$A_{1,1}$	0.0438	−0.10525	0.043823	0.197075
	$A_{1,2}$	0.0633	0.04387	0.043823	0.300271
	$A_{1,3}$	0.0633	0.19300	0.043823	0.403467
θ_2	$A_{2,1}$	0.1038	−0.01623	0.08097	−0.406247
	$A_{2,2}$	0.1038	0.228138	0.08097	−0.215576
	$A_{2,3}$	0.1038	0.472501	0.08097	−0.024905
θ_3	$A_{3,1}$	0.0031	0.50694	0.00597	0.493359
	$A_{3,2}$	0.0031	0.51423	0.00597	0.507418
	$A_{3,3}$	0.0031	0.52152	0.00597	0.521477
y_1	$A_{4,1}$	0.0002	−0.000001	1×10^{-6}	-5×10^{-6}
	$A_{4,2}$	0.0002	0.000650	1×10^{-6}	-3×10^{-6}
	$A_{4,3}$	0.0002	0.001301	1×10^{-6}	-5×10^{-7}
y_2	$A_{5,1}$	0.0004	−0.002164	7×10^{-6}	1×10^{-6}
	$A_{5,2}$	0.0004	−0.001081	7×10^{-6}	2×10^{-5}
	$A_{5,3}$	0.0004	0.000000	7×10^{-6}	3×10^{-5}

TABLE VIII

MEMBERSHIP FUNCTION PARAMETERS OF FIRST CONTROLLER

Input	Fuzzy Set	T-S FLC 1 Parameters		T-S FLC 2 Parameters	
		a	c	a	c
θ_1	$A_{1,1}$	0.0418	-0.3886	0.0414	-0.3904
	$A_{1,2}$	0.0185	-0.2840	0.0185	-0.2876
θ_2	$A_{2,1}$	0.0262	0.3927	0.0192	0.3917
	$A_{2,2}$	0.0079	0.4561	0.0077	0.4542
θ_3	$A_{3,1}$	0.0033	0.4729	0.0204	0.4952
	$A_{3,2}$	0.0314	0.5316	-0.0029	0.5531
$\dot{\theta}_1$	$A_{1,1}$	0.0261	0.9094	0.0243	0.9217
	$A_{1,2}$	0.0484	0.9793	0.0446	0.9851
$\dot{\theta}_2$	$A_{2,1}$	0.4323	-0.2423	0.4376	-0.2399
	$A_{2,2}$	0.4351	0.7959	0.4381	0.7948
$\dot{\theta}_3$	$A_{3,1}$	0.6707	-0.1089	0.6733	-0.1078
	$A_{3,2}$	0.6732	1.4843	0.6753	1.4835
y_1	$A_{4,1}$	0.0197	-0.0413	0.0350	-0.0353
	$A_{4,2}$	0.0159	0.0354	0.0124	0.0412
y_2	$A_{5,1}$	0.0345	-0.0357	-0.0002	-0.0668
	$A_{5,2}$	0.0124	0.0254	0.0263	-0.0052

TABLE IX

MEMBERSHIP FUNCTION PARAMETERS OF SECOND CONTROLLER

Input	Fuzzy Set	T-S FLC 1 Parameters		T-S FLC 2 Parameters	
		a	c	a	c
θ_1	$A_{1,1}$	0.1191	-0.2681	0.0493	-0.3138
	$A_{1,2}$	0.0447	-0.0509	0.0763	-0.1067
θ_2	$A_{2,1}$	0.0021	0.4318	0.0247	0.4314
	$A_{2,2}$	0.0318	0.4940	0.0231	0.4957
θ_3	$A_{3,1}$	0.0171	0.5107	0.0170	0.5099
	$A_{3,2}$	0.0015	0.5518	-0.0016	0.5498
$\dot{\theta}_1$	$A_{1,1}$	0.1525	0.4524	0.1904	0.4783
	$A_{1,2}$	0.1993	0.9283	0.1867	0.9428
$\dot{\theta}_2$	$A_{2,1}$	0.4647	-0.3690	0.4744	-0.3667
	$A_{2,2}$	0.4683	0.7600	0.4710	0.7572
$\dot{\theta}_3$	$A_{3,1}$	0.0461	-0.2321	0.0928	-0.1997
	$A_{3,2}$	0.0804	-0.0140	0.0779	0.0031
y_1	$A_{4,1}$	-0.0008	-0.0060	0.0125	0.0033
	$A_{4,2}$	0.0138	0.0218	-0.0008	0.0331
y_2	$A_{5,1}$	0.0180	-0.0803	0.0131	-0.0667
	$A_{5,2}$	0.0091	-0.0296	0.0187	-0.0090

TABLE X

MEMBERSHIP FUNCTION PARAMETERS OF THIRD CONTROLLER

Input	Fuzzy Set	T-S FLC 1 Parameters		T-S FLC 2 Parameters	
		a	c	a	c
θ_1	$A_{1,1}$	0.1375	-0.1059	0.13768	-0.1066
	$A_{1,2}$	0.1389	0.2219	0.14065	0.2204
θ_2	$A_{2,1}$	0.2335	-0.0786	0.23411	-0.0780
	$A_{2,2}$	0.2336	0.4724	0.23311	0.4729
θ_3	$A_{3,1}$	0.0081	0.5003	0.00461	0.4994
	$A_{3,2}$	0.0110	0.5177	0.01351	0.5190
$\dot{\theta}_1$	$A_{1,1}$	0.2205	0.4248	0.21962	0.4243
	$A_{1,2}$	0.2191	0.9433	0.21921	0.9431
$\dot{\theta}_2$	$A_{2,1}$	0.6950	-2.0038	0.69503	-2.0037
	$A_{2,2}$	0.6951	-0.3667	0.69490	-0.3665
$\dot{\theta}_3$	$A_{3,1}$	0.0241	-0.0325	0.02631	-0.0318
	$A_{3,2}$	0.0300	0.0353	0.02974	0.0354
y_1	$A_{4,1}$	0.0006	0.0063	-0.00204	0.0155
	$A_{4,2}$	-0.0070	0.0052	-0.00870	0.0028
y_2	$A_{5,1}$	0.0025	-0.0184	-0.00363	-0.0037
	$A_{5,2}$	0.0077	0.0019	-6×10^{-5}	0.0008

TABLE XI

MEMBERSHIP FUNCTION PARAMETERS OF FOURTH CONTROLLER

Input	Fuzzy Set	T-S FLC 1 Parameters		T-S FLC 2 Parameters	
		a	c	a	c
θ_1	$A_{1,1}$	0.0751	0.2246	0.0855	0.2344
	$A_{1,2}$	0.0714	0.3945	0.0332	0.4195
θ_2	$A_{2,1}$	0.1317	-0.3922	0.1275	-0.3934
	$A_{2,2}$	0.1296	-0.0755	0.1251	-0.0732
θ_3	$A_{3,1}$	-0.0101	0.4803	0.0084	0.4819
	$A_{3,2}$	0.0142	0.5133	0.0081	0.5078
$\dot{\theta}_1$	$A_{1,1}$	0.2586	0.9436	0.2596	0.9443
	$A_{1,2}$	0.2569	1.5509	0.2512	1.5536
$\dot{\theta}_2$	$A_{2,1}$	0.1494	-2.3464	0.1585	-2.3436
	$A_{2,2}$	0.1470	-2.0039	0.1426	-2.0034
$\dot{\theta}_3$	$A_{3,1}$	0.1657	-0.4346	0.1428	-0.4482
	$A_{3,2}$	0.1720	-0.0329	0.1765	-0.0387
y_1	$A_{4,1}$	-0.0083	-0.0047	-0.0082	-0.0037
	$A_{4,2}$	-0.0003	-0.0033	-0.0015	-0.0081
y_2	$A_{5,1}$	-0.0093	0.0028	0.0029	0.0001
	$A_{5,2}$	-0.0003	0.0031	0.0019	0.0134

Neuro-Fuzzy Based Output Feedback Controller Design for Biped Robot Walking

Selene L. Cardenas-Maciel[1], Oscar Castillo[2], and Luis T. Aguilar[3]

[1] Universidad Autonoma de Baja California, Tijuana, BC, Mexico
lilettecardenas@ieee.org
[2] Instituto Tecnologico de Tijuana, Mexico
ocastillo@hafsamx.org
[3] Instituto Politecnico Nacional, Mexico
luis.aguilar@ieee.org

Abstract. A neuro-fuzzy learning algorithm is applied to design Takagi-Sugeno Fuzzy Controllers for a biped robot walking problem. The appropriate control signal is provided with a rule to switch between the controllers. A simulation of generation of walking motions is presented to illustrate the effectiveness of this approach.

1 Introduction

Fuzzy logic control as an application area of Fuzzy Logic has attracted attention from scientist and engineers due that through if-then rules can express knowledge of how to control a system incorporating uncertainty. The existence of a big number of variables in the measurable variables space (system o external variables) and the partition needed in these variables, are factors that have influence in the size of the rule base, which implies a nontrivial task into the modeling. In order to overcome this difficulties, Clustering, Adaptive Neuronal Networks and Neuro-fuzzy approaches have been proposed and applied to identification and control tasks where the model of the system to control are not available as in [2]; for observer design proposed in [6] to control of robot manipulators. In biped robot locomotion control, adaptive neural networks and neuro-fuzzy methods are implemented where uses the Zero Moment Point (ZMP) [12] information. For example, in [10] several Adaptive-Network-based Fuzzy Inference System (ANFIS)[7] are proposed to design a locomotion controller and another one to determine the model of the system. A learning algorithm and a grid partition method are proposed in [3] to obtain a walking controller. Neuro-fuzzy approaches applied in ZMP control trajectories are proposed in [4].

O. Castillo et al. (Eds.): Soft Computing for Intell. Control and Mob. Robot., SCI 318, pp. 423–444.
springerlink.com

This paper is related to the application of ANFIS a design tool of an output feedback controller such that it can induce walking motions in a biped robot whose model consider the impact with the environment. The control loop uses an output definition, which include the movement task, if the output is carried to zero the biped robot perform the desired motion. Thus, the controller design is based in the off-line learning of a nonlinear relationship between the state space, the outputs and the control inputs information which are distributed in multiple instances of the learning algorithm which produce a set of Takagi-Sugeno type Fuzzy Logic Controllers specialized in a subspace. The final control input is defined as a switching function dependant of the time.

The rest of this paper is organized as follows: Section 2 introduces the mathematical model of the biped robot. In Section 3, describes some aspects of the neuro-fuzzy approach. Section 4 explains the control strategy used for controller design. Section 5, illustrates simulation results of the closed-loop system. Section 6 provides some conclusions.

2 Biped Robot Model

In this section the dynamical model of a planar biped robot is introduced. The biped robot consists of a torso, hips, and two legs of equal length without ankles and knees. Two torques are applied between the legs and torso. The definition of the angular coordinates and the disposition of the masses of the torso, hips and legs of the biped robot are shown in Fig. 1, the positive angles are computed in a clockwise manner with respect to the indicated vertical lines and all masses of the links are lumped.

The walking cycle takes place in the sagittal plane and on a surface level, and it is assumed as successive phases where only one leg (stance leg) touching the walking surface (swing phase), with the transition from one leg to another taking place in a smaller length of time. During the swing phase, the stance leg is modeled like a pivot and the swing leg is assumed to move into the frontal plane [9] and to renter the plane of the motion when the angle of the stance leg attains a given desired value. The assumptions concerning the walking cycle, define the biped robot model in two parts: the model that describes the swing phase and another one that describes the contact event of the swing leg with the walking surface; which are presented below.

2.1 Swing Phase Model

The dynamical model of the robot during the swing phase is a second order system derived from the Lagrange method [8]:

$$M(\theta)\ddot{\theta} + C(\theta,\dot{\theta})\dot{\theta} + G(\theta) = Bu, \tag{1}$$

where $\theta = [\theta_1, \theta_2, \theta_3]^T$ are the generalized coordinates, θ_1 parameterizes the stance leg, θ_2 the swing leg and θ_3 the torso; $u = [u_1, u_2]^T$ are the input; $M(\theta)$ is a positive-definite inertia matrix, $C(\theta,\dot{\theta})\dot{\theta}$ is the vector of the centripetal and Coriolis forces; and $G(\theta)$ is the vector of the conservative forces and B is the input matrix.

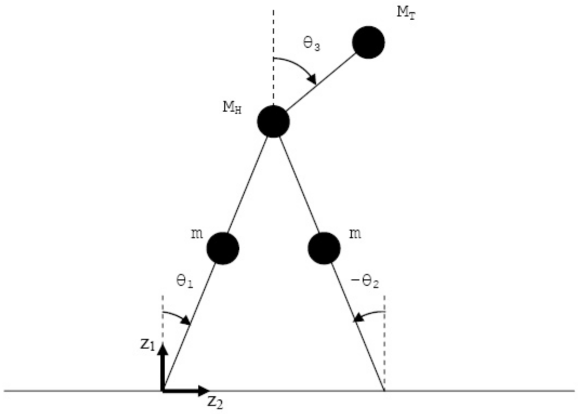

Fig. 1. 3-link biped robot

the state-space form of the second order equation (1) is defined as:

$$\begin{aligned}\dot{x} &:= \frac{d}{dt}\begin{bmatrix}\theta \\ \dot{\theta}\end{bmatrix} = \begin{bmatrix}\dot{\theta} \\ M^{-1}(\theta)[-C(\theta,\dot{\theta})\dot{\theta} - G(\theta) + Bu]\end{bmatrix} \\ &:= f(x) + g(x)u.\end{aligned} \tag{2}$$

2.2 Impact Model

The impact between the swing leg and the ground is modeled as the contact between two rigid bodies. The main objective is to obtain the velocity of the generalized coordinates after the impact of the swing leg with the walking surface in terms of the velocity and position before the impact. The impact model for the biped robot is based on the rigid impact model of [5] and assuming the case where the contact of the swing leg with the walking surface produce either no rebound nor slipping of the swing leg, and the stance leg lifting the walking surface without interaction. the impact model is expressed with equation [13]:

$$\begin{bmatrix}M_e & -E^T \\ E & 0\end{bmatrix}\begin{bmatrix}\dot{\theta}_e^+ \\ F\end{bmatrix} = \begin{bmatrix}M_e\dot{\theta}_e^- \\ 0\end{bmatrix}, \tag{3}$$

where $\theta_e = [\theta_1, \theta_2, \theta_3, z_1, z_2]^T$ are the generalized coordinates resulting of the add the cartesian coordinates $[z_1, z_2]^T$ of the end of the stance leg as shown in Figure 1; M_e is the positive-definite inertia matrix of the biped model with the new generalized coordinates; $F = [F_T, F_N]^T$ represent the tangential and normal forces applied at the end of the swing leg; $\dot{\theta}_e^+$ is the velocity after the impact; $\dot{\theta}_e^-$ is the velocity before the impact and

$$E := \frac{\partial Y}{\partial \theta_e} = \begin{bmatrix} r\cos(\theta_1) & -r\cos(\theta_2) & 0 & 1 & 0 \\ -r\sin(\theta_1) & r\sin(\theta_2) & 0 & 0 & 1 \end{bmatrix}, \tag{4}$$

solving for $\dot{\theta}_e^+$ of equation (3) and a change of coordinates must be done and also a re-initialization of the model (2). The change of coordinates is an expression for $x^+ := (\theta^+, \dot{\theta}^+)$ in terms of $x^- := (\theta^-, \dot{\theta}^-)$, which is given for the mapping function [13]:

$$x^+ := \Delta(x^-) := \begin{bmatrix} \theta_2^- \\ \theta_1^- \\ \theta_3^- \\ \dot{\theta}_2^+(x^-) \\ \dot{\theta}_1^+(x^-) \\ \dot{\theta}_3^+(x^-) \end{bmatrix}. \tag{5}$$

Thus, the overall model of biped walking is the combination of the swing phase model and impact model, as follows:

$$\Sigma_{cl} : \begin{cases} \dot{x} = f(x) + g(x)u(x) & x^- \notin S \\ x^+ = \Delta(x^-) & x^- \in S \end{cases} \tag{6}$$

where

$$S := \{(\theta, \dot{\theta}) | z_1 > 0, z_2 = 0, \theta_1 = \theta_1^d\} \tag{7}$$

3 ANFIS and Fuzzy Models

ANFIS [7] is a class of adaptive neural network whose functionally is equivalent to the T-S fuzzy reasoning mechanism [11]. The ANFIS architecture consist on five layers and the node function for each node of same layer corresponds to the same family functions. The architecture is detailed as follows:

3.1 Layer 1

Every node i in this layer is an adaptive node with a node function

$$O_i^1 = \mu_{A_i}(x) \tag{8}$$

where x is the input to node i and A_i is the linguistic label associated with this node, O_i^1 is the membership function of the fuzzy set A_i, it specifies the grade that the given value x satisfies the quantifier A. The membership function $\mu_{A_i}(x)$ can be parameterized for

$$\mu_{A_i}(x) = \exp\{-\frac{1}{2}(\frac{x - c_i}{a_i})^2\} \tag{9}$$

where a_i and c_i are referred as premise parameters.

3.2 Layer 2

Every node i in this layer is a fixed node labeled Π, whose output is the product of all the incoming signals. For example, consider two linguistic variables A and B characterized by two fuzzy sets each. Then the output of a node i of this layer is obtained by:

$$O_i^2 = w_i = \mu_{A_i}(x)\mu_{B_i}(y)\ ,\ i = 1,2. \tag{10}$$

each node represent the firing strength of a rule.

3.3 Layer 3

Every node in this layer is a fixed node labeled N. The ith node calculate the ratio of the ith rule's firing strength to the sum of the all rules' firing strengths. The outputs of this layer are called normalized firing strengths ($\bar{w}_1$).

$$O_i^3 = \bar{w}_i = \frac{w_i}{\sum i w_i}\ ,\ i = 1,2. \tag{11}$$

3.4 Layer 4

Every node i in this layer is an adaptive node with node function

$$O_i^4 = \bar{w}_i f_i = \bar{w}_i(p_i x + q_i y + r_i),\ i = 1,2. \tag{12}$$

where p_i, q_i, r_i is the parameter set of this node, this are the consequent parameters.

3.5 Layer 5

The single node in this layer is a fixed node labeled Σ, which computes the overall output as the summation of all incoming signals:

$$O_i^5 = \sum_i \bar{w}_i f_i = \frac{\sum_i w_i f_i}{\sum_i w_i} \tag{13}$$

The learning rule combines gradient method and least squares estimate to identify and update the parameters of the network, these parameters are the premise and consequent parameters which describe a Fuzzy Model.

Thus, ANFIS can serve as basis for constructing a set of T-S type fuzzy model [11] with appropriate membership functions starting from a set of input-output data pairs. Consider a T-S fuzzy model with input variables x_1, x_2,..., x_j and output variables u_1, u_2,...,u_k, the lth rule takes the form:

$$\begin{aligned}
R^l\text{: IF}\quad & x_1 \text{ is } A_{1,i} \text{ and } x_2 \text{ is } A_{2,i} \text{ and ... } x_j \text{ is } A_{j,i} \\
\text{THEN}\quad & \\
& u_1 = G(x_1, x_2, \ldots, x_j; p_{1,1}, p_{1,2}, \ldots, p_{1,j}, p_{1,j+1}) \\
& \text{and ... and} \\
& u_k = G(x_1, x_2, \ldots, x_j; p_{k,1}, p_{k,2}, \ldots, p_{k,j}, p_{k,j+1})
\end{aligned} \tag{14}$$

where $A_{j,i}$ with $i = 1,2,\ldots,m_1$ and $j = 1,2,\ldots m_2$, are the ith fuzzy set of the jth input variable; u_k with $k = 1,2,\ldots,m_3$, each $G(\cdot)$ is an crisp continuous function in terms of the inputs with $j+1$ parameters p.

4 Control Strategy

This paper uses the output form proposed in [13], which encode a geometric task for the robot, identifies the zero dynamics of the system model including the presence of impacts and design a feedback controller that generate exponential stable walking motions. The output is defined as follows:

$$y := \begin{bmatrix} y_1 \\ y_2 \end{bmatrix} := \begin{bmatrix} h_1(\theta, a) \\ h_2(\theta, a) \end{bmatrix} := \begin{bmatrix} \theta_3 - h_{d,1}(\theta_1, a) \\ \theta_2 - h_{d,2}(\theta_1, a) \end{bmatrix} \tag{15}$$

where

$$\begin{aligned} h_{d,1}(\theta_1, a) &:= a_1^0 + \cdots + a_1^3(\theta_1)^3 \\ h_{d,2}(\theta_1, a) &:= -\theta_1 + (a_2^0 + \cdots + a_2^3(\theta_1)^3) \times (\theta_1 + \theta_1^d) \times (\theta_1 - \theta_1^d). \end{aligned} \tag{16}$$

The control objective is to find a intelligent control law taking the trajectories of the closed-loop system during a walking cycle obtained in [13] such that the output is driving to zero.

4.1 Controller Design

This paper uses ANFIS for the T-S Fuzzy Logic Controller (T-S FLC) design. In order to accomplish the control objective, the state trajectories $x = [\theta_1, \theta_2, \theta_3, \dot{\theta}_1, \dot{\theta}_2, \dot{\theta}_3]^T$ are considered, the output trajectories $y = [y_1, y_2]^T$ and the control inputs $u = [u_1, u_2]^T$ corresponding to closed-loop system simulation of the work proposed in [13] during a walking cycle, to built the data set (input-output data pairs).

The data set is partitioned to diminish the computational load and the time to the algorithm, and then distributed to different instances of the learning algorithm as follows: 2 ANFIS take each qth partition and use as input data the state and output trajectories; as output data, one of the control inputs. The lth rule of each T-S FLC has the form as:

$$\begin{aligned} R^l: \text{IF} \quad & \theta_1 \text{ is } A_{1,i} \text{ and } \theta_2 \text{ is } A_{2,i} \text{ and } \theta_3 \text{ is } A_{3,i} \text{ and} \\ & \dot{\theta}_1 \text{ is } A_{4,i} \text{ and } \dot{\theta}_2 \text{ is } A_{5,i} \text{ and } \dot{\theta}_3 \text{ is } A_{6,i} \text{ and} \\ & y_1 \text{ is } A_{7,i} \text{ and } y_2 \text{ is } A_{8,i} \\ \text{THEN} \quad & \\ & u_k = p_{1,1}\theta_1 + p_{1,2}\theta_2 + p_{1,3}\theta_3 + p_{1,4}\dot{\theta}_1 + \\ & p_{1,5}\dot{\theta}_2 + p_{1,6}\dot{\theta}_3 + p_{1,7}y_1 + p_{1,8}y_2 + p_{1,9} \end{aligned} \tag{17}$$

where $A_{j,i}$ with $i = 1,2$ are fuzzy sets for each input variable: θ_1, θ_2, θ_3, $\dot{\theta}_1$, $\dot{\theta}_2$, $\dot{\theta}_3$, y_1 and y_2 respectively; u_k with $k = 1,2$ is one control input. The fuzzy sets are parameterized as in (9).

Thus, the overall controller consist of four controllers, each one consists of two first order T-S FLC, and each T-S FLC provides one input control. The overall scheme of proposed controller is presented in Fig. 2. The closed-loop system is shown in Fig. 3, the signal defined as $h_0(\theta)$ are the quantities to control, which represent to the first term of each element of the vector defined in (15).

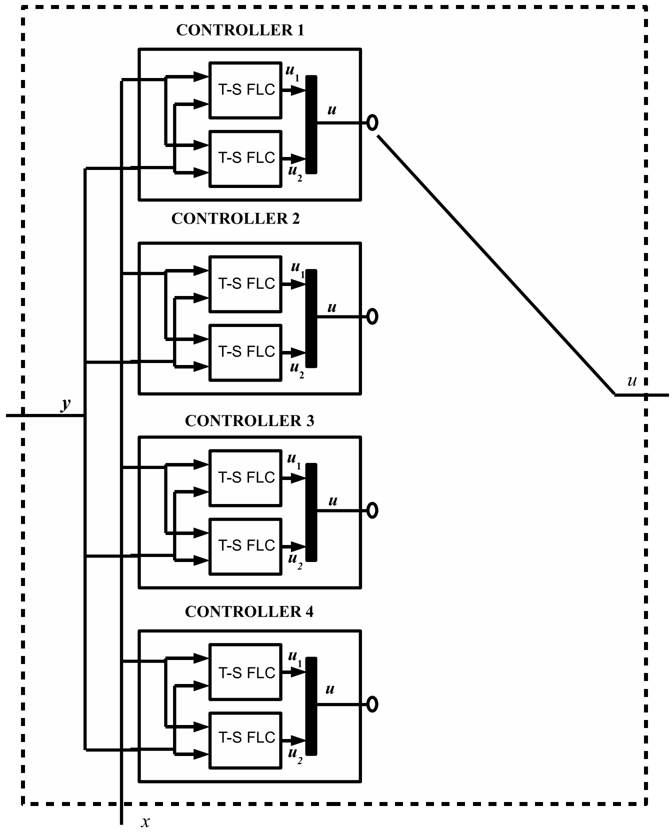

Fig. 2. Controller Structure

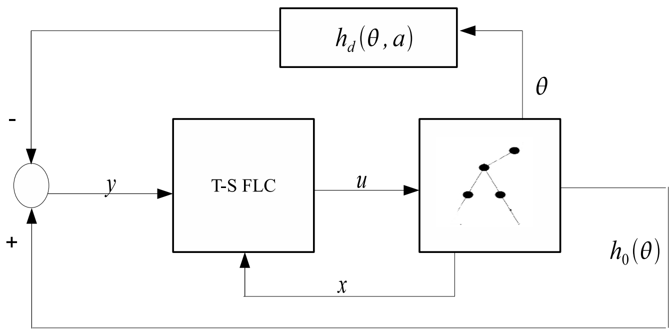

Fig. 3. Closed-loop system block diagram

The control input $u = [u_1^c, u_2^c]^T$ is defined through this function:

$$u(x,y,t) := \begin{cases} u_1^1 = \frac{\sum_i w_i G_i(x,y;p)}{\sum_i w_i} \\ u_2^1 = \frac{\sum_i w_i G_i(x,y;p)}{\sum_i w_i} & ,0 \leq t < t_1 \\ u_1^2 = \frac{\sum_i w_i G_i(x,y;p)}{\sum_i w_i} \\ u_2^2 = \frac{\sum_i w_i G_i(x,y;p)}{\sum_i w_i} & ,t_1 \leq t < t_2 \\ u_1^3 = \frac{\sum_i w_i G_i(x,y;p)}{\sum_i w_i} \\ u_2^3 = \frac{\sum_i w_i G_i(x,y;p)}{\sum_i w_i} & ,t_2 \leq t < t_3 \\ u_1^4 = \frac{\sum_i w_i G_i(x,y;p)}{\sum_i w_i} \\ u_2^4 = \frac{\sum_i w_i G_i(x,y;p)}{\sum_i w_i} & ,t_3 \leq t \leq t_4 \end{cases} \tag{18}$$

where $x = [\theta_1, \theta_2, \theta_3, \dot{\theta}_1, \dot{\theta}_2, \dot{\theta}_3]$, $y = [y_1, y_2]$, $i = 1,2,...,l_c$, l_c is the number of rules in each controller; u_k^c denotes the kth control input provided by cth controller and represents the weight average of rules activation within antecedents projected on the consequents through a time interval; w_i is the firing strength of each rule as in (10); $G(x,y,p)$ is the consequent of the each rule which takes the form as in (12) and p are the consequents parameters of each rule provided by the learning algorithm. The total rule base of the controller comprises 2048 if-then rules, considering that the universe of discourse of each input variable is represented through two membership functions. The parameters which describe each T-S FLC are provided in Section 6.

5 Simulation Results

The numerical verification of the closed-loop system was performed in MatLab, in a Pentium IV computer with 512 MB of RAM, using the software implementation of the biped robot available in [1]. The physical parameters of the biped model are shown in Table 1, and the impact occurs when $\theta_1^d = \pi/8$. The time values that define the interval in (18) are shown in Table 3. The parameters of the output (15)-(16) are given in Table 2. The matrices of the equations (2)-(3) which describe the mathematical model of the biped robot are given at Section 6.

In Fig. 4 to 7 show the state trajectories, output trajectories and input control of closed-loop simulation where the biped robot to perform one step.

Table 1. Biped model parameters

Parameter	Value
Mass of Hips (M_H)	15 kg
Mass of Torso (M_T)	10 kg
Mass of Legs (m)	5 kg
Length of legs (r)	1 m
Length of torso (l)	0.5 m

Table 2. Parameters of the output definition y in (16)

a_1^0	a_1^1	a_1^2	a_1^3	a_2^0	a_2^1	a_2^2	a_2^3
0.512	0.0730	0.0350	-0.8190	-2.2700	3.2600	3.1100	1.8900

Table 3. Time values of the control law definition in (18)

t_1	t_2	t_3	t_4
0.098	0.383	0.980	1.121

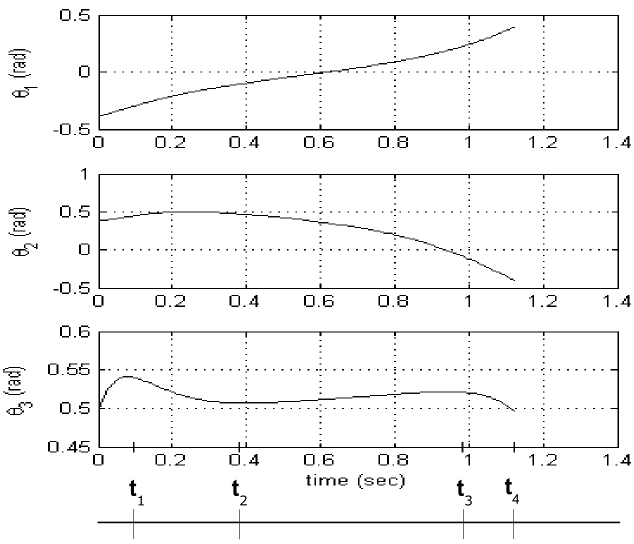

Fig. 4. Joint position trajectories

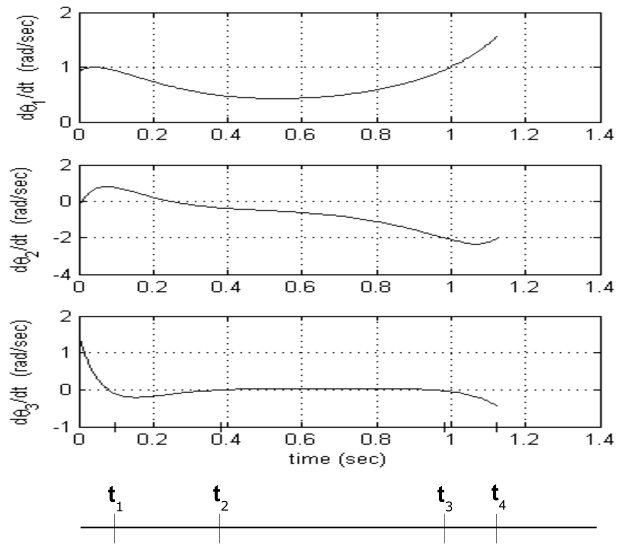

Fig. 5. Joint velocities trajectories

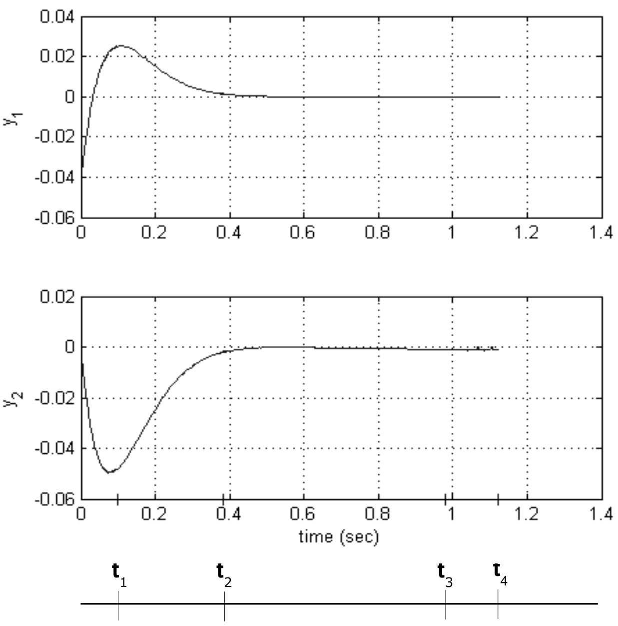

Fig. 6. Output trajectories

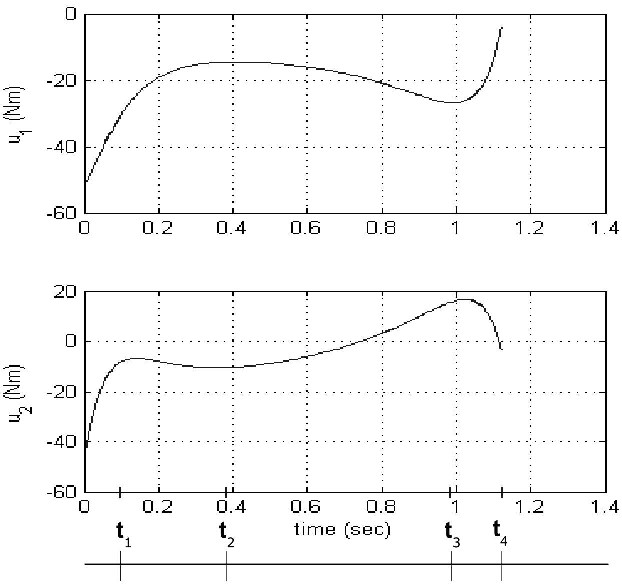

Fig. 7. Control signals

6 Conclusions

In this paper a T-S Fuzzy Logic Controller design to generate walking motions is presented. The control strategy consider an output function imposed in the feedback and several ANFIS are used to adapt the parameters of T-S FLCs such that fit a set of input-output data pairs which represent the evolution of the state variables and the output function during a walking cycle. An intelligent control law as switching function is proposed whose objective is to drive the quantities to control $h_0(\theta)$ to track the output function. The simulations results demonstrate that this method can be applied to solve the problem, its effectiveness is related to the capabilities to perform the data fitting and at this time, the controller is ad hoc for the output function and biped mathematical model parameters presented within the paper.

Appendix 1

Model Details

This section completes the equations of the biped model (2) - (3). In the following, this is the notation used:

$$
\begin{aligned}
s_{1j} &= \sin(\theta_1 - \theta_j), j \in \{2,3\} \\
c_{1j} &= \cos(\theta_1 - \theta_j), j \in \{2,3\}
\end{aligned}
$$

Swing phase Model

$$
M = \begin{bmatrix} (\frac{5}{4}m + M_H + M_T)r^2 & -\frac{1}{2}mr^2 c_{12} & M_T rlc_{13} \\ -\frac{1}{2}mr^2 c_{12} & \frac{1}{4}mr^2 & 0 \\ M_T rlc_{13} & 0 & M_T l^2 \end{bmatrix}
$$

$$
C = \begin{bmatrix} 0 & -\frac{1}{2}mr^2 s_{12}\dot{\theta}_2 & M_T rls_{13}\dot{\theta}_3 \\ \frac{1}{2}mr^2 s_{12}\dot{\theta}_1 & 0 & 0 \\ -M_T rls_{13}\dot{\theta}_1 & 0 & 0 \end{bmatrix}
$$

$$
G = \begin{bmatrix} -\frac{1}{2}g(2M_H + 3m + 2M_T)r\sin(\theta_1) \\ \frac{1}{2}gmr\sin(\theta_2) \\ -gM_T l\sin(\theta_3) \end{bmatrix}
$$

$$
B = \begin{bmatrix} -1 & 0 \\ 0 & -1 \\ 1 & 1 \end{bmatrix}
$$

Impact Model

The inertia matrix M_e has the entries:

$$
\begin{aligned}
M_e^{11} &= (\frac{5}{4}m + M_H + M_T)r^2 \\
M_e^{12} &= -\frac{1}{2}mr^2 c_{12} \\
M_e^{13} &= M_T rlc_{13} \\
M_e^{14} &= (\frac{3}{2}m + M_H + M_T)r\cos(\theta_1) \\
M_e^{15} &= -(\frac{3}{2}m + M_H + M_T)r\sin(\theta_1) \\
M_e^{22} &= \frac{1}{4}mr^2 \\
M_e^{24} &= -\frac{1}{2}mr\cos(\theta_2) \\
M_e^{25} &= \frac{1}{2}mr\sin(\theta_2) \\
M_e^{33} &= M_T l^2 \\
M_e^{34} &= M_T l\cos(\theta_3) \\
M_e^{35} &= -M_T l\sin(\theta_3) \\
M_e^{44} &= 2m + M_H + M_T \\
M_e^{55} &= 2m + M_H + M_T
\end{aligned}
$$

Appendix 2

T-S Fuzzy Controllers Parameters

Antecedent Parameters

This subsection Tables 4 to 7 show the membership functions parameters of each of the controller explained in the section 4.

Table 4. Membership function parameters of first Controller

Input	Fuzzy Set	T-S FLC 1 Parameters a	T-S FLC 1 Parameters c	T-S FLC 2 Parameters a	T-S FLC 2 Parameters c
θ_1	$A_{1,1}$	0.04179	−0.38862	0.04136	−0.39037
	$A_{1,2}$	0.01850	−0.28397	0.01845	−0.28763
θ_2	$A_{2,1}$	0.02619	0.39265	0.01917	0.39171
	$A_{2,2}$	0.00797	0.45614	0.00766	0.45421
θ_3	$A_{3,1}$	0.00331	0.47294	0.02037	0.49516
	$A_{3,2}$	0.03138	0.53158	−0.00288	0.55305
$\dot{\theta}_1$	$A_{1,1}$	0.02612	0.90943	0.02432	0.92174
	$A_{1,2}$	0.04841	0.97931	0.04458	0.98509
$\dot{\theta}_2$	$A_{2,1}$	0.43232	−0.24231	0.43764	−0.23986
	$A_{2,2}$	0.43512	0.79588	0.43810	0.79484
$\dot{\theta}_3$	$A_{3,1}$	0.67073	−0.10894	0.67329	−0.10776
	$A_{3,2}$	0.67316	1.48427	0.67532	1.48346
y_1	$A_{4,1}$	0.01973	−0.04125	0.03504	−0.03530
	$A_{4,2}$	0.01592	0.03541	0.01244	0.04119
y_2	$A_{5,1}$	0.03453	−0.03573	−0.00024	−0.06683
	$A_{5,2}$	0.01242	0.02543	0.02626	−0.00515

Table 5. Membership function parameters of second Controller

Input	Fuzzy Set	T-S FLC 1 Parameters a	T-S FLC 1 Parameters c	T-S FLC 2 Parameters a	T-S FLC 2 Parameters c
θ_1	$A_{1,1}$	0.11912	−0.26805	0.04926	−0.31383
	$A_{1,2}$	0.04469	−0.05091	0.07628	−0.10665
θ_2	$A_{2,1}$	0.00209	0.43179	0.02466	0.43144
	$A_{2,2}$	0.03183	0.49398	0.02314	0.49563
θ_3	$A_{3,1}$	0.01710	0.51069	0.01704	0.50994
	$A_{3,2}$	0.00148	0.55181	−0.00160	0.54978
$\dot{\theta}_1$	$A_{1,1}$	0.15245	0.45236	0.19035	0.47829
	$A_{1,2}$	0.19932	0.92833	0.18665	0.94280
$\dot{\theta}_2$	$A_{2,1}$	0.46471	−0.36901	0.47436	−0.36670
	$A_{2,2}$	0.46829	0.76003	0.47100	0.75723
$\dot{\theta}_3$	$A_{3,1}$	0.04614	−0.23211	0.09284	−0.19973
	$A_{3,2}$	0.08043	−0.01404	0.07787	0.00310
y_1	$A_{4,1}$	−0.00075	−0.00595	0.01248	0.00329
	$A_{4,2}$	0.01384	0.02182	−0.00078	0.03306
y_2	$A_{5,1}$	0.01796	−0.08025	0.01307	−0.06672
	$A_{5,2}$	0.00909	−0.02957	0.01867	−0.00895

Table 6. Membership function parameters of third Controller

Input	Fuzzy Set	T-S FLC 1 Parameters a	T-S FLC 1 Parameters c	T-S FLC 2 Parameters a	T-S FLC 2 Parameters c
θ_1	$A_{1,1}$	0.13746	−0.10592	0.13768	−0.10662
	$A_{1,2}$	0.13887	0.22189	0.14065	0.22035
θ_2	$A_{2,1}$	0.23348	−0.07858	0.23411	−0.07802
	$A_{2,2}$	0.23356	0.47241	0.23311	0.47289
θ_3	$A_{3,1}$	0.00812	0.50028	0.00461	0.49942
	$A_{3,2}$	0.01100	0.51772	0.01351	0.51900
$\dot{\theta}_1$	$A_{1,1}$	0.22045	0.42482	0.21962	0.42427
	$A_{1,2}$	0.21908	0.94333	0.21921	0.94308
$\dot{\theta}_2$	$A_{2,1}$	0.69502	−2.00380	0.69503	−2.00372
	$A_{2,2}$	0.69512	−0.36665	0.69490	−0.36648
$\dot{\theta}_3$	$A_{3,1}$	0.02408	−0.03254	0.02631	−0.03178
	$A_{3,2}$	0.03000	0.03532	0.02974	0.03535
y_1	$A_{4,1}$	0.00061	0.00626	−0.00204	0.01551
	$A_{4,2}$	−0.00696	0.00520	−0.00870	0.00277
y_2	$A_{5,1}$	0.00253	−0.01839	−0.00363	−0.00373
	$A_{5,2}$	0.00774	0.00191	-6.53×10^{-5}	0.00076

Table 7. Membership function parameters of fourth Controller

Input	Fuzzy Set	T-S FLC 1 Parameters a	T-S FLC 1 Parameters c	T-S FLC 2 Parameters a	T-S FLC 2 Parameters c
θ_1	$A_{1,1}$	0.07507	0.22460	0.08552	0.23442
	$A_{1,2}$	0.07136	0.39446	0.03315	0.41950
θ_2	$A_{2,1}$	0.13168	−0.39218	0.12745	−0.39340
	$A_{2,2}$	0.12964	−0.07554	0.12509	−0.07315
θ_3	$A_{3,1}$	−0.01008	0.48029	0.00837	0.48193
	$A_{3,2}$	0.01417	0.51326	0.00808	0.50781
$\dot{\theta}_1$	$A_{1,1}$	0.25863	0.94355	0.25958	0.94432
	$A_{1,2}$	0.25689	1.55087	0.25120	1.55362
$\dot{\theta}_2$	$A_{2,1}$	0.14937	−2.34638	0.15849	−2.34355
	$A_{2,2}$	0.14704	−2.00387	0.14260	−2.00340
$\dot{\theta}_3$	$A_{3,1}$	0.16569	−0.43464	0.14283	−0.44816
	$A_{3,2}$	0.17196	−0.03286	0.17654	−0.03871
y_1	$A_{4,1}$	−0.00826	−0.00474	−0.00815	−0.00371
	$A_{4,2}$	−0.00034	−0.00333	−0.00145	−0.00814
y_2	$A_{5,1}$	−0.00932	0.00284	0.00288	0.00011
	$A_{5,2}$	−0.00032	0.00309	0.00189	0.01339

Consequent Parameters

This subsection presents the consequent parameters of the controller explained in the section 4. In Tables 8 to 13 provide the consequent parameters of 151 rules of the first controller.

Table 8. Consequent parameters of the Controller 1 - T-S FLC 1 (1 of 3)

R^l	$p_{1,1}$	$p_{1,2}$	$p_{1,3}$	$p_{1,4}$	$p_{1,5}$
R^1	-2.36×10^{-10}	2.36×10^{-10}	2.98×10^{-10}	5.55×10^{-10}	-1.48×10^{-10}
R^2	-5.26×10^{-11}	5.26×10^{-11}	6.65×10^{-11}	1.24×10^{-10}	-3.29×10^{-11}
R^3	-1.55×10^{-15}	1.55×10^{-15}	1.95×10^{-15}	3.64×10^{-15}	-9.93×10^{-16}
R^4	-3.60×10^{-16}	3.60×10^{-16}	4.54×10^{-16}	8.47×10^{-16}	-2.28×10^{-16}
R^5	-4.06×10^{-09}	4.07×10^{-09}	5.13×10^{-09}	9.57×10^{-09}	-2.54×10^{-09}
R^6	-9.00×10^{-10}	9.00×10^{-10}	1.14×10^{-09}	2.12×10^{-09}	-5.61×10^{-10}
R^7	-2.71×10^{-14}	2.71×10^{-14}	3.42×10^{-14}	6.38×10^{-14}	-1.73×10^{-14}
R^8	-6.23×10^{-15}	6.23×10^{-15}	7.87×10^{-15}	1.47×10^{-14}	-3.93×10^{-15}
R^9	-1.33×10^{-11}	1.33×10^{-11}	1.68×10^{-11}	3.13×10^{-11}	-8.40×10^{-12}
R^{10}	-2.30×10^{-12}	3.00×10^{-12}	3.79×10^{-12}	7.07×10^{-12}	-1.88×10^{-12}
R^{11}	-8.42×10^{-17}	8.42×10^{-17}	1.06×10^{-16}	1.98×10^{-16}	-5.47×10^{-17}
R^{12}	-2.00×10^{-17}	2.00×10^{-17}	2.53×10^{-17}	4.72×10^{-17}	-1.28×10^{-17}
R^{13}	-2.30×10^{-10}	2.30×10^{-10}	2.90×10^{-10}	5.41×10^{-10}	-1.45×10^{-10}
R^{14}	-5.15×10^{-11}	5.15×10^{-11}	6.51×10^{-11}	1.21×10^{-10}	-3.22×10^{-11}
R^{15}	-1.49×10^{-15}	1.49×10^{-15}	1.88×10^{-15}	3.51×10^{-15}	-9.61×10^{-16}
R^{16}	-3.49×10^{-16}	3.49×10^{-16}	4.41×10^{-16}	8.23×10^{-16}	-2.22×10^{-16}
R^{17}	-1.57×10^{-10}	1.57×10^{-10}	1.98×10^{-10}	3.69×10^{-10}	-9.91×10^{-11}
R^{18}	-3.54×10^{-11}	3.54×10^{-11}	4.47×10^{-11}	8.34×10^{-11}	-2.22×10^{-11}
R^{19}	-9.98×10^{-16}	9.97×10^{-16}	1.26×10^{-15}	2.35×10^{-15}	-6.48×10^{-16}
R^{20}	-2.37×10^{-16}	2.37×10^{-16}	2.99×10^{-16}	5.58×10^{-16}	-1.51×10^{-16}
R^{21}	-2.71×10^{-09}	2.71×10^{-09}	3.42×10^{-09}	6.39×10^{-09}	-1.71×10^{-09}
R^{22}	-6.07×10^{-10}	6.07×10^{-10}	7.67×10^{-10}	1.43×10^{-09}	-3.79×10^{-10}
R^{23}	-1.76×10^{-14}	1.76×10^{-14}	2.23×10^{-14}	4.15×10^{-14}	-1.14×10^{-14}
R^{24}	-4.13×10^{-15}	4.12×10^{-15}	5.21×10^{-15}	9.72×10^{-15}	-2.62×10^{-15}
R^{25}	-8.75×10^{-12}	8.74×10^{-12}	1.10×10^{-11}	2.06×10^{-11}	-5.57×10^{-12}
R^{26}	-2.00×10^{-12}	2.00×10^{-12}	2.53×10^{-12}	4.72×10^{-12}	-1.26×10^{-12}
R^{27}	-5.35×10^{-17}	5.34×10^{-17}	6.74×10^{-17}	1.26×10^{-16}	-3.52×10^{-17}
R^{28}	-1.30×10^{-17}	1.30×10^{-17}	1.65×10^{-17}	3.07×10^{-17}	-8.40×10^{-18}
R^{29}	-1.52×10^{-10}	1.52×10^{-10}	1.92×10^{-10}	3.59×10^{-10}	-9.65×10^{-11}
R^{30}	-3.45×10^{-11}	3.45×10^{-11}	4.36×10^{-11}	8.14×10^{-11}	-2.17×10^{-11}
R^{31}	-9.57×10^{-16}	9.56×10^{-16}	1.21×10^{-15}	2.25×10^{-15}	-6.24×10^{-16}
R^{32}	-2.29×10^{-16}	2.29×10^{-16}	2.89×10^{-16}	5.40×10^{-16}	-1.47×10^{-16}
R^{33}	3.01×10^{-01}	-3.04×10^{-01}	-3.89×10^{-01}	-7.27×10^{-01}	9.32×10^{-02}
R^{34}	1.65×10^{-01}	-1.63×10^{-01}	-2.02×10^{-01}	-3.75×10^{-01}	1.82×10^{-01}
R^{35}	7.07×10^{-02}	-9.53×10^{-02}	-1.20×10^{-01}	-2.14×10^{-01}	-1.65×10^{-01}
R^{36}	9.21×10^{-07}	-8.66×10^{-07}	-1.02×10^{-06}	-1.88×10^{-06}	2.24×10^{-06}
R^{37}	4.66×10^{-00}	-4.66×10^{-00}	-5.80×10^{-00}	-10.8×10^{-00}	4.25×10^{-00}
R^{38}	4.42×10^{-00}	-4.40×10^{-00}	-5.52×10^{-00}	-10.3×10^{-00}	3.57×10^{-00}
R^{39}	1.38×10^{-02}	-1.66×10^{-02}	-2.14×10^{-02}	-3.92×10^{-02}	-2.38×10^{-02}
R^{40}	1.89×10^{-05}	-1.91×10^{-05}	-2.50×10^{-05}	-4.70×10^{-05}	-2.90×10^{-06}
R^{41}	9.66×10^{-02}	-1.06×10^{-01}	-1.39×10^{-01}	-2.60×10^{-01}	-1.11×10^{-01}
R^{42}	8.36×10^{-04}	-8.38×10^{-04}	-9.49×10^{-04}	-1.71×10^{-03}	2.20×10^{-03}
R^{43}	9.81×10^{-01}	-1.32×10^{-00}	-1.66×10^{-00}	-2.98×10^{-00}	-2.31×10^{-00}
R^{44}	1.55×10^{-07}	-2.21×10^{-07}	-3.18×10^{-07}	-5.99×10^{-07}	-1.15×10^{-06}
R^{45}	3.71×10^{-01}	-3.77×10^{-01}	-4.81×10^{-01}	-8.99×10^{-01}	9.85×10^{-01}
R^{46}	9.93×10^{-02}	-9.79×10^{-02}	-1.19×10^{-01}	-2.21×10^{-01}	1.42×10^{-01}
R^{47}	1.27×10^{-01}	-1.64×10^{-01}	-2.09×10^{-01}	-3.79×10^{-01}	-2.87×10^{-01}
R^{48}	-1.17×10^{-06}	1.24×10^{-06}	1.77×10^{-06}	3.41×10^{-06}	3.24×10^{-06}
R^{49}	2.46×10^{-00}	-2.62×10^{-00}	-3.46×10^{-00}	-6.49×10^{-00}	-2.28×10^{-00}
R^{50}	3.98×10^{-02}	-3.98×10^{-02}	-4.93×10^{-02}	-9.14×10^{-02}	4.05×10^{-02}
R^{51}	2.25×10^{-00}	-2.65×10^{-00}	-3.45×10^{-00}	-6.36×10^{-00}	-3.84×10^{-00}

Table 9. Consequent parameters of the Controller 1 - T-S FLC 1 (cont. 1 of 3)

R^l	$p_{1,6}$	$p_{1,7}$	$p_{1,8}$	$p_{1,9}$
R^1	8.95×10^{-10}	-2.53×10^{-11}	2.17×10^{-13}	6.00×10^{-10}
R^2	2.00×10^{-10}	-5.65×10^{-12}	3.65×10^{-14}	1.34×10^{-10}
R^3	5.89×10^{-15}	-1.67×10^{-16}	2.40×10^{-18}	3.93×10^{-15}
R^4	1.37×10^{-15}	-3.88×10^{-17}	4.06×10^{-19}	9.15×10^{-16}
R^5	1.54×10^{-08}	-4.36×10^{-10}	3.35×10^{-12}	1.03×10^{-08}
R^6	3.41×10^{-09}	-9.66×10^{-11}	5.62×10^{-13}	2.29×10^{-09}
R^7	1.03×10^{-13}	-2.93×10^{-15}	3.70×10^{-17}	6.90×10^{-14}
R^8	2.37×10^{-14}	-6.71×10^{-16}	6.26×10^{-18}	1.59×10^{-14}
R^9	5.04×10^{-11}	-1.43×10^{-12}	1.46×10^{-14}	3.38×10^{-11}
R^{10}	1.14×10^{-11}	-3.22×10^{-13}	2.47×10^{-15}	7.63×10^{-12}
R^{11}	3.22×10^{-16}	-9.15×10^{-18}	1.60×10^{-19}	2.14×10^{-16}
R^{12}	7.63×10^{-17}	-2.16×10^{-18}	2.73×10^{-20}	5.10×10^{-17}
R^{13}	8.72×10^{-10}	-2.47×10^{-11}	2.25×10^{-13}	5.85×10^{-10}
R^{14}	1.95×10^{-10}	-5.53×10^{-12}	3.79×10^{-14}	1.31×10^{-10}
R^{15}	5.68×10^{-15}	-1.62×10^{-16}	2.49×10^{-18}	3.79×10^{-15}
R^{16}	1.33×10^{-15}	-3.77×10^{-17}	4.21×10^{-19}	8.89×10^{-16}
R^{17}	5.95×10^{-10}	-1.69×10^{-11}	1.70×10^{-13}	3.99×10^{-10}
R^{18}	1.34×10^{-10}	-3.80×10^{-12}	2.86×10^{-14}	9.00×10^{-11}
R^{19}	3.81×10^{-15}	-1.08×10^{-16}	1.86×10^{-18}	2.54×10^{-15}
R^{20}	9.01×10^{-16}	-2.58×10^{-17}	3.17×10^{-19}	6.03×10^{-16}
R^{21}	1.03×10^{-08}	-2.92×10^{-10}	2.61×10^{-12}	6.90×10^{-09}
R^{22}	2.30×10^{-09}	-6.52×10^{-11}	4.40×10^{-13}	1.55×10^{-09}
R^{23}	6.72×10^{-14}	-1.91×10^{-15}	2.88×10^{-17}	4.49×10^{-14}
R^{24}	1.57×10^{-14}	-4.45×10^{-16}	4.89×10^{-18}	1.05×10^{-14}
R^{25}	3.33×10^{-11}	-9.44×10^{-13}	1.14×10^{-14}	2.23×10^{-11}
R^{26}	7.61×10^{-12}	-2.16×10^{-13}	1.93×10^{-15}	5.10×10^{-12}
R^{27}	2.05×10^{-16}	-5.83×10^{-18}	1.24×10^{-19}	1.36×10^{-16}
R^{28}	4.97×10^{-17}	-1.41×10^{-18}	2.12×10^{-20}	3.32×10^{-17}
R^{29}	5.79×10^{-10}	-1.64×10^{-11}	1.76×10^{-13}	3.88×10^{-10}
R^{30}	1.31×10^{-10}	-3.71×10^{-12}	2.97×10^{-14}	8.79×10^{-11}
R^{31}	3.66×10^{-15}	-1.04×10^{-16}	1.92×10^{-18}	2.44×10^{-15}
R^{32}	8.73×10^{-16}	-2.48×10^{-17}	3.28×10^{-19}	5.83×10^{-16}
R^{33}	-1.05×10^{-00}	2.76×10^{-02}	4.29×10^{-03}	-7.75×10^{-01}
R^{34}	-6.98×10^{-01}	2.15×10^{-02}	-3.83×10^{-03}	-4.14×10^{-01}
R^{35}	-1.65×10^{-02}	-4.40×10^{-03}	1.05×10^{-02}	-2.22×10^{-01}
R^{36}	-5.10×10^{-06}	1.82×10^{-07}	-8.01×10^{-08}	-2.21×10^{-06}
R^{37}	-18.8×10^{-00}	5.64×10^{-01}	-6.52×10^{-02}	-11.8×10^{-00}
R^{38}	-17.5×10^{-00}	5.15×10^{-01}	-4.14×10^{-02}	-11.2×10^{-00}
R^{39}	-1.60×10^{-02}	-2.96×10^{-04}	1.59×10^{-03}	-4.01×10^{-02}
R^{40}	-5.86×10^{-05}	1.32×10^{-06}	6.74×10^{-07}	-4.90×10^{-05}
R^{41}	-1.90×10^{-01}	1.46×10^{-03}	8.20×10^{-03}	-2.66×10^{-01}
R^{42}	-4.61×10^{-03}	1.69×10^{-04}	-7.82×10^{-05}	-2.06×10^{-03}
R^{43}	-1.98×10^{-01}	-6.28×10^{-02}	1.47×10^{-01}	-3.08×10^{-00}
R^{44}	6.88×10^{-07}	-4.82×10^{-08}	6.03×10^{-08}	-5.31×10^{-07}
R^{45}	-1.28×10^{-00}	3.31×10^{-02}	6.10×10^{-03}	-9.57×10^{-01}
R^{46}	-4.50×10^{-01}	1.46×10^{-02}	-3.82×10^{-03}	-2.48×10^{-01}
R^{47}	-5.58×10^{-02}	-6.95×10^{-03}	1.83×10^{-02}	-3.88×10^{-01}
R^{48}	8.12×10^{-07}	6.76×10^{-08}	-1.86×10^{-07}	3.23×10^{-06}
R^{49}	-5.57×10^{-00}	7.03×10^{-02}	1.81×10^{-01}	-6.63×10^{-00}
R^{50}	-1.65×10^{-01}	5.01×10^{-03}	-7.52×10^{-04}	-1.01×10^{-01}
R^{51}	-2.81×10^{-00}	-4.16×10^{-02}	2.56×10^{-01}	-6.48×10^{-00}

Table 10. Consequent parameters of the Controller 1 - T-S FLC 1 (2 of 3)

R^l	$p_{1,1}$	$p_{1,2}$	$p_{1,3}$	$p_{1,4}$	$p_{1,5}$
R^{52}	2.05×10^{-05}	-2.16×10^{-05}	-2.89×10^{-05}	-5.45×10^{-05}	-2.30×10^{-05}
R^{53}	5.85×10^{-00}	-6.08×10^{-00}	-7.87×10^{-00}	-14.7×10^{-00}	-1.60×10^{-00}
R^{54}	1.44×10^{-00}	-1.43×10^{-00}	-1.76×10^{-00}	-3.27×10^{-00}	1.62×10^{-00}
R^{55}	1.05×10^{-00}	-1.20×10^{-00}	-1.58×10^{-00}	-2.95×10^{-00}	-1.83×10^{-00}
R^{56}	-2.44×10^{-06}	3.36×10^{-07}	-2.68×10^{-08}	2.09×10^{-07}	-2.93×10^{-05}
R^{57}	5.32×10^{-00}	-5.98×10^{-00}	-7.88×10^{-00}	-14.7×10^{-00}	-8.07×10^{-00}
R^{58}	3.09×10^{-03}	-3.07×10^{-03}	-3.91×10^{-03}	-7.31×10^{-03}	1.66×10^{-03}
R^{59}	4.43×10^{-00}	-7.27×10^{-00}	-7.81×10^{-00}	-12.49×10^{-00}	1.33×10^{-00}
R^{60}	1.48×10^{-05}	-1.60×10^{-05}	-2.06×10^{-05}	-3.83×10^{-05}	-7.89×10^{-06}
R^{61}	6.12×10^{-00}	-6.52×10^{-00}	-8.58×10^{-00}	-16.1×10^{-00}	-5.52×10^{-00}
R^{62}	3.38×10^{-02}	-3.41×10^{-02}	-4.34×10^{-02}	-8.10×10^{-02}	1.42×10^{-02}
R^{63}	6.65×10^{-00}	-7.32×10^{-00}	-9.77×10^{-00}	-18.3×10^{-00}	-10.4×10^{-00}
R^{64}	5.77×10^{-05}	-5.97×10^{-05}	-7.90×10^{-05}	-1.49×10^{-04}	-3.97×10^{-05}
R^{65}	-4.19×10^{-24}	4.18×10^{-24}	5.29×10^{-24}	9.87×10^{-24}	-2.62×10^{-24}
R^{66}	-9.24×10^{-25}	9.24×10^{-25}	1.17×10^{-24}	2.18×10^{-24}	-5.74×10^{-25}
R^{67}	-2.83×10^{-29}	2.83×10^{-29}	3.57×10^{-29}	6.67×10^{-29}	-1.80×10^{-29}
R^{68}	-6.45×10^{-30}	6.45×10^{-30}	8.15×10^{-30}	1.52×10^{-29}	-4.06×10^{-30}
R^{69}	-7.17×10^{-23}	7.17×10^{-23}	9.06×10^{-23}	1.69×10^{-22}	-4.47×10^{-23}
R^{70}	-1.58×10^{-23}	1.58×10^{-23}	1.99×10^{-23}	3.72×10^{-23}	-9.78×10^{-24}
R^{71}	-4.92×10^{-28}	4.92×10^{-28}	6.21×10^{-28}	1.16×10^{-27}	-3.11×10^{-28}
R^{72}	-1.11×10^{-28}	1.11×10^{-28}	1.40×10^{-28}	2.62×10^{-28}	-6.96×10^{-29}
R^{73}	-2.38×10^{-25}	2.38×10^{-25}	3.00×10^{-25}	5.60×10^{-25}	-1.49×10^{-25}
R^{74}	-5.30×10^{-26}	5.30×10^{-26}	6.70×10^{-26}	1.23×10^{-25}	-3.31×10^{-26}
R^{75}	-1.57×10^{-30}	1.57×10^{-30}	1.98×10^{-30}	3.69×10^{-30}	-1.01×10^{-30}
R^{76}	-3.64×10^{-31}	3.63×10^{-31}	4.59×10^{-31}	8.57×10^{-31}	-2.30×10^{-31}
R^{77}	-4.09×10^{-24}	4.09×10^{-24}	5.17×10^{-24}	9.64×10^{-24}	-2.56×10^{-24}
R^{78}	-9.06×10^{-25}	9.06×10^{-25}	1.14×10^{-24}	2.14×10^{-24}	-5.64×10^{-25}
R^{79}	-2.74×10^{-29}	2.74×10^{-29}	3.46×10^{-29}	6.46×10^{-29}	-1.75×10^{-29}
R^{80}	-6.29×10^{-30}	6.29×10^{-30}	7.94×10^{-30}	1.48×10^{-29}	-3.96×10^{-30}
R^{81}	-2.80×10^{-24}	2.80×10^{-24}	3.54×10^{-24}	6.61×10^{-24}	-1.76×10^{-24}
R^{82}	-6.25×10^{-25}	6.24×10^{-25}	7.89×10^{-25}	1.47×10^{-24}	-3.89×10^{-25}
R^{83}	-1.85×10^{-29}	1.85×10^{-29}	2.34×10^{-29}	4.37×10^{-29}	-1.19×10^{-29}
R^{84}	-4.29×10^{-30}	4.29×10^{-30}	5.42×10^{-30}	1.01×10^{-29}	-2.71×10^{-30}
R^{85}	-4.82×10^{-23}	4.82×10^{-23}	6.09×10^{-23}	1.14×10^{-22}	-3.02×10^{-23}
R^{86}	-1.07×10^{-23}	1.07×10^{-23}	1.35×10^{-23}	2.52×10^{-23}	-6.64×10^{-24}
R^{87}	-3.24×10^{-28}	3.24×10^{-28}	4.09×10^{-28}	7.64×10^{-28}	-2.07×10^{-28}
R^{88}	-7.42×10^{-29}	7.42×10^{-29}	9.37×10^{-29}	1.75×10^{-28}	-4.67×10^{-29}
R^{89}	-1.58×10^{-25}	1.58×10^{-25}	2.00×10^{-25}	3.73×10^{-25}	-10.00×10^{-26}
R^{90}	-3.56×10^{-26}	3.56×10^{-26}	4.50×10^{-26}	8.40×10^{-26}	-2.23×10^{-26}
R^{91}	-1.02×10^{-30}	1.01×10^{-30}	1.28×10^{-30}	2.39×10^{-30}	-6.57×10^{-31}
R^{92}	-2.40×10^{-31}	2.40×10^{-31}	3.03×10^{-31}	5.65×10^{-31}	-1.53×10^{-31}
R^{93}	-2.74×10^{-24}	2.73×10^{-24}	3.45×10^{-24}	6.45×10^{-24}	-1.72×10^{-24}
R^{94}	-6.11×10^{-25}	6.11×10^{-25}	7.72×10^{-25}	1.44×10^{-24}	-3.82×10^{-25}
R^{95}	-1.79×10^{-29}	1.79×10^{-29}	2.26×10^{-29}	4.22×10^{-29}	-1.15×10^{-29}
R^{96}	-4.17×10^{-30}	4.17×10^{-30}	5.27×10^{-30}	9.83×10^{-30}	-2.64×10^{-30}
R^{97}	1.61×10^{-04}	-2.33×10^{-04}	-2.86×10^{-04}	-5.03×10^{-04}	-4.08×10^{-04}
R^{98}	1.99×10^{-12}	-2.66×10^{-12}	-3.37×10^{-12}	-6.11×10^{-12}	-5.21×10^{-12}
R^{99}	3.16×10^{-02}	-4.69×10^{-02}	-5.69×10^{-02}	-9.94×10^{-02}	-8.04×10^{-02}
R^{100}	3.72×10^{-10}	-4.89×10^{-10}	-6.23×10^{-10}	-1.14×10^{-09}	-9.88×10^{-10}
R^{101}	1.21×10^{-05}	-1.72×10^{-05}	-2.12×10^{-05}	-3.75×10^{-05}	-3.04×10^{-05}

Table 11. Consequent parameters of the Controller 1 - T-S FLC 1 (cont. 2 of 3)

R^l	$p_{1,6}$	$p_{1,7}$	$p_{1,8}$	$p_{1,9}$
R^{52}	-4.34×10^{-05}	4.09×10^{-07}	1.69×10^{-06}	-5.51×10^{-05}
R^{53}	-16.9×10^{-00}	3.59×10^{-01}	2.48×10^{-01}	-15.4×10^{-00}
R^{54}	-6.11×10^{-00}	1.89×10^{-01}	-3.49×10^{-02}	-3.61×10^{-00}
R^{55}	-1.40×10^{-00}	-1.77×10^{-02}	1.20×10^{-01}	-2.96×10^{-00}
R^{56}	3.96×10^{-05}	-1.76×10^{-06}	1.37×10^{-06}	2.41×10^{-06}
R^{57}	-8.41×10^{-00}	-2.37×10^{-02}	5.48×10^{-01}	-14.9×10^{-00}
R^{58}	-1.15×10^{-02}	3.20×10^{-04}	9.54×10^{-06}	-7.85×10^{-03}
R^{59}	-7.79×10^{-00}	1.72×10^{-01}	1.57×10^{-01}	-15.4×10^{-00}
R^{60}	-3.81×10^{-05}	6.84×10^{-07}	8.25×10^{-07}	-4.00×10^{-05}
R^{61}	-13.9×10^{-00}	1.81×10^{-01}	4.43×10^{-01}	-16.5×10^{-00}
R^{62}	-1.21×10^{-01}	3.27×10^{-03}	3.10×10^{-04}	-8.68×10^{-02}
R^{63}	-10.7×10^{-00}	-3.12×10^{-02}	6.95×10^{-01}	-18.4×10^{-00}
R^{64}	-1.48×10^{-04}	2.45×10^{-06}	3.54×10^{-06}	-1.53×10^{-04}
R^{65}	1.59×10^{-23}	-4.49×10^{-25}	3.15×10^{-27}	1.07×10^{-23}
R^{66}	3.50×10^{-24}	-9.91×10^{-26}	5.28×10^{-28}	2.35×10^{-24}
R^{67}	1.08×10^{-28}	-3.05×10^{-30}	3.49×10^{-32}	7.20×10^{-29}
R^{68}	2.45×10^{-29}	-6.94×10^{-31}	5.90×10^{-33}	1.64×10^{-29}
R^{69}	2.72×10^{-22}	-7.70×10^{-24}	4.84×10^{-26}	1.83×10^{-22}
R^{70}	5.97×10^{-23}	-1.69×10^{-24}	8.09×10^{-27}	4.01×10^{-23}
R^{71}	1.87×10^{-27}	-5.30×10^{-29}	5.38×10^{-31}	1.25×10^{-27}
R^{72}	4.22×10^{-28}	-1.19×10^{-29}	9.08×10^{-32}	2.83×10^{-28}
R^{73}	9.03×10^{-25}	-2.56×10^{-26}	2.12×10^{-28}	6.05×10^{-25}
R^{74}	2.01×10^{-25}	-5.69×10^{-27}	3.57×10^{-29}	1.35×10^{-25}
R^{75}	5.97×10^{-30}	-1.70×10^{-31}	2.34×10^{-33}	3.99×10^{-30}
R^{76}	1.38×10^{-30}	-3.92×10^{-32}	3.97×10^{-34}	9.25×10^{-31}
R^{77}	1.55×10^{-23}	-4.39×10^{-25}	3.27×10^{-27}	1.04×10^{-23}
R^{78}	3.44×10^{-24}	-9.72×10^{-26}	5.48×10^{-28}	2.31×10^{-24}
R^{79}	1.04×10^{-28}	-2.96×10^{-30}	3.61×10^{-32}	6.98×10^{-29}
R^{80}	2.39×10^{-29}	-6.77×10^{-31}	6.12×10^{-33}	1.60×10^{-29}
R^{81}	1.06×10^{-23}	-3.01×10^{-25}	2.46×10^{-27}	7.14×10^{-24}
R^{82}	2.37×10^{-24}	-6.70×10^{-26}	4.14×10^{-28}	1.59×10^{-24}
R^{83}	7.06×10^{-29}	-2.01×10^{-30}	2.72×10^{-32}	4.72×10^{-29}
R^{84}	1.63×10^{-29}	-4.62×10^{-31}	4.61×10^{-33}	1.09×10^{-29}
R^{85}	1.83×10^{-22}	-5.18×10^{-24}	3.79×10^{-26}	1.23×10^{-22}
R^{86}	4.05×10^{-23}	-1.14×10^{-24}	6.35×10^{-27}	2.72×10^{-23}
R^{87}	1.23×10^{-27}	-3.50×10^{-29}	4.20×10^{-31}	8.25×10^{-28}
R^{88}	2.82×10^{-28}	-7.99×10^{-30}	7.10×10^{-32}	1.89×10^{-28}
R^{89}	6.01×10^{-25}	-1.70×10^{-26}	1.66×10^{-28}	4.03×10^{-25}
R^{90}	1.35×10^{-25}	-3.83×10^{-27}	2.79×10^{-29}	9.07×10^{-26}
R^{91}	3.87×10^{-30}	-1.10×10^{-31}	1.82×10^{-33}	2.58×10^{-30}
R^{92}	9.12×10^{-31}	-2.59×10^{-32}	3.09×10^{-34}	6.10×10^{-31}
R^{93}	1.04×10^{-23}	-2.94×10^{-25}	2.55×10^{-27}	6.96×10^{-24}
R^{94}	2.33×10^{-24}	-6.56×10^{-26}	4.29×10^{-28}	1.56×10^{-24}
R^{95}	6.82×10^{-29}	-1.94×10^{-30}	2.81×10^{-32}	4.56×10^{-29}
R^{96}	1.59×10^{-29}	-4.50×10^{-31}	4.77×10^{-33}	1.06×10^{-29}
R^{97}	3.23×10^{-05}	-1.27×10^{-05}	2.58×10^{-05}	-5.29×10^{-04}
R^{98}	-3.25×10^{-14}	-1.48×10^{-13}	3.20×10^{-13}	-6.21×10^{-12}
R^{99}	9.58×10^{-03}	-2.61×10^{-03}	5.12×10^{-03}	-1.05×10^{-01}
R^{100}	-1.01×10^{-11}	-2.78×10^{-11}	6.02×10^{-11}	-1.15×10^{-09}
R^{101}	1.72×10^{-06}	-9.30×10^{-07}	1.92×10^{-06}	-3.92×10^{-05}

Table 12. Consequent parameters of the Controller 1 - T-S FLC 1 (3 of 3)

R^l	$p_{1,1}$	$p_{1,2}$	$p_{1,3}$	$p_{1,4}$	$p_{1,5}$
R^{102}	2.35×10^{-13}	-2.98×10^{-13}	-3.74×10^{-13}	-6.76×10^{-13}	-4.01×10^{-13}
R^{103}	2.13×10^{-03}	-3.12×10^{-03}	-3.80×10^{-03}	-6.65×10^{-03}	-5.36×10^{-03}
R^{104}	3.11×10^{-11}	-4.27×10^{-11}	-5.35×10^{-11}	-9.60×10^{-11}	-8.11×10^{-11}
R^{105}	2.47×10^{-04}	-3.58×10^{-03}	-4.38×10^{-04}	-7.71×10^{-03}	-6.21×10^{-03}
R^{106}	3.96×10^{-11}	-5.53×10^{-11}	-6.88×10^{-11}	-1.27×10^{-10}	-1.02×10^{-10}
R^{107}	4.53×10^{-01}	-6.78×10^{-01}	-8.19×10^{-01}	-1.43×10^{-00}	-1.14×10^{-00}
R^{108}	7.78×10^{-09}	-1.09×10^{-08}	-1.35×10^{-08}	-2.41×10^{-08}	-2.02×10^{-08}
R^{109}	1.93×10^{-04}	-2.73×10^{-04}	-3.37×10^{-04}	-5.97×10^{-04}	-4.83×10^{-04}
R^{110}	3.08×10^{-12}	-4.34×10^{-12}	-5.37×10^{-12}	-9.55×10^{-12}	-7.88×10^{-12}
R^{111}	3.10×10^{-02}	-4.53×10^{-02}	-5.52×10^{-02}	-9.68×10^{-02}	-7.73×10^{-02}
R^{112}	5.79×10^{-10}	-8.20×10^{-10}	-1.01×10^{-09}	-1.80×10^{-09}	-1.49×10^{-09}
R^{113}	1.15×10^{-03}	-1.61×10^{-03}	-2.00×10^{-03}	-3.56×10^{-03}	-2.96×10^{-03}
R^{114}	1.35×10^{-11}	-1.91×10^{-11}	-2.36×10^{-11}	-4.18×10^{-11}	-3.45×10^{-11}
R^{115}	1.96×10^{-01}	-2.69×10^{-01}	-3.36×10^{-01}	-6.02×10^{-01}	-4.98×10^{-01}
R^{116}	2.40×10^{-09}	-3.38×10^{-09}	-4.18×10^{-09}	-7.43×10^{-09}	-6.12×10^{-09}
R^{117}	8.52×10^{-05}	-1.22×10^{-04}	-1.50×10^{-04}	-2.65×10^{-04}	-2.21×10^{-04}
R^{118}	1.05×10^{-12}	-1.47×10^{-12}	-1.82×10^{-12}	-3.22×10^{-12}	-2.55×10^{-12}
R^{119}	1.67×10^{-02}	-2.32×10^{-02}	-2.88×10^{-02}	-5.15×10^{-02}	-4.28×10^{-02}
R^{120}	1.92×10^{-10}	-2.70×10^{-10}	-3.34×10^{-10}	-5.94×10^{-10}	-4.91×10^{-10}
R^{121}	2.12×10^{-02}	-2.97×10^{-02}	-3.69×10^{-02}	-6.57×10^{-02}	-5.47×10^{-02}
R^{122}	2.38×10^{-10}	-3.36×10^{-10}	-4.16×10^{-10}	-7.38×10^{-10}	-6.11×10^{-10}
R^{123}	3.66×10^{-00}	-5.00×10^{-00}	-6.26×10^{-00}	-11.2×10^{-00}	-9.31×10^{-00}
R^{124}	4.24×10^{-08}	-5.92×10^{-08}	-7.36×10^{-08}	-1.31×10^{-07}	-1.08×10^{-07}
R^{125}	1.55×10^{-03}	-2.22×10^{-03}	-2.73×10^{-03}	-4.83×10^{-03}	-4.03×10^{-03}
R^{126}	1.75×10^{-11}	-2.50×10^{-11}	-3.08×10^{-11}	-5.45×10^{-11}	-4.52×10^{-11}
R^{127}	3.12×10^{-01}	-4.33×10^{-01}	-5.39×10^{-01}	-9.63×10^{-01}	-8.01×10^{-01}
R^{128}	3.42×10^{-09}	-4.80×10^{-09}	-5.95×10^{-09}	-1.06×10^{-08}	-8.76×10^{-09}
R^{129}	-6.95×10^{-18}	6.95×10^{-18}	8.77×10^{-18}	1.64×10^{-17}	-4.41×10^{-18}
R^{130}	-1.58×10^{-18}	1.58×10^{-18}	2.00×10^{-18}	3.73×10^{-18}	-9.94×10^{-19}
R^{131}	-4.32×10^{-23}	4.32×10^{-23}	5.45×10^{-23}	1.02×10^{-22}	-2.83×10^{-23}
R^{132}	-1.04×10^{-23}	1.04×10^{-23}	1.32×10^{-23}	2.46×10^{-23}	-6.69×10^{-24}
R^{133}	-1.21×10^{-16}	1.21×10^{-16}	1.52×10^{-16}	2.84×10^{-16}	-7.63×10^{-17}
R^{134}	-2.72×10^{-17}	2.72×10^{-17}	3.44×10^{-17}	6.42×10^{-17}	-1.71×10^{-17}
R^{135}	-7.70×10^{-22}	7.69×10^{-22}	9.71×10^{-22}	1.81×10^{-21}	-4.99×10^{-22}
R^{136}	-1.83×10^{-22}	1.82×10^{-22}	2.30×10^{-22}	4.30×10^{-22}	-1.16×10^{-22}
R^{137}	-3.86×10^{-19}	3.85×10^{-19}	4.87×10^{-19}	9.08×10^{-19}	-2.47×10^{-19}
R^{138}	-8.92×10^{-20}	8.92×10^{-20}	1.13×10^{-19}	2.10×10^{-19}	-5.64×10^{-20}
R^{139}	-2.28×10^{-24}	2.28×10^{-24}	2.88×10^{-24}	5.37×10^{-24}	-1.52×10^{-24}
R^{140}	-5.69×10^{-25}	5.69×10^{-25}	7.18×10^{-25}	1.34×10^{-24}	-3.69×10^{-25}
R^{141}	-6.74×10^{-18}	6.74×10^{-18}	8.51×10^{-18}	1.59×10^{-17}	-4.29×10^{-18}
R^{142}	-1.54×10^{-18}	1.54×10^{-18}	1.95×10^{-18}	3.64×10^{-18}	-9.72×10^{-19}
R^{143}	-4.13×10^{-23}	4.12×10^{-23}	5.20×10^{-23}	9.71×10^{-23}	-2.72×10^{-23}
R^{144}	-1.01×10^{-23}	1.01×10^{-23}	1.27×10^{-23}	2.37×10^{-23}	-6.48×10^{-24}
R^{145}	-4.56×10^{-18}	4.56×10^{-18}	5.75×10^{-18}	1.07×10^{-17}	-2.92×10^{-18}
R^{146}	-1.05×10^{-18}	1.05×10^{-18}	1.33×10^{-18}	2.48×10^{-18}	-6.65×10^{-19}
R^{147}	-2.71×10^{-23}	2.71×10^{-23}	3.42×10^{-23}	6.38×10^{-23}	-1.80×10^{-23}
R^{148}	-6.74×10^{-24}	6.74×10^{-24}	8.51×10^{-24}	1.59×10^{-23}	-4.37×10^{-24}
R^{149}	-7.97×10^{-17}	7.96×10^{-17}	1.01×10^{-16}	1.88×10^{-16}	-5.07×10^{-17}
R^{150}	-1.82×10^{-17}	1.82×10^{-17}	2.30×10^{-17}	4.29×10^{-17}	-1.15×10^{-17}
R^{151}	-4.90×10^{-22}	4.89×10^{-22}	6.17×10^{-22}	1.15×10^{-21}	-3.22×10^{-22}

Table 13. Consequent parameters of the Controller 1 - T-S FLC 1 (cont. 3 of 3)

R^l	$p_{1,6}$	$p_{1,7}$	$p_{1,8}$	$p_{1,9}$
R^{102}	-2.35×10^{-13}	-5.98×10^{-15}	2.73×10^{-14}	-7.04×10^{-13}
R^{103}	5.05×10^{-04}	-1.70×10^{-04}	3.42×10^{-04}	-7.03×10^{-03}
R^{104}	2.34×10^{-12}	-2.39×10^{-12}	5.02×10^{-12}	-9.86×10^{-11}
R^{105}	4.37×10^{-04}	-1.93×10^{-04}	3.94×10^{-04}	-8.11×10^{-03}
R^{106}	4.52×10^{-12}	-3.07×10^{-12}	6.38×10^{-12}	-1.27×10^{-10}
R^{107}	1.43×10^{-01}	-3.72×10^{-02}	7.30×10^{-02}	-1.52×10^{-00}
R^{108}	1.14×10^{-09}	-6.13×10^{-10}	1.26×10^{-09}	-2.50×10^{-08}
R^{109}	1.96×10^{-05}	-1.46×10^{-05}	3.05×10^{-05}	-6.24×10^{-04}
R^{110}	3.68×10^{-13}	-2.38×10^{-13}	4.93×10^{-13}	-9.93×10^{-12}
R^{111}	6.43×10^{-03}	-2.43×10^{-03}	4.93×10^{-03}	-1.02×10^{-01}
R^{112}	9.48×10^{-11}	-4.56×10^{-11}	9.33×10^{-11}	-1.87×10^{-09}
R^{113}	1.36×10^{-04}	-8.89×10^{-05}	1.85×10^{-04}	-3.69×10^{-03}
R^{114}	1.89×10^{-12}	-1.05×10^{-12}	2.16×10^{-12}	-4.35×10^{-11}
R^{115}	7.18×10^{-04}	-1.44×10^{-02}	3.10×10^{-02}	-6.22×10^{-02}
R^{116}	2.06×10^{-10}	-1.82×10^{-10}	3.83×10^{-10}	-7.72×10^{-09}
R^{117}	1.74×10^{-05}	-6.85×10^{-06}	1.38×10^{-05}	-2.77×10^{-04}
R^{118}	1.05×10^{-14}	-7.44×10^{-14}	1.61×10^{-13}	-3.37×10^{-12}
R^{119}	1.16×10^{-03}	-1.26×10^{-03}	2.66×10^{-03}	-5.33×10^{-03}
R^{120}	2.19×10^{-11}	-1.48×10^{-11}	3.07×10^{-11}	-6.18×10^{-10}
R^{121}	2.63×10^{-03}	-1.65×10^{-03}	3.41×10^{-03}	-6.82×10^{-02}
R^{122}	3.41×10^{-11}	-1.86×10^{-11}	3.82×10^{-11}	-7.69×10^{-10}
R^{123}	-2.26×10^{-02}	-2.67×10^{-01}	5.78×10^{-01}	-11.57×10^{-00}
R^{124}	2.98×10^{-09}	-3.20×10^{-09}	6.75×10^{-09}	-1.36×10^{-07}
R^{125}	3.47×10^{-04}	-1.26×10^{-04}	2.52×10^{-04}	-5.04×10^{-04}
R^{126}	3.47×10^{-12}	-1.40×10^{-12}	2.83×10^{-12}	-5.70×10^{-11}
R^{127}	2.22×10^{-02}	-2.37×10^{-02}	4.99×10^{-02}	-9.96×10^{-01}
R^{128}	3.74×10^{-10}	-2.63×10^{-10}	5.47×10^{-10}	-1.10×10^{-08}
R^{129}	2.64×10^{-17}	-7.50×10^{-19}	8.42×10^{-21}	1.77×10^{-17}
R^{130}	6.01×10^{-18}	-1.70×10^{-19}	1.42×10^{-21}	4.03×10^{-18}
R^{131}	1.65×10^{-22}	-4.70×10^{-24}	9.20×10^{-26}	1.10×10^{-22}
R^{132}	3.97×10^{-23}	-1.13×10^{-24}	1.57×10^{-26}	2.65×10^{-23}
R^{133}	4.59×10^{-16}	-1.30×10^{-17}	1.30×10^{-19}	3.07×10^{-16}
R^{134}	1.03×10^{-16}	-2.93×10^{-18}	2.19×10^{-20}	6.93×10^{-17}
R^{135}	2.94×10^{-21}	-8.35×10^{-23}	1.42×10^{-24}	1.96×10^{-21}
R^{136}	6.94×10^{-22}	-1.97×10^{-23}	2.42×10^{-25}	4.64×10^{-22}
R^{137}	1.47×10^{-18}	-4.17×10^{-20}	5.65×10^{-22}	9.81×10^{-19}
R^{138}	3.39×10^{-19}	-9.61×10^{-21}	9.57×10^{-23}	2.27×10^{-19}
R^{139}	8.75×10^{-24}	-2.50×10^{-25}	6.12×10^{-27}	5.80×10^{-24}
R^{140}	2.17×10^{-24}	-6.18×10^{-26}	1.05×10^{-27}	1.45×10^{-24}
R^{141}	2.56×10^{-17}	-7.28×10^{-19}	8.72×10^{-21}	1.72×10^{-17}
R^{142}	5.86×10^{-18}	-1.66×10^{-19}	1.47×10^{-21}	3.93×10^{-18}
R^{143}	1.58×10^{-22}	-4.50×10^{-24}	9.50×10^{-26}	1.05×10^{-22}
R^{144}	3.83×10^{-23}	-1.09×10^{-24}	1.62×10^{-26}	2.56×10^{-23}
R^{145}	1.74×10^{-17}	-4.93×10^{-19}	6.55×10^{-21}	1.16×10^{-17}
R^{146}	4.00×10^{-18}	-1.13×10^{-19}	1.11×10^{-21}	2.68×10^{-18}
R^{147}	1.04×10^{-22}	-2.97×10^{-24}	7.10×10^{-26}	6.90×10^{-23}
R^{148}	2.57×10^{-23}	-7.32×10^{-25}	1.22×10^{-26}	1.72×10^{-23}
R^{149}	3.03×10^{-16}	-8.60×10^{-18}	1.01×10^{-19}	2.03×10^{-16}
R^{150}	6.91×10^{-17}	-1.96×10^{-18}	1.71×10^{-20}	4.63×10^{-17}
R^{151}	1.87×10^{-21}	-5.34×10^{-23}	1.10×10^{-24}	1.25×10^{-21}

References

1. Feedback control of dynamic bipedal robot locomotion book webpage (2007), `http://www.dynamicbipedcontrol.org`
2. Ahtiwas, O.M., Abdulmuin, M.Z., Siraj, S.-F.: A neural-fuzzy logic approach for modeling and control of nonlinear systems. In: IEEE International Symposium on Intelligent Control, pp. 270–275 (2002)
3. Ferreira, J., Amaral, T., Pires, V., Crisostomo, M., Coimbra, A.: A neural-fuzzy walking control of an autonomous biped robot. In: Proceedings of World Automation Congress, vol. 15, pp. 253–258 (2004), doi:10.1109/WAC.2004.185229
4. Ferreira, J., Crisóstomo, M., Coimbra, A.P.: Neuro-fuzzy zmp control of a biped robot. In: SMO 2006: Proceedings of the 6th WSEAS International Conference on Simulation, Modelling and Optimization, pp. 331–337. World Scientific and Engineering Academy and Society (WSEAS), Stevens Point (2006)
5. Hurmuzlu, Y., Marghitu, D.B.: Rigid body collisions of planar kinematic chains with multiple contact points. Int. J. Robot Res. 13(1), 82–92 (1994)
6. Islam, S., Liu, P.X.: Adaptive fuzzy output feeedback control for robot manipulators. In: IEEE International Conference on Systems, Man and Cybernetics, SMC 2009, pp. 2630–2635 (2009)
7. Jang, J.-S.R.: Anfis: adaptive-network-based fuzzy inference system. IEEE Transactions on Systems, Man and Cybernetics 23(3), 665–685 (1993), doi:10.1109/21.256541
8. Kelly, R., Santibáñez, V., Loría, A.: Control of Robot Manipulators in Joint Space. In: Advanced Textbooks in Control and Signal Processing, Springer, Heidelberg (2005)
9. McGeer, T.: Passive dynamic walking. Int. J. Robot Res. 9(2), 62–82 (1990)
10. Shieh, M.-Y., Chang, K.-H., Chuang, C.-Y., Chiou, J.-S., Li, J.-H.: Anfis based controller design for biped robots. In: IEEE International Conference on Mechatronics, pp. 1–6 (2007), doi:10.1109/ICMECH.2007.4280017
11. Sugeno, M., Kang, T.: Structure identification of fuzzy model. Fuzzy Sets and Systems 28, 15–33 (1988)
12. Vukobratovic, M., Juricic, D.: Contribution to the synthesis of biped gait. IEEE Transactions on Biomedical Engineering 16(1), 1–6 (1969)
13. Westervelt, E.R., Grizzle, J.W., Chevallereau, C., Choi, J.-H., Morris, B.: Systematic Design of Within-Stride Feedback Controllers for Walking. In: Feedback Control of Dynamic Bipedal Robot Locomotion, pp. 137–190. Taylor & Francis/CRC (2007)

Applied Soft Computing 11 (2011) 5306–5314

Contents lists available at ScienceDirect

Applied Soft Computing

journal homepage: www.elsevier.com/locate/asoc

Generation of walking periodic motions for a biped robot via genetic algorithms☆

Selene L. Cardenas-Maciel [a,b,*], Oscar Castillo [b], Luis T. Aguilar [c]

[a] Facultad de Ciencias Quimicas e Ingenieria, Universidad Autonoma de Baja California, Calzada Universidad No. 14418. Mesa de Otay, Tijuana, BC 22390, Mexico
[b] Division de Estudios de Posgrado e Investigacion, Instituto Tecnologico de Tijuana, Calzada Tecnologico S/N, Tijuana, BC 22414, Mexico
[c] Centro de Investigacion y Desarrollo de Tecnologia Digital, Instituto Politecnico Nacional, Av. del Parque No. 1310, Mesa de Otay, Tijuana, BC 22510, Mexico

ARTICLE INFO

Article history:
Received 27 June 2009
Received in revised form 15 July 2010
Accepted 1 May 2011
Available online 20 May 2011

Keywords:
Periodic motions design
Genetic algorithms
Constrained optimization
Biped robot walking

ABSTRACT

This paper presents the design of walking motions of a biped robot by a computational intelligent method. The proposed method finds the parameters of the output functions that produce such motion in the closed-loop system which fulfill the requirements of stability and minimal energy control by formulating a constrained optimization problem. A set of parameters which produces periodic motions with low energy control magnitudes and its closed-loop system trajectories are shown through a numerical study case of a 3-DOF biped robot.

1. Introduction

In recent years several results have been provided for the stabilization of biped robot locomotion, which usually are based on finding a suitable reference trajectory (i. e. walking pattern) such that it guarantees performing stable steps while obeying a certain criteria such as walking velocity, step length, step frequency, including energy minimization [1,2] and then, enforcing the mechanism to follow it using a tracking controller.

Some proposed methods for the walking pattern synthesis use as a main design criteria the energy minimization and incorporate the zero moment point approach (ZMP) [3] as an indicator of stability of the biped motion, Qiang et. al. [4] consider the ground condition and walking patterns with small torque and velocity of the joint actuators are obtained. Capi et. al. in [5] generate the joint trajectories for walking and going up-stairs based on consumed energy and torque change. Denk and Schmidt [6] propose a systematic approach for the design of a walking pattern database using optimal control techniques and ZMP for prevention of the foot rotation and ensure the feasibility of the walking; Kajita et. al. [7] introduce a method for a walking pattern generation by using a preview control of ZMP that uses ZMP as future reference. In others, the main idea is to find a set of functions which characterize the trajectories of either joint and velocities coordinate, then, to obtain the walking pattern through the application of optimization techniques. Bessonnet et al. [8] define the generalized coordinates as spline functions and by a formulation of an optimal control problem and a quadratic programming method find the functions such that fulfill the minimization of the amount of the driving torques. The genetic algorithms (GAs) has been used as optimization method by Choi et. al. [9] to determine the shape of velocities and accelerations trajectories for obtain smooth and stable walking. Likewise, Park and Choi [10] use GAs to obtain an optimal locomotion pattern with minimal energy consumption by finding the parameters of a four order polynomial and the optimal locations of the center of mass of each links of the robot.

On the other hand, early literature focuses on the incorporation of analysis and control techniques, which generate periodic motions without requiring of a preplanned walking pattern, designing feedbacks such that to allow reach stabilization to an limit cycle [11,12].

In this paper, the later approach in [11,12] is adopted as one important part in the generation of walking motions unlike related publications as [5,10,13] where with the ZMP approach periodic motions are not established as a necessary condition to determining the walking patterns and these results are expressed as functions in the time. A feedback controller where holonomic constraints are imposed into the outputs with the objective of driving the outputs to zero is used, the outputs are polynomial-type functions in terms of joint positions which express the desired dynamic behavior. Thus, the motion generation is formulated as a constrained optimization problem, and a genetic algorithm is applied as an optimization method, where the main task is to find the

☆ This work was supported in part by Conacyt under Grant 127575 and by DGEST under Grant 4378.11-P.

* Corresponding author. Tel.: +52 6646827681; fax: +52 6646827681.
E-mail addresses: lilettecardenas@ieee.org (S.L. Cardenas-Maciel), ocastillo@hafsamx.org, luis.aguilar@ieee.org (L.T. Aguilar).

1568-4946/$ – see front matter © 2011 Elsevier B.V. All rights reserved.
doi:10.1016/j.asoc.2011.05.030

Nomenclature

$\lvert\alpha\rvert$	absolute value of α
$\lvert\lvert x\rvert\rvert$	Euclidean norm of x
sign(α)	Signum function
$M \in \Re^{n\times n}$	is the inertia matrix
$C \in \Re^{n\times n}$	is the Coriolis matrix
$G \in \Re^{n}$	is the conservative forces vector
$B \in \Re^{n\times m}$	is the input matrix

parameters of the output functions such that input energy injected to the mechanism during the walking be minimal while periodic walking motions are obtained and satisfying the biped model assumptions.

The paper is organized as follows: Section 2 presents the mathematical model of a biped robot. In Section 3, the problem formulation is summarized. Section 4, describes the optimization method and their implementation details according to the problem. Section 5, presents the parameters obtained with the GA, and the trajectories generated by the simulation of the closed-loop system for a 3-DOF planar biped robot. Section 6 provides the conclusions.

2. Biped robot model

In this section the dynamical model of a planar biped robot is introduced. The biped robot consists of a torso, hips, and two legs of equal length without ankles and knees. Two torques are applied between the legs and torso. The definition of the angular coordinates and the disposition of the masses of the torso, hips and legs of the biped robot are shown in Fig. 1, the positive angles are computed in a clockwise manner with respect to the indicated vertical lines and all masses of the links are lumped.

The walking cycle takes place in the sagittal plane and on a surface level, and it is assumed as successive phases where only one leg (stance leg) touching the walking surface (the swing phase), and the transition from one leg to another taking place in a smaller length of time. During swing the phase, the stance leg is modeled like a pivot and the swing leg is assumed to move into the frontal plane [14] and to renter the plane of the motion when the angle of the stance leg attains a given desired value. The assumptions concerning the walking cycle, define the biped robot model in two parts: the model that describes the swing phase and another one that describes the contact event of the swing leg with the walking surface; which are presented below.

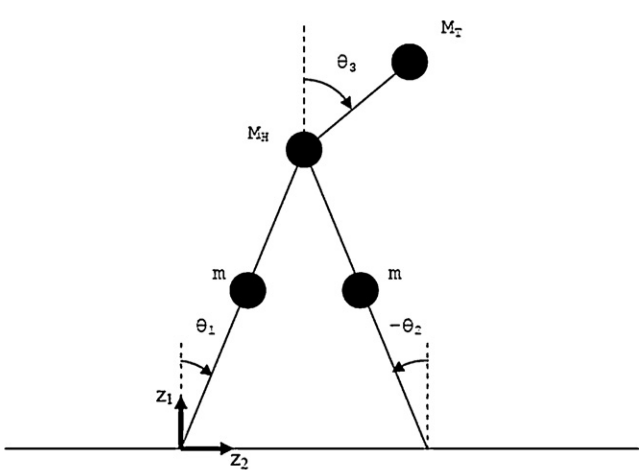

Fig. 1. 3-link biped robot.

2.1. Dynamic model

The dynamical model of the robot during the swing phase is a second order system obtained from the Lagrange method [15]:

$$M(\theta)\ddot{\theta} + C(\theta, \dot{\theta})\dot{\theta} + G(\theta) = Bu, \tag{1}$$

where $\theta = [\theta_1, \theta_2, \theta_3]^T$ are the generalized coordinates, θ_1 parameterizes the stance leg, θ_2 the swing leg and θ_3 the torso; $u = [u_1, u_2]^T$ are the input.

The second order differential Eq. (1) is rewritten into state-space form by defining

$$\begin{aligned} \dot{x} \; &:= \frac{d}{dt}\begin{bmatrix} \theta \\ \dot{\theta} \end{bmatrix} = \begin{bmatrix} \dot{\theta} \\ M^{-1}(\theta)[-C(\theta,\dot{\theta})\dot{\theta} - G(\theta) + Bu] \end{bmatrix} \\ &:= f(x) + g(x)u. \end{aligned} \tag{2}$$

2.2. Impact model

The impact between the swing leg and the ground is modeled as the contact between two rigid bodies. The main objective is to obtain the velocity of the generalized coordinates after the impact of the swing leg with the walking surface in terms of the velocity and position before the impact. The impact model for the biped robot is based on the rigid impact model of Ref. [16] and assuming the case where the contact of the swing leg with the walking surface produce either no rebound nor slipping of the swing leg, and the stance leg lifting the walking surface without interaction. The conditions in Ref. [16] for these assumptions to be valid are that:

1. The impact takes place over an infinitesimally small period of time;
2. The external forces during impact can be represented by impulses;
3. Impulsive forces may result in an instantaneous change in the velocities of the generalized coordinates, but positions remain continuous;
4. The torques supplied by the actuators are not impulsional.

Taking into account the previous assumptions, the impact model is expressed with equation [17]:

$$\begin{bmatrix} M_e & -E^T \\ E & 0 \end{bmatrix}\begin{bmatrix} \dot{\theta}_e^+ \\ F \end{bmatrix} = \begin{bmatrix} M_e\dot{\theta}_e^- \\ 0 \end{bmatrix}, \tag{3}$$

where $\theta_e = [\theta_1, \theta_2, \theta_3, z_1, z_2]^T$ are the generalized coordinates resulting of the add the cartesian coordinates $[z_1, z_2]^T$ of the end of the stance leg as shown in Fig. 1; M_e is the positive-definite inertia matrix of the biped model with the new generalized coordinates; $F = [F_T, F_N]^T$ represent the tangential and normal forces applied at the end of the swing leg; $\dot{\theta}_e^+$ is the velocity after the impact; $\dot{\theta}_e^-$ is the velocity before the impact and

$$E := \frac{\partial \Upsilon}{\partial \theta_e} = \begin{bmatrix} r\cos(\theta_1) & -r\cos(\theta_2) & 0 & 1 & 0 \\ -r\sin(\theta_1) & r\sin(\theta_2) & 0 & 0 & 1 \end{bmatrix}, \tag{4}$$

where

$$\Upsilon := \begin{bmatrix} z_1 + r\sin(\theta_1) - r\sin(\theta_2) \\ z_2 + r\cos(\theta_1) - r\cos(\theta_2) \end{bmatrix}. \tag{5}$$

Solving for $\dot{\theta}_e^+$ of Eq. (3), a change of coordinates must be done and also a re-initialization of the model (2). The change of coordinates is an expression for $x^+ := (\theta^+, \dot{\theta}^+)$ in terms of $x^- := (\theta^-, \dot{\theta}^-)$, which is given for the mapping function [18]:

$$x^+ = \Delta(x^-) := \begin{bmatrix} \theta_2^- & \theta_1^- & \theta_3^- & \dot{\theta}_2^+(x^-) & \dot{\theta}_1^+(x^-) & \dot{\theta}_3^+(x^-) \end{bmatrix}. \tag{6}$$

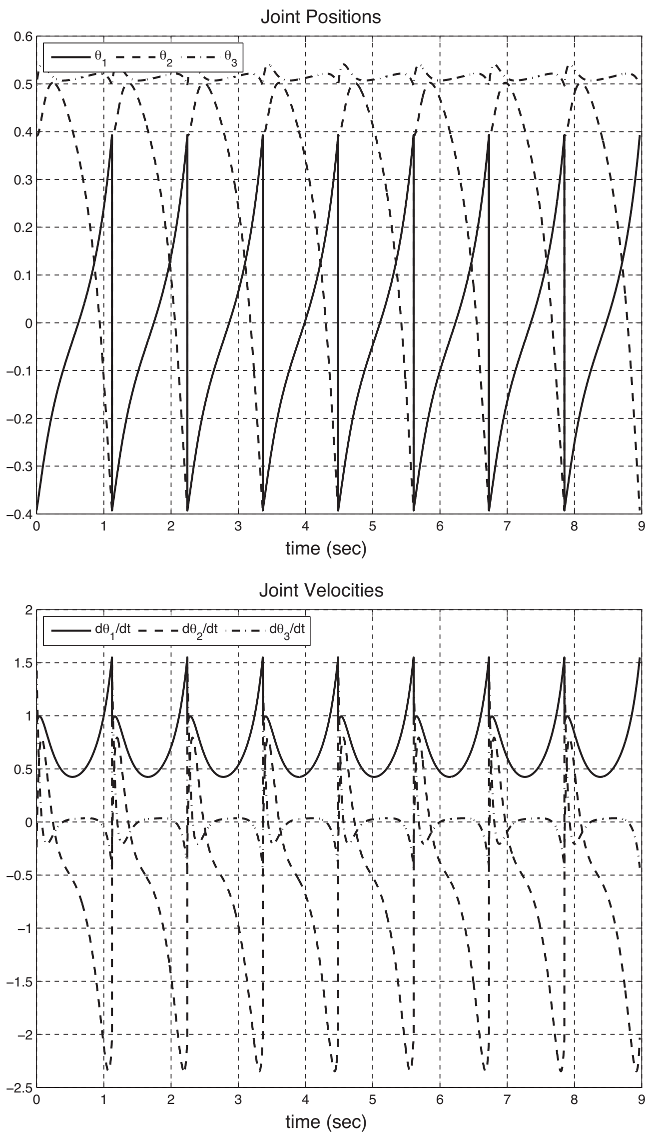

Fig. 2. Joint positions and velocities trajectories corresponding to the closed-loop system simulation using the parameters of Table 4.

Table 1
Genetic algorithm parameters.

Parameter	Value
Number of individuals	100
Generations	400
Crossover rate	0.9
Mutation rate	0.2
Selection rate	0.4

Table 2
Biped model parameters.

Parameter	Value
Mass of hips (M_H)	15 kg
Mass of torso (M_T)	10 kg
Mass of legs (m)	5 kg
Length of legs (r)	1 m
Length of torso (l)	0.5 m

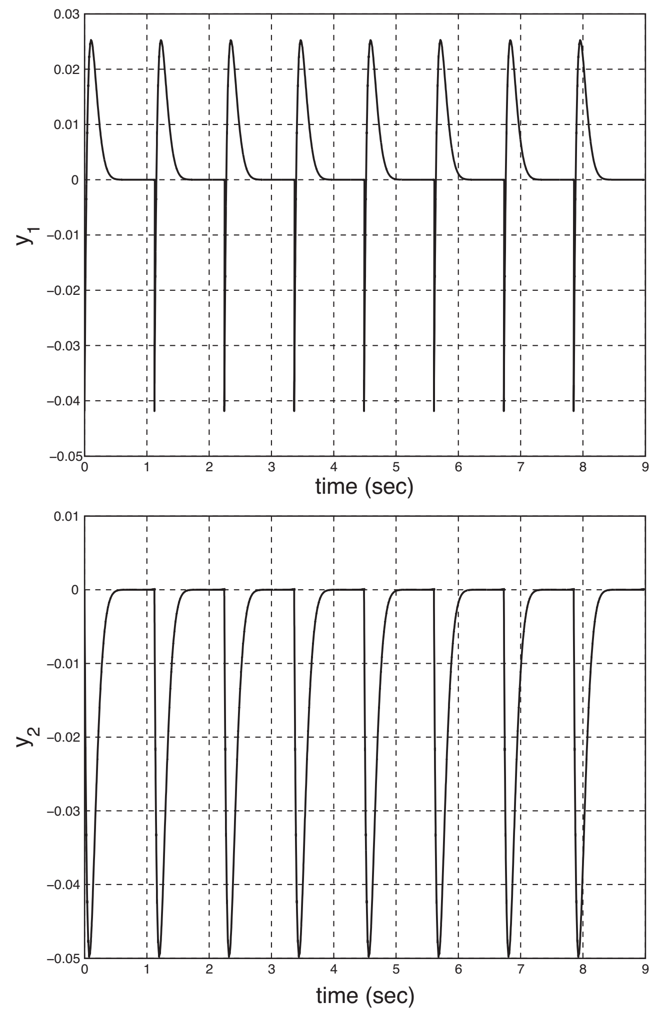

Fig. 3. Output function trajectories corresponding to the closed-loop system simulation using the parameters of Table 4.

Thus, the overall model of biped walking is the combination of the swing phase model and impact model, as follows:

$$\Sigma : \begin{cases} \dot{x} = f(x) + g(x)u & x^- \notin S \\ x^+ = \Delta(x^-) & x^- \in S, \end{cases} \tag{7}$$

where

$$S := \{(\theta, \dot{\theta}) | z_1 > 0, z_2 = 0, \theta_1 = \theta_1^d\}. \tag{8}$$

3. Problem formulation

This paper is based on the feedback controller for walking proposed by Grizzle and co-workers in Ref. [17], which designs a feedback for posture control and swing leg advancement of the biped robot (7), where the posture control means maintaining the torso angle at a desired value and the swing leg advancement consists in driving the swing leg to behave as a mirror image of the stance leg ($\theta_2 = -\theta_1$). Thus, the behavior is encoded into the dynamics of the robot by defining the following output function:

$$y := \begin{bmatrix} y_1 \\ y_2 \end{bmatrix} := \begin{bmatrix} h_1(\theta, a) \\ h_2(\theta, a) \end{bmatrix} := \begin{bmatrix} \theta_3 - h_{d,1}(\theta_1, a) \\ \theta_2 - h_{d,2}(\theta_1, a) \end{bmatrix} \tag{9}$$

where

$$\begin{aligned} h_{d,1}(\theta_1, a) &:= a_1^0 + a_1^1\theta_1 + a_1^2(\theta_1)^2 + a_1^3(\theta_1)^3 \\ h_{d,2}(\theta_1, a) &:= -\theta_1 + (a_2^0 + a_2^1\theta_1 + a_2^2(\theta_1)^2 + a_2^3(\theta_1)^3) \times (\theta_1 + \theta_1^d) \times (\theta_1 - \theta_1^d) \end{aligned} \tag{10}$$

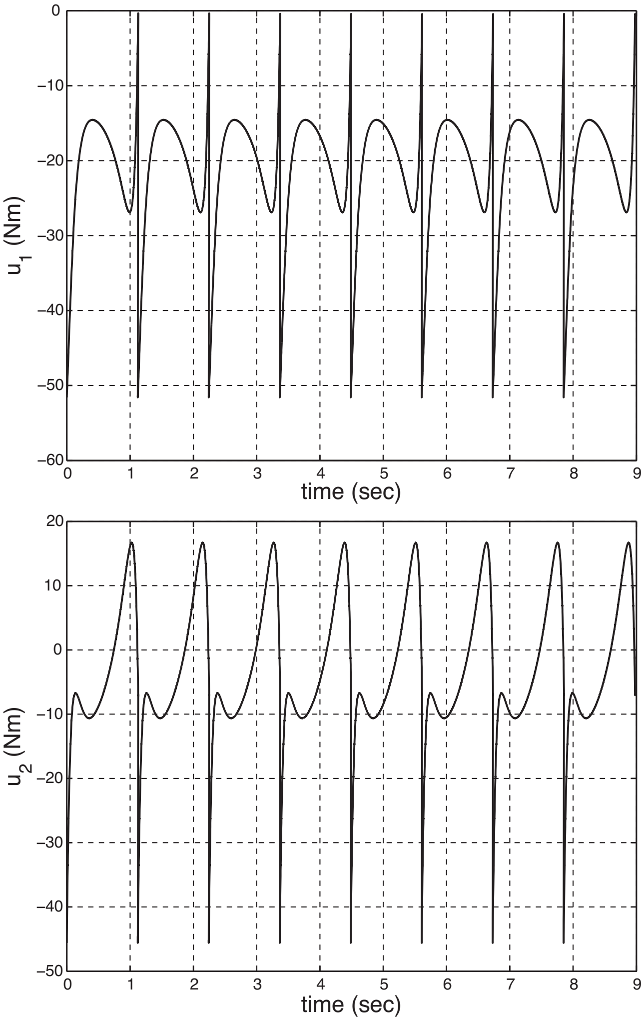

Fig. 4. Control signals corresponding to the closed-loop system simulation using the parameters of Table 4.

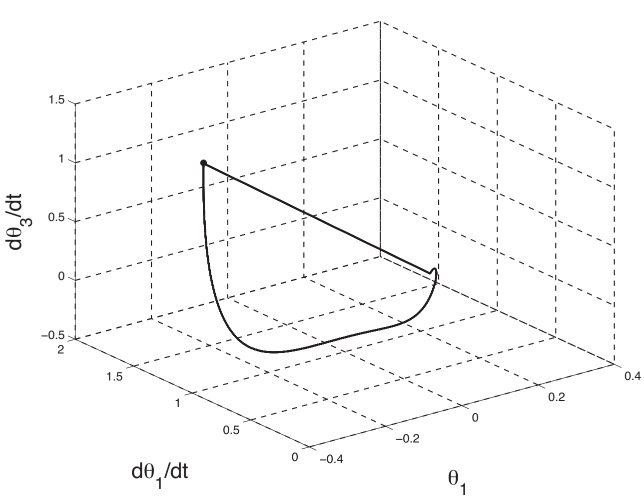

Fig. 5. Orbit corresponding to the closed-loop system simulation using the parameters of Table 4.

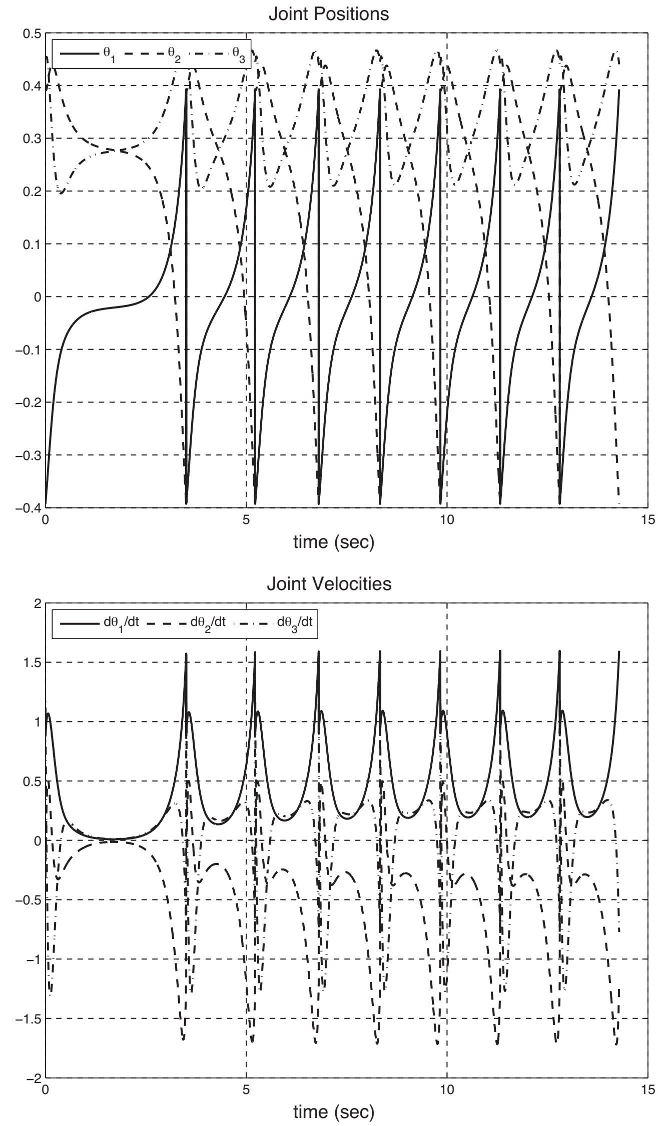

Fig. 6. Joint positions and velocities trajectories corresponding to the closed-loop simulation using the parameters of first row of Table 3.

with the control objective being to zeroing the outputs (9), by defining the feedback

$$u(x) := (L_g L_f h(x))^{-1}(\Psi(h(x), L_f h(x)) - L_f^2 h(x)), \tag{11}$$

with $L_f h(x) = \frac{\partial h}{\partial x} f(x)$, $L_f^2 h(x) = \frac{\partial}{\partial x}\left(\frac{\partial h}{\partial x} f(x)\right) f(x)$ and $L_g L_f h(x) = \frac{\partial}{\partial x}\left(\frac{\partial h}{\partial x} f(x)\right) g(x)$. The Eq. (9) is rewritten in its explicit form:

$$\begin{aligned} u(x) = u(\theta, \dot\theta) \quad &:= \left[\frac{\partial h}{\partial \theta} M^{-1} B u\right]^{-1} \left(\Psi\left(h(\theta, \dot\theta), \begin{bmatrix} \frac{\partial h}{\partial \theta} & \frac{\partial h}{\partial \dot\theta} \end{bmatrix} \begin{bmatrix} \dot\theta \\ M^{-1}[-C\dot\theta - G] \end{bmatrix} \right) \right. \\ &\left. - \begin{bmatrix} \frac{\partial}{\partial \theta}\left(\frac{\partial h}{\partial \theta}\dot\theta\right) & \frac{\partial h}{\partial \theta} \end{bmatrix} \begin{bmatrix} \dot\theta \\ M^{-1}[-C\dot\theta - G] \end{bmatrix} \right), \end{aligned} \tag{12}$$

where

$$\Psi(y, \dot y) := \begin{bmatrix} \frac{1}{\epsilon^2}\psi_\alpha(y_1, \epsilon \dot y_1) \\ \frac{1}{\epsilon^2}\psi_\alpha(y_2, \epsilon \dot y_2) \end{bmatrix}, \tag{13}$$

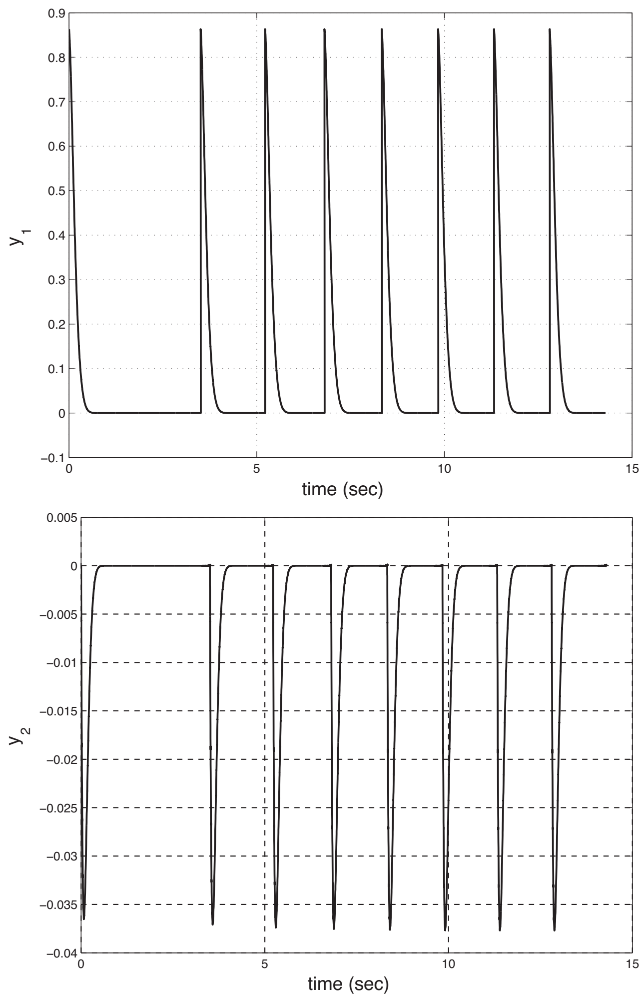

Fig. 7. Output function trajectories corresponding to the closed-loop simulation using the parameters of first row of Table 3.

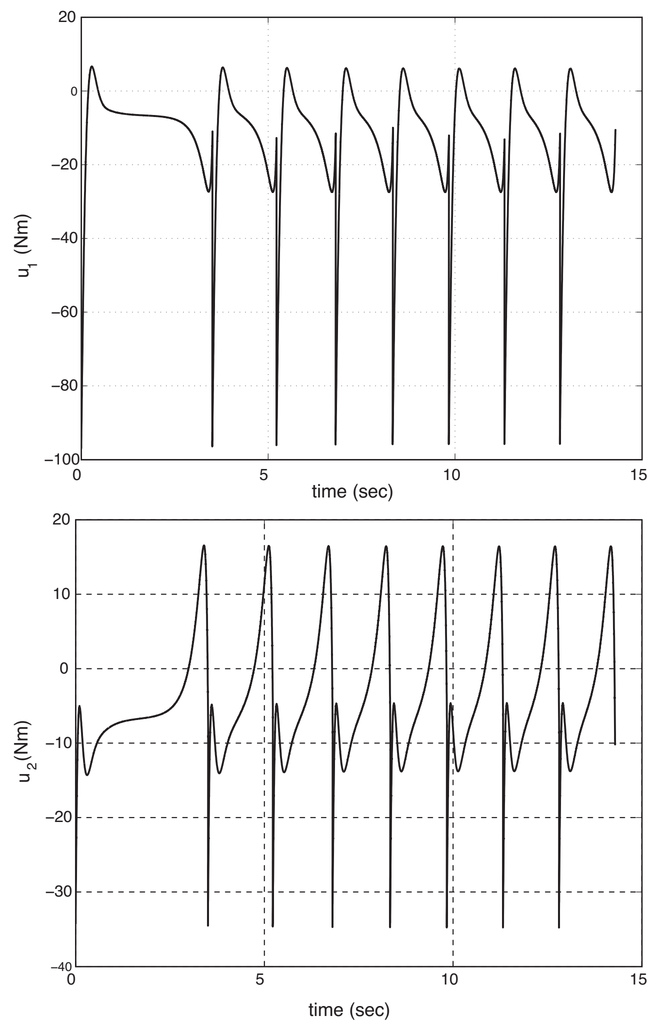

Fig. 8. Control signals corresponding to the closed-loop simulation using the parameters of first row of Table 3.

with $y := [y_1, y_2]$, $\dot{y} := [\dot{y}_1, \dot{y}_2]$ and

$$\psi_\alpha(y_i, \epsilon\dot{y}_i) := -\mathrm{sign}(\epsilon\dot{y}_i)|\epsilon\dot{y}_i|^{\alpha} - \mathrm{sign}(\phi_\alpha(y_i, \epsilon\dot{y}_i))|\phi_\alpha(y_i, \epsilon\dot{y}_i)|^{(\alpha/2-\alpha)} \tag{14}$$

where

$$\phi_\alpha(y_i, \epsilon\dot{y}_i) := y_i + \left(\frac{1}{2-\alpha}\right)\mathrm{sign}(\epsilon\dot{y}_i)|\epsilon\dot{y}_i|^{2-\alpha}, \tag{15}$$

with $i = 1, 2$, $\alpha \in (0, 1)$ and $\epsilon > 0$.

The problem statement is described as follows: Given the biped robot model (7) and the feedback (11), find the parameters a_i^j of the function in (10) such that the closed-loop system produces periodic walking motions with low energy control.

4. Optimization strategy

According to the problem defined above, a GA is proposed to solve the optimization problem. GAs are search algorithms based on natural selection and natural genetic principles [19], these algorithms can be applied to optimization problems that differ from traditional optimization methods in that they use: payoff information (based on an objective function), no derivatives or other auxiliary knowledge issued; a coding of the parameters, not the parameters themselves and probabilistic rules as a tool to guide the search [20].

The implementation of the GA begins with the selection of consistent decision variables to solve the problem, which are then coded into a string called individual, as well as an objective function which provides a numerical value that indicates the goodness degree or fitness of the individual to solve the problem. The GA

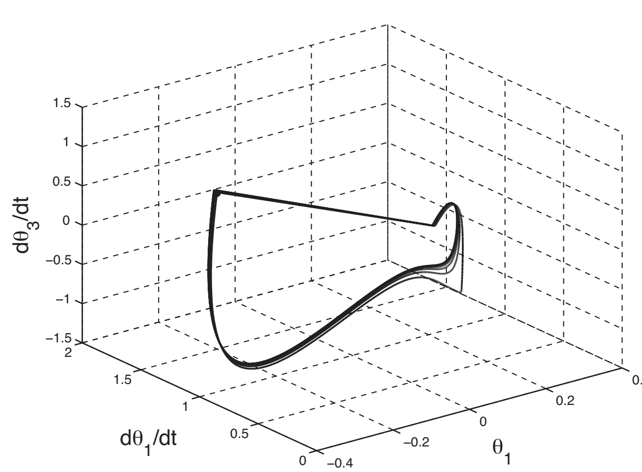

Fig. 9. Orbit corresponding to the closed-loop system simulation using the parameters of the first row of Table 3.

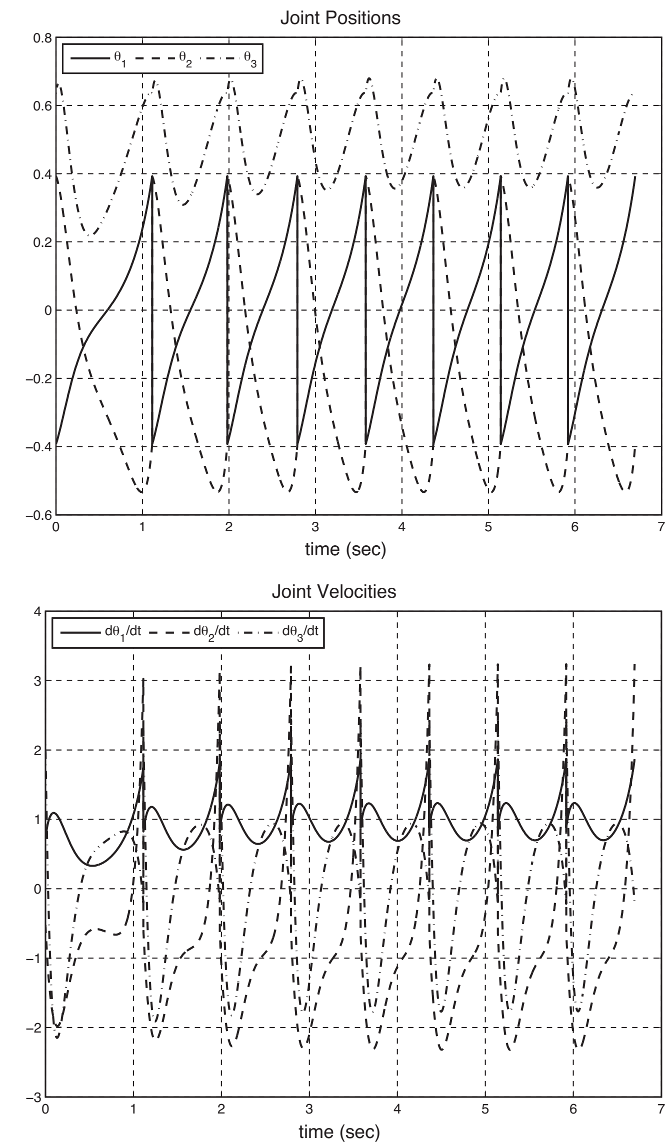

Fig. 10. Joint positions and velocities trajectories corresponding to the closed-loop system simulation sing the parameters of the last row of Table 3.

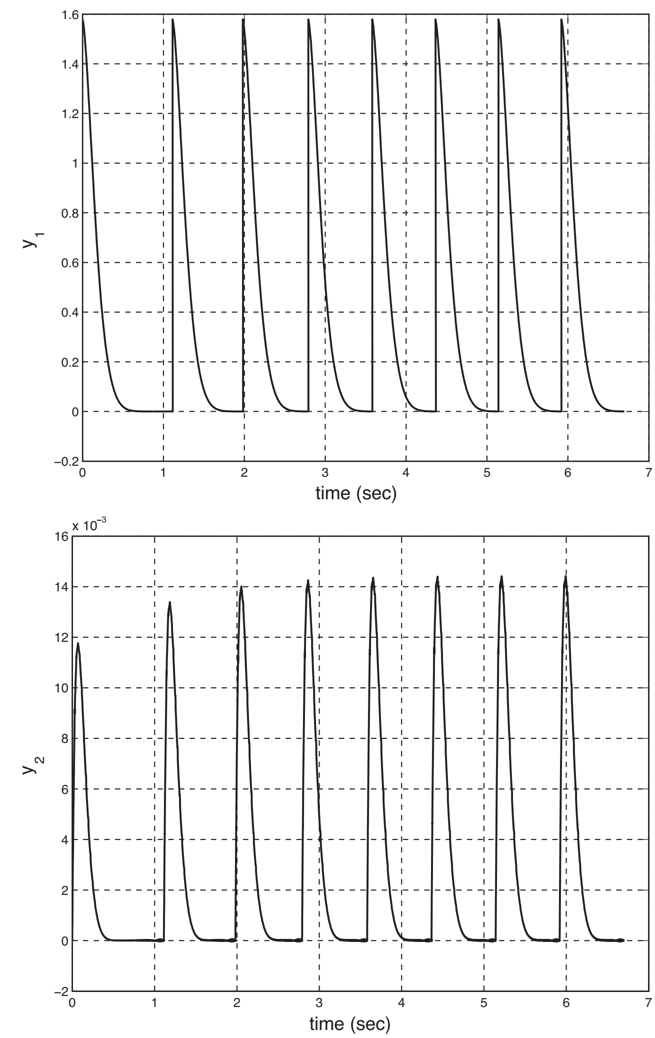

Fig. 11. Output function trajectories corresponding to the closed-loop system simulation sing the parameters of the last row of Table 3.

operation consists of several stages, that imitate the natural principles in which are based: The *initialization* stage where a set of individuals called population is created randomly; the *selection* stage in which each individual is evaluated through the objective function, the values of the evaluation are used by a selection algorithm that identifies and choose the fittest individuals that serve as the parents for the creation of new individuals; the new individuals are created by applying the genetic operations to the individuals selected in the previous stage. These operations are: crossover, which with certain probability, combines the parameters encoded between pairs of individuals producing two individuals with information of both parents, and the mutation, which is the alteration of the value of one parameter encoded in the individual, the goal of this operation is to introduce diversity in the population, this stage is called *reproduction*; the last stage is the *replacement*, and it consist in the creation of the new population with the new individuals and the parents. The overall stages are performed in an iterative manner, and each iteration is called a generation. The GA operation explained above is expressed through an algorithm in pseudocode as shown below:

1. `Begin`
2. $i \leftarrow 0$
3. `Create a population` P_i`of` N`individuals`
4. `Evaluate fitness of all individuals of the population:` $P_i^e \leftarrow Fitness(P_i)$
5. `Repeat the steps until the conditions are reached`

   (a) `Select the parents for matting:` $P_i^s \leftarrow Select(P_i, P_i^e)$
   (b) `Apply crossover and mutation:` $P_i^g \leftarrow Genetic\_Operation(P_i^s)$
   (c) $i \leftarrow i+1$
   (d) `Create the new population:` $P_i \leftarrow New\_Pop(P_i^g, P_{i-1})$
   (e) `Evaluate fitness of new individuals:` $P_i^e \leftarrow Fitness(P_i)$

6. `Print out the best solution`
7. `End`

Thus, the details of our implementation of the each stage are provided below.

4.1. Individual representation

The individual representation selected is the real coding scheme, whose genotype is composed by eight real numbers such they represent each parameter a_i^j with $i=1$, 2 and $j=0, 1, \ldots, 3$ of (10).

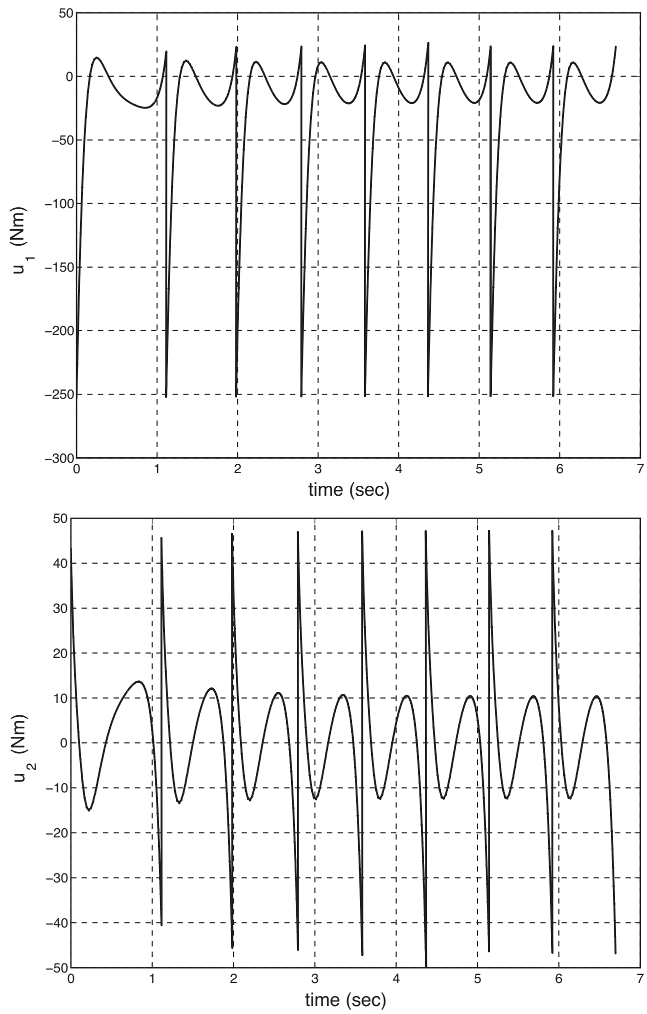

Fig. 12. Control signals corresponding to the closed-loop system simulation sing the parameters of the last row of Table 3.

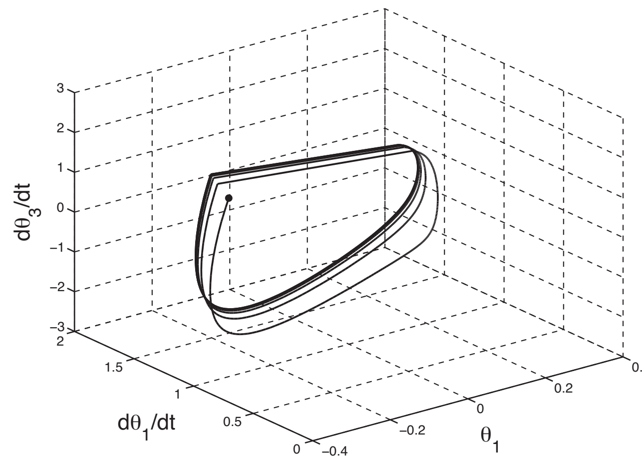

Fig. 13. Orbit corresponding to the closed-loop system simulation using the parameters of the last row of Table 3.

The a_i^j values of the individual are enforced to be within a desired domain. This requirement is preserved in the creation of initial population and the mutation operation. In the initial population, each real number of an individual is obtained through a linear transformation of a random number whose result belonging to the domain $[-5, 5]$. Let an individual represented as $s_v^0 = [v_1^0, v_2^0, v_3^0, \ldots, v_8^0]$. The real number in the initialization stage v_k^0 with $k = 1, 2, \ldots, 8$ is given as

$$v_k^0 = \left(\frac{\mathrm{LB}}{2} + \frac{\mathrm{UB}}{2}\right) + \left(\left(\frac{\mathrm{UB}}{2} - \frac{\mathrm{UL}}{2}\right)(2p-1)\right), \tag{16}$$

where $p \in [0, 1]$ is a random number; LB denotes the lower bound and UB denotes the upper bound of the domain of the real number.

4.2. Objective function

The goal of the GA is the minimization of a cost function, which represents the approximation to the average energy consumed over the walking cycle:

$$\hat{J}(a) = \int_0^T (u_1^2 + u_2^2)dt, \tag{17}$$

where T is such that $\theta_1(T) - \theta_1^d = 0$, and $u = [u_1, u_2]$ is obtained by applying (11) into the closed-loop with the biped robot model (2) and using (9).

Table 3
a_i^j parameters obtained with the GA and energy control.

No.	Parameters								$\hat{J}(a)$
	a_1^0	a_1^1	a_1^2	a_1^3	a_2^0	a_2^1	a_2^2	a_2^3	
1	0.3005	1.1474	-1.8933	−0.3126	−1.5921	3.7716	2.8948	−0.3294	468.8927
2	0.4833	0.6622	−2.276	1.2824	−0.3166	1.8917	1.2474	−0.4689	609.4312
3	0.4833	0.6622	−2.276	1.2824	−0.3166	1.8917	0.8934	0.312	639.8821
4	0.3687	1.3459	−1.6739	−1.6964	−1.5381	2.9158	1.684	2.9733	689.2893
5	0.5893	0.4644	1.5558	−0.0367	−1.2656	1.0308	1.1086	3.7436	719.32
6	0.4857	−0.2815	1.8735	−2.5745	1.5987	4.3327	−2.2472	−2.5773	773.3510
7	0.4317	0.3851	−0.6071	−0.3504	−0.3006	2.0402	2.1131	−0.1945	883.9733
8	0.7098	0.0581	0.0536	−1.0280	−1.9803	2.5752	3.6109	2.0000	1225.40
9	0.3992	0.7515	−2.5759	2.5365	1.8022	0.5344	0.2620	6.0033	1679.20
10	1.0730	−0.4986	−0.4127	1.6194	2.7029	−1.4978	1.6201	−0.8384	2541.70
11	0.2892	1.9435	−2.8760	0.4328	2.0252	4.5643	−0.5546	−4.1460	2980.50

Table 4
a_i^j parameters obtained with SQP method and energy control.

a_1^0	a_1^1	a_1^2	a_1^3	a_2^0	a_2^1	a_2^2	a_2^3	$\hat{J}(a)$
0.5120	0.0730	0.0350	−0.8190	−2.2700	3.2600	3.1100	1.8900	761.00

The cost function is subject to the following constraints taken from [21]:

$$\begin{array}{ll} \hat{\dot{\theta}}_1^- - 0.99\lambda(\hat{\dot{\theta}}_1^-) & \leq 0, \\ \|y(\bar{t})\| & \leq 0, \\ |\frac{F_T}{F_N}| - \mu & \leq 0, \\ -\dot{z}_2^+ & \leq 0, \end{array} \tag{18}$$

where $\hat{\dot{\theta}}_1^-$ is the pre-impact angular velocity of the stance leg and μ is the static friction coefficient.

The first constraint assures the existence of the one fixed point, the second one assures that the controller has converged before the impact and the last two constraints verify the validity of the impact model.

4.3. Genetic operations

The genetic operations comprise the classical one point crossover and non-uniform mutation [20,22]. Non-uniform mutation is defined as follows: if $s_v^t = [v_1,...,v_m]$ is an individual in the generation number t and the element v_k was selected for this mutation, the result is a vector $s_v^t = [v_1, \ldots, v_k^{'}, \ldots, v_m]$ where:

$$v_k^{'} = \begin{cases} v_k + \Delta(t, \mathrm{UB} - v_k); & q = 0 \\ v_k - \Delta(t, v_k - \mathrm{LB}); & q = 1, \end{cases} \tag{19}$$

q is determined as follows: Let $p \in [0, 1]$ a random number, if $0 \leq p < 0.5$, $q = 0$; if $0.5 \leq p \leq 0.5$, $q = 1$. The *LB* and *UB* are the lower an upper domain bounds of v_k.

The function $\Delta(t, y) = y\left(1 - r^{(1-(t/T))^b}\right)$ returns a value in the domain $[0, y]$; $r \in [0, 1]$ is a random number; T is the maximal generation number; b is the dependency degree on the generation number.

The value of b is established as 5 due to need preserve promising solutions by decreasing the value of $\Delta(t, y)$ through the evolutionary process, this mean that in early generations $\Delta(t, y)$ modify to the individual such that produces a global exploration in the search space whereas the exploration becoming local when the generation number approaches to T, because $\Delta(t, y)$ tend to be zero. This parameter value has been used by Refs. [20,23] to mention some works in the literature and its application in this problem allows begin to become a local exploration around of the second half of the process.

5. Simulation results

The GA was developed in MatLab® with the characteristics described in Section 4, running in a Pentium IV computer with 512 MB of RAM using the algorithm parameters shown in Table 1, these parameters were determined by empirical tests based on increments of the typical mutation and selection rate, due to that GA executions with parameters near to the typical showed a slow convergence.

The individual evaluation was made in one walking cycle and uses the software implementation of the 3-DOF model (7) with the controller (11) available in Ref. [24]. The physical parameters of the biped model are shown in Table 2, pre-impact angular velocity is taken as $\dot{\theta}_1^- = 1.55$, the static friction coefficient $\mu = 2/3$, the swing leg reenter to the sagittal plane when $\theta_1^d = \pi/8$ and the controller parameters of Eqs. (13) and (14) are $\epsilon = 0.1$ and $\alpha = 0.9$, respectively. Details of the biped model can be found in Appendix A.

Table 3 shows the parameters a_i^j of the function (10) obtained of eleven independent GA executions as well as the energy control computed by the closed-loop system simulation with each parameters.

The parameters in Table 4 were obtained using sequential quadratic programming (SQP) method which are reported in [21].

In the following are shown the state trajectories, the output, the control signals and orbits projected onto $\theta_1, \dot{\theta}_1$ and $\dot{\theta}_3$ corresponding to the closed-loop system simulation which represents the system performing eight steps. From Figs. 2–5 the results using the parameters given in Table 4, from Figs. 6–9 show the results using the parameters of first row of Table 3, where present an improvement in the energy control although the orbits present slow convergence to the limit cycle regarding to the orbits obtained with parameters found it by SQP and at this time is not a criteria into the optimization. It should be note that the parameters presented in Table 3 allow to reach the control objective and to obtain periodic walking motions in spite of some have energy control that not improve the energy control obtained with SQP. Simulation results corresponding to this case are presented in Figs. 10–13.

6. Conclusions

In this paper a GA for the generation of walking motions of a biped robot was presented. The design approach consisted in the search of suitable parameters of the output functions which impose the desired behavior of the system such that produce walking motions while keeping a low energy control. The closed-loop system simulations using the parameters obtained with GA show that this approach is feasible to obtain the parameters that produce periodic walking motions and minimize the energy control.

Appendix A. Model details

This appendix completes the equations of the biped model (2) and (3). In the following, this is the notation used:

$$\begin{array}{ll} \omega & = \dot{\theta} \\ s_{1j} & = \sin(\theta_1 - \theta_j), j \in \{2, 3\} \\ c_{1j} & = \sin(\theta_1 - \theta_j), j \in \{2, 3\} \end{array}$$

A.1. Mechanical model

$$M = \begin{bmatrix} (\frac{5}{4}m + M_H + M_T)r^2 & -\frac{1}{2}mr^2c_{12} & M_Trlc_{13} \\ -\frac{1}{2}mr^2c_{12} & \frac{1}{4}mr^2 & 0 \\ M_Trlc_{13} & 0 & M_Tl^2 \end{bmatrix} \tag{20}$$

$$C = \begin{bmatrix} 0 & -\frac{1}{2}mr^2s_{12}\omega_2 & M_Trls_{13}\omega_3 \\ \frac{1}{2}mr^2s_{12}\omega_1 & 0 & 0 \\ -M_Trls_{13}\omega_1 & 0 & 0 \end{bmatrix} \tag{21}$$

$$G = \begin{bmatrix} -\frac{1}{2}g(2M_H + 3m + 2M_T)r\sin(\theta_1) \\ \frac{1}{2}gmr\sin(\theta_2) \\ -gM_Tl\sin(\theta_3) \end{bmatrix} \tag{22}$$

$$B = \begin{bmatrix} -1 & 0 \\ 0 & -1 \\ 1 & 1 \end{bmatrix} \tag{23}$$

A.2. Impact model

The inertia matrix M_e has the entries:

$$
\begin{aligned}
M_e^{11} &= (\frac{5}{4}m + M_H + M_T)r^2 \\
M_e^{12} &= -\frac{1}{2}mr^2 c_{12} \\
M_e^{13} &= M_T r l c_{13} \\
M_e^{14} &= (\frac{3}{2}m + M_H + M_T)r\cos(\theta_1) \\
M_e^{15} &= -(\frac{3}{2}m + M_H + M_T)r\sin(\theta_1) \\
M_e^{22} &= \frac{1}{4}mr^2 \\
M_e^{23} &= 0 \\
M_e^{24} &= -\frac{1}{2}mr\cos(\theta_2) \\
M_e^{25} &= \frac{1}{2}mr\sin(\theta_2) \\
M_e^{33} &= M_T l^2 \\
M_e^{34} &= M_T l\cos(\theta_3) \\
M_e^{35} &= -M_T l\sin(\theta_3) \\
M_e^{44} &= 2m + M_H + M_T \\
M_e^{45} &= 0 \\
M_e^{55} &= 2m + M_H + M_T
\end{aligned}
$$

References

[1] L. Roussel, C.C. de Wit, A. Goswami, Generation of energy optimal complete gait cycles for biped robots, in: Proceedings of the IEEE International Conference on Robotics and Automation, 1998, pp. 2036–2041.

[2] A.S. Shiriaev, L.B. Freidovich, I.R. Manchester, Can we make a robot ballerina perform a pirouette? orbital stabilization of periodic motions of underactuated mechanical systems, Annual Reviews in Control 32 (2) (2008) 200–211.

[3] M. Vukobratovic, D. Juricic, Contribution to the synthesis of biped gait, IEEE Transactions on Biomedical Engineering 16 (1) (1969) 1–6.

[4] Q. Huang, K. Yokoi, S. Kajita, K. Kaneko, H. Arai, N. Koyachi, K. Tanie, Planning walking patterns for a biped robot, IEEE Transactions on Robotics and Automation 17 (3) (2001) 280–289.

[5] G. Capi, Application of genetic algorithms for biped robot gait synthesis optimization during walking and going up-stairs, Advanced Robotics 15 (October (20)) (2001) 675–694.

[6] J. Denk, G. Schmidt, Synthesis of walking primitive databases for biped robots in 3D-environments, in: Proceedings of the IEEE International Conference on Robotics and Automation (ICRA2003), Taipei, Taiwan, 2003.

[7] S. Kajita, F. Kanehiro, K. Kaneko, K. Fujiwara, K. Harada, K. Yokoi, H. Hirukawa, Biped walking pattern generation by using preview control of zero-moment point, in: Proceedings of ICRA'03. IEEE International Conference on Robotics and Automation 2003, vol. 2, 2003, pp. 1620–1626.

[8] G. Bessonnet, P. Seguin, P. Sardain, A parametric optimization approach to walking pattern synthesis, The International Journal of Robotics Research 24 (7) (2005) 523–536.

[9] S.-H. Choi, Y.-H. Choi, J.-G. Kim, Optimal walking trajectory generation for a biped robot using genetic algorithm, in: Proceedings of IROS '99. IEEE/RSJ International Conference on Intelligent Robots and Systems 1999, vol. 3, 1999, pp. 1456–1461.

[10] J.H. Park, M. Choi, Generation of an optimal gait trajectory for biped robots using a genetic algorithm, JSME International Journal Series C: Mechanical Systems Machine Elements and Manufacturing 47 (2) (2004) 715–721.

[11] J. Grizzle, C. Moog, C. Chevallereau, Nonlinear control of mechanical systems with an unactuated cyclic variable, IEEE Transactions on Automatic Control 50 (5) (2005) 559–576.

[12] A. Shiriaev, J. Perram, C. Canudas-de Wit, Constructive tool for orbital stabilization of underactuated nonlinear systems: virtual constraints approach, IEEE Transactions on Automatic Control 50 (8) (2005) 1164–1176.

[13] G. Dip, V. Prahlad, P.D. Kien, Genetic algorithm-based optimal bipedal walking gait synthesis considering tradeoff between stability margin and speed, Robotica 27 (3) (2009) 355–365.

[14] T. McGeer, Passive dynamic walking, International Journal of Robotics Research 9 (2) (1990) 62–82.

[15] R. Kelly, R. Santibañez, A. Loria, Control of Robots Manipulators in Joint Space, Springer-Verlag London Limited, 2005.

[16] Y. Hurmuzlu, D. Marghitu, Rigid body collisions of planar kinematic chains with multiple contact points, International Journal of Robotics Research 13 (1) (1994) 82–92.

[17] E.R. Westervelt, J.W. Grizzle, C. Chevallereau, J.-H. Choi, B. Morris, Systematic design of within-stride feedback controllers for walking, in: Feedback Control of Dynamic Bipedal Robot Locomotion, Taylor & Francis/CRC, 2007, pp. 137–11891.

[18] J. Grizzle, G. Abba, F. Plestan, Asymptotically stable walking for biped robots: analysis via systems with impulse effects, Automatic Control, IEEE Transactions on 46 (1) (2001) 51–64.

[19] J.M. Holland, Adaptation in Natural and Artificial Systems, University of Michigan Press, Ann Arbor, MI, 1975.

[20] Z. Michalewicz, Genetic Algorithms + Data Structures = Evolution Programs, Springer-Verlag New York, Inc., Secaucus, NJ, USA, 1994.

[21] J. Grizzle, G. Abba, F. Plestan, Proving asymptotic stability of a walking cycle for a 5 DOF biped robot model, in: International Conference on Climbing and Walking Robots, Angleterre, Portsmouth, 1999.

[22] D.E. Goldberg, Genetic Algorithms in Search Optimization and Machine Learning, Addison-Wesley Longman Publishing Co., Inc., Boston, MA, USA, 1989.

[23] F. Herrera, M. Lozano, J. Verdegay, Tacling real-coded genetic algorithms: operators and tools for behavioural analysis, in: Artificial Intelligence Review, vol. 12, Springer, Netherlands, 1998, pp. 265–319.

[24] Feedback control of dynamic bipedal robot locomotion book webpage, http://www.dynamicbipedcontrol.org.